

Fall 2004

Study of the enhancement effect of cyclopentadecanolide on protein permeation through lipid membranes

Zhengmao Li

University of New Hampshire, Durham

Follow this and additional works at: <https://scholars.unh.edu/dissertation>

Recommended Citation

Li, Zhengmao, "Study of the enhancement effect of cyclopentadecanolide on protein permeation through lipid membranes" (2004).
Doctoral Dissertations. 229.

<https://scholars.unh.edu/dissertation/229>

This Dissertation is brought to you for free and open access by the Student Scholarship at University of New Hampshire Scholars' Repository. It has been accepted for inclusion in Doctoral Dissertations by an authorized administrator of University of New Hampshire Scholars' Repository. For more information, please contact nicole.hentz@unh.edu.

**STUDY OF THE ENHANCEMENT EFFECT OF CYCLOPENTADECANOLIDE
ON PROTEIN PERMEATION THROUGH LIPID MEMBRANES**

BY

ZHENGMAO LI

B.S., Peking University, P.R.China, 1998

M.S., Rensselaer Polytechnic Institute, 2000

DISSERTATION

Submitted to the University of New Hampshire

in Partial Fulfillment of

the Requirements for the Degree of

Doctor of Philosophy

in

Engineering: Materials Science

September, 2004

UMI Number: 3144747

INFORMATION TO USERS

The quality of this reproduction is dependent upon the quality of the copy submitted. Broken or indistinct print, colored or poor quality illustrations and photographs, print bleed-through, substandard margins, and improper alignment can adversely affect reproduction.

In the unlikely event that the author did not send a complete manuscript and there are missing pages, these will be noted. Also, if unauthorized copyright material had to be removed, a note will indicate the deletion.

UMI[®]

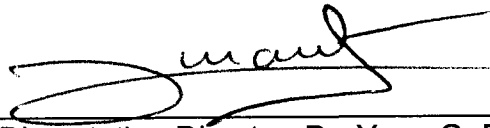
UMI Microform 3144747

Copyright 2004 by ProQuest Information and Learning Company.

All rights reserved. This microform edition is protected against unauthorized copying under Title 17, United States Code.

ProQuest Information and Learning Company
300 North Zeeb Road
P.O. Box 1346
Ann Arbor, MI 48106-1346

This dissertation has been examined and approved.




Dissertation Director, Dr. Yvon G. Durant
Research Associate Professor of Materials
Science



Dr. Donald C. Sundberg
Associate Professor of Chemical Engineering
and Materials Science



Dr. Jerome P. Claverie
Research Associate Professor of Materials
Science



Dr. Thomas M. Laue
Professor of Biochemistry and Molecular
Biology



Dr. Vernon N. Reinhold
Research Professor of Biochemistry and
Molecular Biology and Chemistry

8.4.2004

Date

ACKNOWLEDGEMENTS

First, I would like to express my sincere gratitude to my advisor, Dr. Yvon Durant, for his invaluable mentoring, guidance, support and encouragement during my graduate study. I also want to thank the other committee members: Dr. Donald Sundberg, Dr. Jerome Claverie, Dr. Thomas Laue and Dr. Vernon Reinhold for their time and assistance.

I would like to thank my parents for their guidance and support.

I am grateful to my fellow group members-- Zachary Zguris, Jeffrey Stubbs, Julien Ogier, Floraine Collette, Mingxia Zhang, for their friendship, collaboration and help.

I would like to thank Susan Chase, Kari Hartman, Kathy Gallagher and Nancy Cherim for technical and instrumental help.

Finally, I would like to thank Bentley Pharmaceuticals, Inc., New Hampshire Industrial Research Center and University of New Hampshire for financial support.

TABLE OF CONTENTS

ACKNOWLEDGEMENTS	iii
LIST OF TABLES	vii
LIST OF FIGURES	viii
ABSTRACT	xiii
CHAPTER	PAGE
I. INTRODUCTION	1
1.1. Objective of Thesis	1
1.2. Protein/Peptide Drug Delivery	2
1.2.1. Proteins and Peptides as Pharmaceuticals	2
1.2.2. Protein/Peptide Delivery-- A Booming Research Area	3
1.2.3. Delivery Routes	5
1.2.3.1. Injectable Systems	5
1.2.3.2. Oral Delivery	6
1.2.3.3. Pulmonary Delivery	9
1.2.3.4. Nasal Delivery	10
1.2.3.5. Buccal Delivery	11
1.2.3.6. Transdermal Delivery	11
1.3. Membrane Permeation Enhancers	12
1.4. Membrane Structure	13
1.5. In Vitro Membrane Permeability Models	18
1.5.1. Caco-2	20
1.5.2. PAMPA	21
1.5.3. Liposome	22
1.6. Liposome as an Artificial Membrane Model	23
1.6.1. Preparation of Liposomes	25
1.6.1.1. Multilamellar Vesicles (MLV)	25
1.6.1.2. Large Uni- or Oligolamellar Vesicles	26
1.6.1.2.1. Ether Infusion	26
1.6.1.2.2. Calcium-Induced Fusion	26
1.6.1.2.3. Reverse-Phase-Evaporation (REV)	27
1.6.1.2.4. Rapid Extrusion through Polycarbonate Filter	28
1.6.1.3. Small Unilamellar Liposomes (SUV)	29
1.6.1.3.1. Sonication	29
1.6.1.3.2. Ethanol Injection	30
1.6.1.3.3. Detergent Dialysis	30

1.6.1.3.4. Reverse Micelle Method	31
1.6.2. Removal of Unbound Drug	31
1.6.2.1. Dialysis	32
1.6.2.2. Centrifugation	33
1.6.2.3. Gel Filtration	33
II. METHODOLOGY	35
2.1. Release Concept “In Vivo” Vs. “In Vitro”	35
2.2. In Vitro Release Protocol Design	37
2.2.1. Liposome	37
2.2.2. Model Proteins	40
2.2.3. Release Protocol Flow Chart	41
2.3. Drug Modification	42
2.4. Liposome Synthesis and Size Measurement	50
2.5. Permeation Enhancer Combinations	54
2.6. Liposome Cleaning	57
2.7. Drug Release with Shaker Table	60
2.8. Animal Test Validation	62
III. PROTEIN RELEASE FROM LIPOSOMES	63
3.1. General Procedure for One Release Experiment	63
3.2. Insulin Release from DPPC Liposomes at Different Temperatures	67
3.2.1. Insulin Release from DPPC Liposome at 47 °C at pH 7	67
3.2.2. Insulin Release from DPPC Liposome at 42 °C at pH 7.4	69
3.3. Insulin Release from DPPC Liposomes with Phase Transfer Agent	72
3.3.1. Insulin Release from DPPC Liposome at 42 °C with Cyclodextrins at pH 7	75
3.3.2. Insulin Release from DPPC Liposome at 42 °C with Different Amount of Cyclodextrins at pH 7	78
3.3.3. Insulin Release from DPPC Liposome at 42 °C with Beta-Cyclodextrin at pH 7	81
3.4. Incorporating Cholesterol into DPPC Liposome	84
3.4.1. Insulin Release at 37 °C from DPPC/Cholesterol Liposomes with Different Formulation Components and Simple Combinations	85
3.4.2. Insulin Release at 37 °C from DPPC/Cholesterol Liposomes with Different amount of CPE-215™	89
3.5. Insulin Release from DPPC/Cholesterol Liposomes at Different pH	93
3.5.1. Insulin Release from DPPC/Cholesterol Liposome at 37 °C with Small pH Gradient	93
3.5.2. Insulin Release from DPPC/Cholesterol Liposome at 37 °C at pH 10	96
3.5.3. Insulin Release from DPPC/Cholesterol Liposome at 37 °C at pH 4	98
3.6. BSA Release at 37 °C from DPPC/Cholesterol Liposomes at pH 7	100

IV. RELEASE MECHANISM STUDY	102
4.1. Insulin Solution Properties	102
4.1.1. Insulin Diffusion Coefficient Measurement by NMR	102
4.1.2. Using the Analytical Ultracentrifugation to Determine the Insulin Association State	107
4.2. CPE-215™ Interaction with Liposome (Membrane)	111
4.2.1. Introduction	111
4.2.2. Experiment Design	114
4.2.3. Experimental Section	115
4.2.4. Results and Discussion	118
4.2.5. Conclusion	133
4.3. Insulin Interaction with Liposome (Membrane)	133
4.3.1. Centrifugal Extraction to Determine the Insulin Adsorption Coefficient on Membrane	135
4.3.2. ITC Experiment of Insulin Titration on Liposome	141
4.4. Mechanistic Hypothesis for the Insulin Release from Liposome	147
4.4.1. Diffusion through Lipid Bilayer Membrane	147
4.4.2. The Role of CPE-215™ as a Membrane Permeation Enhancer	151
4.4.3. Proposed Hypothesis for the Whole Insulin Release Process	155
V. QUANTITATIVE RELEASE MODEL	163
5.1. Mathematical Model	163
5.2. Neural Network	168
5.2.1. Introduction to Neural Network	168
5.2.2. Application of Neural Network Model	172
5.2.3. Neural Network Model Analysis	174
5.2.4. Neural Network Prediction	180
VI. CONCLUSION	185
LIST OF REFERENCES	189
APPENDIX	203

LIST OF TABLES

	Page
Table 1 Physical properties of various cyclodextrins	73
Table 2 Sample information in Section 3.4.1	86
Table 3 Sample information in Section 3.4.2	90
Table 4 Composition of different liposomes	116
Table 5 Different liposomes for multiple-heating-cycle experiment	117
Table 6 DSC study summary table	132
Table 7 Centrifugal extraction data	139
Table 8 Modeling parameters for the release experiments	167
Table 9 Neural network matrix	173
Table 10 Experimental data sets for neural network prediction	180
Table 11 Neural network prediction compared with the math model result	181

LIST OF FIGURES

	Page
Figure 1 Molecular structure of Cyclopentadecanolide (CPE-215 [®])	2
Figure 2 Number of published research papers on protein/peptide drug delivery every year from 1985 to 2003	4
Figure 3 Fluid Mosaic Model of biological membrane	14
Figure 4 Molecular structure of some common membrane lipids	16
Figure 5 Cholesterol molecules in lipid bilayer	17
Figure 6 Polymorphic phases, molecular shapes, and the critical packing parameter for some membrane lipids	18
Figure 7 Caco-2 and PAMPA	19
Figure 8 Liposome structure (half)	23
Figure 9 Contrast between in-vivo and in-vitro formulation testing	36
Figure 10 Molecular structure of dipalmitoyl phosphatidylcholine (DPPC)	38
Figure 11 The primary structure of human insulin	40
Figure 12 In vitro release protocol design	42
Figure 13 Molecular structure of the fluorescent probe, fluorescein-5-isothiocyanate	44
Figure 14 Aqueous GPC trace of 4.3 mg/ml BSA, eluant 100 mM KCl 10 mM BTP pH 6.5 buffer	46
Figure 15 Aqueous GPC trace of 4 mg/ml tagged BSA, eluant 100 mM KCl 10 mM BTP pH 6.5 buffer	47
Figure 16 Tagged insulin fluorescence calibration and stability data at pH 7 in phosphate buffer	50
Figure 17 Block diagram of the custom-made liposome extruder	52

Figure 18 Custom-made liposome extruder	53
Figure 19 DPPC liposome size distribution measured by Microtrac S3000 after extrusion through a 400 nm polycarbonate membrane filter	54
Figure 20 DSC trace of CPE-215 [®] (exo up)	55
Figure 21 DSC trace of 3:1 (w/w) CPE-215 [®] : Cottonseed oil	57
Figure 22 Effect of centrifugal extraction on the concentration of free Insulin outside of the liposomes	59
Figure 23 Protein release experiment setup	61
Figure 24 Chemical structure of Triton X-100	66
Figure 25 Insulin release from DPPC liposomes at 47 °C at pH 7	68
Figure 26 Insulin release from DPPC liposome at 42 °C at pH 7.4	70
Figure 27 Molecular structure of α -cyclodextrin	73
Figure 28 Molecular model of α -cyclodextrin (left) and CPE-215 [®] (right) in the same scale	74
Figure 29 Insulin release from DPPC liposomes with cyclodextrins at 42 °C at pH 7	77
Figure 30 Insulin release from DPPC liposomes at 42 °C at pH 7 with different ratio of cyclodextrin over CPE-215 [®]	80
Figure 31 Insulin release from DPPC liposomes at 42 °C with β -cyclodextrin at pH 7	82
Figure 32 Insulin release from DPPC/Cholesterol liposomes at 37 °C at pH 7	87
Figure 33 Insulin release at 37 °C from DPPC/Cholesterol liposomes with different amount of CPE-215 [®] /Cottonseed oil at pH 7	91
Figure 34 Insulin release at 37 °C from DPPC/Cholesterol liposomes at different pH gradients, inside pH is 7	95
Figure 35 Insulin release at 37 °C from DPPC/Cholesterol liposome at pH 10	97

Figure 36 Insulin release at 37 °C from DPPC/Cholesterol liposome at pH 4	99
Figure 37 BSA release at 37 °C from DPPC/Cholesterol liposomes at pH 7	101
Figure 38 Insulin diffusion coefficient measurement by pulsed field gradient NMR at pH 3 at 37 °C	105
Figure 39 Schematic representation of the solute concentration distribution in the centrifuge cell in a sedimentation velocity experiment	109
Figure 40 Result of insulin sedimentation velocity experiment of analytical ultracentrifugation at 20 °C	110
Figure 41 Molecular structure of DPPC, Cholesterol and CPE-215 [®]	111
Figure 42 Phosphatidyl Choline lipid bilayer phase transition	112
Figure 43 DSC of Liposome D (DPPC liposome) and Liposome DC (DPPC/CPE-215 [®] liposome) (exothermal up)	119
Figure 44 DSC of Liposome DH (DPPC/Cholesterol liposome) and DPPC/Cholesterol/CPE liposome (exothermal up)	120
Figure 45 DSC of 2:1 (w/w) CPE-215 [®] : cottonseed oil (exothermal up)	124
Figure 46 Four heating cycles of Liposome D (DPPC liposome) (exothermal up)	125
Figure 47 25 heating cycles of Liposome D (DPPC liposome) with CPE-215 [®] /cottonseed oil mixture	126
Figure 48 Change of phase transition temperature of Liposome D with the number of heating cycles	128
Figure 49 Eight heating cycles of DPPC/Cholesterol liposome with CPE-215 [®] /cottonseed oil mixture (exothermal up)	129
Figure 50 Change of phase transition temperature of Liposome DH with number of heating cycles	130
Figure 51 Change of phase transition ΔH of DPPC in Liposome D (DPPC liposome) with CPE-215 [®] insertion	132

Figure 52 The interaction modes between protein and lipid bilayer membrane	134
Figure 53 The fluorescence signal of the supernatant was measured after each centrifugal extraction for 8 times	138
Figure 54 The VP-ITC raw data of two liposome sample titrations and one control run (endo up)	143
Figure 55 VP-ITC heat data after auto baseline integration, normalized on insulin concentration (0.86 mM)	145
Figure 56 VP-ITC heat data after the sample runs subtracted the control run point by point	146
Figure 57 Simple schematic representation of the solute concentration change while crossing a lipid bilayer membrane according to the solubility-diffusion model	148
Figure 58 Insulin dimer surface property region distribution	154
Figure 59 Insulin release from a DPPC/Cholesterol liposome at 37 °C	155
Figure 60 Scheme of Immediate Impact theory	157
Figure 61 Insulin release at 37°C from different liposomes	160
Figure 62 Close-up of Figure 60 at early times	161
Figure 63 Modeling curves and the experimental release data of the "CPE215" sample in Chapter 3.2.2	166
Figure 64 A simple artificial neuron in Neural Network	169
Figure 65 An example of a fully connected feed-forward network	170
Figure 66 Activation (output) of Neuron j , A_j .	171
Figure 67 The actual vs. forecast for the neural network for predicting a	175
Figure 68 Input importance for each parameter in the network for predicting a	175
Figure 69 The actual vs. forecast (scatter plot) for the neural network for predicting c	177

Figure 70 Input importance for each parameter in the network for predicting c	177
Figure 71 The actual vs. forecast (scatter plot) for the neural network for predicting t^*	179
Figure 72 Input importance for each parameter in the network for predicting t^*	179
Figure 73 Neural network forecast for “CSO+B-CD” sample in Chapter 3.4.1	182
Figure 74 Neural network forecast for “C&C+B-CD” sample in Chapter 3.5.1	183

ABSTRACT

STUDY OF THE ENHANCEMENT EFFECT OF CYCLOPENTADECANOLIDE ON PROTEIN PERMEATION THROUGH LIPID MEMBRANES

By

Zhengmao Li

University of New Hampshire, September 2004

Intranasal drug delivery has been a topic of increasing interest for a decade as a convenient and reliable method for the systemic administration of drugs. The low bioavailability of simple formulation of protein drugs, such as insulin, can be greatly improved by using permeation enhancers. We studied the effect of cyclopentadecanolide (CPE-215[®]) as a permeation enhancer in protein release through lipid bilayer membranes. We successfully designed a novel in-vitro membrane permeability model using liposomes and performed a series of transmembrane protein release experiments. These were carried out under a wide range of conditions in the presence of different permeation enhancer combinations. The experimental results showed that CPE-215[®] is an effective membrane permeation enhancer for proteins and a phase transfer agent, for example, cyclodextrins, can further enhance the effect of CPE-215[®].

Besides the release experiments, studies on insulin solution properties (self-diffusion and self-association states), the interaction between insulin and

liposome and the interaction between CPE-215[®] and liposomes were carried out. Based on the mechanistic study and release data, we hypothesized that CPE-215[®] can form transient “pores” in the lipid bilayer that dissolve when CPE-215[®] distributes homogeneously within the bilayer and restore the barrier function of the lipid bilayer. We performed several experiments that corroborate our hypothesis.

A mathematical model was developed based on our hypothesized release mechanism. A semi-empirical nonlinear equation involving four parameters effectively fits the protein release profiles. The quality of the data fit with this model is good supporting evidence for the validity of our mechanistic model. Finally we used a neural network approach to correlate the different release condition parameters and the four semi-empirical fitting parameters based on our limited data sets. Reasonable neural networks were formed for the three major parameters of the mathematical model and provided acceptable prediction results.

CHAPTER 1

INTRODUCTION

Since our research is related to the mucosal delivery of protein/peptide drugs, an overview of protein/peptide drug delivery is given at the beginning of this chapter, then the topic is narrowed down to our research – protein transport through natural membranes with permeation enhancers. Structure and major components of natural membranes, and different in vitro membrane permeability models (Caco-2, PAMPA, and liposomes) are discussed. Since liposomes were selected as our in vitro membrane model, detailed preparation and purification methods for different kinds of liposomes are presented.

1.1. Objective of Thesis

Cyclopentadecanolide (Figure 1), trademarked as CPE-215[®] is one permeation enhancer with proprietary ownership to Bentley Pharmaceuticals, Inc. Bentley Pharmaceuticals, Inc is using CPE-215[®] to help protein, peptide, and low molecular weight therapeutic drugs transport through natural membranes for delivery to the blood stream. This thesis aims to understand the process behind the permeation effect of CPE-215[®]. Pharmaceutical formulations are always challenged with a need for appropriate animal or human tests. These tests are

typically costly and time consuming, and reproducibility is always difficult. To effectively develop formulations, it is advantageous to construct *in vitro* tests to optimize formulations, before *in vivo* testing. The goal of this thesis is to establish an *in vitro* membrane model for protein transmembrane transport, to understand the release mechanism of CPE-215[®], and to test intranasal formulations.

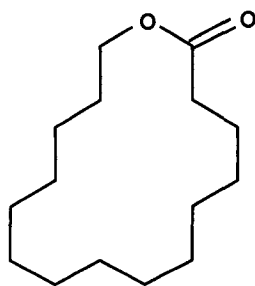


Figure 1 Molecular structure of Cyclopentadecanolide (CPE-215[®]).

1.2. Protein/Peptide Drug Delivery

1.2.1. Proteins and peptides as pharmaceuticals

The use of peptides and proteins for systemic treatment of certain diseases is now well accepted in medical practice. Peptide/protein drugs are increasingly becoming a very important class of therapeutic agents as a result of our gaining more understanding of their role in physiology and pathology as well as the rapid advances in the field of biotechnology and genetic engineering.

Many of these peptides are endogenous molecules that play an important role in maintaining organ function and metabolic homeostasis.

Peptide and protein pharmaceuticals are different than conventional low molecular weight drugs; they are structurally more challenging and complicated; they are often unstable, have large molecular weights and have charges on the outer surface. The last two properties lead to poor permeability through biological membranes and consequently peptides and protein material are difficult to administer except by injection.¹

1.2.2. Protein/Peptide Delivery-- A Booming Research Area

There is presently an urgent need to find new ways to deliver peptides and protein drugs and to control their absorption and distribution in the body. In an editorial in 1998, Rakesh Jain² stated that the delivery of therapeutics can be considered as the next frontier of molecular medicine research. He commented that extraordinary advances in molecular biology and biotechnology have helped identify novel targets and develop a vast array of therapeutic agents. However, (in his view), our understanding of the delivery of therapeutic agents has lagged behind.

In the past, when developing new products, drug delivery scientists have often employed delivery strategies to enhance a property, such as the controlled release of the therapeutic agent. However, for the case of peptides and proteins, drug delivery systems must play a more critical role in enabling a viable product. In doing so, a detailed knowledge of the properties of the compound needs to be

integrated with delivery technology and the relevant aspects of patho/physiology and biology.

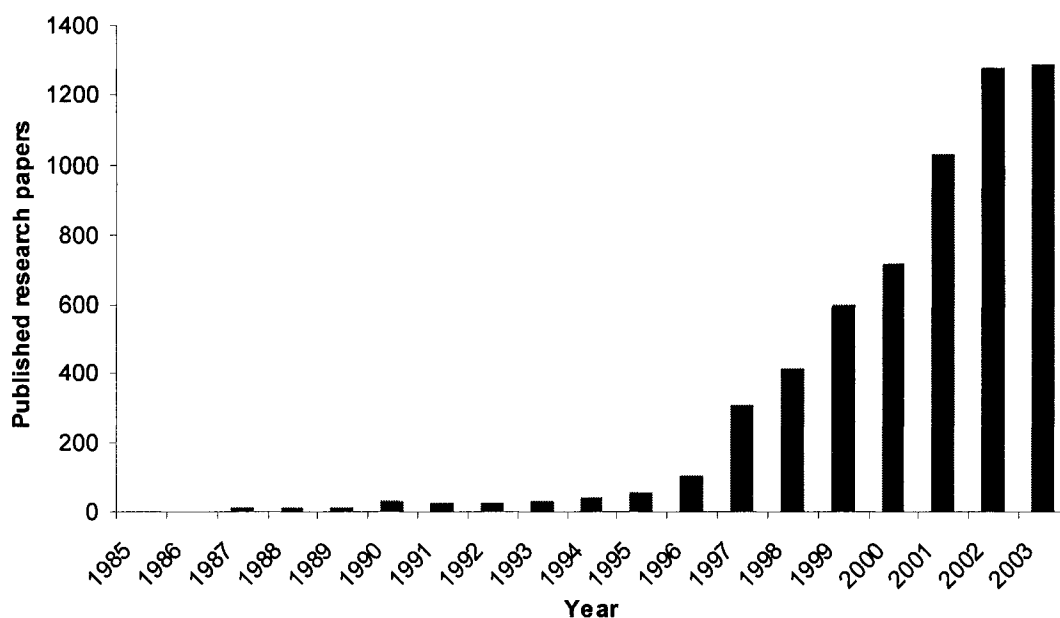


Figure 2 Number of published research papers (journal, letter and patent only) on protein/peptide drug delivery every year from 1985 to 2003.

Usually the number of publications on a research topic shows the magnitude of people's interest in the topic. A publication search on protein/peptide drug delivery using SciFinder Scholar in early 2004, shows that this is really a booming research area. Figure 2 highlights the number of published research papers (journal, letter and patent only) on protein/peptide drug delivery every year from 1985 to 2003. Researchers' interest in protein/peptide drug delivery started in the mid 1980s; for the first decade, there

was a steady and slow increase in the number of publications. However, after the mid 1990s, the number of yearly publications increased drastically, from around 50 a year in 1995 to almost 1300 a year in 2003. There are several key academic researchers in this booming field, such as Dr. Robert Langer (MIT), Dr. Nicholas Peppas (U Texas), Dr. Francis Szoka (UCSF), Dr. William Pardridge (UCLA), Dr. Jacobus Verhoef (Leiden U, Netherlands), Dr. Andreas Bernkop-Schnurch (U Vienna, Austria), Dr. Allan Hoffman (U Washington), and Dr. Lisbeth Illum (U Nottingham, UK), to cite only the most published principal investigators.

1.2.3. Delivery Routes

The choice of delivery routes for drugs is wide (parenteral,³ oral,^{4,5} pulmonary,^{6,7} intranasal,^{8,9} transdermal,^{10,11} buccal,^{12,13} ocular,^{14,15} rectal,¹⁶ vaginal,¹⁷ etc.). The clinical application, drug properties, patient convenience, and required “performance” (e.g. bioavailability), are all key selection factors. The next sections (1.2.3.1 to 1.2.3.6) are an overview of these delivery routes, recent development and their pros and cons.

1.2.3.1. Injectable Systems

Injections are inevitably associated with some degree of pain, irrespective of their route of delivery, whether intramuscular, intravenous, or subcutaneous. The inherent advantages of injectable systems need to be weighed against their disadvantages.

Currently, proteins and peptides are mostly delivered by parenteral administration. Because they are extremely short-acting, repeated injections are often required. Parenteral delivery can be used to target compounds to specific sites (via blood or lymphatic systems), as well as to provide precise pharmacokinetic and pharmacodynamic profiles. Exciting developments have shown how formulation technologies can be used to provide improved parenteral delivery (e.g. nanoparticles, liposomes, PEGylation).^{18,19} Engineering based systems, such as insulin pumps and injection pen systems (for insulin and human growth hormone), have gained considerable success in the market. Needleless injection systems currently under development should have better patient acceptance.²⁰ These include systems employing liquid or powder technologies.

Polymer implants and microspheres based on polylactide-coglycolide (PLGA) have been very successful clinically.²¹ Flamel Technologies developed a self-assembled poly-aminoacid nanoparticles system for parenteral delivery of proteins. However, polymer microspheres are not without problems in terms of loading, drug stability and release profiles. Processing, particularly sterilization, remains an issue. New implant systems based on alternative concepts are currently under investigation including an implantable titanium device.²²

1.2.3.2. Oral Delivery

Oral delivery is the most preferred method for the introduction of therapeutic agents. In 2002, oral delivery technologies accounted for 39% (\$14

billion) of the world market (\$38 billion).²³ This field has been the subject of many peptide and protein delivery attempts, particularly with insulin; but, as yet, few oral polypeptide products have reached the market.

Peptides and proteins are inherently unstable in the harsh conditions of the gastrointestinal tract (pH, enzymes, adsorption to solids); but, even if instability can be avoided, good absorption is not guaranteed. The work of Drew et al. on octreotide is instructive.²⁴ Octreotide is a cyclic polypeptide (a somatostatin analogue) that is very stable even in the small intestines. When orally given to human as a simple solution, the bioavailability is 0.6%. This can increase to 3.3% by using a non-ionic surfactant (polyoxyethylene 24-cholesterol ether). Therefore, for oral administration, it is important to be realistic about potential product performance. If stability is an issue, then enteric coating and enzyme inhibitors can be used.²⁵ Absorption can be improved by selecting a permeation enhancer that can improve transcellular or paracellular transport. Also of importance is the selection of a preferential absorption site. The small intestine and large intestine have both advantages and disadvantages. Therefore, before developing a delivery strategy, it can be important to evaluate the absorption of a candidate biopharmaceutical. Today it is possible to deliver drugs into different regions of the human gastrointestinal tract using “smart” capsules.²⁶ This avoids the highly invasive method of intubation.

Various methods to increase the absorption of challenging molecules from the gastrointestinal tract have been tried. These include permeation enhancers such as surfactants, chitosan (and derivatives thereof), chelating agents, as well

as carriers and complexation systems.²⁷ Some of these strategies use known pharmaceutical excipients (GRAS (Generally Recognized As Safe) status) which can alter cell permeability, usually by modification of the paracellular pathway. Non-covalent complexation strategies have also been reported.²⁸ The modification of peptides and proteins chemically by lipidization or the attachment of hydrophilic and hydrophobic polymeric functions has also been described.^{29,30} Clearly, such modifications result in a new chemical entity and the associated regulatory issues. The covalent attachment of moieties that permit the biopharmaceutical to exploit biological transporters is also an active area of research.^{31,32} Here again, there is the disadvantage of covalent chemistry, but these approaches could offer exciting opportunities in the exploitation of natural pathways. A recent report by Morris et al. could open up new approaches.³³ They found that a 21 residue peptide that had hydrophilic and hydrophobic regions forms stable non-covalent complexes with peptides and proteins. They were able to use this system to deliver a model protein into various cell lines. The system was claimed to have low toxicity but as yet, no in vivo data have been reported.

Alternatively, one may use nanoparticles for the delivery of peptide and protein drugs into the systemic circulation from the gastrointestinal tract. It is well known that certain specialized cells (M-cells) in the gastrointestinal tract can take up and transport particles.³⁴ The size and surface properties of the particles are key factors. This process is important for the development of oral vaccine systems. However, the quantities of material transported are low, even with systems with specific surface markers that provide enhanced interaction between

particles and cells. Some clinical phase II trials suggested that particle uptake resulted in less than 0.1% of the administered dose being sequestered.³⁵ This could be sufficient for a beneficial immune response when developing an oral vaccine but will surely be of no benefit for the oral delivery of peptides.

1.2.3.3. Pulmonary Delivery

Patton has claimed that the lung is a logical target for non-invasive drug delivery.³⁶ It should provide rapid onset of action and a variety of delivery devices (Metered Dose Inhalers (MDI), Dry Powder Inhalers (DPI), nebulizers). Good absorption, even of polar drugs, can be achieved, if the drug is delivered to the deep lung. Good patient compliance is to be expected provided that the device and delivery system are properly engineered. Similarly, good reliability should also be attainable. Understandably, insulin has been the molecule of choice and a number of different companies are pursuing novel pulmonary delivery systems using liquid and powder systems. Reported bioavailabilities, versus s.c. (subcutaneous) injection, range from 10-20% and reliability would appear to be as good as or better than for injectable insulin (s.c.). Various products are now in Phase II/Phase III clinical evaluation and the results look to be encouraging. However, some concerns over safety (lung function, cough) and increased antibody levels have been raised recently, but it is likely that inhaled products for insulin (and other therapeutic peptides) will reach the market soon. One great advantage of the lung is that it is possible to obtain reasonable absorption (i.e. 50% of the dose delivered) across the mucosal surfaces of the deep lung-

alveolar region using simple formulations. Long term effect of pulmonary delivery has yet to be investigated.

1.2.3.4. Nasal Delivery

The nose is an alternative part of the respiratory system that can be exploited for the delivery of therapeutic peptides and proteins. Nasal products for peptide delivery are on the market, but with low bioavailability.³⁷ Nasal delivery can provide rapid onset of action and good deposition can be achieved readily for both liquid and powder systems. However, using simple formulations, the absorption of biopharmaceuticals from the nose of animal models and human is less than 1%. Therefore, in order to improve reliability and to address cost of goods issues, absorption enhancers may be required. Various materials have been studied over the years. While many are effective, most are associated with problems of irritation and regulatory acceptance.³⁸ Often an increase in absorption (e.g. bioavailability) is associated with a direct effect of membrane damage. However, some materials such as certain phospholipids can provide good absorption with low toxicity; the polysaccharide material chitosan was found to provide increased drug absorption with no evidence of toxic manifestations.³⁹

The nasal route also provides a unique delivery opportunity. The olfactory region of the nose can be exploited to provide direct delivery of drugs into the brain.⁴⁰ Recent studies by Frey et al. have demonstrated that polypeptide materials such as nerve growth factor can reach the CSF and brain tissues.⁴¹ In addition, exciting clinical studies by Fehm and Born⁴² have demonstrated that

materials such as arginine vasopressin, angiotensin II, and insulin can be transported from nose to brain in humans, in low quantities. This could be a novel way to avoid the blood-brain barrier and to provide a novel means of access to the brain.

1.2.3.5. Buccal Delivery

The mouth has been examined as a delivery route for biopharmaceuticals by various groups using animal models and also in humans. The pivotal clinical studies of de Groot and colleagues using sublingual oxytocin suggest a low bioavailability of less than 1%.⁴³ Therefore, the results recently reported on the buccal administration of insulin using a spray device (MDI) are both surprising and potentially exciting. Reported clinical studies in diabetic subjects have demonstrated good efficacy with bioavailabilities in the range of 5-10%.⁴⁴

1.2.3.6. Transdermal Delivery

The transdermal delivery of polypeptides has been evaluated by many groups, but the results so far are not encouraging.⁴⁵ Good results in animal models do not translate well to human (usually because the chosen animal model has little relevance to the human skin). The skin of human provides a good barrier. Novel approaches to “driving” polypeptides across the skin, such as iontophoresis and ultrasound, have been explored but clinical results have been disappointing.^{46,47} Insulin is an interesting case where physiological pH is a

problem when considering iontophoresis. The charge on the molecule changes with pH gradient across the skin. Under electrophoresis, the molecule can be forced into the skin; but, as the pH changes from the skin surface to tissue, the charge on the molecule reverses and the molecule is forced to back out!

A novel transdermal system using “transferosomes” (ultraflexible liposomes with low pore resistance) has been proposed by Cevc.⁴⁸ It is claimed that the system can transport therapeutic amounts of insulin across intact mammalian skin but detailed clinical results are awaited. Alternative engineering approaches, such as microneedles produced by photolithography, could well provide a more reliable transdermal system.⁴⁹

1.3. Membrane Permeation Enhancers

To minimize the health hazard of repeated injection, there is a need to search for another systemic delivery route as a non-invasive alternative to injection. Mucosal delivery routes, such as pulmonary, intranasal and oral routes, will deliver the drugs through the mucosa and reach the general blood circulation via numerous capillary vessels present underneath the mucosa.

In mucosal delivery, therapeutic agents need to go through mucous membranes first; but mucous membranes are not designed to let foreign subjects go through and into the blood system—on the contrary, one of the critical functions of the mucus membranes is the barrier function. Some small and neutral molecules, such as glycerin and vitamins can go through natural membranes easily. But large molecules, for example protein/peptide drugs,

cannot go through mucous membranes and into the blood by themselves, in another words, mucous membranes are not permeable to them. Therefore, improving the bioavailability of the therapeutic agents is the major task for protein/peptide mucosal delivery. In order to go through barrier membranes, protein/peptide drugs need the help of membrane permeation enhancers.

Membrane permeation enhancers are usually small molecules used to interact with the membranes and increase the permeability of membranes. The main concerns with membrane permeation enhancers are safety issues: they can cause irritations and can break the integrity of the membrane. Many molecules have been studied and used as membrane permeation enhancers. Generally speaking, permeation enhancers have experienced three generations.⁵⁰ The first generation is represented by bile salts and surfactants. The second generation is represented by salicylates, enamines, fusidate derivatives, acylcarnitines and phospholipids. Nutrients, hormones and antioxidants form the main force of the third generation of the membrane permeation enhancers. CPE-215[®] may fall in the second generation in this category.

1.4. Membrane Structure

In order to study the permeation property of biological membranes, one must know the structure of the membranes. Despite the variable compositions of biological membranes, the basic structural unit of virtually all biomembranes is the phospholipid bilayer, with embedded proteins (Figure 3). This bilayer is a sheet like structure composed of two layers of phospholipid molecules whose

polar head groups face the surrounding water and whose fatty acyl chains form a continuous hydrophobic interior of 4 nm thick. Each phospholipid layer in this lamellar structure is called a leaflet. The major driving force for the formation of phospholipid bilayers is hydrophobic interaction between the fatty acyl chains of glycolipid and phospholipid molecules. Van der Waals interactions among the hydrocarbon chains favor close packing of these hydrophobic tails. Hydrogen bonding and electrostatic interactions between the polar head groups and water molecules also stabilize the bilayer. Therefore, the membrane has a relatively hydrophilic exterior and a hydrophobic interior.

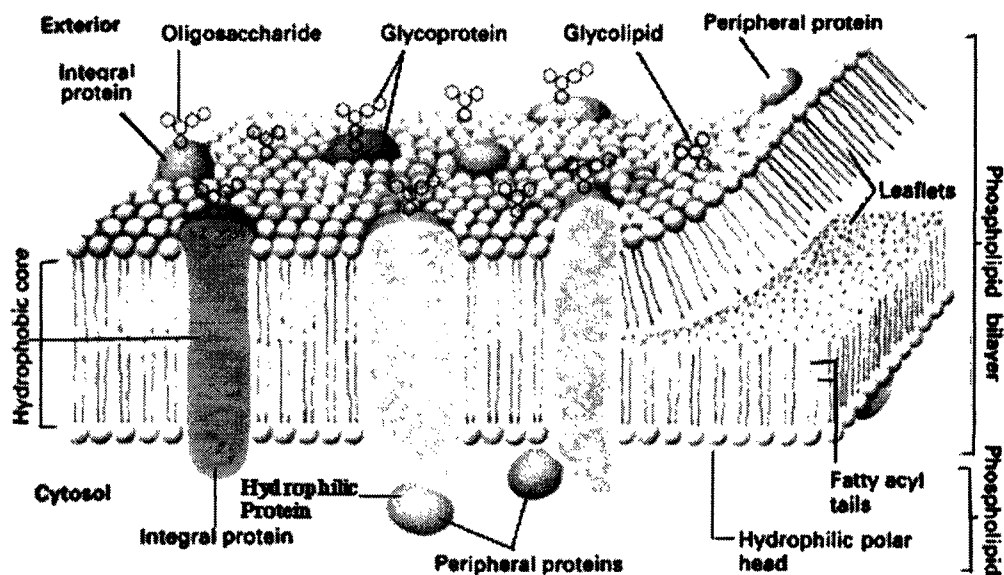


Figure 3 Fluid Mosaic Model of biological membrane.⁵¹

Membrane proteins are embedded in the lipid bilayer. Some may pass through the bilayer as transmembrane proteins. Transmembrane proteins are

amphipathic, which means they have hydrophobic and hydrophilic regions that are oriented in the same regions in the lipid bilayer. Another name for them is “integral proteins”. Other types of proteins may be linked only at the cytoplasmic surface by attachment to a fatty acid chain, or at the external cell surface attached by an oligosaccharide. In other cases, these non-transmembrane proteins may be bound to other membrane proteins. Collectively these are called “peripheral membrane proteins”.

Membrane lipids are numerous and diverse, such as phosphatidylcholine, phosphatidylserine, sphingomyelin, cholesterol, etc. The lipid components of biological membranes in animal cells consist predominantly of phospholipids. The phospholipids have two fatty acyl chains esterified to glycerol and a hydrophilic “head group”. In animal cells phosphatidylcholine (PC) is the major phospholipid.

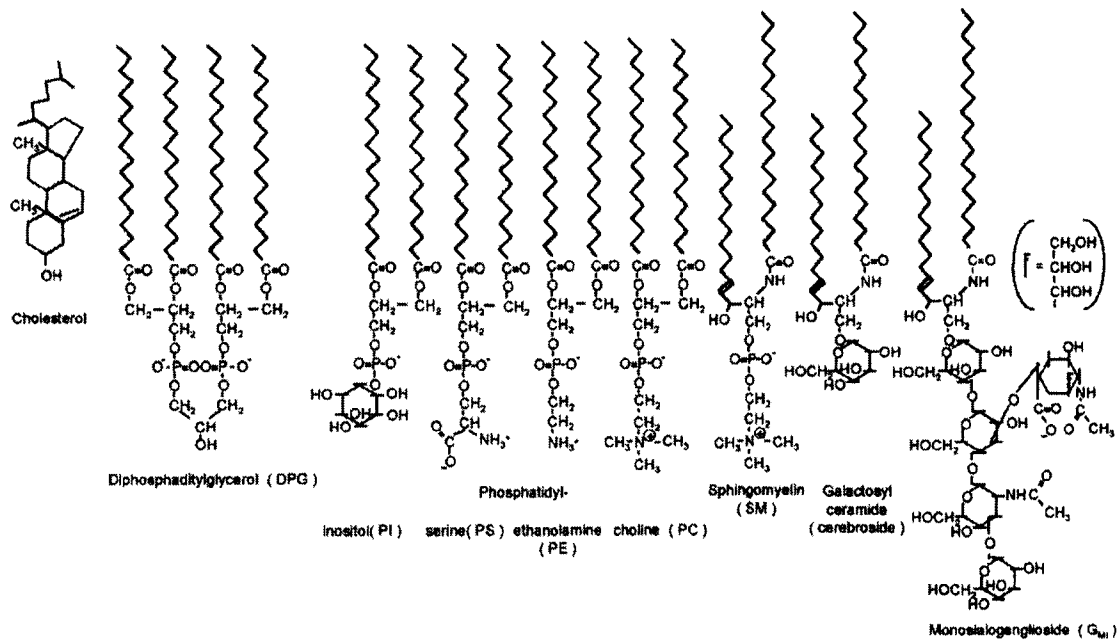


Figure 4 Molecular structure of some common membrane lipids.⁵²

Cholesterol is a particular type of lipid. It is a membrane constituent widely found in biological systems which serves the unique purpose of modulating membrane fluidity, elasticity, and permeability. It literally fills in the gaps created by imperfect packing of other lipid species when proteins are embedded in the membrane. Cholesterol serves much the same purpose in model membranes. The cholesterol molecule inserts itself in the membrane with the same orientation as the phospholipid molecules. Figure 5 shows phospholipid molecules with a cholesterol molecule inserted. Note that the polar head of the cholesterol is aligned with the polar head of the phospholipids.

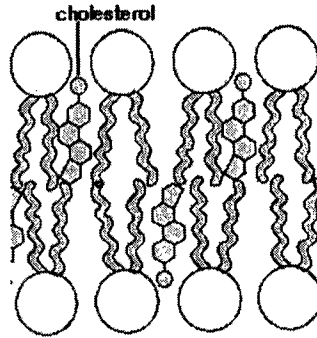


Figure 5 Cholesterol molecules in lipid bilayer.⁴⁹

Different lipids can have different conformations in water when they gather together, and those conformations are usually determined by their molecular shapes (Figure 6). Lipids with a big hydrophilic anionic “head” and a small hydrophobic hydrocarbon “tail”, for example common detergents, have the shape of an inverted cone, and will form micelles in water. Lipids with a hydrophilic “head” and two hydrophobic “tails”, for example most lipids in natural membranes, have a cylindrical shape, and will form lipid bilayers in water. These lipid bilayers are thermodynamically stable.

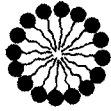

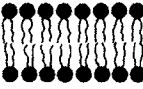

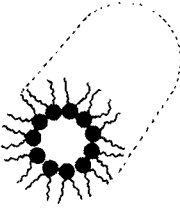

LIPID	PHASE	MOLECULAR SHAPE	CRITICAL PACKING PARAMETER (v/l.s.)
Lysophospholipids Detergents	 Micellar	 Inverted Cone	$< \frac{1}{3}$ (Sphere) $\frac{1}{3}$ to $\frac{1}{2}$ (Globular Shapes; Rods)
Phosphatidylcholine Sphingomyelin Phosphatidylserine Phosphatidylinositol Phosphatidylglycerol Phosphatidic Acid Cardiolipin Digalactosyldiglyceride	 Bilayer	 Cylindrical	$\frac{1}{2}$ to 1
Phosphatidylethanolamine (Unsaturated) Cardiolipin - Ca^{2+} Phosphatidic Acid - Ca^{2+} (pH < 6.0) Phosphatidic Acid (pH < 3.0) Phosphatidylserine (pH < 4.0) Monogalactosyldiglyceride	 Hexagonal (H_{II})	 Cone	> 1

Figure 6 Polymorphic phases, molecular shapes, and the critical packing parameter for some membrane lipids.⁵³

1.5. In Vitro Membrane Permeability Models

It costs pharmaceutical companies hundreds of millions of dollars to test drugs in Phase II & III. This makes a compound that demonstrates low bioavailability during clinical trials unacceptable. To prevent this problem, drug candidates are screened for their absorption potential early in the discovery and development phase, when investment in a compound is low, as a filter to remove poor performers and identify candidates that need to be potentially modified.

Initially, *in silico* methods were favored. But computational models based on molecular properties typically fail when large sets of diverse compounds are analyzed. This is particularly a problem when conformationally flexible compounds are used. Membrane retention is also an important phenomenon. Two compounds can have the same permeability but different membrane retention characteristics. This retention is often misunderstood or neglected, which leads to incorrect membrane permeability estimates and calculations. The failure of physiochemistry-based predictions led to the development of simple assays to evaluate compound absorption. As a result, two permeability assays have become prevalent in the past five years: the Caco-2 cell permeability assay and the parallel artificial membrane permeability assay (PAMPA). These assays have risen to play important roles in industry, and most companies perform at least one of them in their research programs.

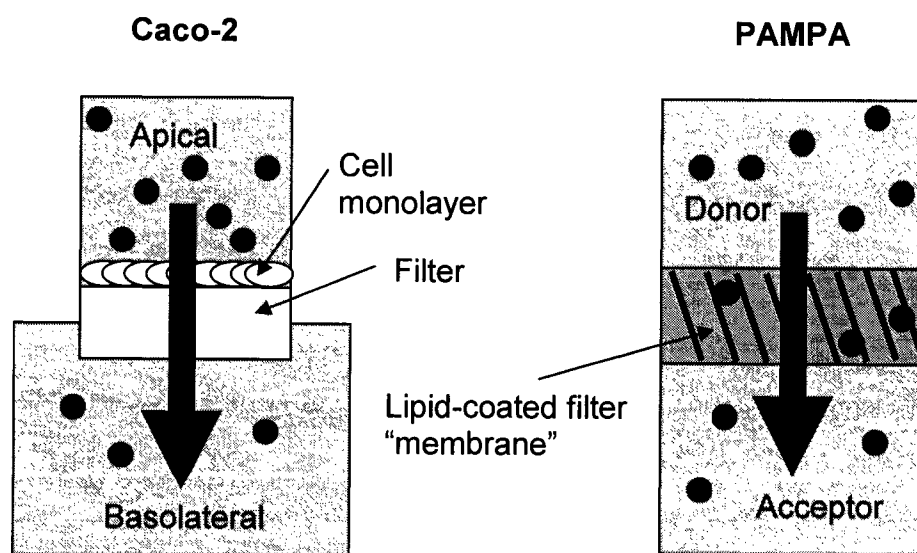


Figure 7 Caco-2 and PAMPA. Caco-2 uses compartments of different volumes separated by a monolayer of cell grown on a filter. PAMPA uses chambers of the same size, separated by a filter coated with lipid in organic solvent.

Liposomes are usually used as model membranes to study the properties of pure lipids and lipid mixtures. In the drug delivery field, they are mostly used as drug delivery carriers. However, we found that they can also be used as membrane permeability models due to their lipid bilayer structure.

1.5.1. Caco-2

First described in the early 1990s, cell permeability studies came to industry from academia, where several groups worked to develop cell-based assays that mimicked the passage of drugs through the intestinal mucosa^{54,55}--- the Caco-2 assay was the result.

In typical experiments, a monolayer of cells is grown on a filter separating two stacked microwell plates. The permeability of compounds through the cells is determined after the introduction of a drug on one side of the filter. The entire process has been automated, and when used in conjunction with LC-MS detection, it enables any compound's permeability to be determined. It is recognized by the FDA as one of the few means to measure permeability as part of the bioequivalence waiver process. Since its introduction, Caco-2 has been championed as a standard for measuring permeability, but it is not without some shortcomings.

Caco-2 experiments require up to 20 days for the preparation of stable monolayers, and the cells must be maintained in protective environments, free from contamination, and examined for tight-junction formation prior to use. The

method requires careful sample analysis to calculate permeability correctly. Interlaboratory variation is a problem because of differences in cell line strains. Caco-2 cells also contain endogenous transporter and efflux systems, the latter of which work against the permeability process and can complicate data interpretation for some compounds. In addition, test compound solubility appears to be a problem in Caco-2 assays because of the assay conditions.

1.5.2. PAMPA

As a less expensive alternative to Caco-2, Manfred Kansy et al. developed PAMPA.⁵⁶ A “PAMPA sandwich” is prepared from two plates that are similar to those used for traditional Caco-2 experiments (Figure 7). One plate contains a porous filter disk at the bottom of each well. The other one is a reservoir plate that is precisely molded to sit under the filter plate so that contact between the two occurs at the filter. The filter is coated with a solution of lipid material in inert organic solvent to prepare the artificial membrane. The wells of one plate are then filled with donor solution (i.e., drug), and the other with acceptor solution (i.e., buffer); the plates are then stacked to create the sandwich and are incubated. The drug concentration in the donor and acceptor wells is then determined by UV or LC-MS methods, and permeability is calculated.⁵⁷ The whole PAMPA process is easily automated and commercially available.

The lipid choice is flexible and often varies by research group, ranging from mixtures that reflect the lipid composition of mammalian cell membranes to

simple synthetic phospholipids.⁵⁸ Some even forgo the lipid altogether and use non-polar organic solvents.⁵⁹

With PAMPA, the emphasis is on simplicity. Because the membrane has no transporters or efflux systems, only passive permeability is observed. And because there is no growth period, the analysis can be set up quickly from standard stock supplies without concern about contamination. This allows PAMPA to be run without restructuring laboratories to create sterile environments, making PAMPA experiments easier, faster, and much less expensive to run than Caco-2 assays.

1.5.3. Liposome

Due to the lack of experience with cell culture and uncertainty with cell lives, we did not use Caco-2 as the membrane permeability model. As to PAMPA, its artificial membrane is a filter coated with a solution of lipid materials in inert organic solvent, which is quite different from the lipid bilayer structure of biological membranes. In that case, PAMPA will not be a good membrane analog for us to study the interaction of our hydrophobic permeation enhancer with biological membranes.

Liposomes have a spherical lipid bilayer structure, which is very similar to the lipid bilayer structure in biological membranes. Since liposomes can encapsulate solutions inside and separate the inside solution from the outside, we found that liposome can be used as a passive membrane permeability model. By encapsulating the drug solution inside of liposomes and detecting the drug

concentration in the outside solution, we can monitor the drug transport across the lipid bilayer.

The research on liposomes is mostly focused on using liposomes as drug delivery carriers,^{60,61} and structural model membranes. However, no one has yet reported using liposomes as passive membrane permeability models before.

More information about liposomes will be introduced in the following section.

1.6. Liposome as an Artificial Membrane Model

The term “liposome” can be defined as any lipid bilayer structure which encloses a volume (Figure 8).^{62,63,64} Many phospholipids, when dispersed in water, spontaneously form a heterogeneous mixture of vesicular structures which contain multiple bilayers forming a series of concentric shells.

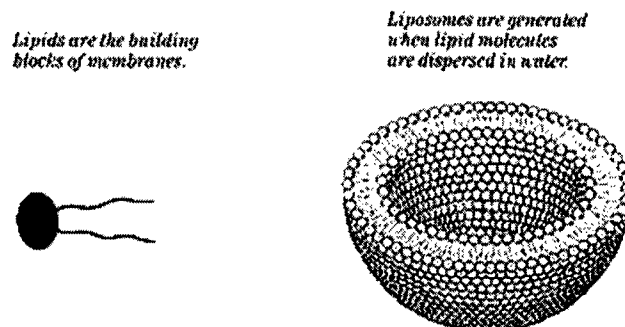


Figure 8 Liposome structure (half).⁶⁵

There are different kinds of liposomes (vesicles): multilamellar vesicles (MLV), large unilamellar vesicles (LUV) and small unilamellar vesicles (SUV, < 100 nm in diameter). Practical applications of liposomes have been explored in three main areas of research, namely in model membrane studies, in controlled and targeted drug delivery in vivo, and in transfer of genetic and other material into cells in culture.

One important property of liposome is its thermal phase transition. The phase transition temperature (T_c) is defined as the temperature required to induce a change in the lipid physical state from the ordered gel phase, where the hydrocarbon chains are fully extended and closely packed at low temperature, to the disordered liquid crystalline phase, where the hydrocarbon chains are randomly oriented and fluid at more elevated temperature. There are several factors which directly affect the phase transition temperature including hydrocarbon length, unsaturation, charge, and headgroup species. As the hydrocarbon length is increased, van der Waals interactions become stronger requiring more energy to disrupt the ordered packing, thus the phase transition temperature increases. Likewise, introducing a double bond into the acyl group puts a kink in the chain which requires much lower temperatures to induce an ordered packing arrangement. This property will be the object of a specific study in Chapter 4.2.

1.6.1. Preparation of Liposomes

When considering the preparative methodology of liposomes, it has to be recognized that different applications require different types of liposomes.

1.6.1.1. Multilamellar Vesicles (MLV)

Multilamellar liposomes were first described by Bangham et al.⁶⁶ The procedure used by them still remains the simplest and the most widely used. This involves the deposition of a thin lipid film from an organic solvent medium on the walls of a container, followed by agitation with an aqueous solution of the material to be encapsulated. Provided the agitation is carried out at temperatures above the characteristic gel-liquid crystal phase transition temperature of the phospholipid and the lipid film is indeed thin, MLV should form spontaneously with little effort. However, the degree of agitation required to form a good dispersion of MLV (without poorly hydrated lipid globules) will depend upon the thickness of the lipid film. With relatively thicker films produced by more concentrated lipid solutions and/or smaller evaporation vessels, more vigorous agitation is required.

The MLV appear to be attractive because of the ease of their preparation and relative stability on storage. However, the disadvantages include low encapsulation efficiency and inconsistency of properties.

1.6.1.2. Large Uni- or Oligolamellar Vesicles

Relatively large liposomes with either one or a few lamellae, as for example the reverse-phase-evaporation vesicles (REV), occupy an intermediate position between the MLV and small unilamellar vesicles (SUV). Some common large unilamellar liposome preparation methods will be briefly introduced below.

1.6.1.2.1. Ether Infusion

Ether infusion techniques^{67,68} can be used to prepare large unilamellar liposomes. The basic principle is the injection of a solution of lipids in ether into an aqueous solution of the material to be encapsulated at a temperature high enough for the rapid evaporation of the solvent. Large molecules such as proteins and DNA have been encapsulated into liposomes using this technique. Although the encapsulation efficiency is very low, relatively large aqueous space volumes have been reported.⁶⁹ Additionally, the size distribution of the liposomes is heterogeneous.

1.6.1.2.2. Calcium-Induced Fusion

This method, developed by Papahadjopoulos et al.⁷⁰ relies on the effect of calcium ions on acidic phospholipids to form initially cochleate cylindrical structures, which are then transformed into large unilamellar vesicles (LUV) by the addition of the chelating agent EDTA. Although the preparative procedure and efficiency of encapsulation are attractive,⁷¹ the presence of calcium ions and the sequestrant during the formation of the liposomes and consequent

contamination of the liposomes with these may be unacceptable. Furthermore, this rather specialized technique is valid only for acidic lipids.

1.6.1.2.3. Reverse-Phase-Evaporation (REV)

This method was introduced by Szoka and Papahadjopoulos⁷² for the preparation of large uni- or oligolamellar liposomes incorporating a variety of drugs and biologically active materials. The efficiency of drug encapsulation, generally around 50%, is very good. The method appears suitable for use with a variety of lipids and lipid mixtures and for the encapsulation of even large macromolecular materials. The aqueous space in these liposomes is 7 to 10 l/mol lipid, which is very high in comparison to MLV and SUV.⁸ Liposomal dispersions prepared in this manner are said to be mixtures of large unilamellar and oligolamellar liposomes with the size and number of lamellae being dependent upon the nature of the lipid mixture, and possibly the exact procedure.^{6,73}

The relatively high encapsulation efficiency for a variety of compounds and the basic principle of going from an emulsion to a liposomal dispersion are very attractive from scale-up and processing considerations. Greater reproducibility of liposome size range and drug encapsulation can be expected due to the absence of the “dry lipid” stage. One of the disadvantages of this method is the need for sonication of the mixture of the lipid solution and the aqueous drug solution to form an “adequate” emulsion. This step would be difficult to operate on a large scale in a reproducible manner. Although Szoka

and Papahadjopoulos⁶ stressed the need for sonication in order to ensure a homogeneous emulsion, and thus a primarily unilamellar liposomal dispersion, other emulsification techniques may be equally effective. Other drawbacks of this procedure include the presence of the organic solvent in contact with the material to be encapsulated and the temperature needed for the evaporation of the solvent under reduced pressure. These conditions may be too severe for peptides and proteins.

1.6.1.2.4. Rapid Extrusion through Polycarbonate Filter

Lipid extrusion is a technique in which a lipid suspension is forced under pressure through polycarbonate filters with defined pore sizes to yield particles with a mean diameter that reflects that of the filter pore.⁷⁴ Prior to extrusion through the final pore size, LMV suspensions are disrupted either by several freeze-thaw cycles or by prefiltering the suspension through a larger pore size. This method helps prevent the membranes from fouling and improves the homogeneity of the size distribution of the final suspension. As with all procedures for downsizing LMV dispersions, the extrusion should be done at a temperature above the T_c of the lipid. Attempts to extrude below the T_c will be unsuccessful as the membrane has a tendency to foul with rigid membranes which cannot pass through the pores.

Preparing liposomes by extrusion allows the size of the liposomes to be specified by selecting a polycarbonate membrane filters with a specific pore size.

Mean particle size is quite reproducible from batch to batch. Liposomes made from extrusion process usually have narrow size distributions.

1.6.1.3. Small Unilamellar Liposomes (SUV)

Small unilamellar liposomes (SUV) are of great interest in drug delivery because of their potential for controlled drug release in the blood stream and for targeting to non-reticuloendothelial cells and tissues. The slow clearance of SUV from circulation after i.v. administration⁷⁵ offers these possibilities. SUV also have a potential for fusion with target cell membranes. Methods for the preparation of SUV are examined in the following sections.

1.6.1.3.1. Sonication

The most widely used procedure for the preparation of SUV consists of sonicating MLV using either a probe or a sonication bath.^{76,77} Electron microscopic techniques are used to visualize the unilamellar structure and to estimate the size, typically about 50 nm as the mean diameter. In general, adequate ultrasonic treatment leads to a homogeneous preparation in terms of size. One of the consequences of the small size of the SUV is the limited aqueous space inside the liposomes and the low encapsulation efficiency.⁹ Application of ultrasonic energy as a means of converting MLV to SUV is unlikely to be a reliable and consistent operation in large-scale manufacture.

1.6.1.3.2. Ethanol Injection

This procedure, introduced by Batzri and Korn,⁷⁸ is reported to produce relatively small unilamellar liposomes. Although this technique is, in principle, similar to the ether injection method,³ the size and degree of heterogeneity of the liposomes are dependent upon the concentration of the lipids and the relative volumes of the alcoholic and the aqueous phases. The basic procedure is amenable to scale-up and needs to be examined further. Two major drawbacks of this method are the low drug encapsulation levels and the yield of liposomes as a very dilute dispersion at the end of the process. An additional concentration step is required to produce an adequate liposomal dispersion.

1.6.1.3.3. Detergent Dialysis

The detergent dialysis procedure was developed by Milsmann et al.⁷⁹ In this method, mixed micelles are first formed by dispersing a phospholipid and a surfactant in an aqueous solution of the material to be encapsulated. This dispersion of mixed micelles is then dialyzed extensively, when the surfactant is gradually removed and the phospholipid assumes a unilamellar liposome structure. Homogeneous dispersions of SUV are formed by this technique. An additional advantage is the absence of an evaporation step and elevated temperatures. This allows encapsulation of labile materials under mild conditions.

The degree of encapsulation is, however, very low because of the loss of material during dialysis (while the liposomes are being formed), except in the case of encapsulation of macromolecular compounds. Another disadvantage of

this method is the presence of considerable amounts of residual surfactant in the final liposomal dispersion at the end of dialysis.

1.6.1.3.4. Reverse Micelle Method

The reverse micelle method was described in a patent by the Battelle Memorial Institute.⁸⁰ In this method, a small quantity of an aqueous solution of the material to be encapsulated is initially dispersed in a volatile organic solvent containing the lipid mixture. The inverted micellar dispersion is then redispersed in an aqueous buffer medium to form a water-in-oil-in-water type emulsion. Upon evaporation of the solvent under reduced pressure or by means of a stream of nitrogen, unilamellar liposomes are obtained.

Very high degrees of drug encapsulation, in terms of the encapsulated drug as a percentage of the total drug used, are claimed. However, it should be pointed out that the drug solution only forms the interior aqueous phase of the emulsion. Consequently, the final liposomal dispersion is dilute with respect to the encapsulated drug, although the apparent degree of encapsulation is high. This technique has potential for large-scale application and should be explored further.

1.6.2. Removal of Unbound Drug

When lipophilic drugs of appropriate structure are associated with liposomes by inclusion in the bilayer phase, the degree of "encapsulation" is

dependent upon the saturation of the lipid phase. Under these circumstances, it is possible to achieve degrees of encapsulation of over 90%, making it unnecessary to remove the unbound drug. However, in the case of water-soluble drugs, the encapsulated drug is only a fraction of the total drug used. An additional process step is required to remove the unbound drug from the drug-loaded liposomes in dispersion. Dialysis, centrifugation, and gel filtration have been used for this purpose.

1.6.2.1. Dialysis

Dialysis is probably the simplest and most widely used procedure for the removal of the unbound drug, except when macromolecular compounds are involved.⁸¹ It is a technique requiring no complicated or expensive equipment and is capable of being scaled up. Dialysis is effective in removing nearly the entire free drugs with a sufficient number of changes of the dialyzing medium. Dialysis is, however, a slow process. Typically, removal of over 95% of the free drug in a liposomal dispersion might require a minimum of 3 changes of the external medium over 10 to 24 hr at room temperature. Additionally, the volume of the liposomal dispersion will alter during dialysis, unless care is taken to balance the osmotic strengths of the liposomal dispersion and the dialyzing medium. It is also possible that the presence of the external dialyzing medium in equilibrium with the liposomal dispersion might induce leakage of the encapsulated drug.

1.6.2.2. Centrifugation

Centrifugation at various g values is an effective means of isolating various kinds of liposomes from the free drug in the suspending medium.⁸² Two or more resuspension and centrifugation steps are usually included to effect a complete removal of the free drug. The centrifugal force required to pull liposomes down into a pellet is dependent upon the size of the liposomes, and to a certain extent, on the flocculation state of the dispersion. The lowest speed possible to achieve pelleting is best since higher speeds could induce deformation and/or fusion of liposomes. High g values and conditions of refrigeration are required for liposomes in the small to medium size ranges.

Clearly, the use of refrigerated centrifuges operating at high speeds with large volumes of liposomal dispersions is energy intensive and expensive, when feasible. Therefore, this method may not be suitable for the isolation of small liposomes. For relatively large liposomes, low speed centrifugation offers the advantages of a short time scale of operation and an opportunity to concentrate or dilute the original dispersion to the required extent. It is essential to ensure that the osmotic strength of the resuspending medium is matched with that of original liposomal dispersion in order to avoid osmotic shock and rupture of liposomes.

1.6.2.3. Gel Filtration

Gel permeation chromatographic technique is used extensively both to separate liposomes from unbound drug and also to fractionate heterogeneous

liposomal dispersions.⁸³ The technique is very effective and rapid at the laboratory level. Although gel filtration is used in the purification of biological materials such as insulin on a large scale, the technique is difficult and expensive. Additionally, dilution of the liposomal dispersion with the eluting medium may necessitate another concentration step. Much remains to be established in regard to recovery levels and lipid losses on the column materials.

Centrifugation is the fastest way to remove unbound drugs from liposomes among the three; it works fine with large liposomes, but not very well with small liposomes (<100 nm). Dialysis takes longer time, but it is easier and cheaper than gel filtration. Gel filtration is a universal method to remove unbound drugs from liposomes, but it involves gel column packing and may dilute the liposome suspension after the process.

CHAPTER 2

METHODOLOGY

In this chapter, the focus is on the design and development of a novel and valid *in vitro* membrane release model for protein/peptide drugs. We selected the kind of lipid that would be used to prepare liposomes and the model proteins, and determined the protocol for the release experiments. Then improvements on the liposome preparation, protein detection, and release experiment procedure are discussed.

2.1. Release Concept “In Vivo” Vs. “In Vitro”

In a conventional intranasal drug delivery configuration, the peptide drug and the permeation enhancer are formulated together to achieve delivery across the natural membrane. In our model, we encapsulate the peptide inside the liposome, and use the formulated permeation enhancer to “free” the peptide from the liposome. This simple permutation of location is illustrated in Figure 9.

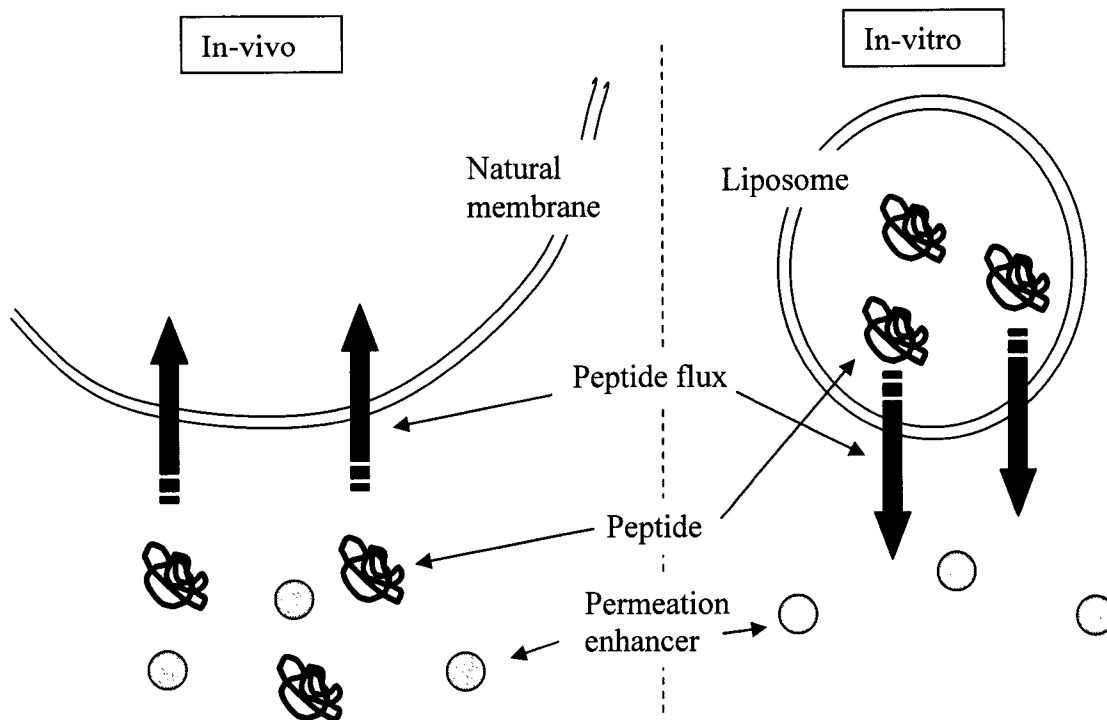


Figure 9 Contrast between in vivo and in vitro formulation testing.

Indeed, our liposome model differs from the mechanism of in vivo intranasal delivery. In in vivo intranasal delivery, the peptide drug is in the vicinity of the permeation enhancer and diffuses into the biological membrane. In the present liposome model, the peptide is encapsulated inside the liposome, while the permeation enhancer is added outside. The outside peptide concentration is measured to quantify the permeation enhancing effect. In both instances the peptide is required to travel across the membrane. In both situations, the “assistance” of the permeation enhancer is necessary to achieve faster release (or permeation) rates. If the peptide release is faster with the addition of a specific formulation of permeation enhancers, then we know this formulation can effectively interact with the loaded liposome to let the peptide cross through the

bilayer. The methodology needed to test the efficiency of a permeation enhancer formulation is less complex and expensive compared to an in vivo test.

2.2. In Vitro Release Protocol Design

The concept is to encapsulate the protein/peptide drugs inside liposomes, separate the liposomes from the unencapsulated drugs, then add the permeation enhancer outside of the liposomes and monitor how fast the encapsulated drugs can release out of the liposomes. In the following sections, the choice of liposome lipid, protein and release probes will be discussed.

2.2.1 Liposome

In order to make full use of the lipid, obviously unilamellar liposomes are more desirable than multilamellar liposomes. During the liposome encapsulation process of an aqueous solution of drugs, lipids form spherical lipid bilayers and encapsulate part of the solution inside; after the formation of the liposomes, the concentrations of the aqueous solutions inside and outside of liposomes are the same. To increase the liposome encapsulation efficiency, or to encapsulate the maximum amount of solution with a given amount of lipids, one must answer the question of how to occupy the maximum total volume with the same total surface area. The answer to this question is to make one giant unilamellar liposome, but there is no practical value to make a liposome that big. The practical way to get high encapsulation efficiency is to make narrow size distribution of large

unilamellar liposomes, instead of small unilamellar liposomes. What size of unilamellar liposome is appropriate? Due to the structural strength of the lipid bilayer sphere, it is hard to make large unilamellar liposomes even at the micron scale. We think unilamellar liposomes with 400 nm in diameter should be both large enough to reach high encapsulation efficiency, and strong enough to maintain their shape. Considering the thickness of unilamellar lipid bilayer is about 5 nm,⁸⁴ selecting 400 nm as liposome diameter can also reduce the curvature effect on the permeation study.

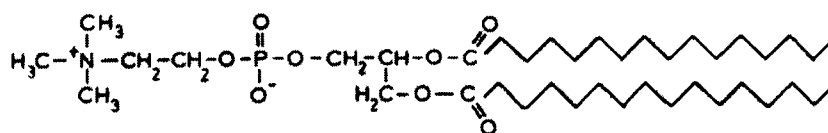


Figure 10 Molecular structure of dipalmitoyl phosphatidylcholine (DPPC).

At first we used only one phospholipid, dipalmitoyl phosphatidylcholine (DPPC), to prepare the simplest liposome model. Figure 10 shows the molecular structure of DPPC. DPPC was selected because of its popular usage in liposome related research and its high concentration and occurrence in natural membranes.

As seen before, cholesterol is a membrane constituent widely found in animal systems, which serves a unique purpose of modulating membrane fluidity, elasticity, and permeability. It literally fills in the gaps created by imperfect packing of other lipid species when proteins are embedded in the membrane. In

order to make our liposome model a better analog of natural membrane, later we made 4:1 (w/w) DPPC: Cholesterol liposomes for the release study.

The total inner aqueous volume ratio V , (liters per 1.0 liter of liposome suspension) of the unilamellar liposomes can be determined by the following equations. The total number of lipid molecules N_p was expressed as the function of the initial concentration of the lipid, C (mole·liter⁻¹),

$$N_p = N_0 \cdot C, \quad [2.1]$$

where N_0 was Avogadro's number. N_1 , the number of lipid molecules composing one unilamellar liposome with radius r (Å), was expressed as

$$N_1 = 4\pi(r^2 + (r - d)^2) / S, \quad [2.2]$$

where S and d were the average surface area per lipid molecule in square angstroms and the thickness of the bilayer membrane in angstrom, respectively. N , the number of liposomes with radius r in the solution containing C (mole·liter⁻¹) lipids, was therefore expressed as

$$N = \frac{N_p}{N_1} = \frac{N_0 \cdot C \cdot S}{4\pi(r^2 + (r - d)^2)}. \quad [2.3]$$

The total inner aqueous volume (V) was defined as

$$V = N \cdot \frac{4}{3} \pi (r - d)^3 \times 10^{-27} \quad [2.4]$$

In the case of 400 nm unilamellar DPPC liposomes, where $C = 3.4 \times 10^{-3}$ mole·liter⁻¹ (=0.25 wt%), $r = 2000$ Å, $S = 58$ Å², and $d = 37$ Å,^{85,86} the total inner volume was calculated to be 3.8×10^{-2} (liter per 1.0 liter of liposome suspension), i.e., 3.8% by volume.

2.2.2 Model Proteins

This project focuses on quantifying the permeation of proteins/peptides through membranes and characterizing the enhancement effect of CPE-215[®]. Insulin (Figure 11) was selected as the protein model for this study because it is one of the least expensive low molecular weight small proteins available, and also because it is one of Bentley's target drugs.

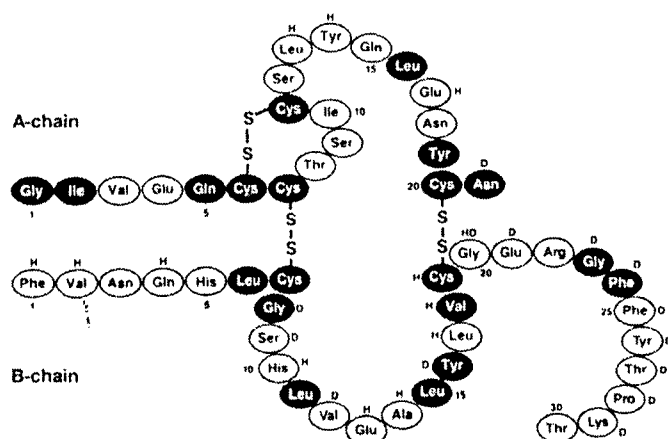


Figure 11 The primary structure of human insulin. The black residues designate the amino acids which are invariant among species of insulin. The letters indicate the residues involved in association of the molecule. D, dimer formation. H, hexamer formation.⁸⁷

Insulin, the hormone that regulates blood glucose levels, is a small protein (MW 5.8 KDa) comprising two peptide chains connected by disulfide bonds, A (21 amino acids) and B (30 amino acids). Due to the functional groups on the chain ends, insulin dissolves in water only at pH below 4.5 and above 7.0. When insulin concentration is high in solution, with or without the help of zinc, it forms

dimers or even higher association states, such as tetramers and hexamers.

Monomeric insulin is observed only at low concentration ($< 0.1 \mu\text{M}$, $\sim 0.6 \mu\text{g/ml}$).⁸⁷

Bovine serum albumin (BSA) is one of the most widely studied proteins with a high solubility in water around 5g/100ml. BSA was used as a second model protein for its higher molecular weight, about 66 KDa, which is about 10 times the molecular weight of insulin.

2.2.3 Release Protocol Flow Chart

The general strategy behind our release studies is illustrated in Figure 12. We first prepared an insulin buffer solution, and then used the extrusion method to prepare narrow size distribution large unilamellar liposomes to encapsulate some of the insulin solution inside, and then separated the liposomes from the unencapsulated insulin with a gel filtration column at 4 °C. Then liposomes were collected for the release study. After adding the permeation enhancer formulation, the liposome solution was held at 37 °C, and small amount of liposome samples were periodically taken out and released insulin was separated from liposomes. Finally we measured the insulin concentration outside the liposomes.

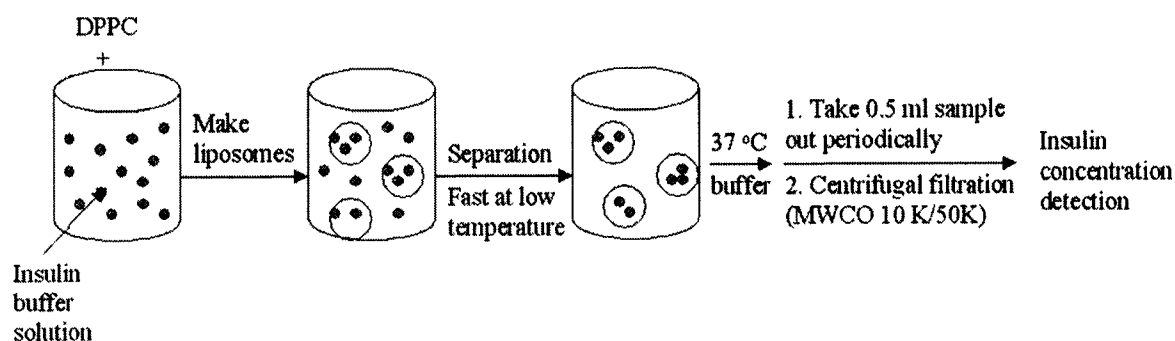


Figure 12 In vitro release protocol design.

2.3. Drug Modification

Although insulin is one of the smallest proteins, it is still a large molecule compared to lipids. The lipid DPPC has a molecular weight of only 734 Da, while insulin in monomeric form has more than 50 amino acids with a molecular weight near 6000 Da, not taking into account the insulin that may be present in the hexameric form. There is an equilibrium between insulin monomers, dimers and tetramers (possibly hexamers) in solution. Since small and neutral molecules, such as water, glycerol and vitamins, can go through biological membranes fairly easy, at first we suspected the protein membrane permeation process is size and charge controlled. We assumed that the smaller the protein, the easier it could go through the lipid bilayer. In that case, we would like to use the lower association states of insulin, such as monomers or dimers, to do the release experiments, then we need very dilute insulin solution (insulin monomer concentration limit is $0.1 \mu\text{M}$, $\sim 0.6 \mu\text{g/ml}$)⁸⁷.

Such very dilute insulin concentrations make detecting insulin a challenge in itself. The UV technique is not sensitive enough at such low concentration.

Fluorescence is much more sensitive, and insulin has intrinsic fluorescence signal due to its tyrosine and phenylalanine amino acid residues, but that is not a strong fluorescence signal.

To improve the detection sensitivity of insulin molecule, we decided to attach a fluorescent label to insulin. Amine-reactive reagents may be conjugated with virtually any protein or peptide. After consideration of many possibilities, an amine-reactive fluorescent analog, fluorescein-5-isothiocyanate (Figure 13), was selected because it has a relatively high ϵ_{MAX} (77,000 at pH 9) with a relatively low price. The isothiocyanate group reacts with basic amine groups at high pH and forms a covalent bond to derivatize the protein. Besides the two amine groups at the two N-terminals, insulin has two basic amine groups from the side chains of lysine and arginine; therefore, there should be no more than 4 fluorescence probes on each insulin molecule after the labeling reaction. The labeling reaction is done in a mild condition: mix the insulin in a pH 9 bicarbonate buffered solution using dimethyl formamide (DMF) as a solvent with the reagents and stir at room temperature for an hour. Excess reagent is used to react with insulin, and labeled insulin can be easily separated using a gel filtration column.

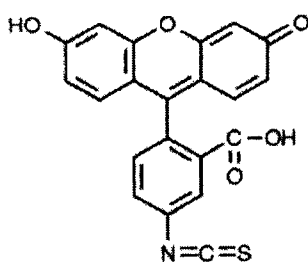


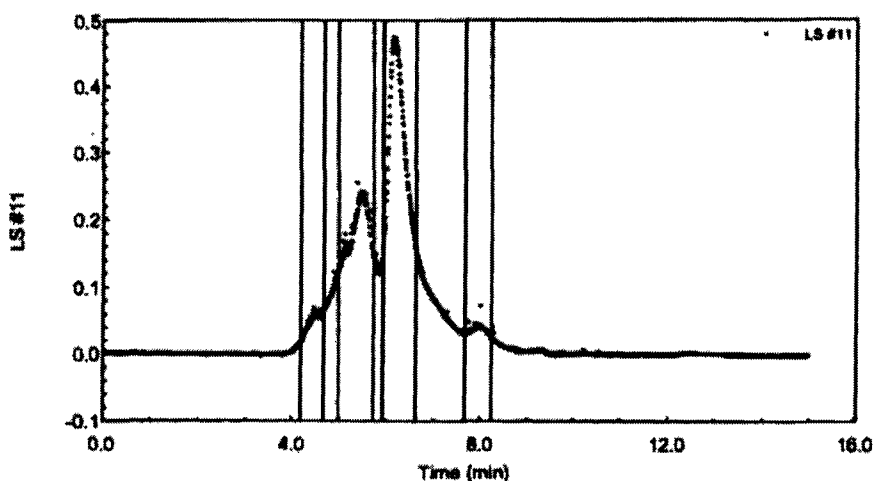
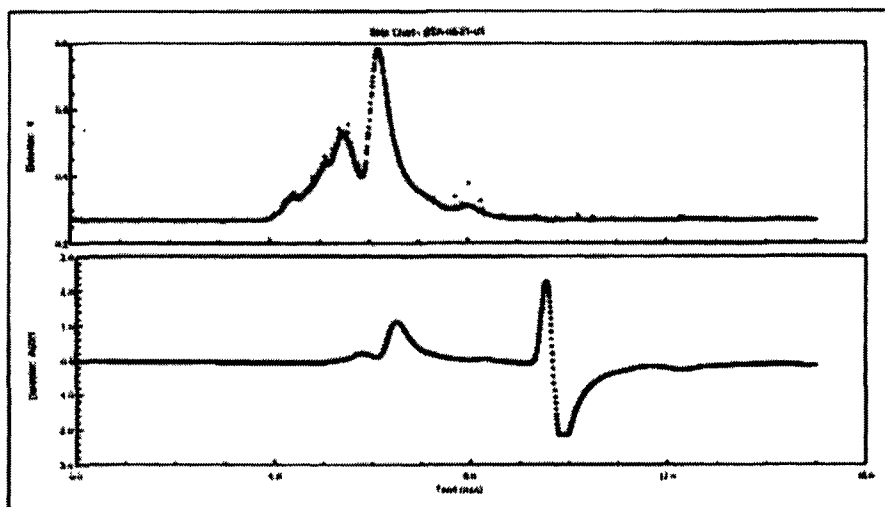
Figure 13 Molecular structure of the fluorescent probe, fluorescein-5-isothiocyanate.

Based on the manufacturer's data, the derivative has an excitation and emission wavelength of 494 nm and 518 nm respectively. In practice, in the SLM AMINCO Bowman® Series 2 luminescence spectrometer, the maximum excitation and emission wavelengths are 492 nm and 516 nm respectively. After the labeling, the detection limits were determined to be 1 ng/mL.

Although the labeling conditions were mild, there was some concern whether the process breaks the bonds within protein, especially the disulfide bonds. Obviously we do not want to see protein degradation due to the fluorescence labeling process. We use the aqueous GPC (Gel Permeation Chromatography) with the Wyatt® light scattering detector (DAWN EOS) and refractive index detector to compare the protein samples before and after the labeling process to see if there is a decrease of protein molecular weight after the labeling.

When a polarized, monochromatic laser beam passes through a solvent containing proteins, the light scattered by the molecules at an angle to the incident beam over the light scattered by the solvent alone is directly proportional

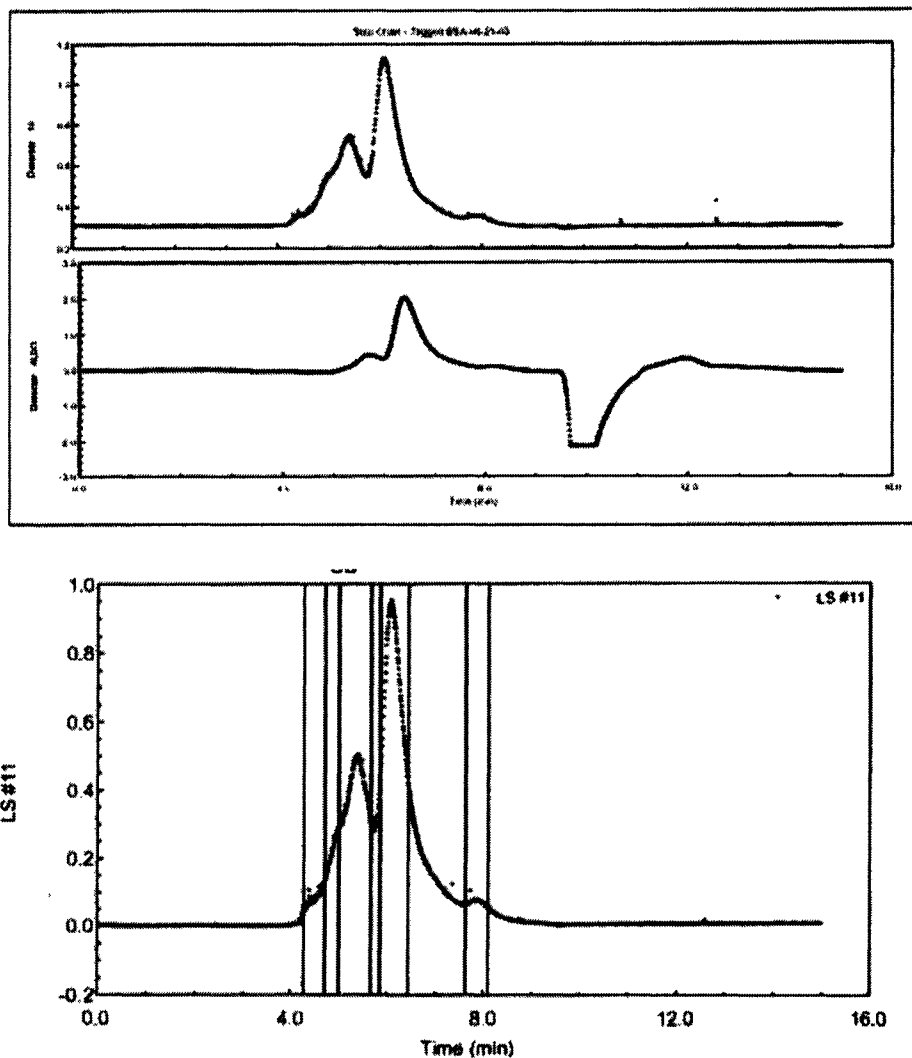
to the molecular weight multiplied by the concentration of the molecule. This characteristic of static light scattering is used for determining the absolute molecular weight of eluting biomolecules.⁸⁸ Therefore, light scattering is not very sensitive to low molecular weight proteins. Since the molecular weight of insulin is small (less than 6 KDa), we used BSA (MW 66 KDa) instead to test the potential degradation effect of the labeling process. Since proteins with higher molecular weight are more complicated and more sensitive to outer environment changes, using BSA to test the labeling process is conceptually more relevant.



RESULTS

	PEAK #1	PEAK #2	PEAK #3	PEAK #4
Time (min.)	: 4.183 - 4.675	: 4.983 - 5.733	: 5.925 - 6.625	: 7.683 - 8.250
Slices	: 60	: 91	: 85	: 69
Mn	: 5.358e+06 (15%)	: 2.166e+05 (0.7%)	: 7.991e+04 (0.4%)	: 9.672e+04 (2.4%)
Mw	: 6.098e+06 (22%)	: 2.286e+05 (0.8%)	: 8.009e+04 (0.4%)	: 1.008e+05 (3%)
Mz	: 7.539e+06 (61%)	: 2.465e+05 (1.8%)	: 8.027e+04 (1.0%)	: 1.126e+05 (9%)

Figure 14 Aqueous GPC trace of 4.3 mg/ml BSA, eluant 100 mM KCl 10 mM BTP pH 6.5 buffer. The upper trace is from the 90° angle light scattering detector, the lower trace is from the refractive index detector. Four interesting peaks in the right 90° angle light scattering trace were selected and the average molecular weights of each peak were given out. The GPC column was TSK G3000SWXL column.



RESULTS

	PEAK #1	PEAK #2	PEAK #3	PEAK #4
Time (min.)	: 4.275 - 4.725	5.008 - 5.667	5.850 - 6.442	7.633 - 8.108
Slices	: 55	80	72	58
Mn	: 2.349e+06 (4%)	2.233e+05 (1.0%)	9.147e+04 (0.7%)	9.623e+04 (5%)
Mw	: 3.513e+06 (10%)	2.304e+05 (1.0%)	9.172e+04 (0.6%)	9.664e+04 (5%)
Mz	: 5.931e+06 (33%)	2.402e+05 (2.3%)	9.197e+04 (1.4%)	9.723e+04 (11%)

Figure 15 Aqueous GPC trace of 4 mg/ml tagged BSA, eluant 100 mM KCl 10 mM BTP pH 6.5 buffer. The upper trace is from the 90° angle light scattering detector, the lower trace is from the refractive index detector. Four interesting peaks in the right 90° angle light scattering trace were selected and the average molecular weights of each peak were given out. The GPC column was TSK G3000SWXL column.

Figure 14 and 15 show the aqueous GPC traces of BSA before and after the fluorescence labeling process. In each figure, the upper left trace is from the 90° angle light scattering detector, and the lower left trace is from the refractive index detector; the right one is the enlarged trace from the 90° angle light scattering detector, four interesting peaks on the trace were selected, and the average molecular weights for each peak were computed. In Figure 14 and 15, the light scattering traces of tagged BSA and original BSA are almost identical, in number of peaks, peak positions and peak shapes. In both figures, peak #1 (from 4.2 min to 4.7 min) is a tiny bump, the major peaks are peak #2 (from 5.0 min to 5.7 min) and peak #3 (from 5.9 min to 6.5 min), peak #4 (from 7.6 min to 8.1 min) is also a tiny bump in the light scattering traces. The peak after 9 min in the refractive index trace is the solvent peak -- the original solvent for the BSA sample came out. Because light scattering is more sensitive to bigger molecules/particles, while refractive index detector only focuses on concentrations, the relative peak area of BSA dimer/trimer (peak #2) comparing to BSA monomer (peak #3) is bigger in the trace of light scattering detector than in the trace of refractive index detector.

From the peak position and the average molecular weight given by the program, peak #3 is identified as the BSA monomer peak, and peak #2 as the peak for the higher association state of BSA. In Figure 14, the molecular weight of original BSA monomer given by the Wyatt® program is 80 KDa, which is a little more than the real number (66 KDa) and may be due to some incorrect parameters in the program. Actually the relative numbers are more important to

us. The molecular weight of higher association state BSA given by the program is about 220 KDa, which is about 2.75 times the molecular weight of monomer and means that is the mixture of BSA dimers and trimers. In Figure 15, the molecular weight of tagged BSA monomer is about 91 KDa, which is more than that of the original BSA monomer and means some fluorescent probes have attached to BSA. The molecular weight of higher association state tagged BSA given by the program is about 230 KDa, which means attached fluorescent probes did not affect the self-association of BSA, tagged BSA can still have higher association states and that is still a mixture of dimers and trimers of tagged BSA.

Every peak in Figure 15 can find its corresponding peak in Figure 14 at almost the same retention time and with almost the same shape, and there is no additional low molecular weight peak appearing in Figure 15 that would indicate BSA degradation by the labeling process. Based on the analysis, this fluorescent probe labeling process is efficient and safe for proteins, no protein degradation is detected after the process and the fluorescence tagged proteins still have self-association ability.

Since a fluorescence signal was used to monitor the insulin release, it was necessary to determine the relationship between the fluorescence signal and tagged insulin concentration; the fluorescence stability of the tagged insulin is also important for long term release studies. Fluorescence measurements of different tagged insulin concentrations at pH 7 in phosphate buffer were carried out. Figure 16 shows the calibration curve of fluorescence signal verse insulin concentration. The data indicate a linear relationship between the fluorescence

signal and concentration. In order to make sure of the fluorescence long-term stability, we stored the tagged insulin solutions with different concentrations at 4 °C and performed fluorescence signal measurement over 90 days. The result (Figure 16) showed the fluorescence signal was stable for at least 90 days.

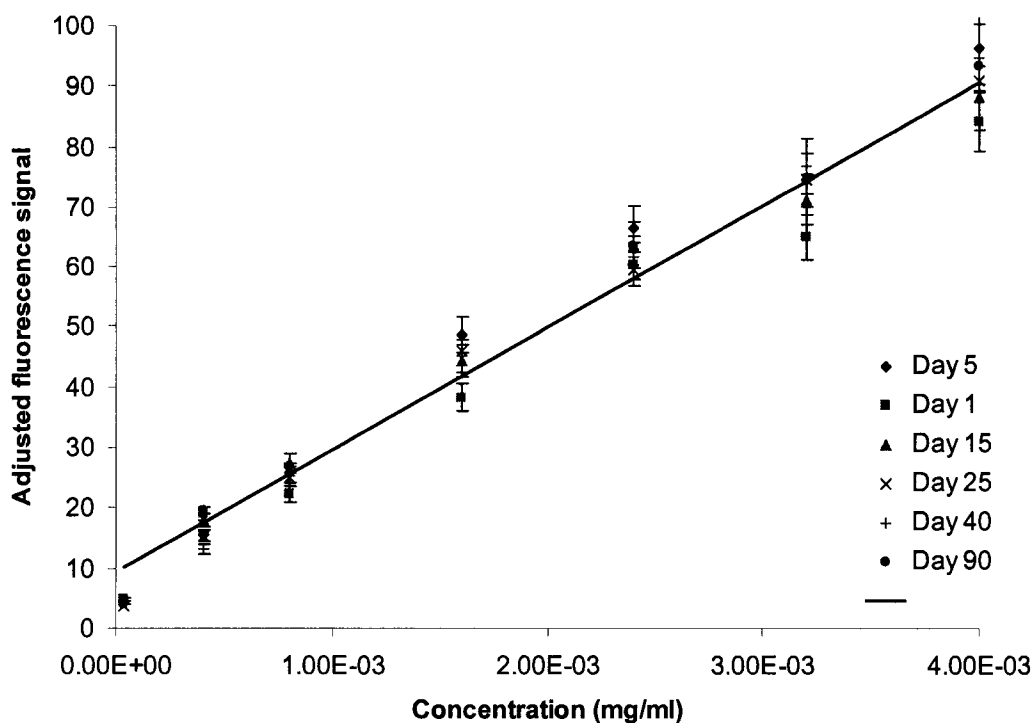


Figure 16 Tagged insulin fluorescence calibration and stability data at pH 7 in phosphate buffer.

2.4. Liposome Synthesis and Size Measurement

The extrusion method can prepare desired size liposomes with relatively narrow size distribution by extruding lipid suspension through a fixed pore size polycarbonate membrane filter at a temperature higher than the transition

temperature of the lipid. Due to obvious advantages over other liposome preparation methods, we chose the extrusion method to prepare liposomes.

The working mechanism of a liposome extruder is not complicated as it only needs a high pressure system, a sample reservoir, a filter holder and a temperature control. Figure 17 shows the design of my custom-made liposome extruder. Valve 1 is a three-way valve, it can connect either A or B to C, or totally closed. Valve 2 is identical to Valve 1, and it can let DE or DF be connected, or close the lines between DE and DF. A is connected to a nitrogen gas cylinder to provide high pressure for the extrusion. B is used to add liposome samples to the sample reservoir loop. E is used to release the high pressure inside the sample reservoir loop after the extrusion making the sample loading/reloading from B possible (without DE open to air, it is impossible to load/reload liposome samples to the reservoir loop from B). The components within the dashed line are submerged in a water bath when the extrusion process begins. The membrane filter is hydrated before it is placed inside the membrane holder. When loading the liposome samples, Valve 1 and 2 are adjusted so that B, C, D, E are connected. A syringe is used to load the raw liposomes from B to the reservoir loop. After the loading, Valve 1 and 2 are adjusted so that A, C, D, F, G are connected, then the reservoir loop and membrane filter holder are submerged in the water bath, then the gas pressure is established to start the extrusion. Multiple extrusions are needed to make narrow size distribution liposomes, so the liposomes need to be reloaded in the reservoir loop after each extrusion. After the extrusion is performed, the high pressure gas inlet is closed, and the

extruder is removed from the water bath. Valve 2 is turned to connect DE and release the remaining pressure inside of the sample reservoir loop. Then Valve 1 is turned to connect BC and the liposomes are loaded for the next extrusion.

Since the phase transition temperature of DPPC is 41 °C and the water bath temperature should be higher than the lipid phase transition temperature, we selected 50 °C as the water bath temperature.

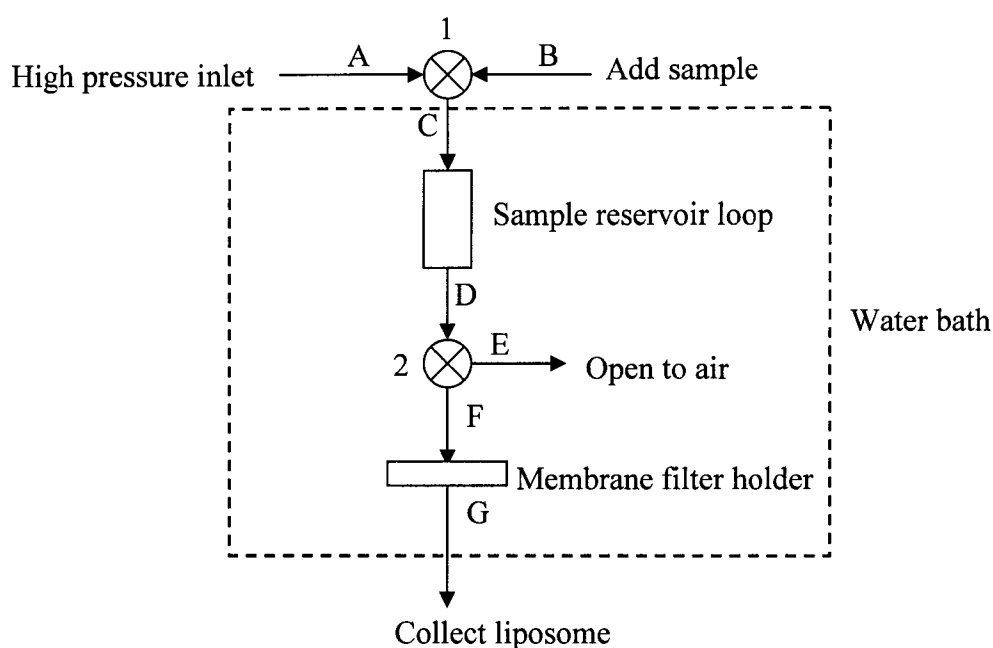


Figure 17 Block diagram of the custom-made liposome extruder. Valve 1 is a three-way valve, it can either let AC connected or BC connected, or totally close the lines of AC and BC. Valve 2 is the same as Valve 1, and it can let DE or DF connected, or close the lines of DE and DF. A is connected to a nitrogen gas cylinder to provide high pressure for the extrusion. B is used to add liposome samples to the sample reservoir loop. E is used to release the high pressure inside the sample reservoir loop after the extrusion and make the sample loading/reloading from B possible. The components within the dashed line will be submerged in the water bath when the extrusion process begins.



Figure 18 Custom-made liposome extruder (without showing the water bath and high pressure gas inlet).

We chose a 400 nm pore size polycarbonate membrane filters to make large unilamellar liposomes. The thickness of one lipid bilayer is about 5 nm, and using 400 nm diameter large unilamellar liposome can greatly reduce the curvature effect of the liposome, so that the liposome leakage profile is similar to that of a planar lipid bilayer.

We used a light scattering instrument (Microtrac S3000) to measure the liposome size and distribution after extrusion. Figure 19 shows one example of DPPC liposome size distribution after extrusion through a 400 nm membrane filter. This shows an essentially monodispersed distribution: volume-average diameter 354 nm, area-average diameter 351 nm, number-average diameter 345 nm.

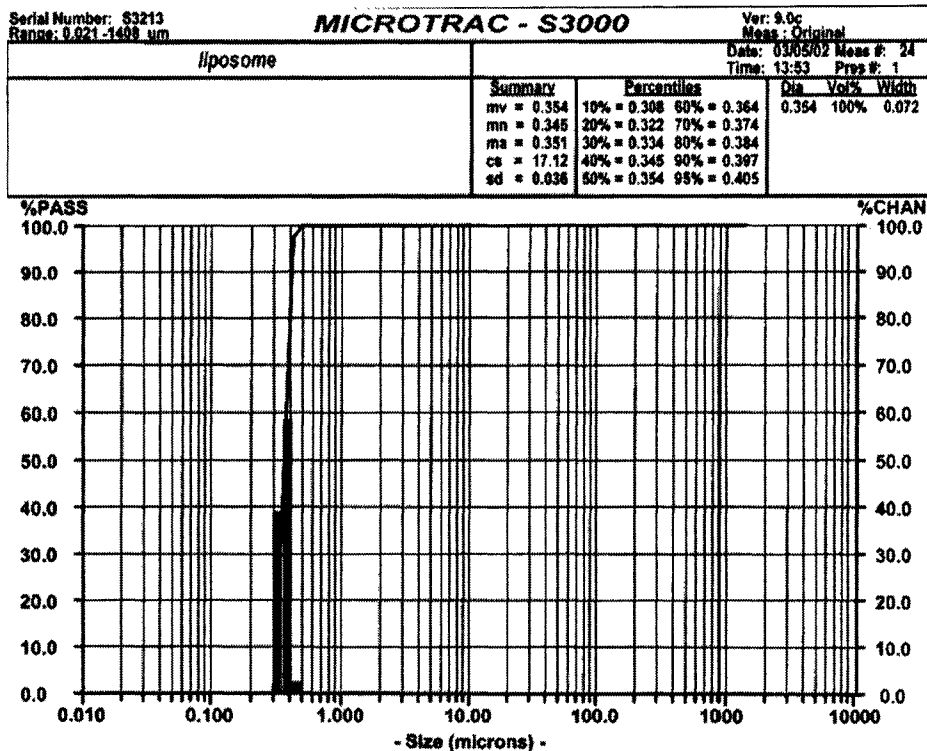


Figure 19 DPPC liposome size distribution measured by Microtrac S3000 after extrusion through a 400 nm polycarbonate membrane filter. This shows a very narrow distribution: volume-average diameter 354 nm, area-average diameter 351nm, number-average diameter 345 nm.

2.5. Permeation Enhancer Combinations

CPE-215[®] is the permeation enhancer Bentley uses for the intranasal emulsion formulations, but its melting point makes a problem for emulsion formulation. CPE-215[®] has a melting point of 34 °C, which makes it a solid at room temperature. Figure 20 shows the thermal property of CPE-215[®] by Differential Scanning Calorimeter (Q100 series modulated DSC from TA Instrument, Inc). In Figure 20, CPE-215[®] was equilibrated at -20 °C first, then heated at 3 °C /min to 100 °C, and then cooled at 3 °C /min back to -20 °C. The top trace shows the cooling process, and the large exothermic peak indicates

crystallization which starts at 33.5 °C. The bottom trace shows the heating process, and the large endothermic peak indicates melting process which starts at 34 °C. In order to make a practical formulation, we need to be sure that CPE-215[®] will not crystallize at storage temperature and while in use.

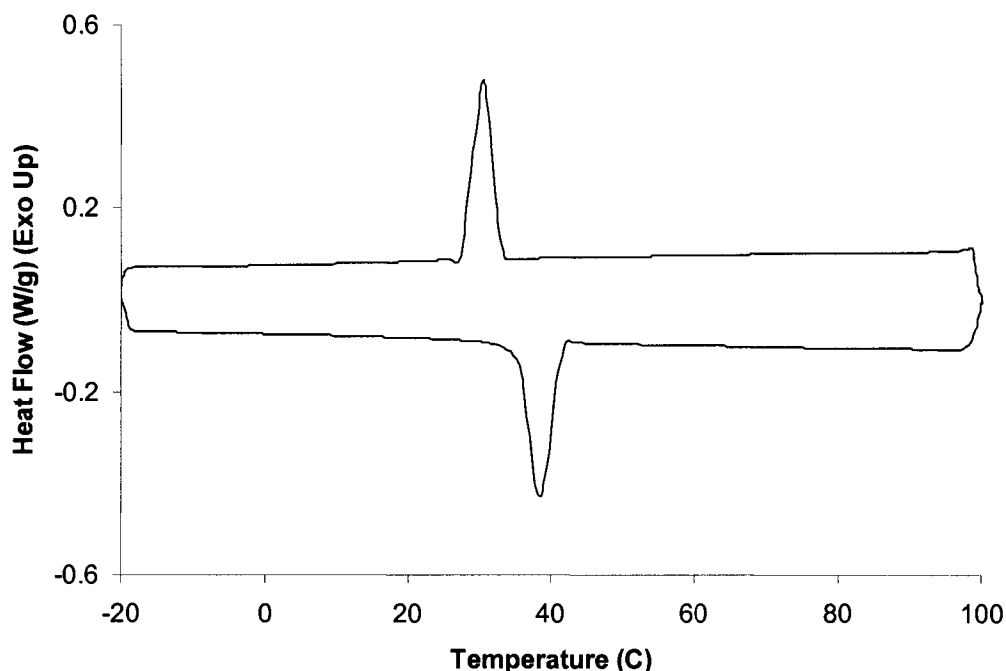


Figure 20 DSC trace of CPE-215[®] (exo up). The sample was equilibrated at -20 °C first, then heated at 3 °C/min to 100 °C, and then cooled at 3 °C/min back to -20 °C. The top trace shows the cooling process, and the large exothermic peak indicates crystallization. The bottom trace shows the heating process, and the large endothermic peak indicates melting process.

We tried to use different additives, such as sesame oil, cottonseed oil, and soybean oil, to lower the melting temperature of CPE-215[®], and found that cottonseed oil could successfully lower the melting and crystalline temperature of CPE-215[®]. Figure 21 shows the thermal property of 3:1 (w/w) CPE-215[®]:

cottonseed oil by DSC (Q100 series modulated DSC from TA Instrument, Inc). In Figure 21, the mixture was equilibrated at -20 °C first, then heated at 3 °C /min to 100 °C, and then cooled at 3 °C /min back to -20 °C. The top trace shows the cooling process, and the crystallization peak shows that the mixture does not crystallize until cooled to 5 °C. The bottom trace shows the heating process, it is hard to identify the exact temperature at which the mixture starts to melt, but it appears around 5 °C. The mixture only has one melting/crystalline peak at much lower temperature compared to pure CPE-215[®], which shows complete miscibility between CPE-215[®] and cottonseed oil. In our study, all the CPE-215[®]/cottonseed oil mixture we used were 3:1 (w/w) oil mixtures.

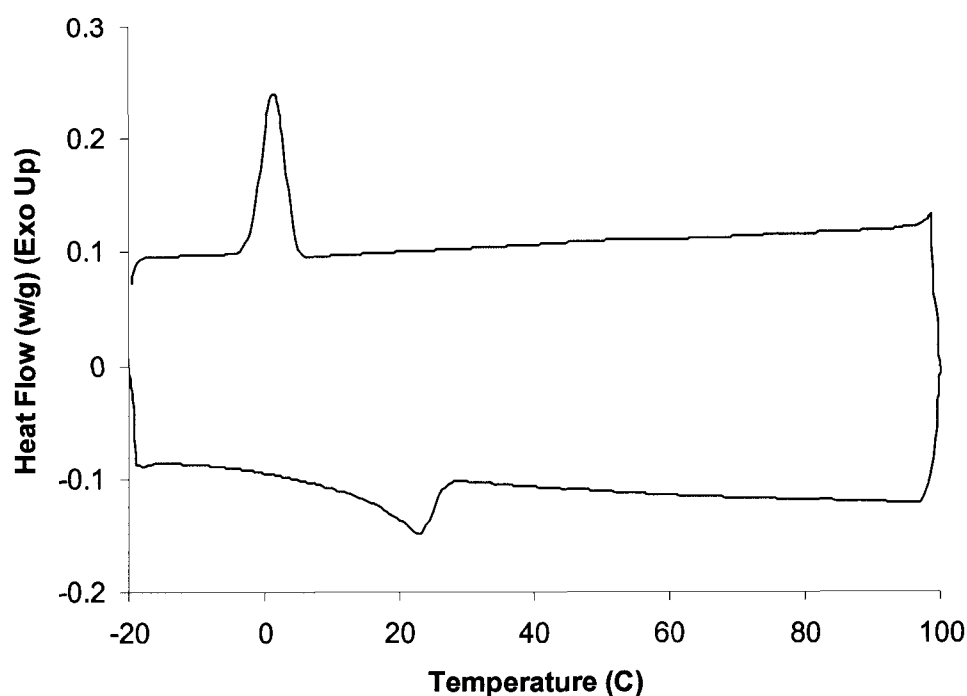


Figure 21 DSC trace of 3:1 (w/w) CPE-215[®]: Cottonseed oil. The sample was equilibrated at -20 °C first, then heated at 3 °C/min to 100 °C, and then cooled at 3 °C /min back to -20 °C. The top trace shows the cooling process, and the large exothermal peak indicates crystallization. The bottom trace shows the heating process, and the large endothermal peak indicates melting process.

2.6. Liposome Cleaning

After the extrusion, narrow size distribution large unilamellar liposomes are made, but there are insulin molecules remaining both inside and outside of the liposomes. Separating the outside free insulin molecules from the liposomes is the last step before release studies.

At first we used gel filtration to separate the outside insulin from liposomes. However, after we collected the liposomes by gel filtration and preformed the insulin release experiment, at the beginning of the release

experiment, the fluorescence signals of free insulin in solution at time “zero” were much higher than we expected. We assumed it could be due to the adsorption of insulin on the outside surface of the liposomes. During the gel filtration, the adsorbed insulin eluted with the liposomes; after gel filtration, the outside insulin concentration was so low that the adsorbed insulin desorbed from the liposomes and went into the solution, which produced the high fluorescence signal at the starting points. Further gel filtrations might be a way to solve that problem, but that could also further dilute the liposome suspension, and the gel filtration process involved more labor and time.

Since it was found that our liposomes had a slightly higher density than water, a centrifuge technique was studied to make the outside of liposomes “insulin free”. For this to be accomplished, the liposome suspension after extrusion was centrifuged at 650 g at 4 °C for 30 minutes, then the supernatant was taken out and fresh buffer was added; then the same procedure was repeated. This may be called centrifugal extraction, which is similar to dialysis but faster and does not require a membrane.

After each cycle of centrifugal extraction, some clear supernatant was taken out for fluorescence measurement to detect the free insulin concentration in the supernatant. Figure 22 shows the result of the measurement and the effect of centrifugal extraction on the free insulin concentration outside of the liposomes. After 10 cycles of centrifugal extraction, the requirement of “substantially insulin free” outside the liposome could be reached.

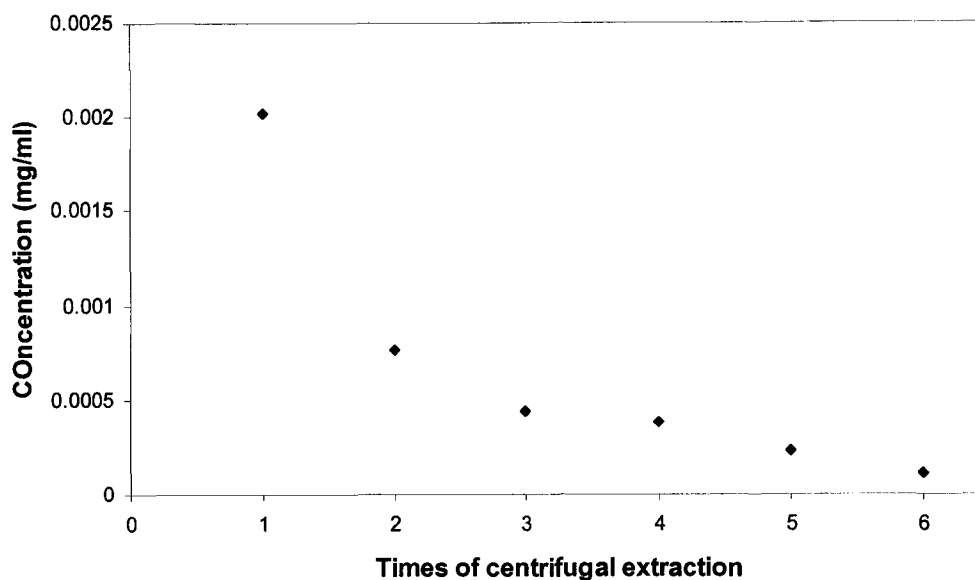


Figure 22 Effect of centrifugal extraction on the concentration of free insulin outside of the liposomes.

During the insulin release experiment, after taking out the liposome samples from the release tubes and before the fluorescence measurement for the released insulin concentration, free insulin molecules outside need to be separated from liposomes again. This time the outside insulin is what we need and the insulin concentration should not be changed after the separation. Therefore, this time we used centrifugal filtration.

The process of centrifugal filtration uses semi-permeable membrane filters and centrifugal force to separate molecular species on the basis of size and shape. The disposable centrifugal units consist of a sample filter unit and a filtration collection tube. A sample is loaded in the filter unit that is then put into the collection tube. Together the filter unit and collection tube are put in a centrifuge and spun at the appropriate speed. Since the size of our liposomes is

around 400 nm in diameter and the size of hexamer insulin is less than 10 nm in diameter, a membrane filter with the nominal molecular weight limits (NMWL) of 50 KDa can retain the liposomes and let insulin molecules go through without any problems. However, liposomes do not have a solid surface, therefore, the centrifuge conditions need to be adjusted to make sure the liposomes will not break during the process of centrifugal filtration. We did a test by performing the centrifugal filtration at different speed at 4 °C with 400 nm DPPC liposomes and found that filtration at 500 g not only did not break the liposomes, but also provided reasonable separation times. Another concern is that too many liposomes might clog the filter membrane. To solve this problem, before placing the liposomes into the sample filter unit, we centrifuge them at 500 g at 4 °C for 20 minutes and only take the supernatant to perform the centrifugal filtration process. In this case, fewer liposomes have a chance to contact the filter membrane.

2.7. Drug Release with Shaker Table

Once we obtain “clean” liposomes with insulin solution inside, we can start the release experiments. In order to keep the liposome samples at controlled temperature, we use 15ml centrifuge tubes to contain the liposome samples and fit the tubes in the necks of the three-neck jacketed flasks, which are connected to a temperature controlled water bath (Figure 23). Both the inside and jacketed flasks are filled with water; in this case the temperature inside the flask is controlled by the water bath, and the sample temperature is controlled by the

water inside of the flask. We found that once they reached temperature equilibrium, there was almost no temperature difference between water bath and liposome samples. A shaker table is used to give gentle shaking to the liposome samples so that there is no concentration gradient in each tube to affect the insulin release.

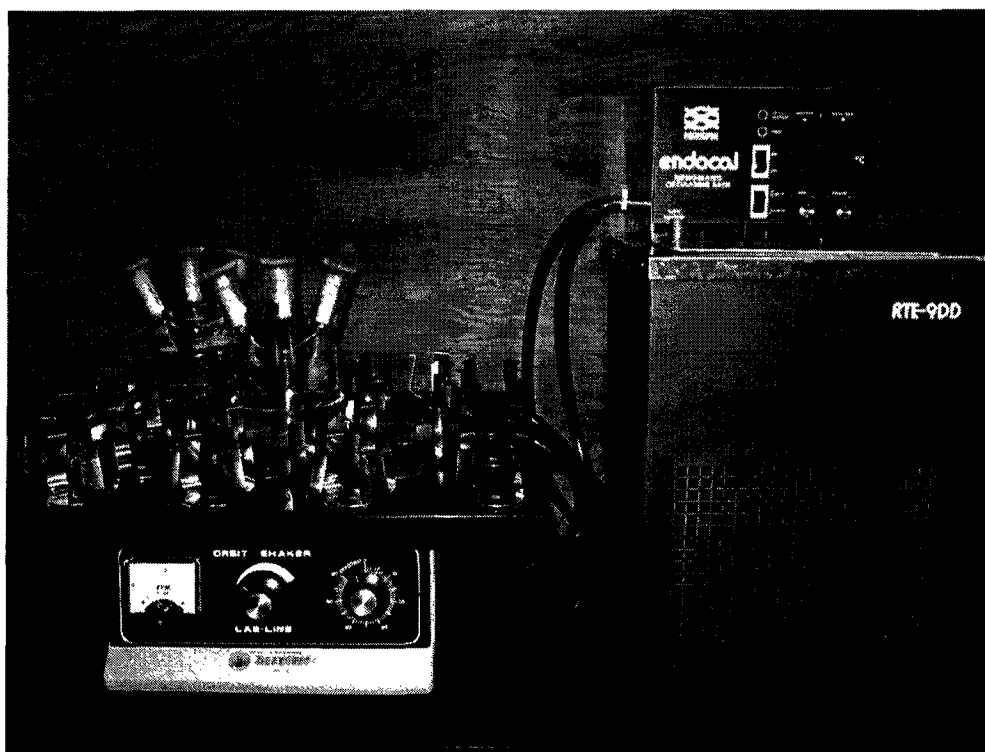


Figure 23 Protein release experiment setup. The release liposome samples are in the red-capped centrifuge tubes. The tubes are inserted in the necks of the three-neck jacketed flasks, and the flasks are used as water baths to control the sample temperature. The shaker table is used to give gentle steering to the liposome samples.

2.8. Animal Test Validation

All the experiments we designed and performed were membrane permeation in vitro tests, and needed in vivo animal tests to validate the model. If the in vitro test results were significantly different from those of the in vivo animal tests, then it would mean some of our assumptions were incorrect.

Bentley Pharmaceuticals, Inc. used pigs to perform the in vivo tests for intranasal insulin delivery with CPE-215[®] formulations. The results showed that right after the spray of certain intranasal insulin formulations into the pigs' noses, the body glucose level in the pigs dropped quickly, which indicated the insulin did go through the nasal membranes with the help of CPE-215[®] and into the blood system. CPE-215[®] is an effective membrane permeation enhancer for insulin. Formulation lacking the enhancer showed no alterations in blood insulin level.

Since the animal test is not the object of this thesis and the test results are proprietary of Bentley Pharmaceutical, we will not talk about it in detail here.

CHAPTER 3

PROTEIN RELEASE FROM LIPOSOMES

In order to study the property and function of CPE-215[®] as a permeation enhancer for natural membranes, we performed some insulin release experiments with our liposome model under different conditions.

As described in the last chapter, liposomes are used to contain the fluorescein-tagged insulin solutions, then different CPE-215[®] formulations are added externally, and external insulin fluorescence is measured. Different formulations provided insight on factors causing release.

3.1. General Procedure for One Release Experiment

First, about 0.1 g of lipid mixture (sometimes DPPC lipid only, sometimes mixture of 4:1 (w/w) DPPC/cholesterol) was dissolved in 4 ml of chloroform to assure a homogeneous mixture of lipids. Once the lipids were thoroughly mixed in chloroform, the chloroform was removed by rotary evaporation yielding a thin lipid film on the side of a 50-ml round bottom flask. The lipid film was thoroughly dried to remove residual chloroform by placing the flask under vacuum overnight at room temperature. Then 8 ml 0.2 mg/ml fluorescein-tagged insulin pH 7 phosphate buffer solution was added into the flask to hydrate the dry lipid film at

50 °C, which allowed the lipid to hydrate in its fluid phase with adequate agitation. A ten-second bath-type sonication was found to greatly reduce the hydration time, making the sizing process easier and improving the homogeneity of the size distribution. The product of hydration was a suspension of large, multilamellar liposomes analogous in structure to an onion, with each lipid bilayer separated by a water layer.⁸⁹ Typically liposome suspensions were extruded five times through a 400 nm pore size polycarbonate membrane filter at 50 °C (Attempts to extrude below the T_c of lipids were unsuccessful as the membrane has a tendency to foul with rigid membranes which cannot pass through the pores).

After extrusion, centrifugal extraction was carried out to remove the unencapsulated tagged insulin molecules. To make sure the liposomes were free of external insulin, 6 ml of liposome suspension was centrifuged at 650 g for 30 minutes at 4 °C, then the supernatant was taken out and fresh 50 mM pH 7 phosphate buffer was added, and then the same procedure was repeated. Ten cycles of centrifugal extraction were performed.

The process of liposome extrusion and centrifugal extraction can result in some lipid loss. We did one blank run (extrude liposome suspension without insulin, after 10 cycles of centrifugal extraction, dry the remaining liposome suspension to determine the dry lipid content) to determine how much lipid was left after the process of liposome extrusion and centrifugal extraction, and found that 70% of lipid content was left after the process.

After the centrifugal extraction, the “cleaned” liposomes were evenly distributed into six 15-ml plastic centrifuge tubes, which were used as the containers for the release experiments. According to the requirement of the experiment, buffer (most of the time, it was 50 mM pH 7 phosphate buffer) and different excipients were added to the tubes. Usually one of the tubes was used as blank release (no permeation excipient added). Finally each tube had 4 ml of liposome suspension inside, and an aliquot sample was taken from each tube for the release value at time=0. The centrifuge tubes were fit in the necks of the three-neck jacketed flasks, which were on a shaker table and connected to the temperature controlled water bath. The shaker table was set to 150 rpm arbitrarily, and the influence of this shear parameter was not studied, though it would be expected to have influence on the release results.

At various times, 400 μ l of liposome sample was taken from each tube. After 20 minutes' centrifuging at 500 g at 4 °C, 200 μ l supernatant of each 400 μ l sample was taken for the centrifugal filtration process at 500 g at 4 °C for another 30 minutes. A membrane filter with the nominal molecular weight limits (NMWL) of 50 KDa was usually used to retain the liposomes and let insulin molecules go through. 40 μ l of the filtrate was diluted with the 50 mM pH 7 phosphate buffer to 400 μ l for the final fluorescence measurement.

Finally, 100% release was achieved by sonicating the remaining liposomes in the presence of Triton X-100 to break the lipid bilayers. Triton X-100 (Figure 24) is a strong water-soluble surfactant, which disrupts the bilayer packing of liposomes and makes them leak.

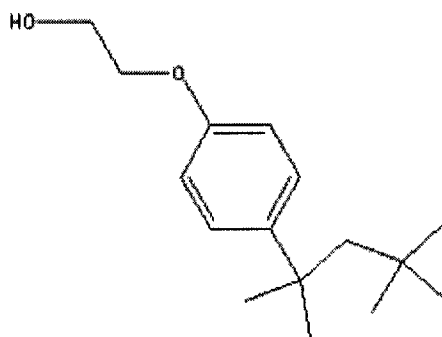


Figure 24 Chemical structure of Triton X-100.

The reproducibility of the release data has been improved over the course of this study. Release data were estimated to have a reproducibility error of 10% for Section 3.2 to 3.3. This error was reduced to 3-5% in Section 3.4 to 3.6. Only a very limited data set was reproduced in Section 4.4.3 towards the end of this study and the error was found to be less than 2%. The relative trend of the release data (i.e. which sample had the faster/slower release rate) was reproducible.

Point #0 for each sample was taken right after the emulsion/suspension was added into the release tubes (before that, everything inside each tube was identical), so theoretically their signals should be identical. However, practically the liposomes release insulin even at low temperature. Only after centrifugal filtration is complete, the outside insulin concentration is constant. The centrifugal filtration process for each sample took about half an hour, from the time taking the samples out to the end of the centrifugation. The signal difference of the

Point #0 between the various formulations partially indicates the membrane permeation enhancing effects of different formulations during the first 30 minutes.

3.2. Insulin Release from DPPC Liposomes at Different Temperatures

At first, we used only DPPC to prepare the liposomes. The transition temperature of DPPC lipid bilayer is 42 °C. Below this temperature, the lipid is in the rigid gel state; above it, the lipid is in the so called liquid crystalline state, with freedom of motion in 2 dimensions without true melting. The liquid crystalline state is the structural basis allowing mobility of membrane components within an organized framework. The dynamic properties of membranes rely on the fluid environment within the plane of the membrane, which means in the natural membranes the overall transition temperature of the lipids is below 37 °C. In order to make our liposome system more closely resemble the natural membrane situation, higher release temperatures were used.

3.2.1. Insulin Release from DPPC Liposome at 47 °C At pH 7

An insulin release experiment of DPPC liposome at 47 °C was conducted, which is 5 °C higher than the phase transition temperature of DPPC. Equal amount and same concentration of DPPC liposomes in 50 mM pH 7 phosphate buffer were put in three 15-ml plastic centrifuge tubes; pH 7 phosphate buffer, cottonseed oil emulsion and CPE-215[®]/cottonseed oil emulsion were added into three tubes respectively. The amount of CPE-215[®] is based on the molar ratio of

CPE-215[®]: DPPC = 1:2, the weight ratio of CPE-215[®]: cottonseed oil = 3:1. The tubes were placed into the 47 °C water bath on a shaker table at 150 rpm.

Figure 25 shows that the insulin release from DPPC liposome at 47 °C was so fast that most of the insulin came out in 6 hours; and the temperature was so high that there was almost no difference between the insulin release rates among the three different tubes. At this temperature, the lipid bilayer was already too permeable

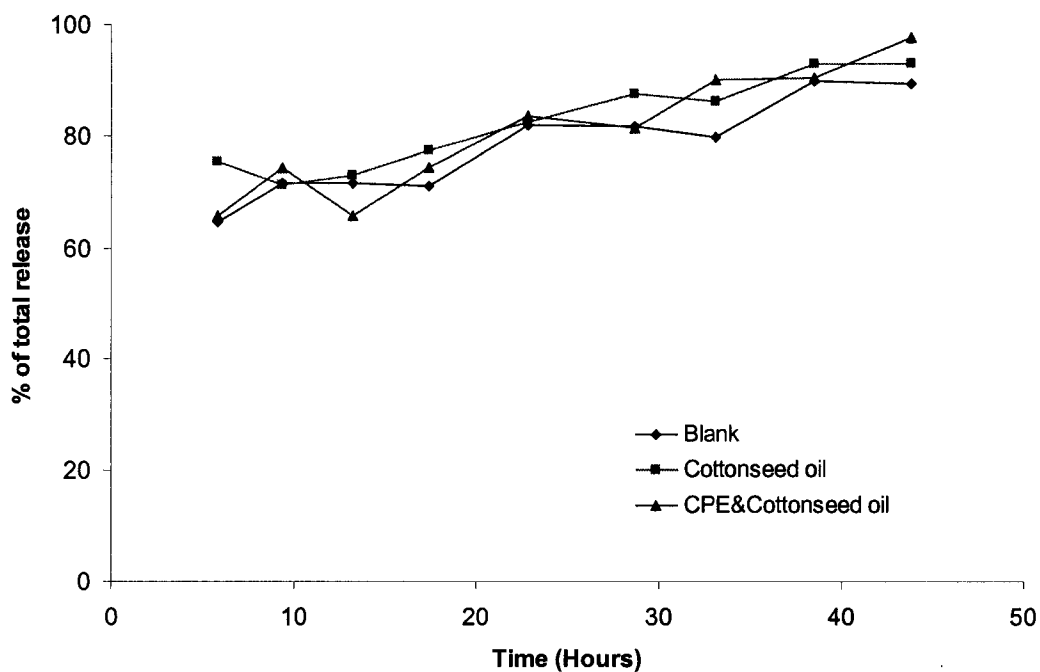


Figure 25 Insulin release from DPPC liposomes at 47 °C at pH 7. In the “Blank” sample, there were only DPPC liposomes encapsulating insulin solution. In “Cottonseed oil” sample, besides DPPC liposomes, there was some cottonseed oil added. In “CPE&Cottonseed oil” sample, besides DPPC liposomes, there was some mixture of 3:1(w/w) CPE-215[®]/Cottonseed oil added.

This was the first insulin release experiment. Therefore, there were some flaws in it. I did not expect the release rates to be that fast, and I did not take samples in the first 6 hours and missed most of the information at the beginning. In later release experiments, the sampling rate was increased at early times. In Figure 25, although the trend of the data points was increasing with time, for one sample (either "Blank", or "Cottonseed oil", or "CPE&Cottonseed oil"), some release points at later time even had lower fluorescence signals than the earlier ones. Theoretically, since those points were taken from the same release tube at different times, the later sample points should not have lower fluorescence signals than the earlier ones. That problem might be due to my sample handling techniques, which needed to be improved. However, from this experiment, we did know that 47 °C was too high for the DPPC liposome release experiments, and we needed to use lower temperature for the future release experiments.

3.2.2. Insulin Release from DPPC Liposome at 42 °C at pH 7.4

Since we did not want to perform DPPC liposome release experiments at temperature below the phase transition temperature of DPPC, and 47 °C was proven to be too high, we decided to carry out the release experiment at the phase transition of DPPC (42 °C). This time we would like to see the individual effect of cottonseed oil and CPE-215[®] on the insulin release from DPPC liposomes at pH 7.4.

DPPC liposomes were made with pH 7.4 tagged insulin phosphate buffer solution. Three different release samples were made -- one at pH 7.4 with CPE-

215[®] suspension only, one at pH 7.4 with cottonseed oil suspension only, the last one at pH 7.4 was the blank control. In each 15-ml plastic centrifuge tube, there was 4 ml DPPC liposome buffer suspension with 0.0076 g DPPC inside; 1 g of different emulsion/suspension was added later. CPE-215[®] was handled in a warm water bath so that it was in the liquid state (mp 34 °C). This time the CPE-215[®] amount was based on the molar ratio of CPE-215[®]: DPPC = 125:1.

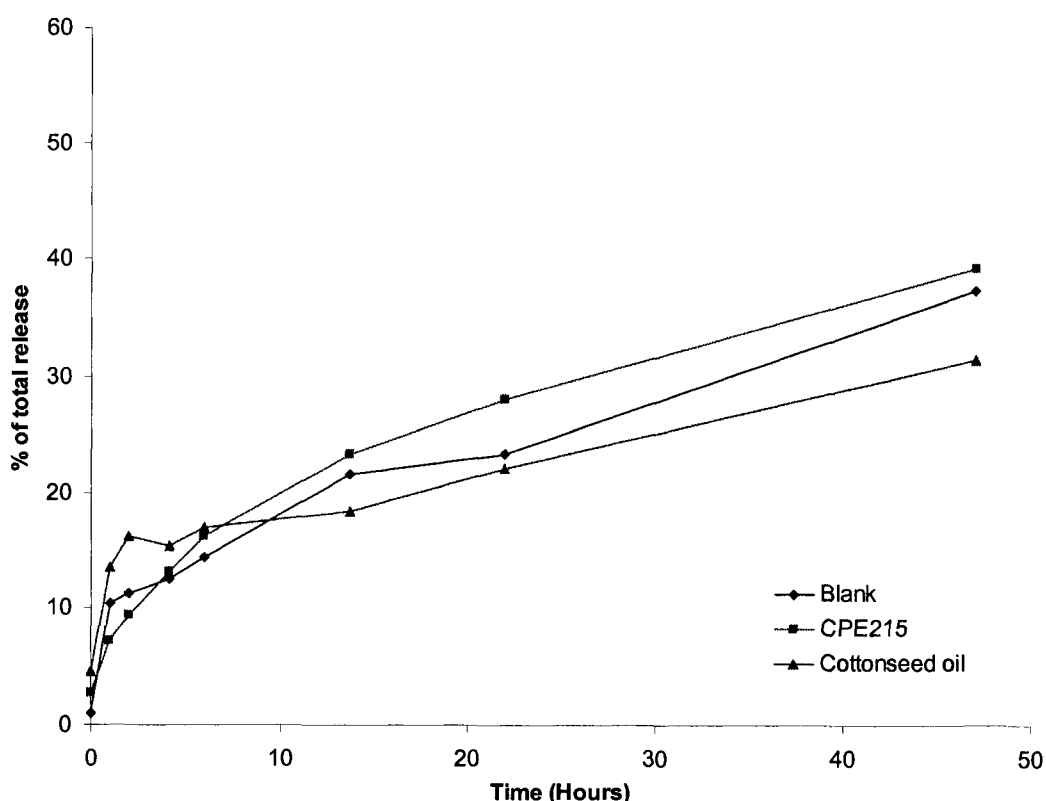


Figure 26 Insulin release from DPPC liposome at 42 °C at pH 7.4. In the “Blank” sample, there were only DPPC liposomes encapsulating insulin solution. In “Cottonseed oil” sample, besides DPPC liposomes, there was some cottonseed oil added. In “CPE-215” sample, besides DPPC liposomes, there was some CPE-215[®] added. The amount of CPE-215[®] added was based on the molar ratio of CPE-215[®]: DPPC = 125:1. Cottonseed oil amount was based on CPE-215[®]: cottonseed oil (w/w) = 3:1.

The release tubes were placed in a 42 °C water bath on a shaker table at 150 rpm. In the “CPE215” sample, most of the CPE-215[®] was on the top of the solution; phase separation was due to its low solubility in water and its low density. Oil-water phase separation happened in “Cottonseed oil” sample, too.

In Figure 26, those Point #0s are different, which partially indicates that CPE-215[®] and cottonseed oil do have permeation enhancing effects on the DPPC liposome release capacity. The sequence of initial fluorescence signals from high to low is “Cottonseed oil”, “CPE215” and “Blank”.

Insulin release in “Cottonseed oil” was the fastest at the beginning, while insulin release in “CPE215” was the slowest. But the release rate of “Cottonseed oil” slowed down after it reached certain point, and finally was caught up by “CPE215” and “Blank”. In this group, it seems that the sample releasing the fastest (“Cottonseed oil”) at the beginning had the lowest data point in the end, while the slowest one at the beginning (“CPE215”) had the highest data point. It seems that cottonseed oil can help make a burst release at the beginning while CPE-215[®] can keep the release from liposome at a higher rate. According to the literature⁹⁰, cottonseed oil is a mixture of triglycerides. 18-carbon fatty acids with two unsaturated double bonds count for 53% of the total amount of fatty acids in cottonseed oil. Cottonseed oil is a mixture of lipids, similar to DPPC. Therefore, it can have good interactions with the lipids in the liposomes, which may account for its membrane permeation enhancing effect.

3.3. Insulin Release from DPPC Liposomes with Phase Transfer Agent

CPE-215[®] is a crystalline solid at room temperature, and cottonseed oil is added to lower its melting point. The CPE-215[®]/cottonseed oil mixture is very hydrophobic and not soluble in aqueous solutions. During the release experiments, most of the CPE-215[®]/cottonseed oil mixture was phase-separated from the aqueous buffer solution and floating on the top, which means most of the CPE-215[®] added into the system did not have the chance to make contact with liposomes, let alone help the release of insulin. In order for the permeation excipient to take effect, how much and how fast CPE-215[®] can interact with the liposomes and be incorporated in the lipid bilayer is more important than how much CPE-215[®] emulsion is added to the system. Only the soluble portion of CPE-215[®], which is very limited, counts. This is the interpretation of why the release enhancement effect of CPE-215[®] was so small in previous experiment.

Getting more CPE-215[®] into the lipid bilayer may be the key for faster release rate. We need a phase-transfer carrier to transport more CPE-215[®] from the oil phase through the water phase to the liposome membrane to facilitate the release of insulin out of the liposomes. Cyclodextrins are well-known for their phase transport properties.

Structurally, Cyclodextrins consist of 6, 7, or 8 (α , β and γ respectively) D-glucopyranosyl units connected by alpha-(1,4) glycosidic linkages. Figure 27 shows the molecular structure of α -cyclodextrin. The most stable three dimensional molecular configuration for these non-reducing cyclic oligosaccharides takes the form of a toroid with the upper (larger) and lower

(smaller) opening of the toroid presenting secondary and primary hydroxyl groups, respectively, to the solvent environment. The interior of the toroid is hydrophobic as a result of the electron rich environment provided in large part by the glycosidic oxygen atoms, which can be used to carry or encapsulate small water-insoluble molecules.

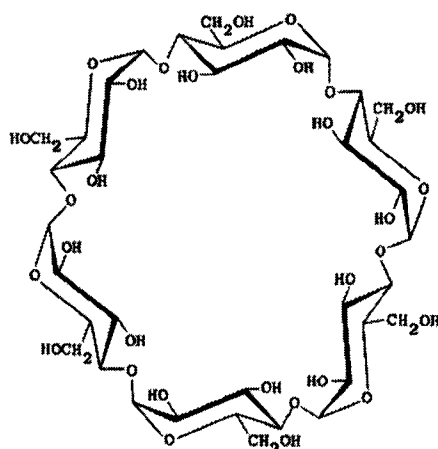


Figure 27 Molecular structure of α -cyclodextrin.

Table 1 Physical properties of various cyclodextrins⁹¹

	Alpha	Beta	Gamma
Molecular weight	972	1135	1297
Glucose monomers	6	7	8
Internal cavity diameter (angstroms)	5	6	8
Water solubility (g/100ml, at 25 °C)	14.2	1.85	23.2
Melting rang (°C)	255-260	255-265	240-245
Water molecules in cavity	6	11	17

According to the information from Table 1, one more glucose unit in cyclodextrin can result in huge cavity volume increase, it is surprising that the

water solubility of β -cyclodextrin is only about 1/10 of that of α - or γ -cyclodextrin. γ -Cyclodextrin has the largest internal cavity, but it is much more expensive than the other two and not economical to use. β -Cyclodextrin is the cheapest among the three and has a larger cavity than α -cyclodextrin, so β -cyclodextrin was used as the promising phase transfer candidate.



Figure 28 Molecular model of α -cyclodextrin (left) and CPE-215[®] (right) in the same scale. Hydrogen atoms are white, carbon atoms are grey, and oxygen atoms are red. α -Cyclodextrin is in a rod model, and CPE-215[®] is in a stick-and-ball model.

Figure 28 shows the molecular model of α -cyclodextrin and CPE-215[®] at the same scale. It seems that the internal cavity of α -cyclodextrin is large enough for a CPE-215[®] molecule.

3.3.1. Insulin Release from DPPC Liposome at 42 °C with Cyclodextrins at pH 7

We decided to add cyclodextrins to our release formulations to see if they can work as phase transfer carriers as we expected. First we would like to know if cyclodextrin can further enhance the permeation effect of CPE-215[®] and cottonseed oil, then we would like to know if cyclodextrin itself has permeation enhancing effect, and determine which cyclodextrin is better (alpha or beta).

We used a release tube with only DPPC liposomes inside as the blank control; β -cyclodextrin buffer solution was added in one DPPC liposome suspension as the "B-CD" sample to see the membrane permeation enhancing effect of β -cyclodextrin itself; CPE-215[®]/Cottonseed oil mixture emulsion was added to one DPPC liposome tube as the "CPE&CSO" sample to see the membrane permeation enhancing effect of CPE-215[®]/Cottonseed oil mixture; CPE-215[®]/Cottonseed oil mixture in β -cyclodextrin buffer solution was added into one DPPC liposome tube as the "B-CD+CPE&CSO" sample to see if the presence of β -cyclodextrin can further boost the effect of CPE-215[®]/Cottonseed oil mixture; CPE-215[®]/Cottonseed oil mixture in α -cyclodextrin buffer solution was added into one DPPC liposome tube as the " α -CD+CPE&CSO" sample to see if α -cyclodextrin is better than β -cyclodextrin.

Phosphate buffer at pH 7 was used to make liposomes and prepare different release samples. Five different 1 g emulsion/suspension formulations were added to the identical liposome suspension in five release tubes, each with 4 ml DPPC liposome buffer suspension and 0.0063 g DPPC inside: one was the

blank control buffer solution, one was the β -cyclodextrin buffer solution, one was the β -cyclodextrin buffer solution with mixture of CPE-215[®] & cottonseed oil, one was the simple mixture of CPE-215[®] & cottonseed oil, one was the α -cyclodextrin buffer solution with mixture of CPE-215[®] & cottonseed oil.

The amount of CPE-215[®] added was based on a molar ratio of CPE-215[®]: DPPC = 125:1. The amount of cyclodextrin was planned to be added according to the weight ratio of CPE-215[®]: cyclodextrin = 2:1, but unfortunately, neither α -cyclodextrin nor β -cyclodextrin could be dissolved to that extent in the buffer solution, so saturated cyclodextrin solutions were used (α -cyclodextrin is much more water soluble than β -cyclodextrin).

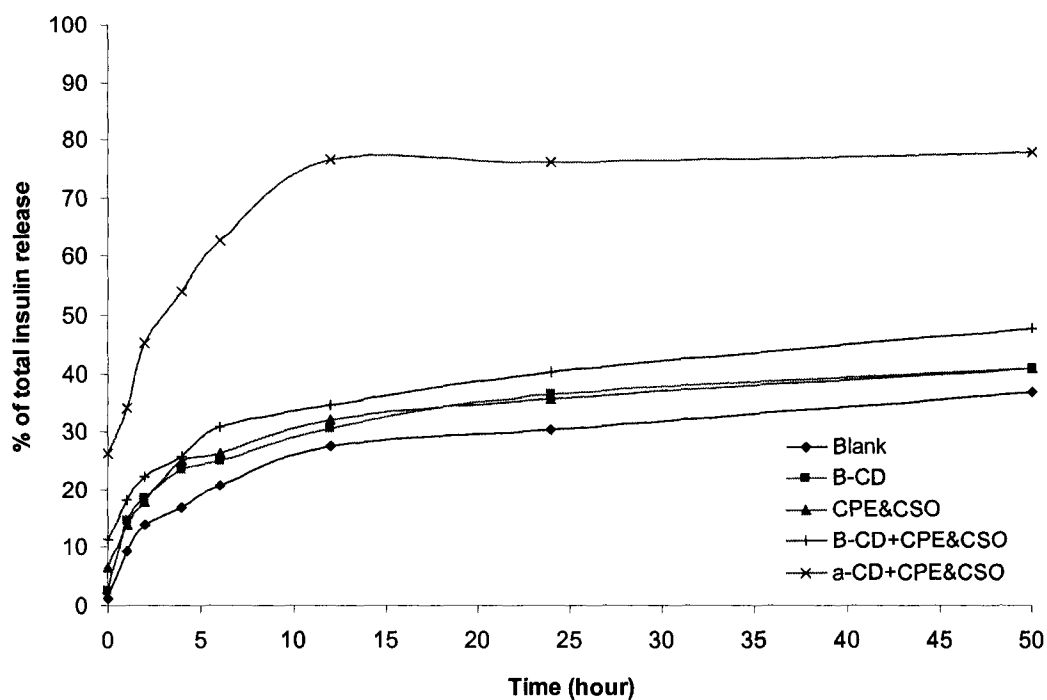


Figure 29 Insulin release from DPPC liposomes with cyclodextrins at 42 °C at pH 7. Sample tube with DPPC liposomes only was the “Blank”; β -cyclodextrin buffer solution was added in one DPPC liposome suspension as the “B-CD” sample; CPE-215[®]/Cottonseed oil mixture emulsion was added to one DPPC liposome tube as the “CPE&CSO” sample; CPE-215[®]/Cottonseed oil mixture in β -cyclodextrin buffer solution was added into one DPPC liposome tube as the “B-CD+CPE&CSO” sample; CPE-215[®]/Cottonseed oil mixture in α -cyclodextrin buffer solution was added into one DPPC liposome tube as the “a-CD+CPE&CSO” sample.

The release tubes were placed in a 42 °C water bath on a shaker table at 150 rpm. Figure 29 shows the result of this insulin release experiment with cyclodextrins at pH 7.

All samples showed similar release pattern: insulin release rates were very fast at the very beginning (ideal for intranasal drug delivery), followed by slower rate after 10 hours, but different samples showed different starting points.

The experimental data showed that the sample with α -cyclodextrin buffer solution and mixture of CPE-215[®] & cottonseed oil had the highest starting point and the fastest release rate at the beginning; the next one was the one with β -cyclodextrin and mixture of CPE-215[®] & cottonseed oil. The blank control one had the lowest starting point and the slowest release rate, as expected. For the ones with only β -cyclodextrin or mixture of CPE-215[®] & cottonseed oil, it is hard to tell which one is faster; they have almost the same effects on the release of insulin.

All the samples with cyclodextrin show obvious permeation enhancement effects, and saturated α -cyclodextrin solution has better effect than saturated β -cyclodextrin solution due to the big difference in water solubility. Cyclodextrin itself has just a small permeation enhancing effect; it mainly acts as a phase transfer carrier.

Finally, CPE-215[®] is an effective permeation enhancer, but needs a phase transition carrier like cyclodextrin; otherwise it can reach the membrane only with great difficulty due to its limited water solubility.

3.3.2. Insulin Release from DPPC Liposome at 42 °C with Different Amount of Cyclodextrins at pH 7

We have known that cyclodextrin can further enhance the membrane permeation effect caused by CPE-215[®] and cottonseed oil, now we would like to know how much cyclodextrin is needed and what the proper ratio of CPE-215[®] to cyclodextrin is.

This time, we added the same amount of CPE-215[®]/Cottonseed oil mixture with different amount of α -cyclodextrin into each liposome suspension to determine the best ratio of cyclodextrin to CPE-215[®]. In the previous experiment, saturated α -cyclodextrin showed better permeation enhancing effect with CPE-215[®] than saturated β -cyclodextrin, but in that case, much more α -cyclodextrin was added than β -cyclodextrin due to higher solubility of α -cyclodextrin, so it is difficult to determine which one is better. This time we compared α -cyclodextrin with β -cyclodextrin at the same molar ratio of CPE-215[®].

Similar amount of 3:1 (w/w) CPE-215[®]/Cottonseed oil mixture were added to every release tube. The amount of CPE-215[®] added was based on the molar ratio of CPE-215[®]: DPPC = 20:1. A 50 mM pH 7 phosphate buffer was used to make liposomes and prepare different release samples. Three liposome samples were used to see the effect of different amount of α -cyclodextrin on the insulin release rate. In "C&C+1x a-CD" sample, molar ratio of α -cyclodextrin: CPE-215[®] = 1:100; in "C&C+5x a-CD" sample, molar ratio of α -cyclodextrin: CPE-215[®] = 1:20; in "C&C+20x a-CD" sample, molar ratio of α -cyclodextrin: CPE-215[®] = 1:5. In "C&C+20x B-CD" sample, molar ratio of β -cyclodextrin: CPE-215[®] = 1:5.

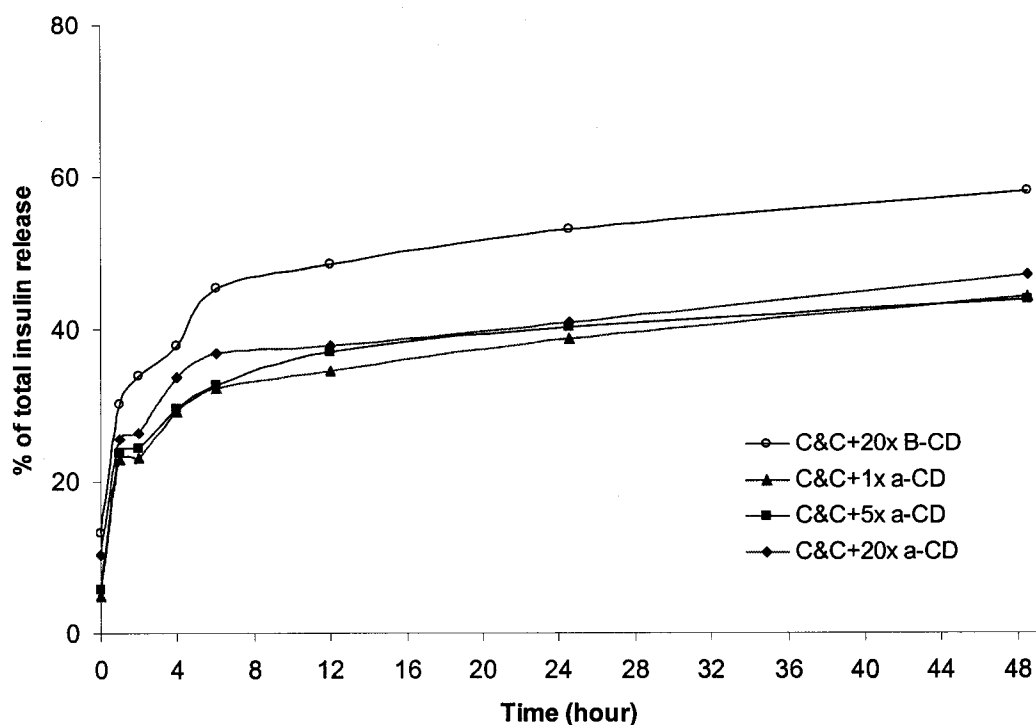


Figure 30 Insulin release from DPPC liposomes at 42 °C at pH 7 with different ratio of cyclodextrin over CPE-215[®]. Same amount of 3:1 (w/w) CPE-215[®]/Cottonseed oil mixture was added to every release tube. The amount of CPE-215[®] added was based on the molar ratio of CPE-215[®]: DPPC = 20:1. In “C&C+1x a-CD” sample, molar ratio of α -cyclodextrin: CPE-215[®] = 1:100; in “C&C+5x a-CD” sample, molar ratio of α -cyclodextrin: CPE-215[®] = 1:20; in “C&C+20x a-CD” sample, molar ratio of α -cyclodextrin: CPE-215[®] = 1:5. In “C&C+20x B-CD” sample, molar ratio of β -cyclodextrin: CPE-215[®] = 1:5.

The release tubes were placed in a 42 °C water bath on a shaker table at 150 rpm. Figure 30 showed the results of this insulin release experiment with different amounts of cyclodextrin at 42 °C at pH 7. The shapes of the four insulin release curves were similar: the release rate was very fast at the very beginning, then the insulin release rate slowed down and after 6 hours reached a gentle slope. The starting points for each release curve were not the same. We could

almost predict which sample would have the maximum final insulin release by looking at the insulin fluorescence signals at Time Zero – the higher the fluorescence signal at Time Zero, the more final released insulin for that sample.

By comparing the release curves, we can see that the more cyclodextrin, the more insulin released from DPPC liposomes; at the same molar ratio to CPE-215[®], β -cyclodextrin is better than α -cyclodextrin, which makes sense because β -cyclodextrin has a bigger hydrophobic cavity than α -cyclodextrin.

3.3.3. Insulin Release from DPPC Liposome at 42 °C with Beta-Cyclodextrin at pH 7

In order to know the effect of β -cyclodextrin on different components of the intranasal formulation, such as CPE-215[®], cottonseed oil and mixture of CPE-215[®] and cottonseed oil, we carried out another insulin release experiment.

“Cleaned” DPPC liposomes encapsulating insulin pH 7 phosphate buffer solution were evenly divided into four plastic centrifuge tubes. As usual we used one tube of DPPC liposomes as the “Blank” sample. In “CSO+B-CD” sample, cottonseed oil in pH 7 β -cyclodextrin buffer solution was added; in “CPE+B-CD” sample, CPE-215[®] in pH 7 β -cyclodextrin buffer solution was added; in “CPE+CSO+B-CD” sample, CPE-215[®]/Cottonseed oil mixture in β -cyclodextrin buffer solution was added. We used 2% β -cyclodextrin buffer solution, which is almost its saturation concentration. The amount of CPE-215[®] added was based on the molar ratio of CPE-215[®]: β -cyclodextrin =1:1, molar ratio of DPPC: CPE-

215[®] = 1:5. The 50 mM pH 7 phosphate buffer was used to prepare liposomes for these different release samples.

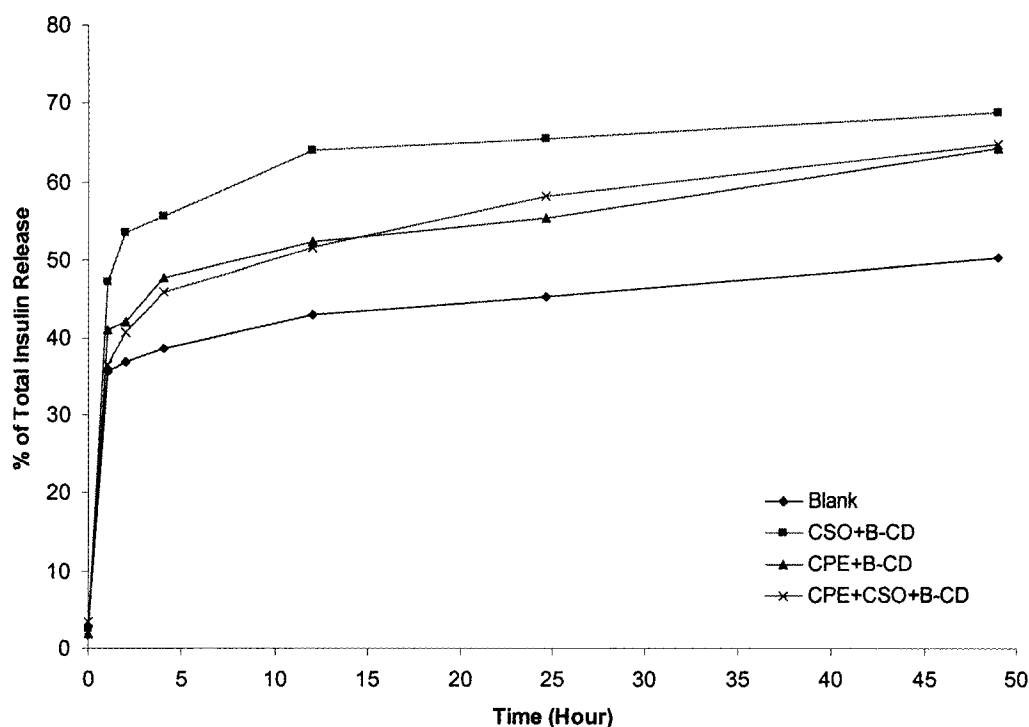


Figure 31 Insulin release from DPPC liposomes at 42 °C with β -cyclodextrin at pH 7. In “Blank” sample, there was only DPPC liposomes, as the blank control for insulin release. In “CSO+B-CD” sample, cottonseed oil in pH 7 β -cyclodextrin buffer solution was added into liposomes; in “CPE+B-CD” sample, CPE-215[®] in pH 7 β -cyclodextrin buffer solution was added into liposomes; in “CPE+CSO+B-CD” sample, CPE-215[®]/Cottonseed oil mixture in β -cyclodextrin buffer solution was added into liposomes. The amount of CPE-215[®] added was based on the molar ratio of CPE-215[®]: β -cyclodextrin =1:1, molar ratio of DPPC: CPE-215[®] = 1:5.

The release tubes were placed in a 42 °C water bath on a shaker table at 150 rpm. Figure 31 showed the insulin DPPC liposome release result of β -cyclodextrin with different formulation components. There was also a very fast

release rate at the very beginning, then the rate slowed down and reached a plateau. The insulin released from liposomes in “Blank” sample was the smallest, as expected. Although the “Blank” here was different from the “Blank” in Figure 26 , which meant we had some reproducibility issue, the relative trends of them were similar. The amounts of insulin released in “CPE+B-CD” and “CPE+CSO+B-CD” samples were average; the “CSO+B-CD” sample had the maximum insulin release. It is interesting to see that cottonseed oil showed better membrane permeation enhancing effect than CPE-215[®] in this experiment. In comparison with previous results of insulin release experiments, we can say β -cyclodextrin can further enhance the insulin release from DPPC liposomes.

Based on the structure of cyclodextrins and the results of the insulin release experiments, we confirmed that cyclodextrins increased the availability of CPE-215[®] and cottonseed oil to the liposomes. Cyclodextrins and the hydrophobic CPE-215[®]/ cottonseed oil formed inclusion complexes by hydrophobic interaction and when the cyclodextrins collided with the liposomes, CPE-215[®] and cottonseed oil could be released into the hydrophobic lipid bilayers of liposomes. The direct conclusion out of this hypothesis is that cyclodextrin could greatly increase the apparent solubility of CPE-215[®] in water. However, in a simple solubility test of CPE-215[®] in β -cyclodextrin solution, even when the molar ratio of β -cyclodextrin: CPE-215[®] reached to 10:1, we could still see some CPE-215[®] floating on the aqueous surface. Probably β -cyclodextrin did increase the solubility of CPE-215[®] in water, maybe by 10 or 100 fold, but not as much as we thought (we thought by forming an inclusion complex with CPE-

215[®], one β -cyclodextrin could take one CPE-215[®] into the aqueous phase). I did a literature search on cyclodextrins, and found that cyclodextrins were widely used to increase the water solubility of hydrophobic molecules by forming a 1:1 inclusion complex; but not every cyclodextrin molecule could form a complex with those hydrophobic molecules, there were different formation constants for different molecules. In one recent paper on the use of β -cyclodextrin to increase the solubility of a highly hydrophobic drug, furosemide, the drug solubility was increased by 11 fold with the help of cyclodextrin.⁹²

3.4. Incorporating Cholesterol into DPPC Liposome

Cholesterol is a membrane constituent widely found in animal systems which serves a unique purpose of modulating membrane fluidity, elasticity, and permeability. In order to make our liposome model more similar to natural membrane, cholesterol was incorporated with DPPC to prepare the liposomes. The fluid-phase behavior of binary mixtures of cholesterol with phosphatidylcholines was well studied.^{93,94} When cholesterol content is higher than 30 mol%, there is only one phase in DPPC and cholesterol mixture from 20 °C to 55 °C. In order to make cholesterol evenly distributed in the lipid bilayer, the weight ratio of DPPC to cholesterol in our new membrane model was 4:1, in which cholesterol counts for 32 mol% of total lipid. With this adjustment to the liposome model, the insulin release temperature was adjusted to the human body temperature of 37 °C.

3.4.1. Insulin Release at 37 °C from DPPC/Cholesterol Liposomes with Different Formulation Components and Simple Combinations

After we decided to incorporate cholesterol into DPPC liposomes, we wanted to see if the change in the liposome model and temperature could result in a change of the insulin release profile. We wanted to see the effect of CPE-215[®] only, cottonseed oil only and with β -cyclodextrin combination on this improved membrane model. Therefore, we did a similar insulin release experiment for this DPPC/Cholesterol liposome at 37 °C.

We used a high molar ratio of β -cyclodextrin: CPE-215[®], which was 1:1. Due to the solubility limitation of β -cyclodextrin, the molar ratio of CPE-215[®]: DPPC turned out to be 4:1. Cottonseed oil is a mixture of triglycerides with the average molecular weight of 275. In this experiment, the molar ratio of β -cyclodextrin: cottonseed oil was also 1:1. A 50 mM pH 7 phosphate buffer was used to prepare these liposomes.

“Cleaned” DPPC/Cholesterol liposomes encapsulating insulin phosphate buffer solutions were evenly divided into six plastic centrifuge tubes, with 2 ml of DPPC/Cholesterol liposomes in each tube. We added 2 ml of pH 7 buffer into one tube of liposomes and used it as the “Blank” control sample. In the “CPE-215 only” sample, CPE-215[®] and 2 ml of pH 7 phosphate buffer were added to the 2 ml liposomes; in the “Cottonseed oil only” sample, cottonseed oil and 2 ml of pH 7 phosphate buffer were added to the liposomes; in the “1:1 B-cyclodextrin: CPE-215” sample, CPE-215[®] and 2 ml of 2% β -cyclodextrin pH 7 phosphate buffer solution were added to the 2 ml liposomes; in the “1:1 B-cyclodextrin: CSO”

sample, cottonseed oil and 2 ml of 2% β -cyclodextrin pH 7 phosphate buffer solution were added to the 2 ml liposomes.

In this experiment, we also wanted to see the effect of different oil droplet size of cottonseed oil on the insulin release profile. In “Cottonseed oil only” and “1:1 B-cyclodextrin: CSO” samples, cottonseed oil was added as droplets. However, in the “CSO emulsion” sample, cottonseed oil was added to the liposomes in the form of emulsion made with a high shear mixer (Ultra Turrex®).

Table 2 Sample information in Section 3.4.1

Sample	Content	Note
Blank	2 ml liposome +2 ml phosphate buffer	The amount of CPE-215® used in different samples was the same, so was cottonseed oil. The amount of CPE-215® and cottonseed oil used was based on 1:1 molar ratio to β -CD.
CPE-215 only	2 ml liposome +2 ml phosphate buffer+CPE-215®	
Cottonseed oil only	2 ml liposome +2 ml phosphate buffer+ cottonseed oil drop	
CSO emulsion	2 ml liposome +2 ml cottonseed oil emulsion	
1:1 B-cyclodextrin: CPE-215	2 ml liposome +2ml 2% β -CD buffer solution + CPE-215®	
1:1 B-cyclodextrin: CSO	2 ml liposome +2ml 2% β -CD buffer solution + cottonseed oil drop	

Before the experiment, we thought since CPE-215® crystal started to melt at 34 °C, it would be in liquid state at 37 °C. But during the release experiment at 37 °C, in the samples containing CPE-215®, we could see some solid CPE-215® floating on the aqueous surface, which further decreased the availability of CPE-215® to the liposomes. Consequently, in all the further release experiments at 37

°C, CPE-215[®] was added in company of cottonseed oil, in order to eliminate solid CPE-215[®] phase.

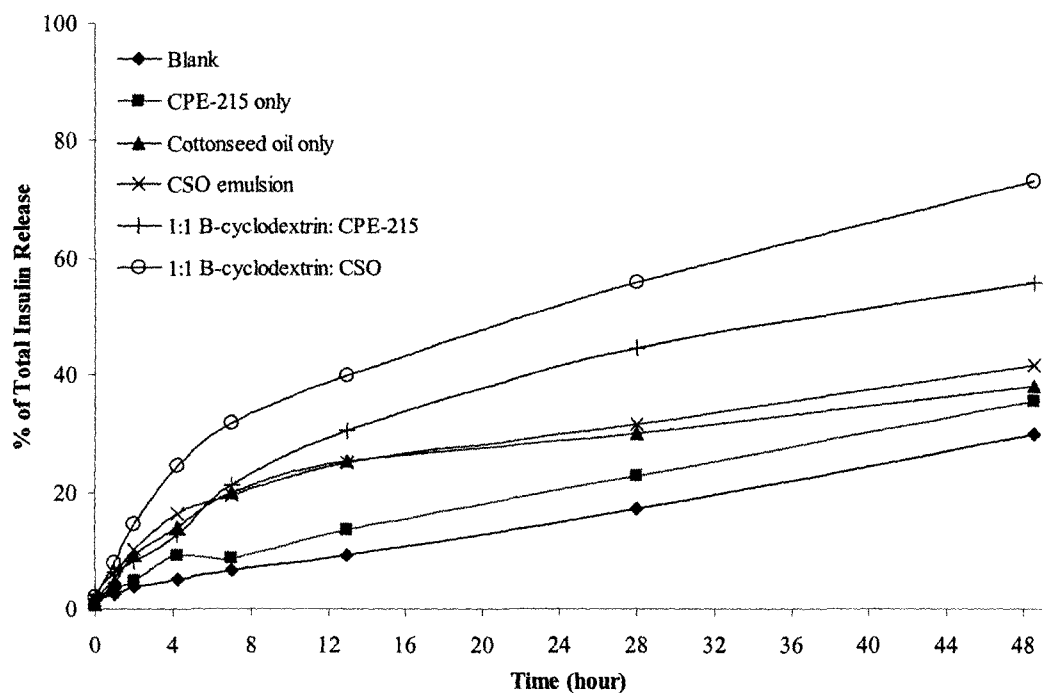


Figure 32 Insulin release from DPPC/Cholesterol liposomes at 37 °C at pH 7. In the “Blank” sample, there was only DPPC/Cholesterol liposomes, as the blank control for insulin release. Molar ratio of β -cyclodextrin: CPE-215[®]: cottonseed oil = 1:1:1.

Figure 32 showed the result of insulin release from DPPC/Cholesterol liposomes at 37 °C at pH 7. The release data were good and as expected—the data curve of the “Blank” sample was the lowest among all the sample release curves, and the released insulin signals increased with time in all the samples. All the insulin release data points are independent, which means that there is no

guarantee for fluorescence signal of the next point to be higher than the one before, although it should be—any mistakes can result in unreasonable curves. Therefore, a reasonable curve (the fluorescence signals increase with time and the “Blank” curve shows the slowest release) not only shows the insulin release information, but also shows that the experimental procedures (sample handling, liposome separation and fluorescence signal measurement, etc.) were done properly. The reproducibility of our data was also good.

From Figure 32, we can establish a list of samples from the minimum amount of released insulin from DPPC/Cholesterol liposomes to the maximum amount of released insulin, and comes in order “Blank”, “CPE-215 only”, “Cottonseed oil only”, “CSO emulsion”, “1:1 B-cyclodextrin: CPE-215” and “1:1 B-cyclodextrin :CSO”. The difference between “Cottonseed oil only” and “CSO emulsion” samples was really small, which shows that the difference in the oil droplet size of cottonseed oil did not make a difference in the insulin release profile. Since adding oil droplets is much easier than making oil emulsions, in the following experiments, cottonseed oil and mixture of CPE-215[®]/Cottonseed oil were added into DPPC/Cholesterol liposomes as large oil droplets.

This experiment showed again that adding β -cyclodextrin could further enhance the insulin release from liposomes and cottonseed oil had better membrane permeation enhancing effect than CPE-215[®]. CPE-215[®] is a good permeation enhancer, but needs a phase transfer carrier to increase its availability to the liposomes.

3.4.2. Insulin Release at 37 °C from DPPC/Cholesterol Liposomes with Different amount of CPE-215[®]

From the results of previous insulin release experiments with cyclodextrins, it seemed that the insulin release was controlled by the availability of CPE-215[®] to the liposomes, not by the amount of CPE-215[®] added into the release tube. If that conclusion is true, then under the same conditions, adding more CPE-215[®] into the release tube will not make the insulin release rate from liposomes faster, since the water is already saturated with CPE-215[®]. In order to test this theory, we designed a new release experiment.

This time, we used six release tubes. One was still used as blank control; one was used to see the permeation enhancing effect of β -cyclodextrin only, without CPE-215[®]; two were used to compare the insulin release rate with different amount of CPE-215[®]/Cottonseed oil mixture; the last two were used to compare the insulin release rate with different amount of CPE-215[®]/Cottonseed oil mixture with the same amount of β -cyclodextrin present.

In DPPC/Cholesterol liposome, weight ration of DPPC: cholesterol was still 4:1. The weight ratio of CPE-215[®]: cottonseed oil was still 3:1. In the "1X CPE&CSO" sample, molar ratio of CPE-215[®]: DPPC was 4:1; in the "3X CPE&CSO" sample, molar ratio of CPE-215[®]: DPPC was 12:1. In the "1XCPE&CSO+B-CD", molar ratio of β -cyclodextrin: CPE-215[®]: DPPC was 4:4:1; in the "3XCPE&CSO+B-CD" sample, molar ratio of β -cyclodextrin: CPE-215[®]: DPPC was 4:12:1. In the "B-CD only" sample, molar ratio of β -cyclodextrin:

DPPC was 4:1. A 50 mM pH 7 phosphate buffer was used to prepare these liposomes.

Table 3 Sample information in Section 3.4.2

Sample	CPE-215 [®] :Cottonseed oil (weight)	CPE-215 [®] :DPPC:β-CD (molar)
Blank	N/A	N/A
B-CD only	N/A	0:1:4
1X CPE&CSO	3:1	4:1:0
3X CPE&CSO	3:1	12:1:0
1XCPE&CSO+B-CD	3:1	4:1:4
3XCPE&CSO+B-CD	3:1	12:1:4

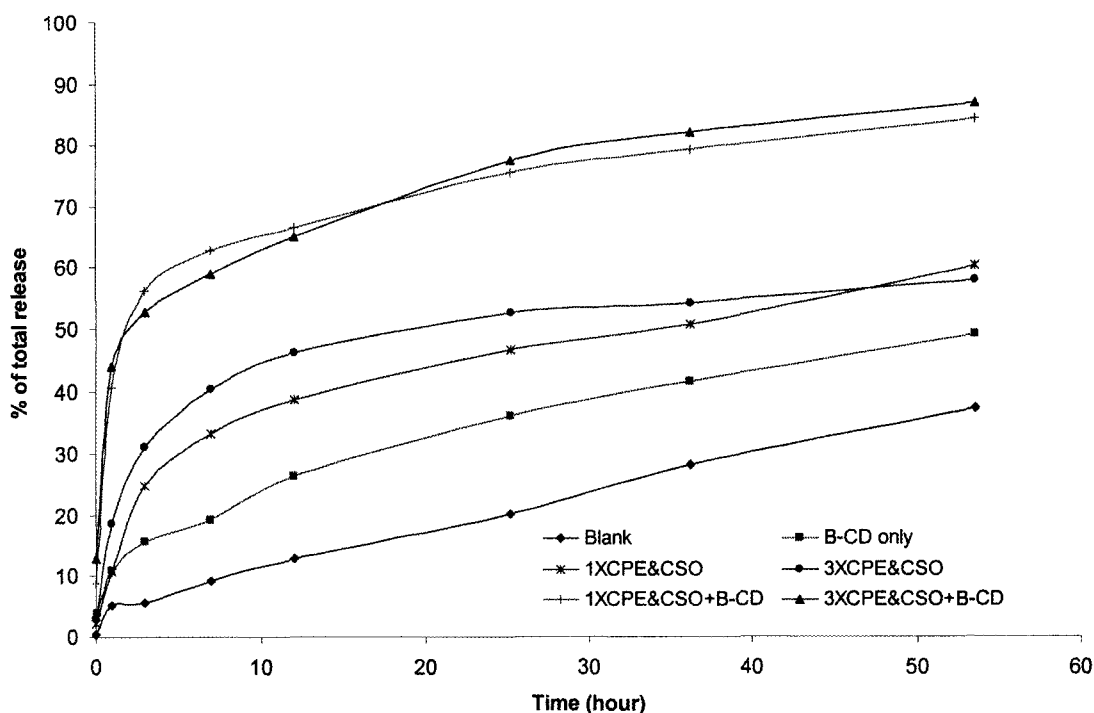


Figure 33 Insulin release at 37 °C from DPPC/Cholesterol liposomes with different amount of CPE-215[®]/Cottonseed oil at pH 7. The weight ratio of CPE-215[®]: cottonseed oil was still 3:1. In the “1X CPE&CSO” sample, molar ratio of CPE-215[®]: DPPC was 4:1; in the “3X CPE&CSO” sample, molar ratio of CPE-215[®]: DPPC was 12:1. In the “1XCPE&CSO+B-CD”, molar ratio of β -cyclodextrin: CPE-215[®]: DPPC was 4: 4:1; in the “3XCPE&CSO+B-CD” sample, molar ratio of β -cyclodextrin: CPE-215[®]: DPPC was 4:12:1. In the “B-CD only” sample, molar ratio of β -cyclodextrin: DPPC was 4:1.

Figure 33 showed the result of insulin release from DPPC/Cholesterol liposomes with different amount of CPE-215[®]/Cottonseed oil mixture at pH 7. The “Blank” sample showed a steady intrinsic insulin leakage rate from DPPC/Cholesterol liposomes. The other samples all showed a much higher insulin release rate than the “Blank” sample at the beginning, then the release rates decreased and finally the insulin release rates were similar to the blank

control. The “B-CD only” sample showed that β -cyclodextrin itself also had membrane permeation enhancing effect, but the faster release rate only lasted for about an hour, then went back down to the blank control rate. The “1XCPE&CSO” sample had almost the same starting release rate as the “B-CD only” sample, but lasted for a longer time, about 3 hours, then the rate went back down to the blank control rate. The “3XCPE&CSO” sample had a little bit faster starting release rate than the “1XCPE&CSO” sample, but not much. The “1XCPE&CSO+B-CD” sample and the “3XCPE&CSO+B-CD” sample had almost the same release profiles, though the amount of CPE-215[®]/Cottonseed oil in these two samples was different; their insulin release rate was much faster than the other samples. Obviously the fast insulin release rate was not due to the simple effects of β -cyclodextrin and CPE-215[®]/Cottonseed oil, but showed the synergy between β -cyclodextrin and CPE-215[®]/Cottonseed oil on the membrane permeation effect.

This experiment successfully supported the assumption that the insulin release was controlled by the availability of CPE-215[®] to the liposomes, not by the amount of CPE-215[®] added into the release tube. β -Cyclodextrin could increase the availability of hydrophobic CPE-215[®] to the aqueous phase, which resulted in great insulin release rate increases from “1XCPE&CSO” to “1XCPE&CSO+B-CD”, and from “3XCPE&CSO” to “3XCPE&CSO+B-CD”. With the same amount of β -cyclodextrin in the solution, which meant with the same amount of “transporters” available, different amount of CPE-215[®] results in the same insulin release rate.

3.5. Insulin Release from DPPC/Cholesterol Liposomes at Different pH

Twenty different amino acids are the elementary constituents of all natural proteins. Those amino acids can be grouped according to the characteristics of the side chains, such as acidic, basic, polar, and non-polar. Changing pH changes the charges on the acidic and basic amino acid side chains, and results in changes in the total charge of the protein: the higher the pH value, the more negative charge on the protein. For human insulin, the isoelectric point is around pH 5.3.⁹⁵ We wished to see the effect of pH on the insulin release rate from DPPC/Cholesterol liposomes. The change of pH could also affect the charge on the lipids and the liposome structure, but the charge on DPPC does not change in the pH range from 4 to pH 10.

3.5.1. Insulin Release from DPPC/Cholesterol Liposome at 37 °C with Small pH Gradient

We wanted to see what the insulin release profile would be when there is a pH gradient across the membrane (the insulin solution inside of liposomes at different pH value from the outside buffer solution). In this experiment, we tested three gradients (inside to outside of liposome): pH 7 to pH 5.7, pH 7 to pH 7, pH 7 to pH 8.2. There were two samples for each gradient: one as the blank release control, the other was added CPE-215[®]/cottonseed oil mixture and β -

cyclodextrin. However, the result was not what we expected. Finally we realized that it is hard to keep a pH gradient across the lipid bilayer.

When we prepared the 4:1 (w/w) DPPC/Cholesterol liposomes, 50 mM pH 7 phosphate buffer was used, so that the insulin solution inside of liposome was pH 7. When we did the centrifugal extractions at 4 °C, 50 mM pH 7 phosphate buffer was also used. Then 3 ml of concentrated liposomes were evenly distributed into six 15-ml plastic centrifuge tubes. In “pH 5.7 Blank”, 3.5 ml of pH 5 phosphate solution was added to 0.5 ml of pH 7 liposomes, the final pH turned out to be 5.7. In “pH 7 Blank”, 3.5 ml of pH 7 phosphate buffer was added to 0.5 ml of pH 7 liposomes. In “pH 8.2 Blank”, 3.5 ml of pH 9 phosphate solution was added to 0.5 ml of pH 7 liposomes, the final pH turned out to be 8.2. In “pH 5.7 C&C+B-CD”, 3.5 ml of 2% β -cyclodextrin pH 5 phosphate solution and mixture of CPE-215[®]/Cottonseed oil were added to 0.5 ml of pH 7 liposomes. In “pH 7 C&C+B-CD”, 3.5 ml of 2% β -cyclodextrin pH 7 phosphate solution and mixture of CPE-215[®]/Cottonseed oil were added to 0.5 ml of pH 7 liposomes. In “pH 8.2 C&C+B-CD”, 3.5 ml of 2% β -cyclodextrin pH 9 phosphate solution and mixture of CPE-215[®]/Cottonseed oil were added to 0.5 ml of pH 7 liposomes.

The weight ratio of CPE-215[®]: cottonseed oil was still 3:1. The molar ratio of CPE-215[®]: β -cyclodextrin: DPPC was 4:4:1.

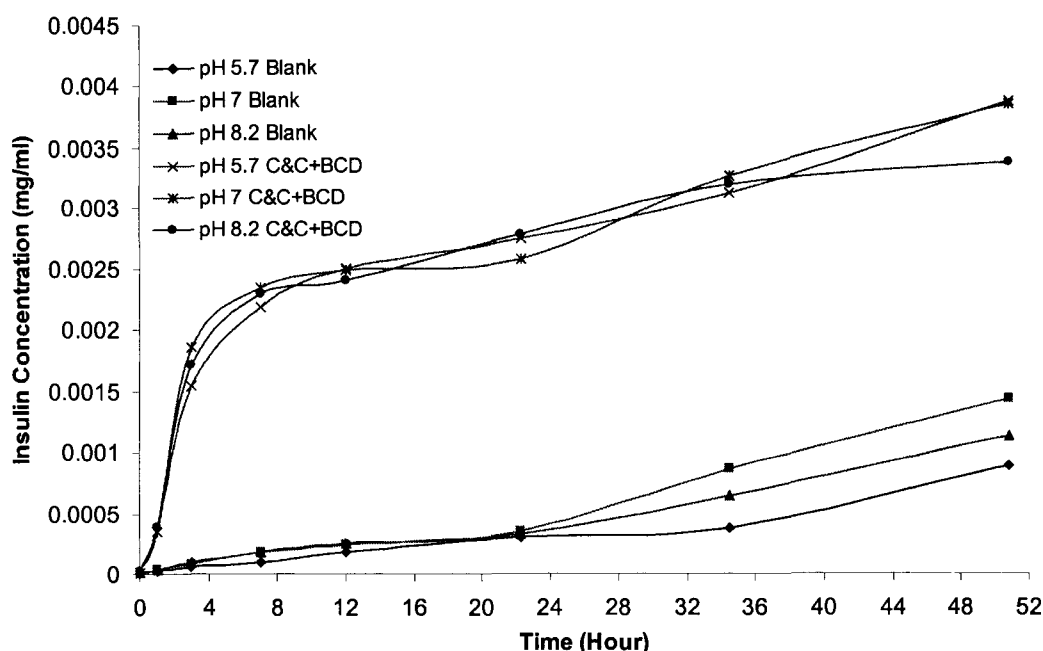


Figure 34 Insulin release at 37 °C from DPPC/Cholesterol liposomes at different pH gradients, inside pH is 7. The 100% insulin release point was 0.0045 mg/ml. We tested three gradients (inside to outside of liposome): pH 7 to pH 5.7, pH 7 to pH 7, pH 7 to pH 8.2. There were two samples for each gradient, one for the blank release control, the other was added CPE-215[®]/cottonseed oil mixture and β -cyclodextrin. The weight ratio of CPE-215[®]: cottonseed oil was still 3:1. The molar ratio of CPE-215[®]: β -cyclodextrin: DPPC was 4:4:1.

Figure 34 showed the result of insulin release from DPPC/Cholesterol liposomes at different pH gradients. To our surprise, it seemed that the pH gradients had no effect on the insulin release rate from liposomes: no matter at what pH gradient, all the blank control samples seemed to have the same insulin release rate, and all the samples with CPE-215[®]/Cottonseed oil and β -cyclodextrin had the same insulin release rate, too. The samples with CPE-215[®]/Cottonseed oil and β -cyclodextrin showed much faster insulin release rates at the beginning, similar to the previous release experiments at pH 7.

In Figure 34, instead of showing the percent of total insulin release in the Y-axis as before, insulin concentration was used as the Y-axis. The 100% insulin release point corresponded to the insulin concentration of 0.0045 mg/ml.

After some literature search on the membrane permeability to protons, I found that lipid bilayers are remarkably permeable to protons.⁹⁶ It is clear that proton permeability is at least 10^6 greater than for the other simple ions, and this is true for biomembranes as well as for model membranes.⁹⁷ Therefore, in our experiment, due to the great permeability of protons through membrane, there might not be a pH gradient between the inside and outside of liposomes, though we tried to establish one; the release results are likely to have shown the insulin release rates at pH around 6, 7 and 8, without pH gradients.

3.5.2. Insulin Release from DPPC/Cholesterol Liposome at 37 °C at pH 10

In order to find out how pH affects insulin release, we performed the insulin release from 4:1 (w/w) DPPC/Cholesterol liposomes at pH 10. At pH 10, insulin has a negative overall charge of about -5.

We did the liposome extrusion and the centrifugal extraction both at pH 10, so that we were certain there was no pH gradient from the inside to the outside of the liposome. The liposomes were evenly distributed into three 15-ml plastic centrifuge tubes. One tube was used as blank release control, one received a CPE-215[®]/Cottonseed oil mixture, the other one received a CPE-215[®]/Cottonseed oil mixture and β -cyclodextrin. The weight ratio of CPE-215[®]:

cottonseed oil was still 3:1. The molar ratio of CPE-215[®]: β -cyclodextrin: DPPC was 4:4:1.

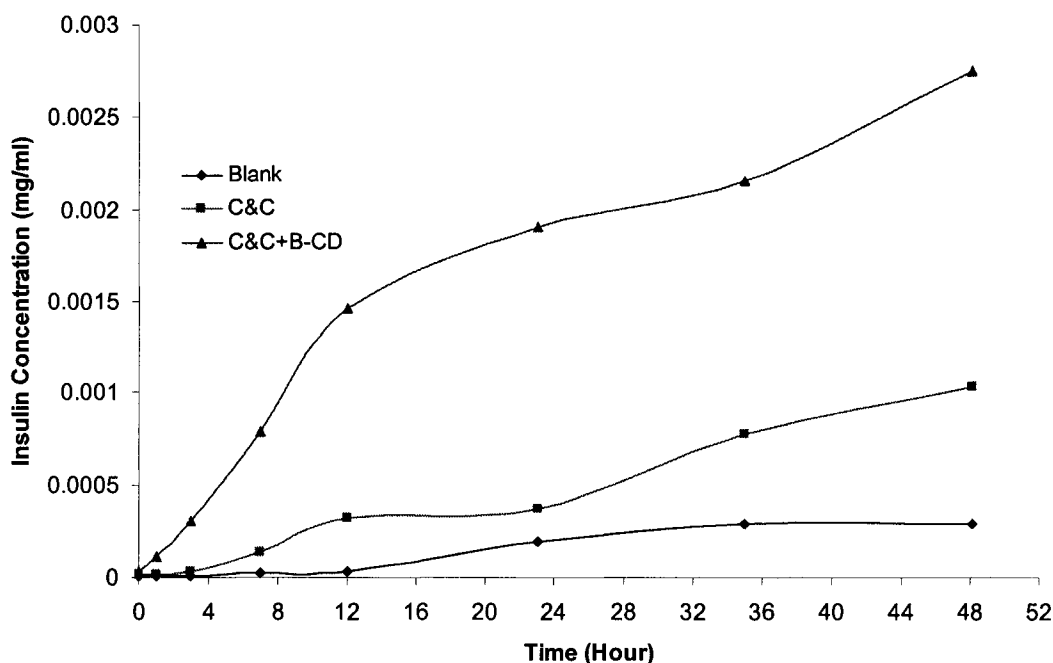


Figure 35 Insulin release at 37 °C from DPPC/Cholesterol liposome at pH 10. The 100% insulin release point was 0.003 mg/ml. The weight ratio of CPE-215[®]: cottonseed oil was still 3:1. The molar ratio of CPE-215[®]: β -cyclodextrin: DPPC was 4:4:1.

Figure 35 showed the result of insulin release from DPPC/Cholesterol liposomes at pH 10. Insulin concentration was used as the Y-axis. The 100% insulin release point corresponded to the insulin concentration of 0.003 mg/ml. Insulin release at pH 10 showed a similar trend: CPE-215[®]/Cottonseed oil mixture could make more insulin come out of liposomes; adding β -cyclodextrin

could further enhance the permeation effect of CPE-215[®]. However, compared with the release data at pH 7 (Figure 33), insulin release at pH 10 seems more difficult: slower release rate with low insulin blank release rate.

3.5.3. Insulin Release from DPPC/Cholesterol Liposome at 37 °C at pH 4

We also performed the insulin release from 4:1 (w/w) DPPC/Cholesterol liposomes at pH 4. At pH 10, insulin has a positive overall charge, about +3.

We carried out the liposome extrusion and the centrifugal extraction at pH 4, so that we were certain that there was no pH gradient. The liposomes were evenly distributed into three 15-ml plastic centrifuge tubes. One tube was used as blank release control; "C&C" received a CPE-215[®]/Cottonseed oil mixture; "C&C+B-CD" received a CPE-215[®]/Cottonseed oil mixture and β -cyclodextrin. The weight ratio of CPE-215[®]: cottonseed oil was 3:1. The molar ratio of CPE-215[®]: β -cyclodextrin: DPPC was 4:4:1.

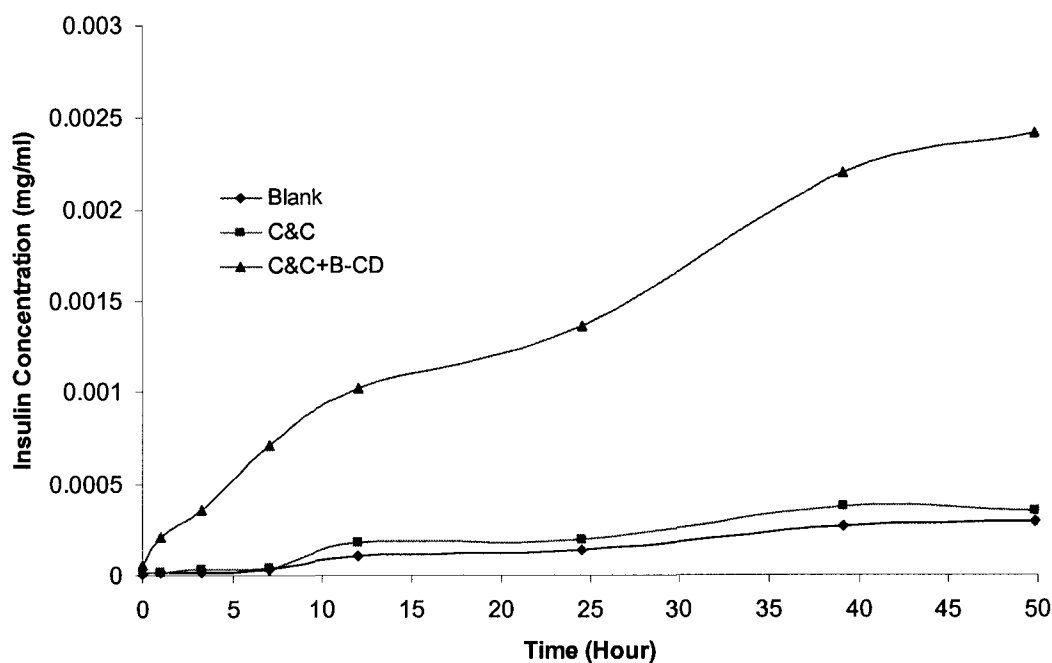


Figure 36 Insulin release at 37 °C from DPPC/Cholesterol liposome at pH 4. The 100% insulin release point was 0.003 mg/ml. The weight ratio of CPE-215[®]: cottonseed oil was 3:1. The molar ratio of CPE-215[®]: β -cyclodextrin: DPPC was 4:4:1.

Figure 36 showed the result of insulin release from DPPC/Cholesterol liposomes at pH 4. Insulin concentration was used as the Y-axis. The 100% insulin release point corresponded to the insulin concentration of 0.003 mg/ml. Insulin release curve of “C&C” was only a little higher than the release curve of “Blank”, but “C&C+B-CD” still showed much faster insulin release from liposomes. Comparing the release data at pH 4 (Figure 36) and pH 7 (Figure 33), we can see it is much harder for insulin to permeate through lipid bilayers at pH 4 than at pH 7, even with the help of CPE-215[®]/cottonseed oil and β -cyclodextrin.

3.6. BSA Release at 37 °C from DPPC/Cholesterol Liposomes at pH 7

Previously we used insulin molecules, which were tagged with fluorescence probes, to do the release experiments from liposomes with CPE-215[®], and found that liposomes are a good membrane model and CPE-215[®] is a good membrane permeation enhancer. To see if CPE-215[®] is protein kind and size specific, we used a larger protein instead of insulin (MW 6 KDa) to do another release experiment. Bovine serum albumin (BSA, MW 66 KDa) was selected to be the other model protein. In order to improve the detection sensitivity, again we used the fluorescence labeling process to attach a fluorescence probe to BSA.

We performed both the liposome extrusion and the centrifugal extraction at pH 7. The 4:1 (w/w) DPPC/Cholesterol liposomes were evenly distributed into three 15-ml plastic centrifuge tubes. One tube was used as the blank release control; in the "CPE" sample, CPE-215[®] solid was added; in the "CPE&CSO" sample, CPE-215[®]/Cottonseed oil mixture was added. The weight ratio of CPE-215[®]: cottonseed oil was 3:1. The molar ratio of CPE-215[®]: DPPC was 4:1.

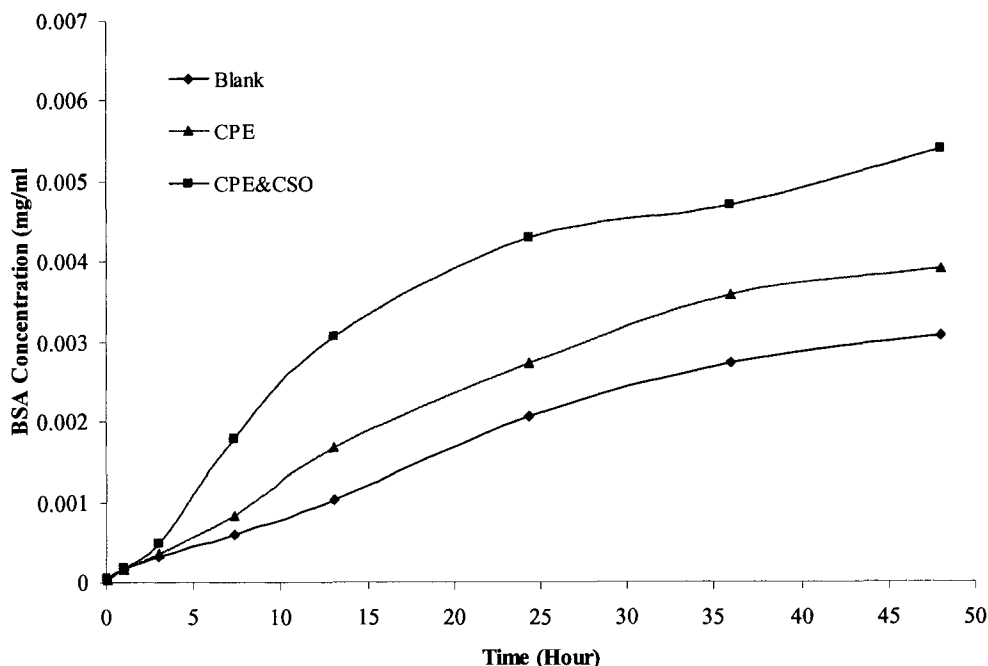


Figure 37 BSA release at 37 °C from DPPC/Cholesterol liposomes at pH 7. The 100% BSA release point was 0.007 mg/ml. The weight ratio of CPE-215[®]: cottonseed oil was 3:1. The molar ratio of CPE-215[®]: DPPC was 4:1. In the “CPE” sample, CPE-215[®] solid was added; in the “CPE&CSO” sample, CPE-215[®]/Cottonseed oil mixture was added.

Figure 37 showed the result of BSA release at 37 °C from DPPC/Cholesterol liposomes at pH 7. BSA concentration was used as the Y-axis. The 100% BSA release point was 0.007 mg/ml. The BSA release data showed that CPE-215[®] can also enhance the release of big proteins, for example 66 KDa BSA, through lipid bilayers. CPE-215[®]/Cottonseed oil mixture gave better result than CPE-215[®] alone, maybe because at 37 °C, most of CPE-215[®] is still a solid, making it less available to the liposomes than CPE-215[®]/Cottonseed oil mixture. The BSA release rate with CPE-215[®]/Cottonseed oil was slow at the beginning when compared with the insulin release data, which might be due to the larger size of BSA.

CHAPTER 4

RELEASE MECHANISM STUDY

The experiments of insulin release from liposomes have proved that CPE-215[®] is an effective membrane permeation enhancer. The next step is to investigate the mechanism behind the fact that CPE-215[®] facilitates the insulin transport through lipid bilayers. Studies focusing on the properties of our system were carried out, such as the insulin solution properties (self-diffusion and self-association states of insulin), the interaction between insulin and liposome and the interaction between CPE-215[®] and liposomes. Based on these studies and the experimental data, a hypothesis was proposed and the result of a special testing experiment proved the validity of the hypothesis for the protein release profile from liposomes.

4.1. Insulin Solution Properties

4.1.1. Insulin Diffusion Coefficient Measurement by NMR

Nuclear Magnetic Resonance (NMR) is a common non-destructive technique, which is widely used to obtain information on functional group analysis (chemical shifts), bonding connectivity and orientation (J coupling), through space connectivity (Overhauser effect), molecular conformations, DNA, peptide

and enzyme sequence and structure, etc. It can also be used to determine the self-diffusion coefficient by the spin-echo technique with pulsed field gradient.^{98,99}

Molecules in liquid or solution states move. This translational motion is, in contrast to rotational motion, known as Brownian molecular motion and is often simply called diffusion or self-diffusion. It depends on a lot of physical parameters such as size and shape of the molecule, temperature and viscosity. Assuming a globular or spherical shape for the molecule, the diffusion coefficient, D , is described by the Stokes-Einstein equation

$$D = \frac{kT}{6\pi\eta r_s} \quad [4.1]$$

where k is the Boltzmann constant, T the temperature, η the viscosity of the liquid and r_s the hydrodynamic radius of the molecule.

Pulsed field gradient NMR spectroscopy can be used to measure the translational diffusion coefficient of molecules and is sometimes referred to as q-space imaging. Through the use of a gradient, molecules can be spatially labeled, i.e. marked depending on their spatial position in the sample tube. If they move after this encoding during the following diffusion time Δ , their new position can be decoded by a second gradient. The measured signal is the integral over the whole sample volume and the NMR signal intensity is attenuated depending on the diffusion time Δ and the gradient parameters (g , δ). This intensity change is described by

$$I = I_0 \cdot e^{-D\gamma^2 g^2 \delta^2 (\Delta - \delta/3)} \quad [4.2]$$

where I is the observed intensity, I_0 the reference intensity (unattenuated signal intensity), D the diffusion coefficient, γ the gyromagnetic ratio of the observed nucleus, g the gradient strength, δ the length of the gradient, and Δ the diffusion time. If bipolar gradients are used for dephasing and rephasing, a correction for the time τ between those bipolar gradients has to be applied:

$$I = I_0 \cdot e^{-D\gamma^2 g^2 \delta^2 (\Delta - \delta/3 - \tau/2)} \quad [4.3]$$

Briefly, a spin echo pulse sequence is used in combination with a pair of gradients on both sides of the 180° pulse. The echo amplitude decay was measured and the value of the self-diffusion coefficient was determined from that signal.

Usually in NMR experiments, the higher the concentration, the better the signal/noise. We used low pH to dissolve more insulin in the NMR tube: deuterated hydrochloride acid was used to adjust D_2O to pH 3, which was near the pH value of the intranasal insulin formulations of Bentley Pharmaceuticals, and then insulin was dissolved to reach 2 mg/ml solution.

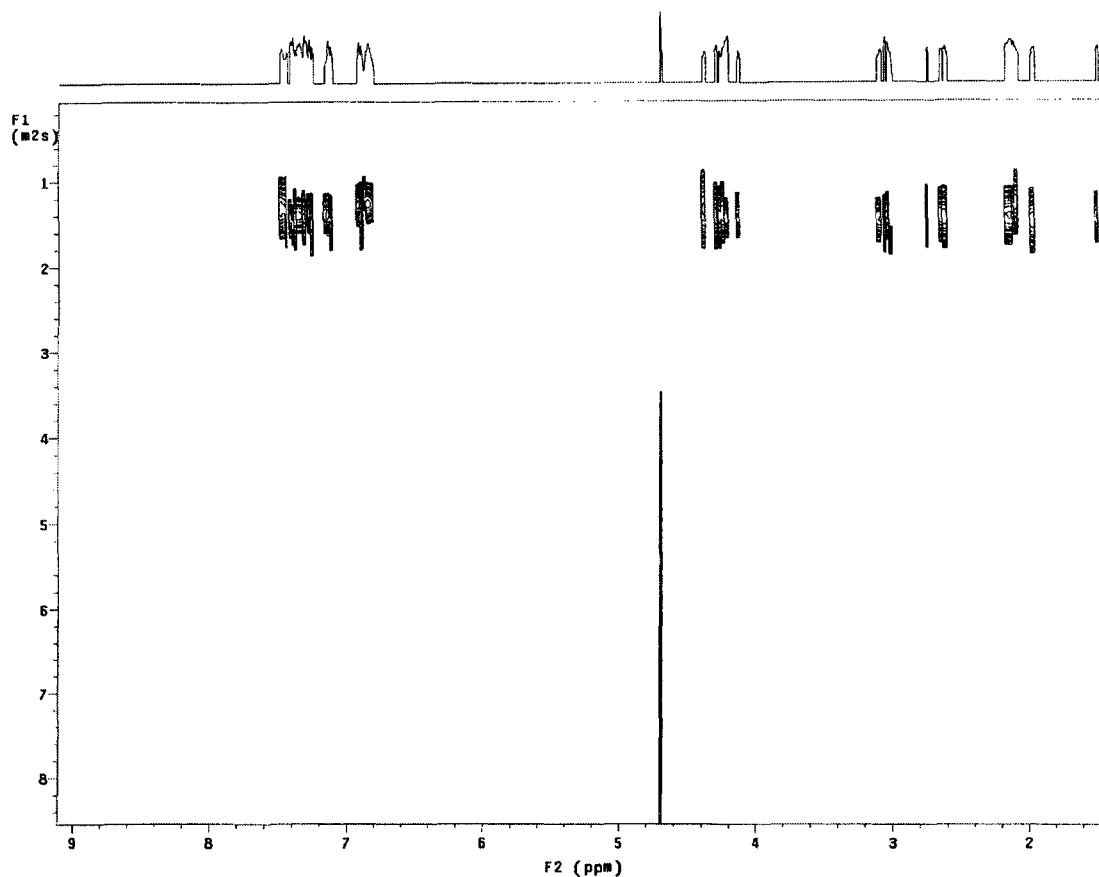


Figure 38 Insulin diffusion coefficient measurement by pulsed field gradient NMR at pH 3 at 37 °C. The X-axis shows the chemical shifts of ^1H NMR spectrum; the Y-axis shows the diffusion coefficient, the unit is $10^{-10} \text{ m}^2/\text{s}$, i.e. $10^{-6} \text{ cm}^2/\text{s}$.

Figure 38 shows the insulin diffusion coefficient measured by pulsed field gradient NMR at pH 3 at 37 °C. It is a 2D NMR spectrum: the X-axis shows the ^1H NMR spectrum, the value in the Y-axis corresponds to the diffusion coefficient of the molecule for that specific proton. This 2D NMR spectrum shows the diffusion coefficients of different protons in the solution; therefore, even if there are different molecules in the solution, as long as the chemical shifts can be identified individually, the diffusion coefficients of different molecules can be

obtained from the 2D DOSY NMR spectrum at the same time. In Figure 38, most protons have the diffusion coefficient of $1.4 \times 10^{-10} \text{ m}^2/\text{s}$, the other proton with a chemical shift at 4.7 ppm has a much faster and broader diffusion coefficient. Based on its chemical shift position and diffusion coefficient, the peak at 4.7 ppm should be due to the proton of water molecules. Insulin consists of 51 amino acids and should have a ^1H NMR spectrum with numerous peaks. Therefore, the remaining peaks in Figure 38 should belong to insulin, and insulin diffusion coefficient at pH 3 at 37°C is $1.4 \times 10^{-10} \text{ m}^2/\text{s}$, or $1.4 \times 10^{-6} \text{ cm}^2/\text{s}$.

Assuming the insulin molecule is a globular protein, from the Stokes-Einstein equation (Eq. [4.1]),

$$r_s = \frac{kT}{6\pi\eta D} \quad [4.4]$$

The viscosity for a dilute aqueous is approximately equal to that of water, which is approximately, 1.0 centipoise (cP) or $1.0 \times 10^{-3} \text{ Pa}\cdot\text{s}$. Thus, the hydrodynamic radius of insulin

$$r_s = \frac{(1.38 \times 10^{-23} \text{ J}\cdot\text{K}^{-1})(310\text{K})}{6\pi \cdot (1.0 \times 10^{-3} \text{ Pa}\cdot\text{s})(1.40 \times 10^{-10} \text{ m}^2 \cdot \text{s}^{-1})} = 1.6 \times 10^{-9} \text{ m} = 1.6 \text{ nm}$$

We calculate that the insulin at pH 3 at 2 mg/ml concentration at 37°C behaves like a globular protein with a radius of 1.6 nm or with a diameter of 3.2 nm.

Lin, et al. studied the insulin aggregates with pulsed-field gradient nuclear magnetic resonance spectroscopy at pH 9.4 at 25°C .¹⁰⁰ They found that at 4 mg/ml, the insulin dimer is the predominant species in the solution, the hydrodynamic diameters calculated for the dimer is 3.6 nm, and the diffusion

coefficient detected for the dimer by PFG NMR is $1.38 \times 10^{-6} \text{ cm}^2/\text{s}$ at 25 °C, which is similar to our result at pH 3.

4.1.2. Using the Analytical Ultracentrifugation to Determine the Insulin Association State

Human insulin exists in different association states, from monomer to hexamer, depending on the conditions.^{101,102,103} In the presence of zinc, the "normal" state is a hexamer. Zinc ions are not involved in dimer formation but are involved in the association of dimers to give the hexamer.¹⁰⁴ Zinc-free insulin can have different aggregation levels, six monomers ↔ three dimers ↔ one hexamer, or monomer ↔ dimer ↔ tetramer ↔ hexamer.¹⁰⁵ We would like to identify the insulin association state under our release condition for the modeling work; and we used the Analytical Ultracentrifugation to do so.

Analytical Ultracentrifugation (AUC) is a very versatile and powerful technique for characterizing the solution-state behavior of macromolecules. It provides a primary method to determine protein molecular weight and size. Using ultracentrifuge to determine protein molecular weight can be traced back to 1920s.¹⁰⁶ The concentration dependence of the molecular weight can provide the same thermodynamic information as light scattering. The rate of movement of molecules provides hydrodynamic size information. The subunit stoichiometry of a protein complex can be calculated from the determined molecular weight. Depending on the quality of the data, this determination can be very accurate; for example, it can be easily established whether the native conformation of a

protein is a dimer, trimer or tetramer. Information about the shape and the conformation of a protein as well as the interaction between macromolecules can be obtained from the sedimentation and diffusion coefficients obtained from a sedimentation velocity experiment.

An analytical ultracentrifuge can be viewed as a combination of a preparative ultracentrifuge and an optical detection system that is capable of directly measuring the sample concentration inside the centrifuge cell during sedimentation. The analytical ultracentrifuge at UNH is a Beckman Optima XL-A. The instrument spins the protein sample at a controlled speed and temperature while at set times recording the spatial concentration distribution. Depending on the rotor, the speed may be as high as 60,000 rpm (which is equivalent to 250,000 x g).

One common type of experiment performed in an analytical ultracentrifuge is sedimentation velocity. Sedimentation velocity is a hydrodynamic technique and is sensitive to the mass and shape of the macromolecular species. In a sedimentation velocity experiment, an initially uniform solution is placed in the cell and a high speed is used to cause rapid sedimentation of solute towards the cell bottom. This produces a depletion of solute near the top solution meniscus and the formation of a sharp boundary between the depleted region and the uniform concentration of sedimenting solute (the plateau) (Figure 39). The rate of movement of this boundary can be measured, which leads to the determination of the sedimentation coefficients.

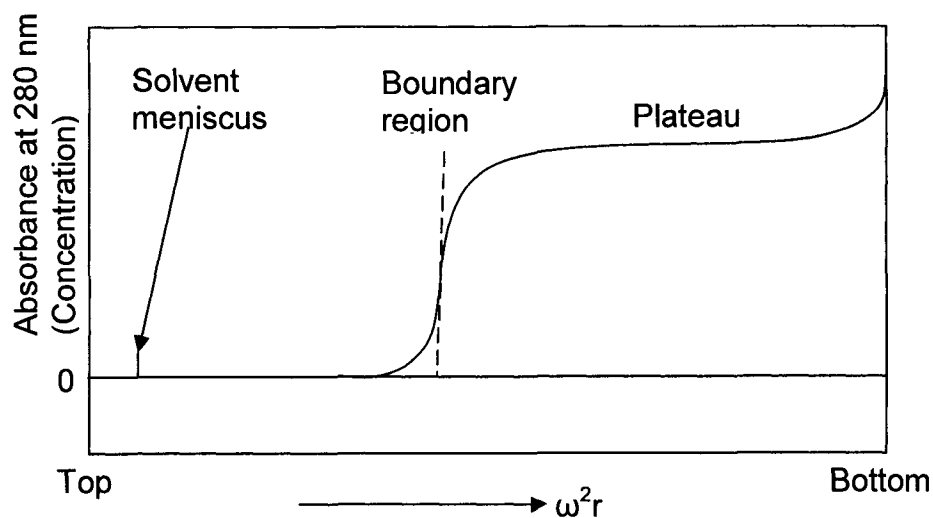


Figure 39 Schematic representation of the solute concentration distribution in the centrifuge cell in a sedimentation velocity experiment.

At their isoelectric points, proteins have the lowest solubility; from their isoelectric points, either raising or lowering the pH, the protein solubility increases. Insulin does not have good solubility at neutral pH, but the ultracentrifugation experiment usually requires a protein concentration of 1 mg/ml. Therefore, we prepared a 1 mg/ml insulin in 50 mM citric acid buffer with 100 mM KCl at pH 3.3, which was also the pH value Bentley Pharmaceutical, Inc. used for their intranasal insulin formulations. Before the ultracentrifugation, the insulin sample was dialyzed for 10 hours with the pH 3.3 citric acid buffer, which was used to dilute the insulin solution later on, to make sure the ionic strengths in the insulin sample and citric acid buffer were the same. Part of the 1 mg/ml insulin sample was diluted to make a 0.5 mg/ml insulin sample (1:2 dilution) and a 0.25 mg/ml insulin sample (1:4 dilution). Then we used the Beckman Optima

XL-A ultracentrifuge at 55,000 rpm and 20 °C to run the sedimentation velocity experiment.

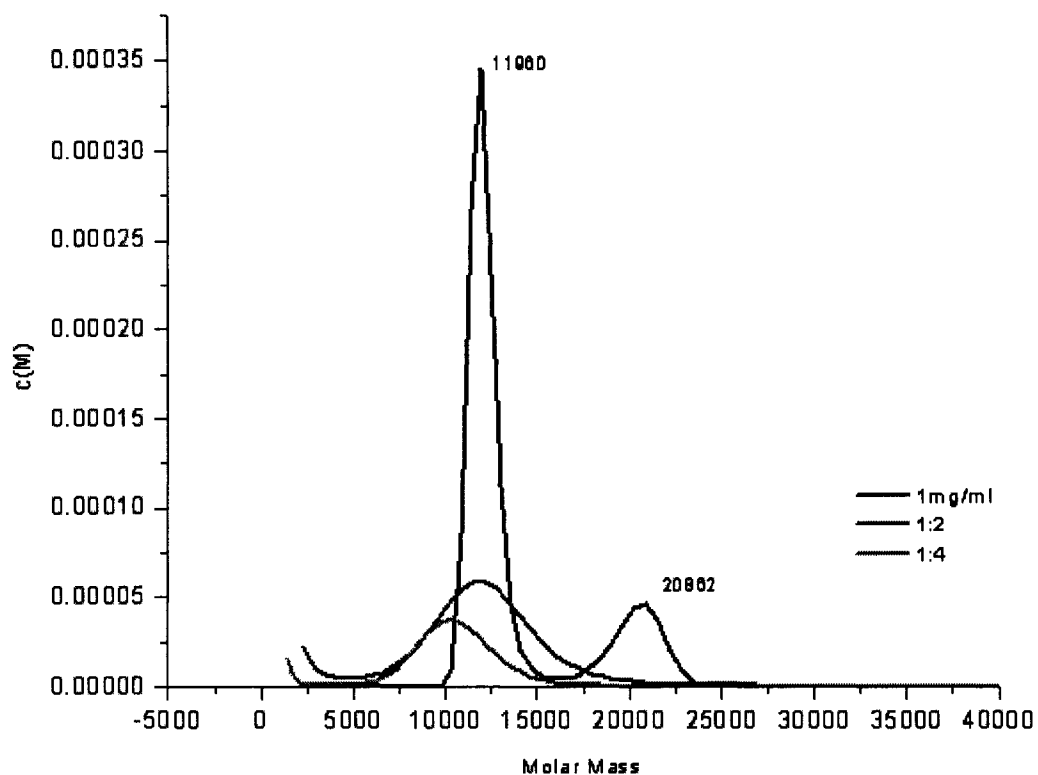


Figure 40 Result of insulin sedimentation velocity experiment of analytical ultracentrifugation at 20 °C. The three curves show the molecular weight distribution of different insulin species in 1 mg/ml, 0.5 mg/ml (1:2 dilution) and 0.25 mg/ml (1:4 dilution) insulin buffer solutions at pH 3.3. The buffer was 50 mM citric acid buffer with 100 mM KCl.

Figure 40 shows the result of the insulin sedimentation velocity experiment. Due to the complex nature of analytical ultracentrifugation, the result shall be interpreted carefully. Peaks in sedimentation velocity diagram have no meanings, and multiple peaks only indicate that the stoichiometry of insulin is

larger than two, which indicates the presence of higher association states of insulin than insulin monomer.

4.2. CPE-215[®] Interaction with Liposome (Membrane)

4.2.1. Introduction

CPE-215[®] is a general-purpose membrane permeation enhancer for protein delivery, which means it is not focusing on specific proteins but interacting with the lipid phase of membranes in general. CPE-215[®] is a hydrophobic molecule, and it interacts with the hydrophobic chains of lipids inside the membranes.

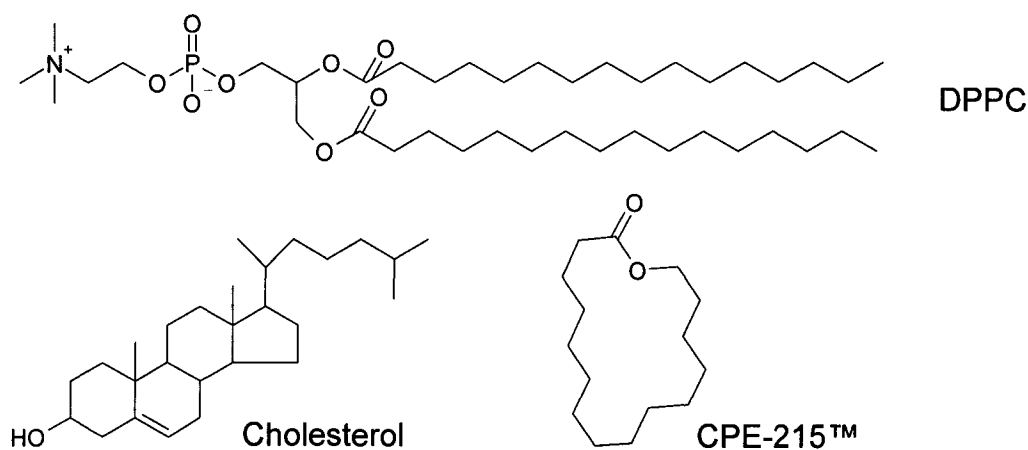


Figure 41 Molecular structure of DPPC, Cholesterol and CPE-215[®].

Figure 41 shows the structure of the three molecules that we focused on in the interaction study between CPE-215[®] and liposome: DPPC was the phospholipid used to form lipid bilayers and liposomes, cholesterol was inserted into the DPPC lipid bilayer to change the fluidity of the lipids, CPE-215[®] was the membrane permeation enhancer.

Lipid bilayers have different phases. The lamellar gel phase is formed at low temperature; the molecules are packed tightly together and the acyl chains are highly ordered, corresponding to the all-*trans* configuration found in the structure of lipid crystals. In lamellar liquid crystalline phase, there is two-dimensional order, but there is considerable disorder in the acyl chains, characterized by *gauche* conformation.¹⁰⁷ The lipid phase transition between the lamellar gel and liquid crystalline phases can be thermally induced, and the phase transition temperature (T_c) is unique to each lipid.

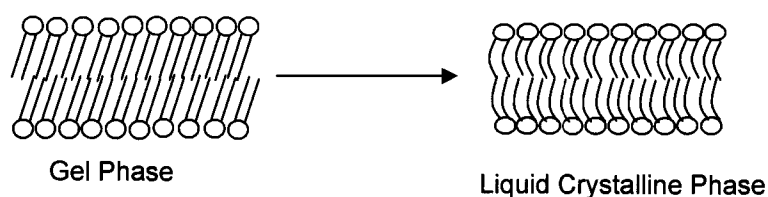


Figure 42 Phosphatidyl Choline lipid bilayer phase transition¹⁰⁸.

The technique commonly applied to determine the lipid phase transition temperature is differential scanning calorimetry (DSC).^{109,110,111,112} It is used to

monitor and characterize changes in physical state in polymorphic lipids and also to characterize the perturbations on pure lipids by the interactions with other materials, such as other lipids, proteins, ions, or small hydrophobic molecules. In DSC, a sample and inert reference are heated independently to maintain an identical temperature in each. The endothermic gel-to-liquid crystalline bilayer transition requires an excess heat over the heat required to maintain the same temperature in the reference. Differential heat flow is then plotted as a function of temperature.

Modulated DSC™ (MDSC®) is a new technique which provides not only the same information as conventional DSC, but also provides unique information not available from conventional DSC by overcoming most of the limitations of conventional DSC.^{113,114} In MDSC, the same “heat flux” cell design is used; however, a different heating profile is applied to the sample and reference. Specifically, a sinusoidal modulation (oscillation) is overlaid on the conventional linear heating or cooling ramp to yield a profile in which the average sample temperature continuously changes with time. The heat capacity (reversible) component of the total heat flow follows the oscillation and can be separated from the kinetic (non- reversible) component of the total heat flow by Fourier Transform. Therefore, more accurate phase transition information can be obtained by MDSC. Furthermore, different from traditional DSC, MDSC can give increased resolution of transitions without loss of sensitivity.

4.2.2. Experiment Design

Earlier, we showed that CPE-215[®] does have a permeation enhancing effect helping insulin go through lipid bilayers. In absence of the permeation enhancer, insulin is not likely to go easily through the membrane by itself. As the membrane permeation enhancer, CPE-215[®] is supposed to interact with the membrane in order to facilitate the crossing of insulin. We wanted to better understand what happens to the membrane in the presence of CPE-215[®].

For a thermal study, the size of the liposome does not need to be narrowly distributed. In that case, all the liposomes used here were made by bath-type sonication at 50 °C for 5 minutes, not by extrusion.

CPE-215[®] is a hydrophobic molecule, and it must interact with the lipid bilayers in order to act as a permeation enhancer. We would like to know if CPE-215[®] molecules formed CPE-215[®] domains inside the lipid bilayers or if they were evenly distributed in the DPPC liposomes and formed a new kind of liposome. First, we mixed CPE-215[®] with DPPC before preparing the liposome, and then we compared the thermal property of this new DPPC/CPE liposome with standard DPPC liposome. We also mixed CPE-215[®] with DPPC and cholesterol before preparing the liposome and compared the thermal property of this DPPC/Cholesterol/CPE-215[®] liposome with the DPPC/Cholesterol liposomes. For convenience, DPPC liposome was called Liposome D, DPPC/CPE liposome was called Liposome DC, DPPC/Cholesterol liposome was called Liposome DH, and DPPC/Cholesterol/CPE-215[®] liposome was called Liposome DHC.

In our insulin release experiment, CPE-215[®] was added outside of the liposomes containing insulin. Therefore, in another experiment, we made Liposome D first and then put CPE-215[®] together with Liposome D and let the MDSC perform multiple heating-cooling cycles. Although CPE-215[®] is hydrophobic, it still has some minimal solubility in water and its solubility increases with temperature. With the increase of temperature, more and more CPE-215[®] can go into the aqueous phase; while when the temperature cools down, super-saturated CPE-215[®] needs to come out of the aqueous phase, and some will reach the liposomes and enter inside the hydrophobic bilayers. With multiple cycles of heating and cooling, conceptually we can see the change of the DPPC liposome thermal properties with CPE-215[®] slowly diffusing into these liposomes. CPE-215[®] has a melting point of 34 °C, which is very close to the liposome phase transition temperature; in order to reduce such interference, we used 2:1 (w/w) mixture of CPE-215[®]/cottonseed oil instead of pure CPE-215[®] (Figure 45), which had no thermal transition above 20 °C. We also run the same experiment with the Liposome DH.

4.2.3. Experimental Section

The DSC instrument was a Modulated DSC Q100 from TA Instruments, Inc. Liposomes were made by sonication. Lipids (DPPC, cholesterol, CPE-215[®]) were mixed and dissolved in chloroform in 50-ml flask, and then dried at reduced pressure with a Rotavapor at room temperature for 6 hours to form a lipid film on the flask wall. The lipid film was hydrated with 10 ml of 50 mM pH 7 phosphate

buffer at 50 °C and then sonicated for 5 minutes in the bath-type sonicator to make liposomes. Then the liposomes were concentrated by centrifugation at 900 g for 30 minutes.

The liposomes were sealed in an aluminum pan to measure the liposome phase transition. After the DSC experiment, a hole was punched in the pan cover and the pan was kept at 70 °C for 5 hours to let the inside water evaporate, finally the weight of dry lipid was obtained. Four different liposomes were characterized for their phase transitions. Table 4 shows the compositions of these four liposomes.

Table 4. Composition of different liposomes.

	Liposome D	Liposome DC	Liposome DH	Liposome DHC
Components weight ratio	N/A	DPPC/CPE 4:1	DPPC/Cholesterol 4:1	DPPC/Cholesterol/CPE 4:1:1
Weight (mg)	5.9	7.5	14.6	12.9
Weight after drying (mg)	1.5	2.8	3.1	3.9
Lipid content	25%	37%	21%	30%

The MDSC in our lab is a Modulated DSC Q100 from TA Instruments, Inc. The following MDSC sequence was used for the purpose of measuring the lipid bilayer phase transition temperature:

1. initial temp at 25 °C
2. equilibrium at 5 °C

3. modulate ± 1 °C/60 sec
4. isotherm for 7 min
5. ramp 5 °C/min to 100 °C
6. isotherm for 2 min

For the multiple heating-cooling experiment of liposomes with CPE-215[®]/cottonseed oil mixture, concentrated liposomes and 2:1 (weight) CPE-215[®]/cottonseed oil mixture were sealed in an aluminum pan and heated from 5 °C to 90 °C for several times. Table 5 shows the different liposomes for the multi-heating-cycle experiment.

Table 5. Different liposomes for multiple-heating-cycle experiment.

	Liposome D only	Liposome D with oil	Liposome DH with oil
CPE/cottonseed oil 2:1 (w/w) (mg)	N/A	2.9	1.6
Liposome (mg)	23.1	19.2	10.1
# of heating cycles	4	25	8

The multiple-heating-cooling program is listed below:

1. initial temp at 25 °C
2. equilibrate at 5 °C
3. modulate ± 0.796 °C/60 sec (heat only)
4. isotherm for 6 min

5. ramp 5 °C/min to 90 °C
6. isotherm for 2 min
7. Repeat from Step 2

In order to see the effect of 2:1 CPE-215[®]/cottonseed oil on the DPPC liposome phase transition DSC curve, 11.9 mg 2:1 CPE-215[®]/cottonseed oil mixture was sealed in an aluminum pan and the thermal scan from 10 °C to 80 °C (modulation \pm 1 °C/60 sec, ramp 5 °C/min) was recorded.

4.2.4. Results and Discussion

The modulated DSC experiments were done for different types of liposomes: Liposome D (DPPC liposome), Liposome DC (DPPC/CPE-215[®] liposome), Liposome DH (DPPC/Cholesterol liposome) and Liposome DHC (DPPC/Cholesterol/CPE-215[®] liposome). Figure 43 and 44 showed the resulting curves. The lipid bilayer phase transition is a reversible, first-order transition; therefore the figures in this section (Figure 43 to Figure 51) show only the reversible heat flow by removing the kinetic (non- reversible) component from the total heat flow.

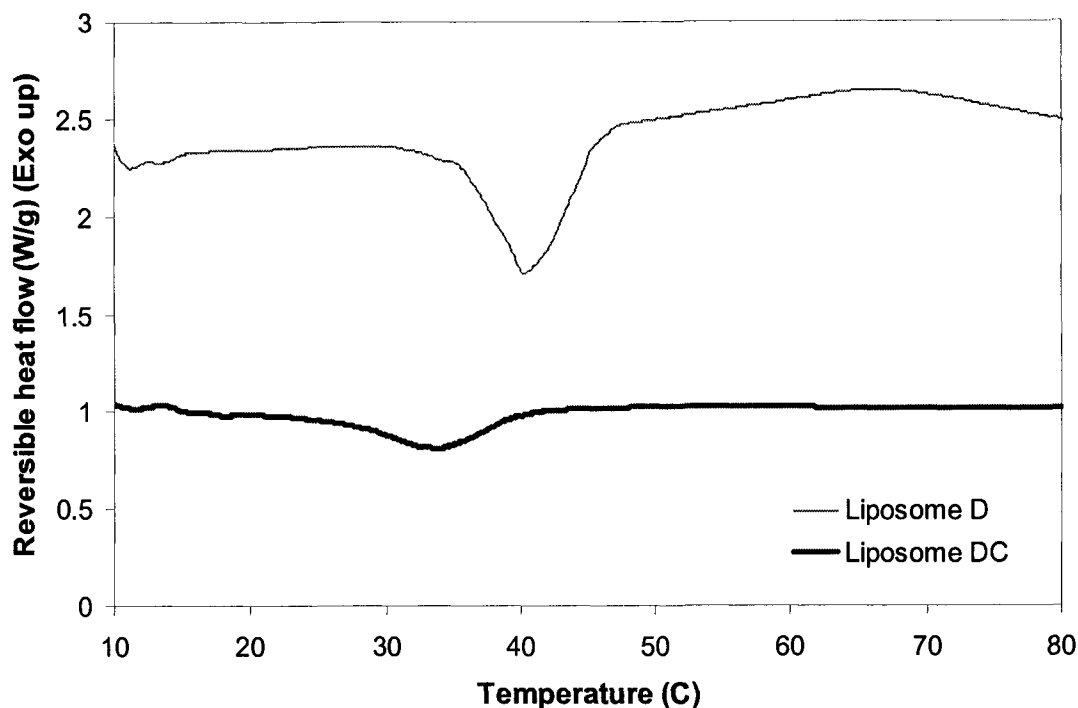


Figure 43 DSC of Liposome D (DPPC liposome) and Liposome DC (DPPC/CPE-215[®] liposome) (exothermal up).

The DSC of Liposome D showed a phase transition temperature at 42 °C (we conveniently took the peak temperature as the phase transition temperature), which was similar to the literature value.¹⁰⁸ The phase transition of highly purified DPPC should be sharp, but in Figure 43, the phase transition peak seemed a little broad, which may be due to minor impurities in the lipid.

The reversible heat flow of Liposome DC (4:1 (w/w) DPPC/CPE-215[®]) showed one broad endothermic peak with the peak value of 34 °C (in our Liposome DC, the molar ratio of DPPC: CPE-215[®] was 1.3). Compared with the reversible heat flow curve of Liposome D, the phase transition temperature of Liposome D was lowered by incorporating CPE-215[®] with DPPC in the

liposomes. Since there was no endothermic peak at 42 °C in the reversible heat flow curve of Liposome DC, there should be no DPPC domains in Liposome DC, or at least the gathering of DPPC in Liposome DC was not significant enough to initiate an endothermic peak in the DSC heat flow curve. As to the question of whether CPE-215[®] formed domains in Liposome DC, unfortunately this could not be answered based on Figure 44 alone because the CPE-215[®] itself has a melting point of 34 °C, the same temperature as the phase transition temperature of Liposome DC. Even if there were CPE-215[®] domains inside, the CPE-215[®] melting peak would be covered by the broad liposome phase transition.

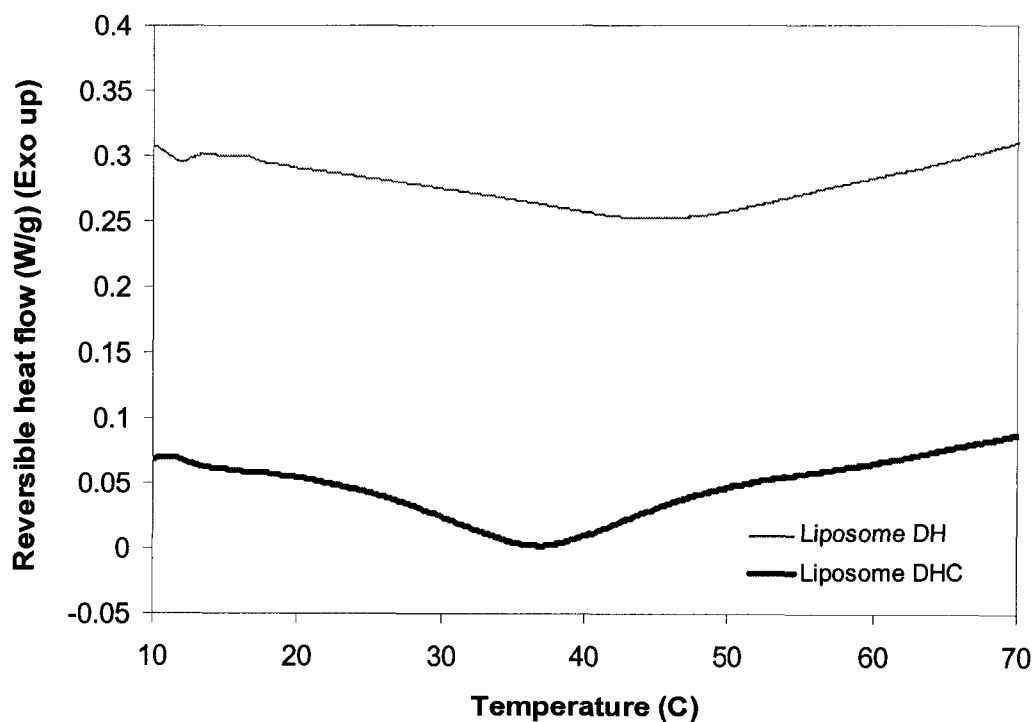


Figure 44 DSC of Liposome DH (DPPC/Cholesterol liposome) and Liposome DHC (DPPC/Cholesterol/CPE liposome) (exothermal up).

Cholesterol is a common lipid in natural membranes. Therefore, we also used Liposome DH (4:1 (w/w) DPPC/cholesterol) as the membrane model and incorporated CPE-215[®] inside to see if the phase transition temperature was also lowered after the addition of CPE-215[®]. Figure 44 showed the modulated DSC reversible heat flow curves of Liposome DH and Liposome DHC (4:1:1 (w/w/w) DPPC/cholesterol/CPE-215[®]), and the phase transition temperatures were 46 °C and 37 °C respectively. Cholesterol made the phase transition of DPPC liposome broader and increased its average value, while CPE-215[®] lowered the liposome phase transition temperature. Figure 44 also showed that there were no CPE-215[®] domains in the final liposome, CPE-215[®] and cholesterol were evenly distributed in the DPPC liposome and formed a liposome with new thermal property.

Among the phase transition peaks of Liposome D, Liposome DC and Liposome DH, the phase transition of Liposome DH was the broadest, the phase transition of Liposome D was the narrowest, while the broadness of the phase transition peak of Liposome DC was intermediate. This might be due to the structure of cholesterol and CPE-215[®] molecules. Cholesterol is a compact, rigid hydrophobic entity with a polar hydroxyl group. With cholesterol in the liposome bilayer, it is difficult for the DPPC lipid to pack the hydrocarbon chains next to the rigid sterol moiety. In the liquid crystalline state, the sterol results in conformational constraints on the phospholipid chain, whereas in the gel state the sterol inhibits optimal packing of the all-*trans* chain configuration. The result is that lipid-cholesterol mixtures behave as intermediate between the gel and

liquid crystalline states of the pure phospholipid, which explains the broadness of the phase transition of Liposome DH. Basically, cholesterol acts as a “spacer” and reduces the attractive forces between the lipid hydrocarbon chains.

Compared to cholesterol, CPE-215[®] is a more flexible lactone of a 16-membered ring and can cooperate better with phospholipid hydrocarbon chains. In the gel phase, the CPE-215[®] can change its conformation so that the phospholipid hydrocarbon chains can pack mostly as *trans* conformation; in the liquid crystalline phase, CPE-215[®] can also change its conformation to minimize the interference with the *gauche* packing of the phospholipid hydrocarbon chains. This can explain why the phase transition of DPPC/CPE-215[®] liposome is narrower than that of Liposome DH. Cholesterol’s rigidity and CPE-215[®]’s flexibility may also account for the phase transition temperature change of the liposomes.

In our insulin release experiments, we started with DPPC (or DPPC/Cholesterol) liposomes and CPE-215[®] was added outside of liposomes; with CPE-215[®] continuously contacted with liposomes and went into the lipid bilayer, Liposome D (or DH) became Liposome DC (or DHC). From Figure 44 and 44, we only learned that the phase transition temperature of Liposome DC (4:1 (w/w) DPPC/CPE-215[®]) was lower than that of Liposome D, but we would also like to know how the DPPC liposome phase transition temperature changed while CPE-215[®] was gradually incorporated inside (Did the phase transition temperature decrease continuously? Or did the phase transition temperatures not change, just the old peak decreasing and the new peak increasing?) It is

similar to the situation that after we discovered the starting point A and the end point B, we would also like to know how to get to B from A.

In order to make CPE-215[®] go into the liposome gradually, we planned to seal the Liposome D with CPE-215[®] inside a 50- μ l aluminum pan with a cover and heat it from 5 °C to 90 °C for multiple cycles with the modulated DSC. Although CPE-215[®] is hydrophobic and has little solubility in water, its solubility can increase with temperature. With the increase of temperature, more and more CPE-215[®] can go into the aqueous phase; while when the temperature cools down, super-saturated CPE-215[®] needs to get out of the aqueous phase, and some will find the liposomes and go inside of bilayers. With multiple cycles of heating and cooling, CPE-215[®] will gradually transport into the lipid bilayers, and we will monitor this continuous change by the modulated DSC. In this experiment, we did not want the sealed mixture to have any thermal phase change, except the liposome phase transition itself, from 20 °C to 60 °C. Due to the melting point of CPE-215[®] at 34 °C, we could not use the pure CPE-215[®] with Liposome D. We found that the mixture of 2:1 (w/w) CPE-215[®]/cottonseed oil did not have thermal phase change from 20 °C to 60 °C (Figure 45), so that we used 2:1 CPE-215[®]/cottonseed oil instead.

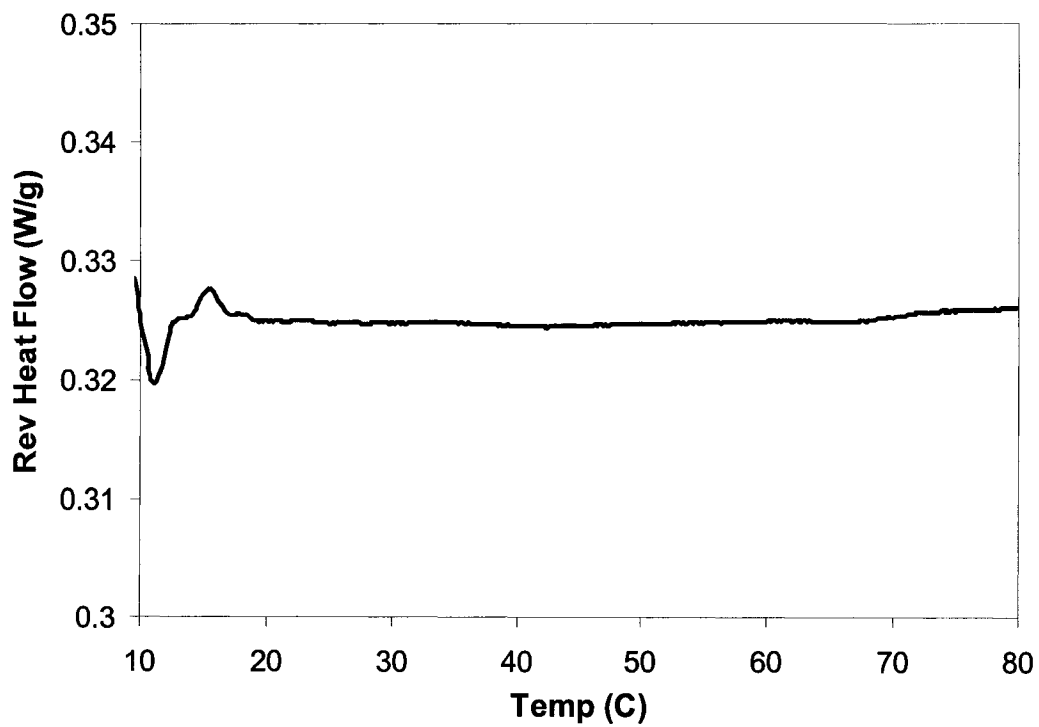


Figure 45 DSC of 2:1 (w/w) CPE-215[®]: cottonseed oil (exothermal up).

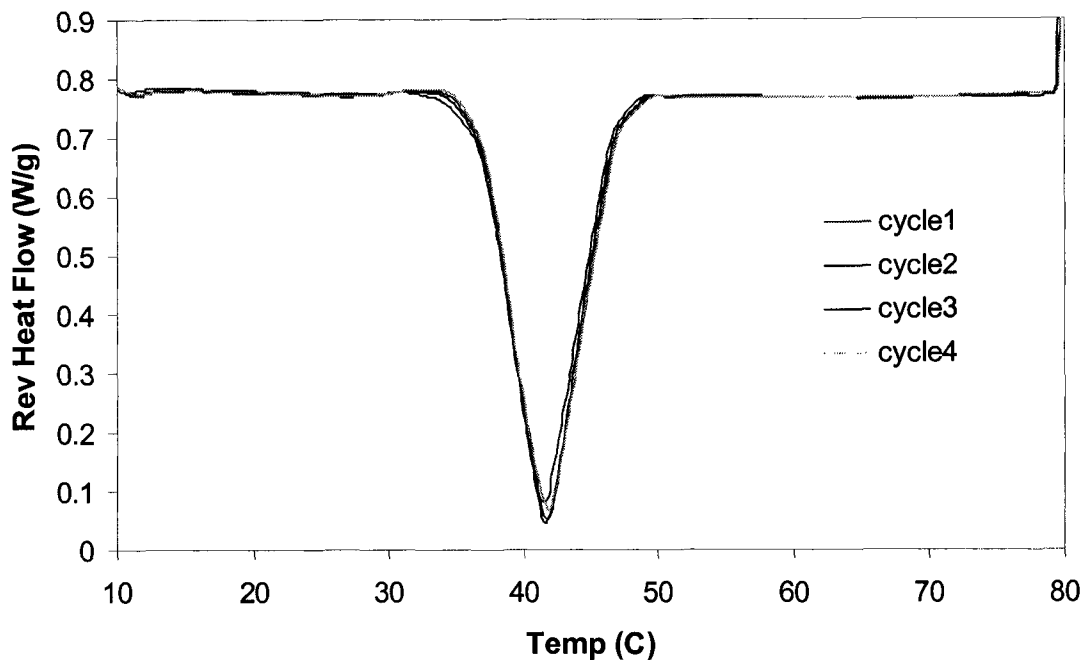


Figure 46 Four heating cycles of Liposome D (DPPC liposome) (exothermal up).

Figure 46 was the reversible heat flow of modulated DSC of four heating cycles of Liposome D. This showed that the phase transition of Liposome D was reversible, transition peak size and position did not change with the number of heating cycles if there was no outside interference. In other words, if the lipid bilayer structure/composition did not change, the phase transition peak size and temperature would not change; if the phase transition size and temperature changed, then there must be changes in the lipid bilayer structure or composition.

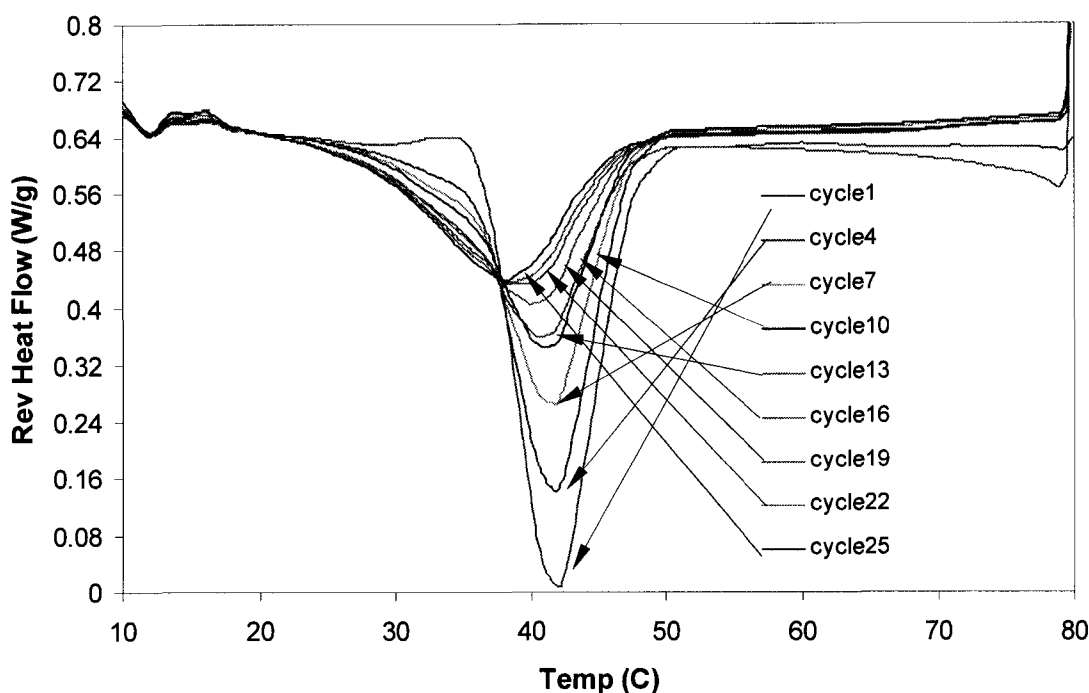


Figure 47 25 heating cycles of Liposome D (DPPC liposome) with CPE-215[®]/cottonseed oil mixture.

Figure 47 shows the result of the multiple heating and cooling of Liposome D and 2:1 (w/w) CPE-215[®]/cottonseed oil mixture. The reduction of the heat of the phase transition and the decrease of the transition temperature are interpreted to be due to CPE-215[®] gradually diffusing inside of DPPC lipid bilayers. Since there was no endothermic peak increasing around 34 °C (mp of CPE-215[®]) and only the whole liposome phase transition peak shifted to low temperature during the cyclic process, we concluded that CPE-215[®] was evenly distributed in liposomes from the beginning, which was thermodynamically favored. If we looked at Figure 47 in detail, we could find that with the number of heating cycles increasing, the starting temperature of the phase transition

decreased, while the ending temperature of the phase transition almost did not change. This meant with more and more CPE-215[®] gradually inserted into the DPPC liposome, lower temperature was required to make the system deviate from ordered packing state, but the same high temperature was still needed to get the whole system away from ordered packing. CPE-215[®] is a small flexible molecule, its gradual insertion into the DPPC lipid bilayer disturbed the *all-trans* ordered packing of phospholipid hydrocarbon chains in the gel state, which resulted in lower starting temperature of the liposome phase transition. However, since the majority was still DPPC lipid, each time the same high temperature was still needed to get all the DPPC chains in the *gauche* conformation to reach the liquid crystalline state.

Figure 48 showed how the liposome phase transition temperature changed with the number of heating cycles, which decreased almost linearly at the beginning and reached a plateau in the end.

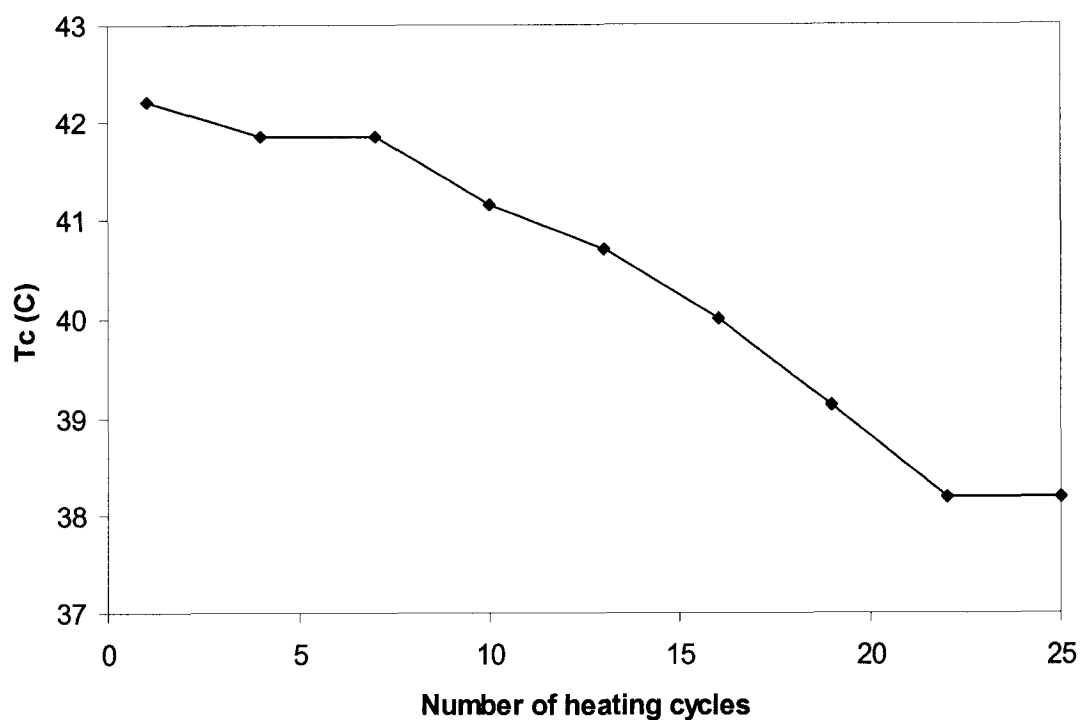


Figure 48 Change of phase transition temperature of Liposome D with the number of heating cycles.

In order to see if CPE-215[®] could only reduce the phase transition temperature of Liposome D, we did the same multi-heating-cycle experiment with Liposome DH. Figure 49 was the DSC result, which also showed that the phase transition temperature of Liposome DH decreased with continuous insertion of CPE-215[®]. Although the phase transition for Liposome DH was very broad, the peak shift with number of heating cycles was still quite noticeable. We took the lowest point of the curve as the phase transition temperature. Figure 50 showed the phase transition temperature decreased with number of heating cycles. The decrease was almost linear with the number of heating cycles.

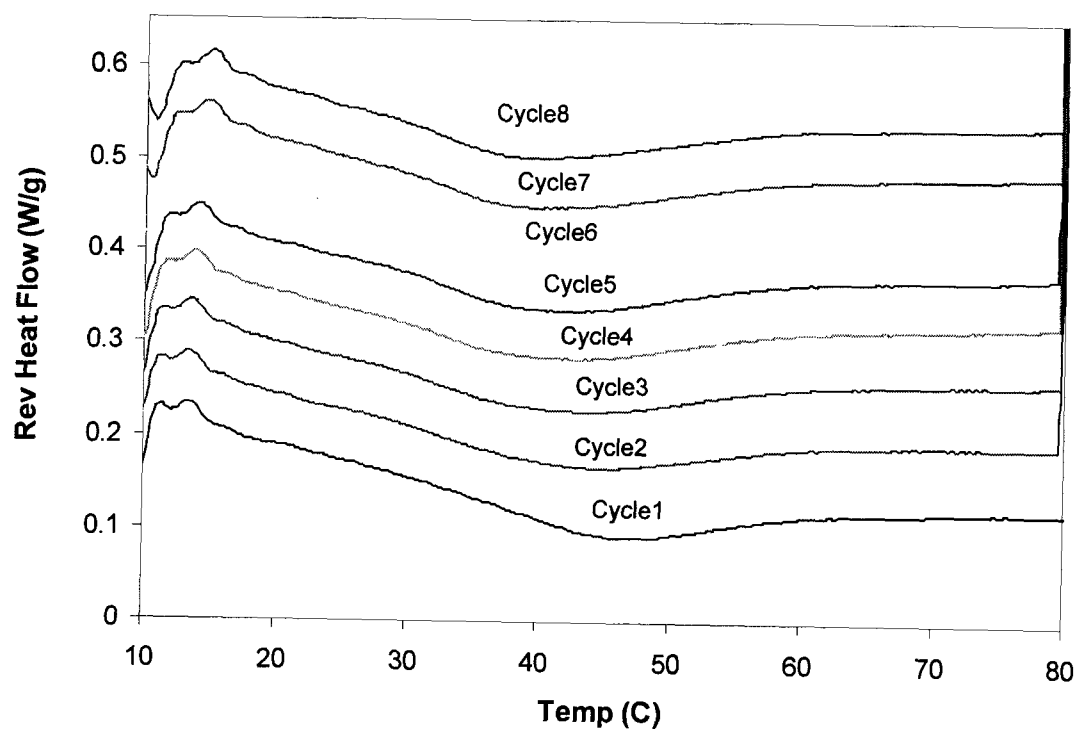


Figure 49 Eight heating cycles of Liposome DH (DPPC/Cholesterol liposome) with CPE-215[®]/cottonseed oil mixture (exothermal up).

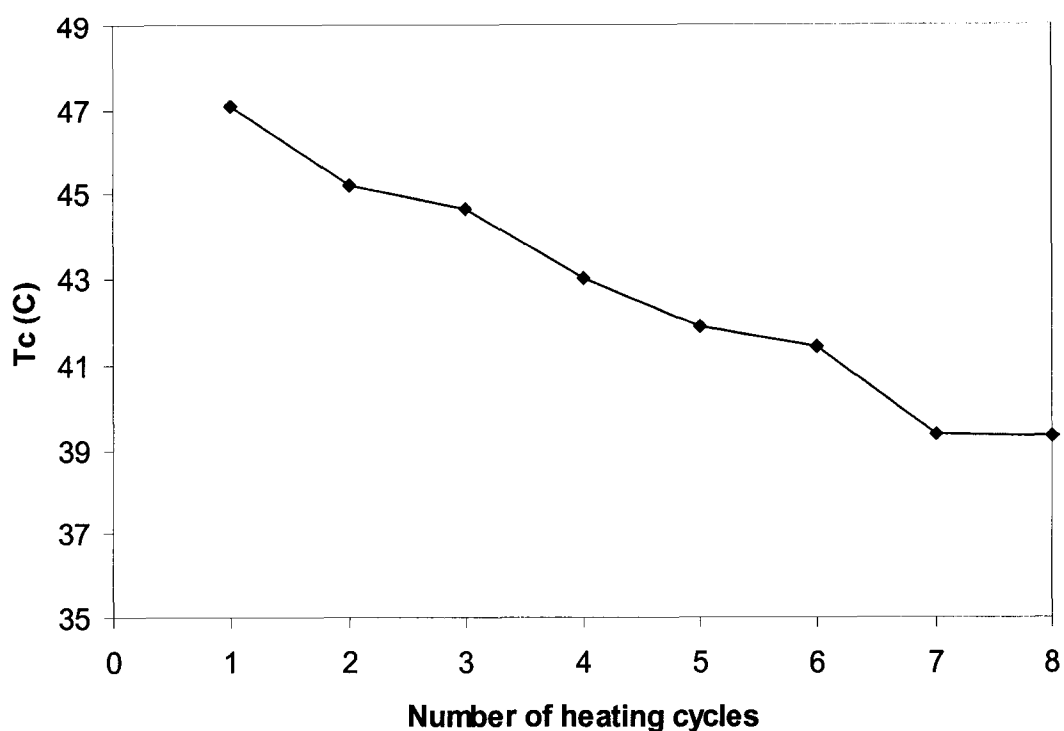


Figure 50 Change of phase transition temperature of Liposome DH with number of heating cycles.

We also looked at the enthalpy change of liposomes during the lipid bilayer phase transitions. Since the phase transitions of cholesterol-containing liposomes are too broad, it is hard to tell the starting and ending points of those transitions and accurately obtain the enthalpy change; in that case, here we only discuss the phase transition of the DPPC liposomes. According to the thermal data of Figure 43, the enthalpy change during the Liposome D phase transition is 37 kJ/mol, which is similar to the literature value.¹⁰⁸ However, the enthalpy change in the phase transition of Liposome DC is only 20 kJ/mol, assuming only DPPC molecules in the liposomes accounted for the enthalpy change, not CPE-

215[®]. The big difference between the enthalpy change of Liposome D and Liposome DC can be explained from the different molecular conformation of DPPC molecules in those two liposomes. As we have discussed before, during the phase transition of Liposome D from lamellar gel phase to lamellar liquid crystalline phase, the conformation of the acyl chains of DPPC molecules are changed from all-*trans* to *gauche*, and the enthalpy change is related to the energy needed to convert the DPPC acyl chains from the highly ordered, low energy level all-*trans* conformation to the *gauche* conformation. In Liposome DC, due to the insertion of CPE-215[®] molecules in the DPPC lipid bilayer, not all the DPPC acyl chains are packed in *trans* conformation in the lamellar gel phase, which increases the energy level of the gel phase of Liposome DC and results in less enthalpy change during the phase transition.

Thermal data from Figure 47 further supported the above explanation. After calculation, we found that with CPE-215[®] diffusing into the DPPC liposomes, the Liposome D phase transition enthalpy change decreased gradually from 37 kJ/mol to 22 kJ/mol after 25 cycles of heating and cooling (Figure 51).

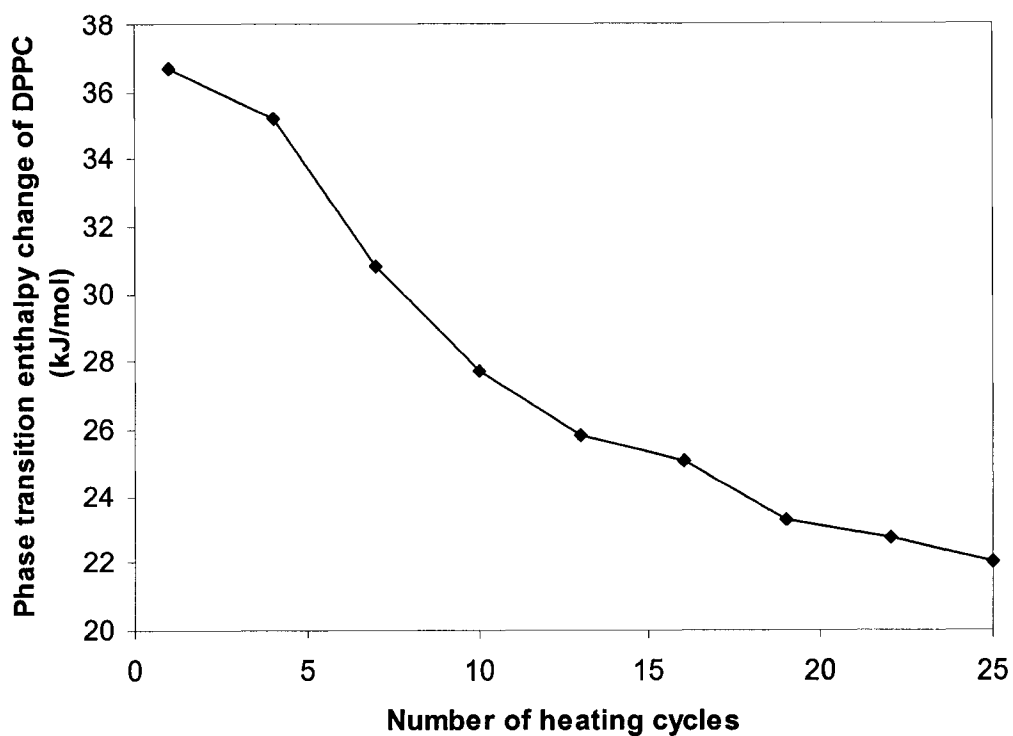


Figure 51 Change of phase transition ΔH of DPPC in Liposome D (DPPC liposome) with CPE-215[®] insertion.

Table 6 DSC study summary table

	T _c (°C)	Transition width	ΔH of DPPC (kJ/mol)
DPPC liposome	42	Narrow	37
DPPC/CPE-215 [®] liposome	34	Broad	20
DPPC/Cholesterol liposome	46	Very road	N/A
DPPC/Cholesterol/CPE-215 [®] liposome	37	Broad	N/A

4.2.5. Conclusion

With the help of the powerful modulated DSC technique, we carried out a series of liposome phase transition studies. We found that adding CPE-215[®] into the lipid bilayer could reduce the phase transition temperature of liposomes. Adding both CPE-215[®] and cholesterol into the lipid bilayer can broaden the phase transition of DPPC liposomes, but CPE-215[®] has less peak broadening effect than cholesterol, which may be due to the rigidity of cholesterol and the flexibility of CPE-215[®]. When inserted into the lipid bilayers, CPE-215[®] was evenly distributed in the bilayers. With CPE-215[®] gradually inserted into the lipid bilayers, the liposome phase transition temperature was gradually shifted to lower temperatures, and the liposome phase transition enthalpy change also decreased gradually.

4.3. Insulin Interaction with Liposome (Membrane)

Depending on the surface properties and the distribution of hydrophilic or hydrophobic regions on the surface, different proteins interact with liposomes in different ways. Usually there are three types of interaction between protein/peptide and lipid bilayer: adsorption, insertion and penetration (Figure 52).

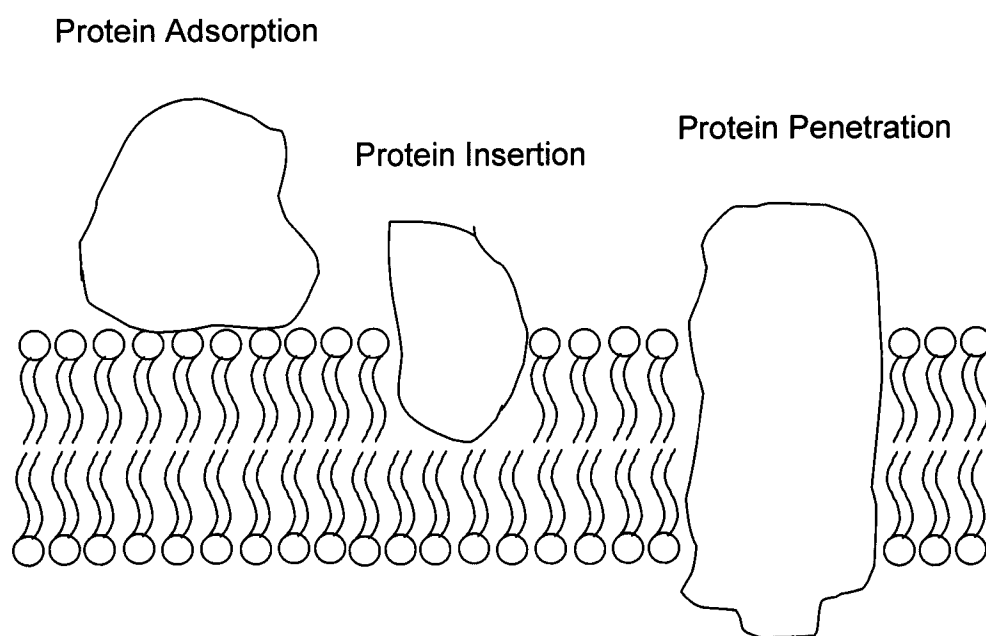


Figure 52 The interaction modes between protein and lipid bilayer membrane.

Understanding the interaction between insulin and liposomes is important to our mechanism study of insulin release from liposomes and permeation enhancing effect of CPE-215[®]. Zhang, et al. studied the interaction between insulin and liposome by fluorescence spectra and microcalorimetry methods.¹¹⁵ They found that the interaction between insulin and liposome was weak; there was no protein insertion or penetration, probably only weak adsorption; the heat effect of the interaction $\Delta H = -1.98$ kcal/mol, which indicates weak non-covalent binding.

4.3.1. Centrifugal Extraction to Determine the Insulin Adsorption Coefficient on Membrane

From our experience in handling insulin molecules during the release experiments, we learned that insulin molecules can adsorb on the surface of liposomes; otherwise, we would not have needed to perform the multiple centrifugal extractions to ensure the outside surface of liposomes was insulin-free before the release experiments.

Each of the 20 amino acids can be distinguished by the R-group substitution on the α -carbon atom. There are two broad classes of amino acids based upon whether the R-group is hydrophobic or hydrophilic. Usually the hydrophilic amino acids tend to interact with the aqueous environment and are often found on the exterior surface of proteins, but some hydrophobic amino acids also exist on the exterior surface, which accounts for the hydrophilic regions and hydrophobic regions on the protein surface. Under the hydrophilic surface, liposomes have the hydrophobic layer to isolate the inside from outside environment. Protein can adsorb on the liposome surface by letting its hydrophilic regions contact the liposome hydrophilic layer.

Our insulin adsorption isotherm is based on three assumptions: adsorption cannot proceed beyond monolayer coverage; all liposome surface sites are equivalent and can accommodate, at most, one adsorbed protein; the ability of a protein molecule to adsorb at a given site is independent of the occupation of neighboring sites. As one can see, our isotherm is similar to a Langmuir isotherm.¹¹⁶

The dynamic equation is: Insulin + Surface \leftrightarrow Insulin-Surface

$$\text{Rate of adsorption } V_a = k_1 C(1 - \theta)$$

where θ is the fractional liposome surface coverage, k_1 is the insulin adsorption rate constant, C is the insulin solution concentration.

$$\text{Rate of desorption } V_d = k_{-1} \theta$$

where k_{-1} is the insulin desorption rate constant.

At equilibrium, the rate of adsorption is equal to the rate of desorption.

Then

$$V_a = V_d$$

$$k_1 C(1 - \theta) = k_{-1} \theta \quad [4.5]$$

$$\text{with } K = \frac{k_1}{k_{-1}}$$

$$\theta = \frac{KC}{1 + KC}. \quad [4.6]$$

We carried out a precise centrifugal extraction experiment to determine the insulin adsorption coefficient, K , on the liposome surface. After the normal procedure of making 400 nm 4:1 (w/w) DPPC/Cholesterol liposomes in insulin solution at pH 7, we performed the centrifugal extraction at 4 °C. We used the DYNAC centrifuge at 2000 rpm, which was slow compared to the ultracentrifuge, but fair enough to concentrate the liposomes to the bottom of the tube. We allowed 1 hour for the insulin desorption and adsorption to reach equilibrium for each centrifugal extraction process. We wanted to see the insulin adsorption

equilibrium at 37 °C, but the lipid bilayer surface is not a solid sphere, and its fluidity depends on its temperature. If we perform the centrifugal extraction at high temperature, for example 37 °C, not only could the liposomes break during the centrifugation, but the inside insulin could come out to interfere with the outside insulin concentration. In that case, this experiment had to be carried out at low temperature, to ensure the hardness of the liposome sphere and minimize the leakage of insulin from inside of liposomes.

Following each centrifugal extraction, we recorded the volume of insulin solution in the centrifuge tube (excluding the volume of liposomes), and used fluorescence to detect the insulin concentration of the supernatant (before the fluorescence measurement, centrifuge filtration with 50 KDa MWCO membrane filters was used to separate insulin solution from liposomes); then we recorded the volume of supernatant that we took out and the volume of fresh buffer we added in. We used the calibration curve to convert the fluorescence signal to insulin concentration.

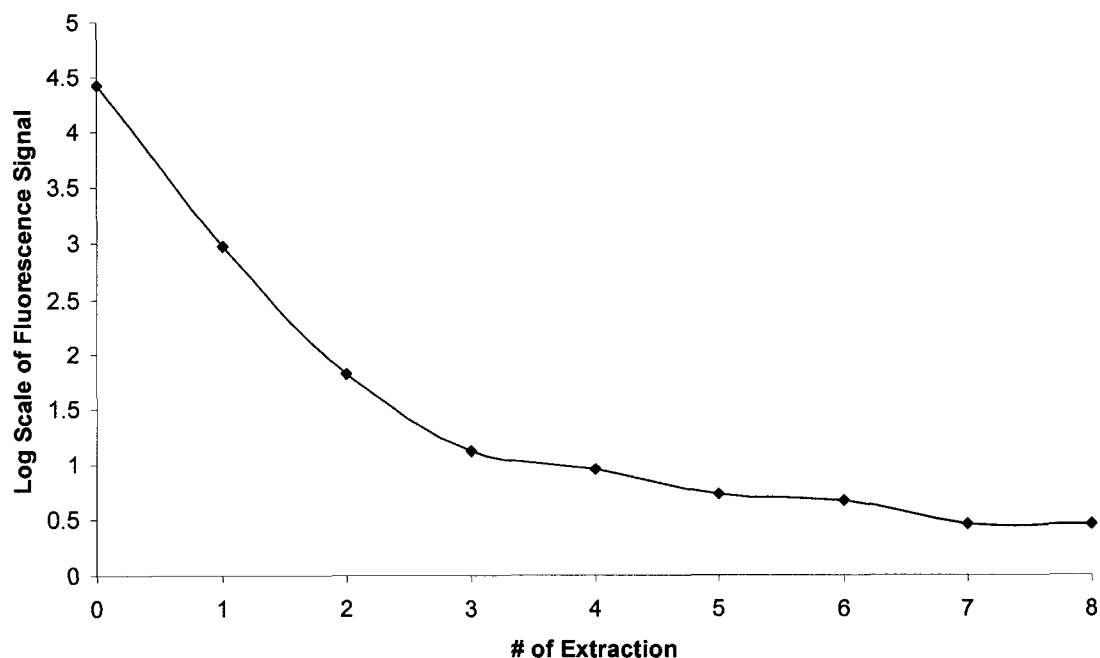


Figure 53 The fluorescence signal of the supernatant was measured after each centrifugal extraction for 8 times. Note the fluorescence signal is on a log scale.

Figure 53 shows the decrease of fluorescence signal of the supernatant with the increase of centrifugal extraction times. Since the decrease in the signal was so drastic for the first couple extractions, the fluorescence signal is shown on a log scale, which indicates that the insulin adsorption on the liposome surface is not a strong interaction. After 3 extractions, the fluorescence signal was near that of the background.

After the i^{th} centrifugal extraction, the insulin concentration, C_i , is the result of dilution and insulin desorption from the liposomes. Therefore, the remaining solution volume (excluding the liposome volume) after removing the supernatant,

V_{ri} , and the final solution volume after adding fresh buffer, V_i , are two important parameters. Then according to the mass balance

$$C_{i-1}V_{ri} + a\theta_{i-1} = C_iV_i + a\theta_i \quad [4.7]$$

where a is the amount of insulin adsorbed on the liposome surface when $\theta=100\%$.

Table 7 Centrifugal extraction data

i	C_i (mg/ml)	V_{ri} (ml)	V_i (ml)
0	0.11	N/A	N/A
1	3.78×10^{-3}	0.33	11.40
2	2.64×10^{-4}	0.11	11.28
3	5.39×10^{-5}	0.17	11.38

Table 7 listed the information from the centrifugal extraction experiment, which were used to calculate the adsorption coefficient, K .

From the equations of

$$C_0V_{r1} + a\theta_0 = C_1V_1 + a\theta_1$$

$$C_1V_{r2} + a\theta_1 = C_2V_2 + a\theta_2$$

$$\theta_0 = \frac{KC_0}{1 + KC_0}$$

$$\theta_1 = \frac{KC_1}{1 + KC_1}$$

$$\theta_2 = \frac{KC_2}{1 + KC_2}$$

we can calculate the values of K , a , θ_1 , θ_2 , θ_3 .

We solved this system of equations and obtained two possible mathematical solutions, one was $K = 97$ ml/mg, the other was $K = 7.13 \times 10^5$ ml/mg. Based on the solutions we got, when $K = 97$ ml/mg, $\theta_0 = 0.914$, $\theta_1 = 0.268$, $\theta_2 = 0.025$, $a = 0.0105$ mg; when $K = 7.13 \times 10^5$ ml/mg, $\theta_0 = 0.999987$, $\theta_1 = 0.99963$, $\theta_2 = 0.9947$, $a = 18.99$ mg. However, the total amount of insulin we put into the system when we prepared the liposomes, both inside and outside of liposomes, was less than 1.4 mg of insulin; hence, it is impossible to have 18.99 mg of insulin adsorbed on the liposome surface. Therefore, $K = 7.13 \times 10^5$ ml/mg is only a mathematical solution, with no physical reality, and was discarded. $K = 97$ ml/mg is the reasonable equilibrium constant for insulin to adsorb on a DPPC/Cholesterol liposome membrane.

Our calculation showed that if the liposome surface was 100% covered by insulin, the amount of insulin on the liposomes surface was 0.0105 mg. In our experiment, after the liposome extrusion process, there were 0.067 g of DPPC and 0.017 g cholesterol in the liposomes. Since cholesterol has a much smaller hydrophilic group than DPPC, we only used the DPPC amount to estimate the liposome surface area. Since the liposomes we made were 400 nm large unilamellar liposomes, we assumed there was no curvature effect and the overall surface area of liposomes was equal to the one side surface of one planar lipid bilayer. A phosphatidylcholine's hydrophilic head group has an average surface area of 50 \AA^2 ,¹¹⁷ the total liposome surface in our experiment $S = 0.067 \text{ g} \div 734 \text{ g/mol} \div 2 \times 6.02 \times 10^{23} \text{ /mol} \times 50 \text{ \AA}^2 = 1.37 \times 10^{21} \text{ \AA}^2$. Therefore, when the

liposome surface was 100% covered by insulin ($\theta = 1$), the area occupied by each insulin molecule was $1.37 \times 10^{21} \text{ \AA}^2 \div (0.0105 \times 10^{-3} \text{ g} \div 5800 \text{ g/mol} \times 6.02 \times 10^{23} / \text{mol}) = 1.26 \times 10^6 \text{ \AA}^2$, which is similar to a square of $112 \text{ nm} \times 112 \text{ nm}$. As we know, the diameter of insulin monomer is less than 3 nm ; therefore, even at 100% coverage, the liposome surface was loosely occupied by insulin molecules, which is another proof of weak interaction. When $\theta = 1$, on the inner surface of each 400 nm liposome, the average number of insulin monomer is $3.14 \times (4000 \text{ \AA})^2 \div 1.26 \times 10^6 \text{ \AA}^2 = 40$; most likely, insulin would exist as dimer when $\theta = 1$, then there would be 20 insulin dimer adsorbed on the inner surface of each 400 nm liposome. This particularly low number of adsorbed insulin molecules indicates that insulin has a very low affinity for the outside of the lipid bilayer.

All these results confirmed that there is interaction between insulin and liposome, but such interaction is weak, most likely through electrostatic interaction.

4.3.2. ITC Experiment of Insulin Titration on Liposome

Isothermal Titration Calorimetry (ITC) is a thermodynamic technique for monitoring any chemical reaction initiated by the addition of a binding component, and has become a method of choice for characterizing biomolecular interactions.^{118,119} When substances bind, heat is either generated or absorbed. Measurement of this heat allows accurate determination of binding constants, reaction stoichiometry, enthalpy and entropy, thereby providing a complete thermodynamic profile of the molecular interaction in a single experiment.

Injection of a ligand into the target molecule (which is accommodated in the calorimeter cell) will result in an endothermic, or exothermic, enthalpic event which will be observed as a heat pulse.

When we used ITC to study the insulin adsorption on liposome surface, insulin was the titrating ligand and the liposome was the target substance. Since the interaction was expected to be weak, insulin solution with high concentration was used to obtain enough signal strength. We prepared 5 mg/ml (0.86 mM) insulin solution and two kinds of liposomes with the lipid content of 5 mg/ml at pH 3.1 in 30mM citrate buffer to study the interaction of insulin with liposomes, i.e. 400 nm 6:1.5:1 (weight) DPPC/Cholesterol/CPE-215[®] unilamellar liposome and 400 nm 4:1 (weight) DPPC/Cholesterol unilamellar liposome. We also sealed insulin solution and liposome solutions into dialysis tubes and put them into the pH3.1 30 mM citrate buffer overnight to make sure they all had the same pH and ionic strength. The dialysis membrane had a molecular weight cutoff of 3500 to make sure insulin and liposome can not pass through.

MicroCal, Inc. kindly agreed to perform the titration experiment for us using their VP-ITC at 37 °C. Besides two liposome sample titrations, a control run was also carried out, i.e. using insulin to titrate pH 3.1 citrate buffer.

Before the titration, the liposomes were placed in the calorimeter cell (1.428 ml cell volume) at 37 °C. The insulin solution was loaded in the syringe, and the titration program adjusted for 10 µl/injection (2 µl for 1st injection), 3.5 min interval between injections, 20 sec per injection.

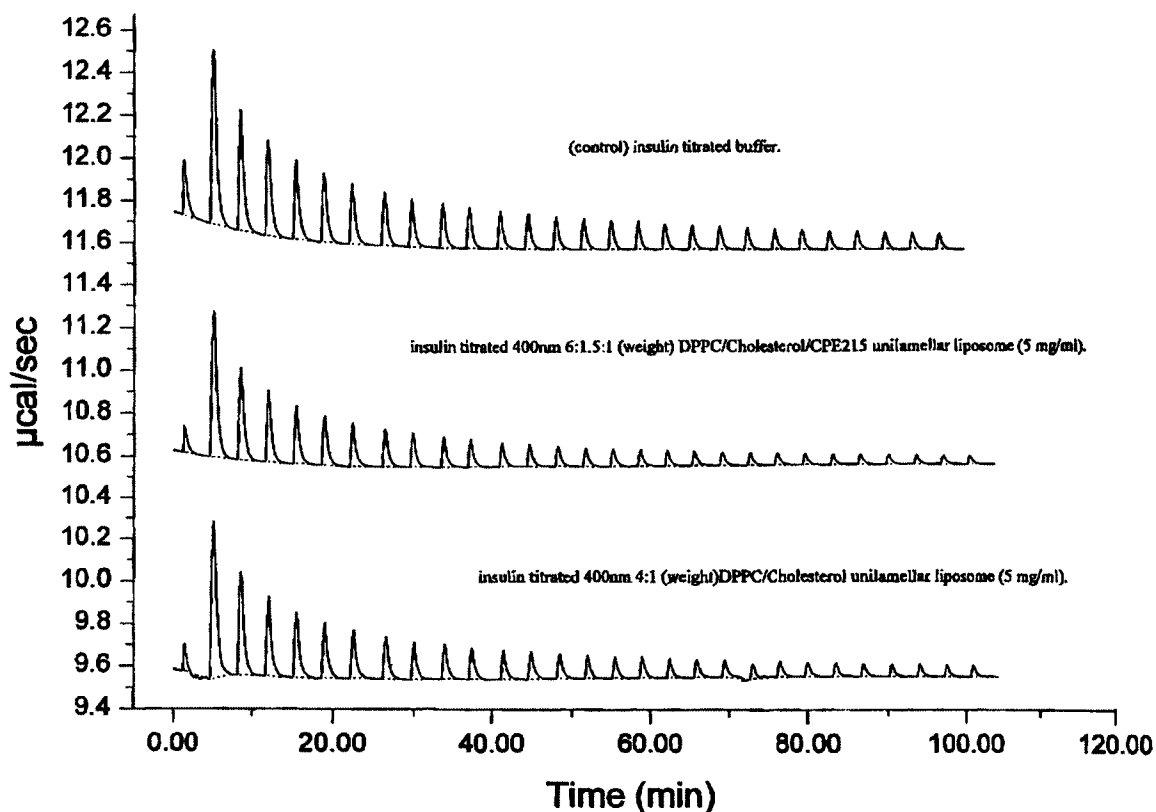


Figure 54 The VP-ITC raw data of two liposome sample titrations and one control run (endo up). Two liposome samples (400 nm 6:1.5:1 (weight) DPPC/Cholesterol/CPE-215[®] unilamellar liposome and 400 nm 4:1 (weight) DPPC/Cholesterol unilamellar liposome) were titrated by insulin (5 mg/ml; 0.86 mM) in 30 mM pH 3.1 citrate buffer at 37 °C. 10 µl/injection (2 µl for 1st injection), 3.5 min interval between injections, 20 sec per injection, 280 rpm stirring.

Figure 54 shows the ITC raw data for two sample titrations and one control run. The heat effects for the control (upper curve) were endothermic and its magnitude decreased quite rapidly as the titration proceeded. Near the end of the titration, the heat effects became very small and constant. These data appeared to be the result of the heat of dilution of a concentrated insulin solution (0.86 mM) injected into a buffer. Due to our dialysis treatment of the samples

before the titration, the large endothermic heat observed for the control run could not be due to pH mismatch. Additionally, a likely source for these endothermic heat effects is the insulin dimer to monomer dissociation when the insulin solution was diluted into the buffer. The heat effects for the two liposome sample titrations are very similar to that of the control, though their endothermic heat effects were slightly smaller than those of the control due to the weak binding of insulin to the liposome surface.

The integrated heats for three titration experiments are shown in Figure 55 after normalizing by the insulin concentration (using 0.86 mM). The differences in the integrated heats between the liposome samples and the control are small. It appears that the sample of DPPC/Cholesterol/CPE-215[®] liposome has a slight larger exothermic net heat than that of DPPC/Cholesterol sample.

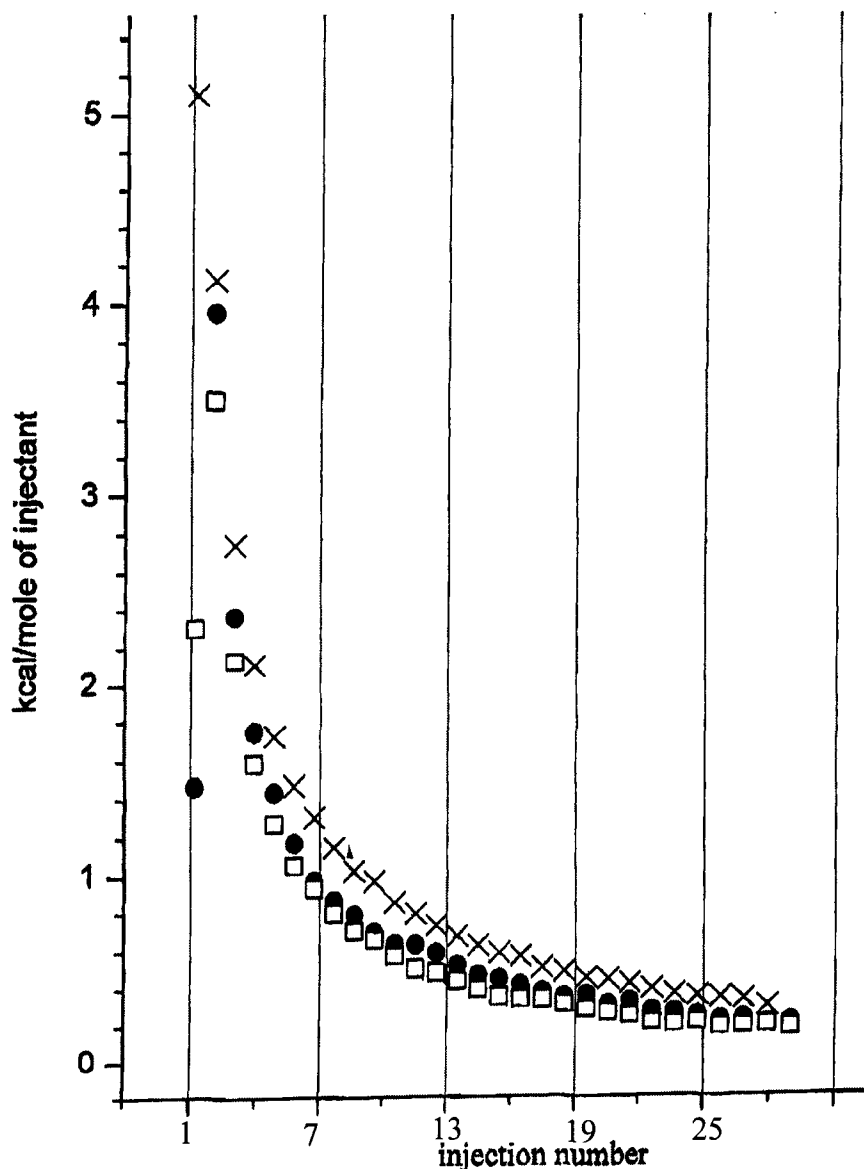


Figure 55 VP-ITC heat data after auto baseline integration, normalized on insulin concentration (0.86 mM). 400 nm 6:1.5:1 (weight) DPPC/Cholesterol/CPE-215[®] unilamellar liposome and 400 nm 4:1 (weight) DPPC/Cholesterol unilamellar liposome) were titrated by insulin (5 mg/ml; 0.86 mM) in 30 mM pH 3.1 citrate buffer at 37 °C. 10 µl/injection (2 µl for 1st injection), 3.5 min interval between injections, 20 sec per injection, 280 rpm stirring. x, control titration; ●, DPPC/Cholesterol liposome; □, DPPC/Cholesterol/CPE-215[®] liposome. Positive heat value means endothermal process.

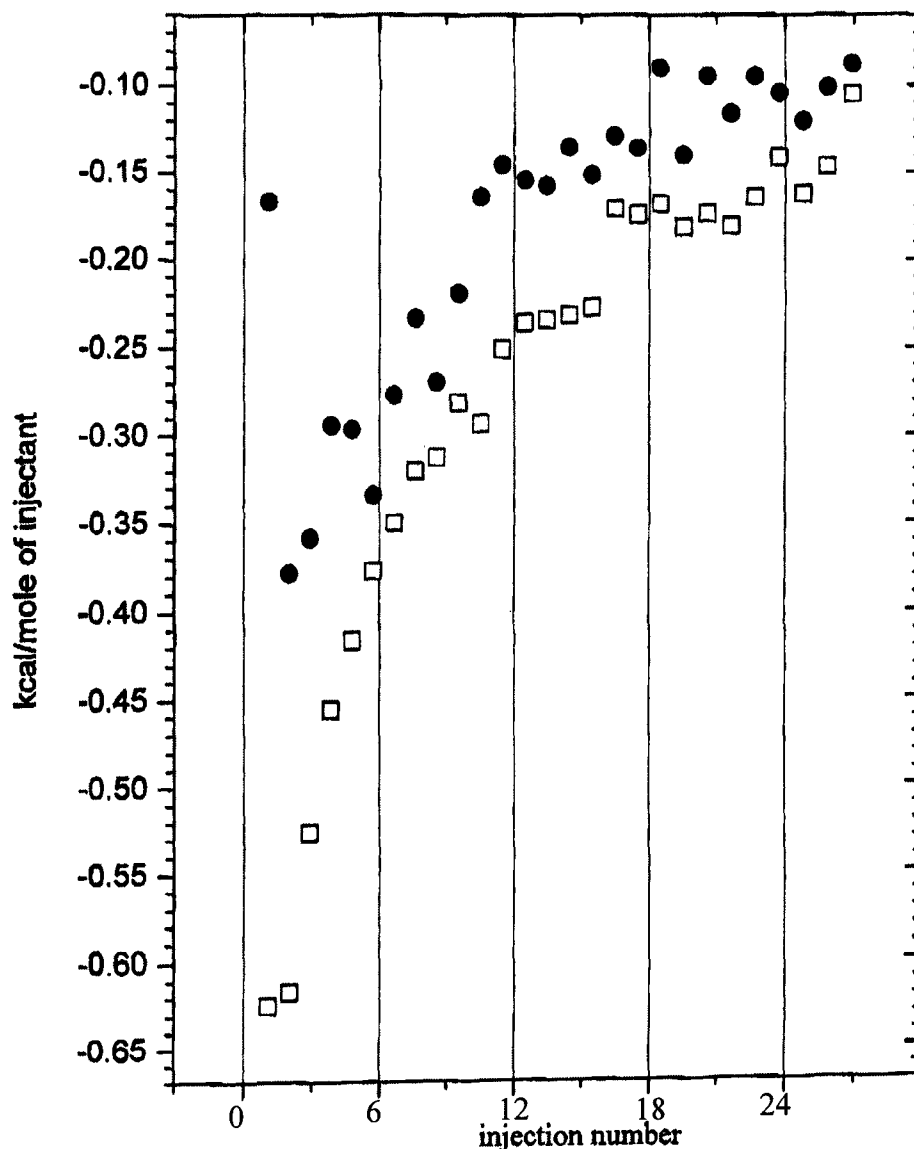


Figure 56 VP-ITC heat data after the sample runs subtracted the control run point by point. ●, DPPC/Cholesterol liposome; □, DPPC/Cholesterol/CPE-215[®] liposome. Negative heat value means exothermal process.

In order to clearly show the net heat effects of insulin adsorption on different liposome surfaces, the heat data of the control run were subtracted from that of liposome samples point by point, and Figure 56 shows the subtraction results. In Figure 56, we can see that DPPC/Cholesterol/CPE-215[®] liposomes

have a larger exothermic net heat than DPPC/Cholesterol liposomes. The net exothermic heat from insulin adsorption on DPPC/Cholesterol/CPE-215[®] liposomes is almost twice that of DPPC/Cholesterol liposomes, which clearly indicates a higher affinity of insulin to the surface of DPPC/Cholesterol/CPE-215[®] liposome than to the surface of DPPC/Cholesterol liposome.

4.4. Mechanistic Hypothesis for the Insulin Release from Liposome

4.4.1. Diffusion through Lipid Bilayer Membrane

Since the permeability of lipid bilayer membranes to small molecules is a well-studied field,^{120,121} at the beginning of our mechanistic study of permeability of insulin through lipid bilayers, we started by testing the mechanism of small molecules crossing lipid bilayer membrane first.

The ability of a small solute molecule to cross the lipid membrane is quantified by its permeability coefficient. For a molecule to cross the bilayer, it must (1) enter the membrane, overcoming any interfacial resistance or free energy barrier to do this, (2) diffuse across the bilayer, and (3) exit the membrane on the opposite side, again, overcoming any possible interfacial resistance. Any of these steps could, in principle, be rate limiting. The permeability of most nonelectrolytes through lipid bilayer membranes can be successfully analyzed by the *solubility-diffusion* model, which makes the assumption that the rate-limiting step is the diffusion within the lipid bilayer and that interfacial barriers for membrane entry and exit are negligible. This allows one to assume a rapid

partition equilibrium between the aqueous and membrane phases (step 1 and 3 in Figure 57). The partition coefficient, K_p , is defined by

$$K_p = \frac{[C_1^m]}{[C_1^{aq}]} = \frac{[C_2^m]}{[C_2^{aq}]} \quad [4.8]$$

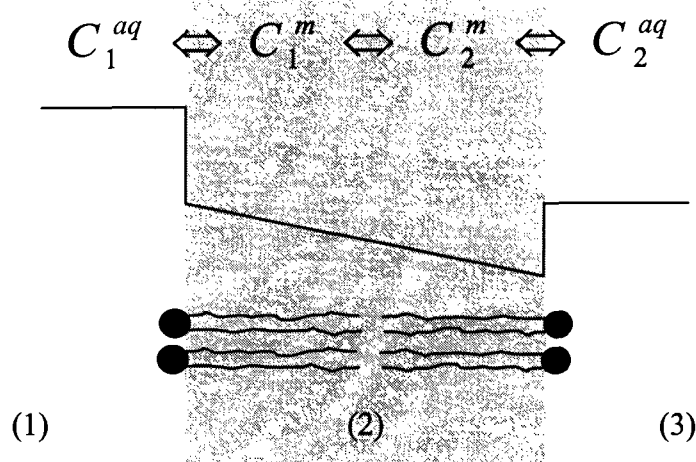


Figure 57 Simple schematic representation of the solute concentration change while crossing a lipid bilayer membrane according to the solubility-diffusion model. The solute concentrations at locations in the membrane (m) and aqueous (aq) phase are indicated. The numbers at the bottom refer to the steps required for a solute to cross the membrane from left to right.

The permeability coefficient, P , in terms of the net flux, from side 1 to side 2, of solute across a membrane of thickness d , is defined by

$$flux = P \cdot (C_1^{aq} - C_2^{aq}) \quad [4.9]$$

This same flux can be expressed in terms of the diffusion coefficient describing the flux of solute within the membrane, D_m , using Fick's first law.

$$flux = -D_m \frac{dC}{dx} \approx -D_m \frac{C_2^m - C_1^m}{d} \quad [4.10]$$

where the concentration gradient is assumed to be linear across the bilayer.

Substituting from equation 4.8 into equation 4.10 yields

$$flux = D_m \frac{C_1^{aq} - C_2^{aq}}{d} K_p \quad [4.11]$$

Comparing equation 4.9 and 4.11 gives

$$P = \frac{K_p D_m}{d} \quad [4.12]$$

The permeability coefficient is a product of the partition coefficient and diffusion coefficient within the membrane, divided by the width of the membrane.

We have already obtained the insulin diffusion coefficient in aqueous solution from NMR, which is $1.4 \times 10^{-6} \text{ cm}^2/\text{s}$ at $37 \text{ }^\circ\text{C}$ for insulin dimer. Since the hydrophobic layer of the bilayer membrane is made of long hydrocarbon chains, we tried to estimate D_m from the insulin diffusion coefficient in decane. Due to the extremely low solubility of insulin in decane, it is very hard to obtain the insulin diffusion coefficient in decane experimentally. According to Stokes-Einstein equation (equation 4.1), the diffusion coefficient is determined by temperature, the viscosity of the liquid and the hydrodynamic radius of the molecule. The viscosity of decane at $20 \text{ }^\circ\text{C}$ is 0.92 cP , which is very similar to that of water at $20 \text{ }^\circ\text{C}$ (1 cP). In that case, at the same temperature, the insulin diffusion coefficient in decane should be very similar to that in water, or at least in the same magnitude of $10^{-6} \text{ cm}^2/\text{s}$. However, the hydrocarbon chains of the lipids in the lipid bilayer are lined up and orderly packed, which is not like the free decane

molecules. From insulin adsorption on the membrane surface to insulin insertion into the membrane, the movement of insulin is associated with the lateral movement of lipids molecules. Therefore, the lateral diffusion (diffusion is restricted to two dimensions) coefficient of lipid should also be considered.¹²² The lateral diffusion coefficient in unilamellar vesicles of DPPC at 50°C was measured to be $8 \times 10^{-8} \text{ cm}^2/\text{s}$.¹²³ According to our DSC data of DPPC liposomes (Figure 43), 37 °C and 50 °C are all in the phase transition range, therefore, the lateral diffusion coefficient in unilamellar vesicles of DPPC at 37°C should be of the order of $10^{-8} \text{ cm}^2/\text{s}$. We would use $10^{-8} \text{ cm}^2/\text{s}$ to estimate the insulin diffusion coefficient in DPPC lipid bilayer at 37 °C.

The thickness of one lipid bilayer is about 4~5 nm. If we assume the insulin permeation through lipid bilayer is a diffusion-controlled process like the small nonelectrolytes, then according to the relation between the diffusion coefficient and the mean-square displacement, $\langle x^2 \rangle$,

$$D_m = \frac{\langle x^2 \rangle}{2t}, \quad [4.13]$$

the time required for insulin molecule to cross the lipid bilayer would be

$$t = \frac{\langle x^2 \rangle}{2D_m} = \frac{(4 \times 10^{-7} \text{ cm})^2}{2 \times 10^{-8} \text{ cm}^2 \cdot \text{s}^{-1}} = 8 \times 10^{-6} \text{ s}$$

This calculation indicates that once insulin is in the lipid bilayer, it takes almost no time for insulin to cross the membrane, but our insulin release experiment data did not show such a fast insulin release rate. Therefore, we can see diffusion is not the rate-limiting step for the insulin release from liposome,

and we cannot ignore the large electric potential energy increase caused by protein surface charges in the bilayer membrane. The partition coefficient, K_p (Equation[4.8]), of insulin in lipid bilayer must be very low. With both low K_p and D_m , it is not surprising that insulin has low permeability in lipid bilayers (Equation [4.12]).

Insulin in water is stabilized by the favorable interaction of the water dipoles, the hydration energy. Moving insulin between media of different dielectric constants, e.g., from an aqueous phase to the bilayer membrane interior, is unfavorable because of the loss of this hydration energy.

4.4.2. The Role of CPE-215[®] as a Membrane Permeation Enhancer

From our release experiments, we know that at 37 °C, insulin has a small leakage rate from liposomes even without the addition of CPE-215[®]; the addition of CPE-215[®] greatly increased the insulin release rate from liposomes. Therefore, our mechanism hypothesis should at least explain these two phenomena.

Liposome leakage has been studied for decades. There are several competing theories, focusing on defects in the packing order of the bilayer. These defects are postulated to form spontaneously, like fluctuating holes¹²⁴, or possibly along boundaries between coexisting lipid gel and liquid crystalline phases¹²⁵. Liposome leakage is maximal at the transition temperature between the gel and liquid crystalline phases¹²⁶, which indicates that the leakage is not due to a simple increase in molecular motion at higher temperatures, but is due

to a transient structural disorder of the lipid packing induced by the phase separation.

Based on this information, we propose that the rate-limiting step for insulin release from liposome is the probability for an insulin molecule to find an appropriate defect in the lipid bilayer to cross the membrane, and the rate of insulin release, V , can be expressed as $V \propto P_i \cdot P_d$, where P_i is the probability of insulin molecules adsorbed on the lipid bilayer surface, P_d is the probability of defects in the lipid bilayer.

Our ITC experimental data show a larger net insulin adsorption exothermic heat on DPPC/Cholesterol/CPE-215[®] liposome surface than on DPPC/Cholesterol liposome surface, which indicates a higher affinity and larger adsorption coefficient of insulin on the surface of DPPC/Cholesterol/CPE-215[®] liposome than on the surface of DPPC/Cholesterol liposome. Therefore, with the addition of CPE-215[®] in the lipid bilayer, more insulin can be adsorbed on the liposome surface, that is, the addition of CPE-215[®] can increase P_i .

Although the hydrophobic CPE-215[®] likes to go into the interior hydrophobic region of the bilayer membrane, there is a hydrophilic layer at the outmost surface of liposome and CPE-215[®] has to cross that layer first to go inside of the bilayer. It is clear that the bilayer is a remarkably good barrier against both hydrophilic and hydrophobic molecules. However, the defects in the liposome surface are perfect places for CPE-215[®] to enter the bilayer. Once CPE-215[®] molecules go into the defect, they stabilize the defect and make a hydrophobic region on the liposome surface attract more CPE-215[®] to make

larger defect. As a result, CPE-215[®] can increase P_d . However, the size of the stabilized defect is limited by the energy cost associated with the creation of a large CPE-215[®]/water interface.

The above analysis shows that CPE-215[®] has positive effect on the two major factors in the rate-limiting step of insulin release. That is our rationale on how CPE-215[®] can facilitate the insulin release from liposomes.

Compared to the totally hydrophobic hydrocarbon chains of the lipids, CPE-215[®] has a better affinity to the insulin molecule due to its polar ester group. Figure 58 shows the insulin dimer surface property region distribution. The insulin dimer structure was obtained from RCSB Protein Data Bank, and was displayed by Swiss-PdbViewer. Those regions are determined by the property of amino acid side groups: the polar regions are red, the non-polar regions are blue, the acidic/basic regions are yellow. The non-polar regions are ready to be in the hydrophobic environment; although the polar regions are not as good as the non-polar regions in the hydrophobic environment, they are much better than the acidic/basic regions; the acidic/basic regions do not want to stay in the hydrophobic environment at all, because they can lose the hydration energy once they move from hydrophilic phase to the hydrophobic phase within the lipid bilayer.

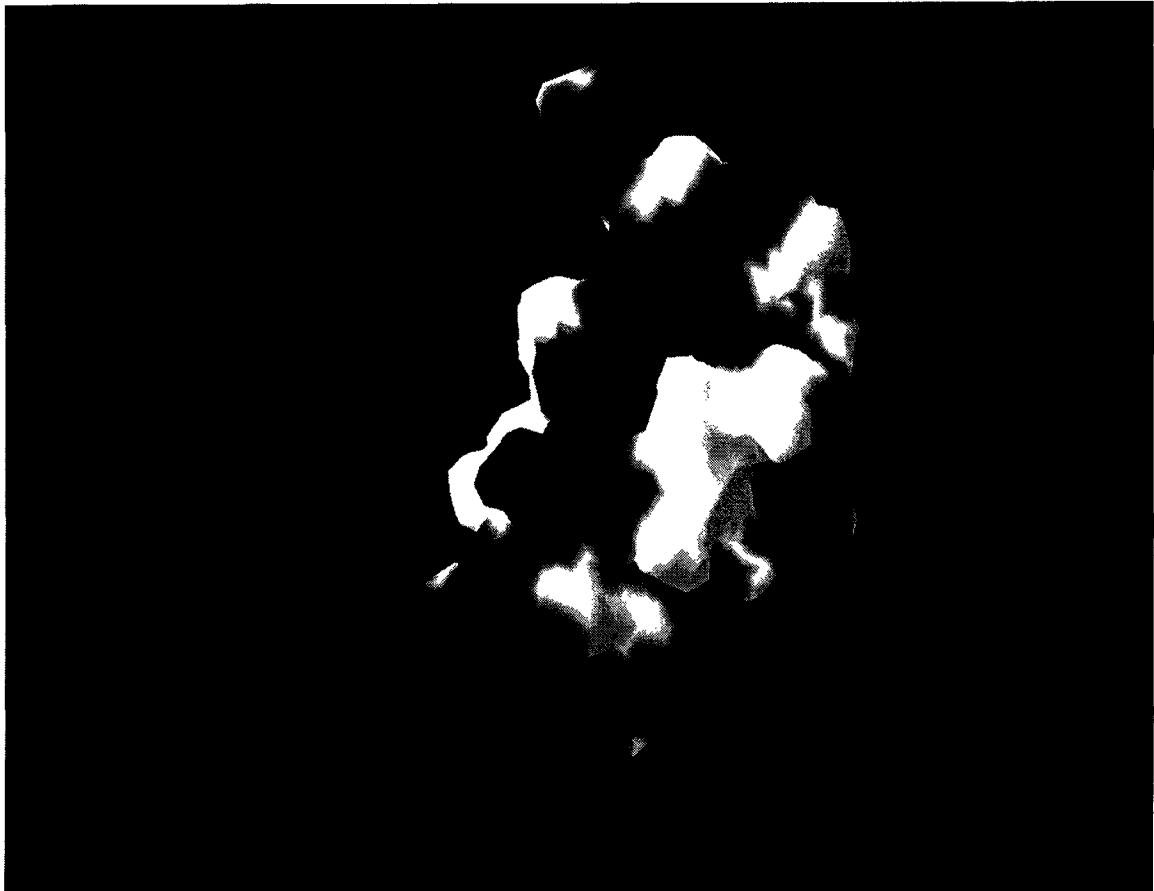


Figure 58 Insulin dimer surface property region distribution: the polar regions are red, the non-polar regions are blue, the acidic/basic regions are yellow.

When insulin dimer enters the defect in the liposome, the CPE-215[®] molecules in the defect can cover the non-polar and polar regions on the dimer surface, some may even cover the acid/basic regions because insulin prefers CPE-215[®] to hydrocarbon chains of lipid anyway. Then the whole insulin dimer molecule can be shielded by CPE-215[®] molecules and cross the bilayer with less energy barrier. This is another possible role of CPE-215[®] as a membrane permeation enhancer, though this may not be the major facilitating effect of CPE-215[®] on the insulin release from liposome process.

4.4.3. Proposed Hypothesis for the Whole Insulin Release Process

From our release data with different formulations and different conditions, we found one similar phenomenon—different formulations can initiate different initial release rates, but high insulin release rates only appeared at early release time, later on all the release rates were similar and independent of enhancer formulation. Figure 59 is an example of this phenomenon that has been systematically observed.

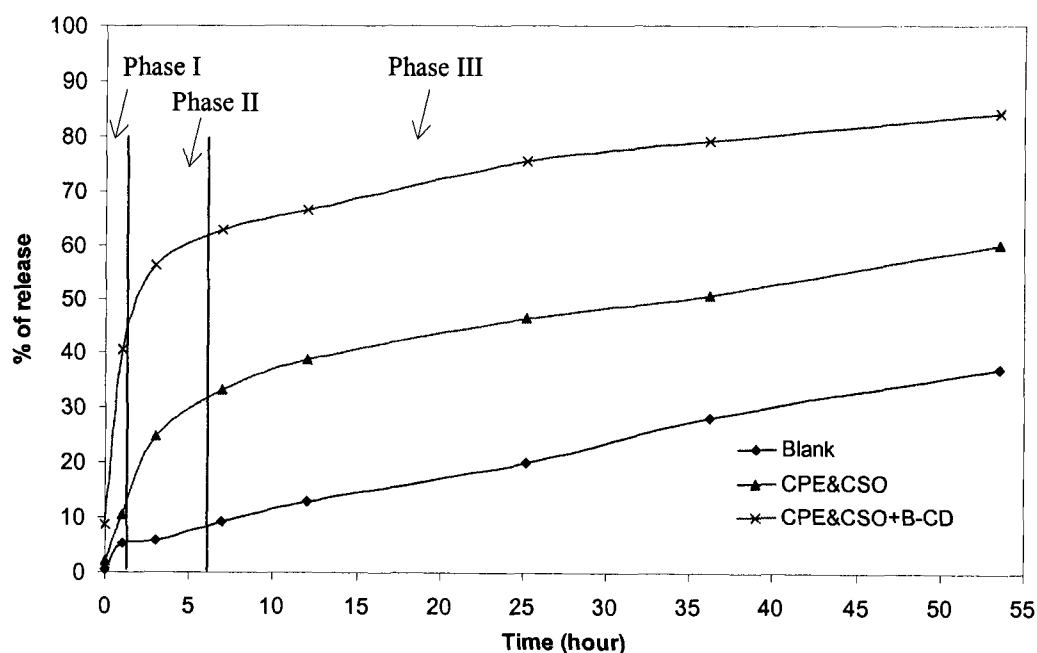


Figure 59 Insulin release from a DPPC/Cholesterol liposome at 37 °C

Figure 59 shows the insulin release from a DPPC/cholesterol (4:1 w/w) liposome at 37 °C. In this experiment, three release tubes contained the same

amount of DPPC/cholesterol (4:1 w/w) liposomes. One tube was used as blank control, one tube received a CPE-215[®]/cottonseed oil (3:1 w/w) mixture, and the other received a CPE-215[®]/cottonseed oil (3:1 w/w) mixture with β -cyclodextrin (1%). The release data showed that the insulin release rate of the blank control almost remained the same throughout the whole experiment, which showed the intrinsic leakage rate of a DPPC/cholesterol liposome. After the addition of CPE-215[®]/cottonseed oil mixture, the release rate was about twice the release rate of the blank control at the beginning, three hours later, the release rate began to slow down, and finally the release rate was equal to the one of the blank control. The formulation containing β -cyclodextrin really boosted the initial insulin release rate (about 8 times from the blank control rate, and 4 times from the formulation containing only CPE-215[®] and cottonseed oil). Later this rate also slowed down to equate to the rate of blank control release. In Figure 59, we divided the release data into three phases: Phase I, when the high initial release rates occur; Phase II, when the release rates begin to decrease; Phase III, when the release rates are all equal to the rate of the blank control.

Figure 60 shows a molecular level illustration of our proposed hypothesis for the whole insulin release process with CPE-215[®]. According to our DSC data (Figure 44), 37 °C is in the phase transition range of DPPC/cholesterol liposome, and there are defects existing in liposome. Due to the reason we discussed earlier, the oil mixture prefers being inserted into the defects of lipid bilayer. Once CPE-215[®] molecules go into the defect, they stabilize the defect and make a hydrophobic region on the liposome surface to attract more CPE-215[®] to form a

domain of CPE-215[®], probably a few nanometers in diameter, which is not detectable by MDSC. As a result, high stress is generated at the outer surface of the liposome, and a transient CPE-215[®] “pore” is formed to facilitate the protein transport through the membrane. That is Phase I in Figure 59 and 60.

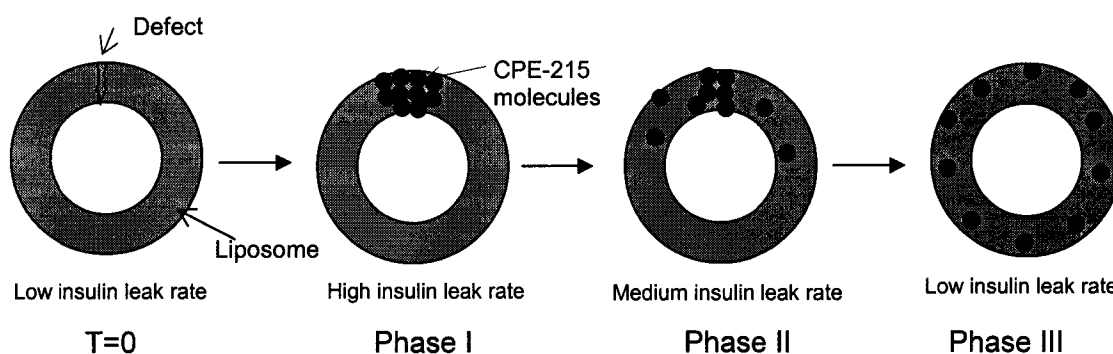


Figure 60 Scheme of Immediate Impact theory

Large CPE-215[®] domains are not favored thermodynamically; entropy causes CPE-215[®] to distribute evenly in the bilayers. When CPE-215[®] molecules begin to diffuse out of the CPE-215[®] rich domain, the transport “pores” begin to disappear, and the insulin release rate starts to decrease. This is what we call Phase II in Figure 59 and 60.

When all the CPE-215[®] molecules in the domains are evenly distributed in the lipid bilayers, no more “pores” exist and the release rate goes back to the blank control leakage rate. We define this mode as Phase III in Figure 59 and 60.

This hypothesis implies that the CPE-215[®]-evenly-distributed liposomes should have a similar leakage rate comparable to the blank control liposomes, and should be able to be reactivated by CPE-215[®]/cottonseed oil droplets. In order to test the validity of the theory, we designed a new release experiment. Two kinds of liposomes were made, one was 4:1 (weight ratio) DPPC/cholesterol liposome, and the other was DPPC/CPE-215[®]/cholesterol liposome. In the DPPC/CPE-215[®]/cholesterol liposome, CPE-215[®] was evenly distributed in the lipid bilayers, DPPC/CPE-215[®] molar ratio was 2:1 (weight ratio 6:1), and DPPC/cholesterol weight ratio was still 4:1. According to our theory and the release data of Figure 59, after 6 hours, CPE-215[®] should be evenly distributed in the lipid bilayers; if another dose of formulation was added then, there should be another enhanced insulin release rate. In this set of experiments, there were five release tubes, two of them were used for controlling the leakage rate of DPPC/cholesterol liposome and DPPC/CPE-215[®]/cholesterol liposome, two of them were used to see the enhanced release effect of adding oil mixture into DPPC/cholesterol liposome and DPPC/CPE-215[®]/cholesterol liposome at time zero, the last one was subjected to a second oil mixture "injection" after 6 hours to see if there would be renewed release boost.

Figure 61 shows the insulin release results of this set of experiments and Figure 62 is a close-up of Figure 61 at early times. The leakage rate of DPPC/CPE-215[®]/cholesterol liposome was similar to that of DPPC/cholesterol liposome, sometimes even slower than that of DPPC/cholesterol liposome, which is in good agreement with our hypothesis theory. Although the third point of the

DPPC/cholesterol liposome release curve was a little low, it was still within the experimental error. Release from the DPPC/CPE-215[®]/cholesterol liposomes was activated by CPE-215[®]/cottonseed oil mixture, similar to what CPE-215[®]/cottonseed oil mixture did to DPPC/cholesterol liposome. Again this agrees with our theory. We think that evenly distributed CPE-215[®] has a function similar to cholesterol in membrane barrier. In DPPC/CPE-215[®]/cholesterol liposome, there was already a large amount of CPE-215[®] evenly distributed in the lipid bilayers, the impact by outside oil mixture should not be as significant as in DPPC/cholesterol liposome, and the “pore” disappearing process should be slower due to reduced driving forces, which explained why in Figure 61 the “DPPC/CPE/Chol C&C” curve had a lower slope than the “DPPC/Chol C&C” curve at the beginning and took longer time to go back to the control leakage rate. The “DPPC/Chol 2C&C” curve showed another boost after a second addition of oil mixture at Hour 6, which is a very strong argument for our theory. All in all, this set of experiment proves the validity of our hypothesis on the membrane permeation enhancing effect of CPE-215[®].

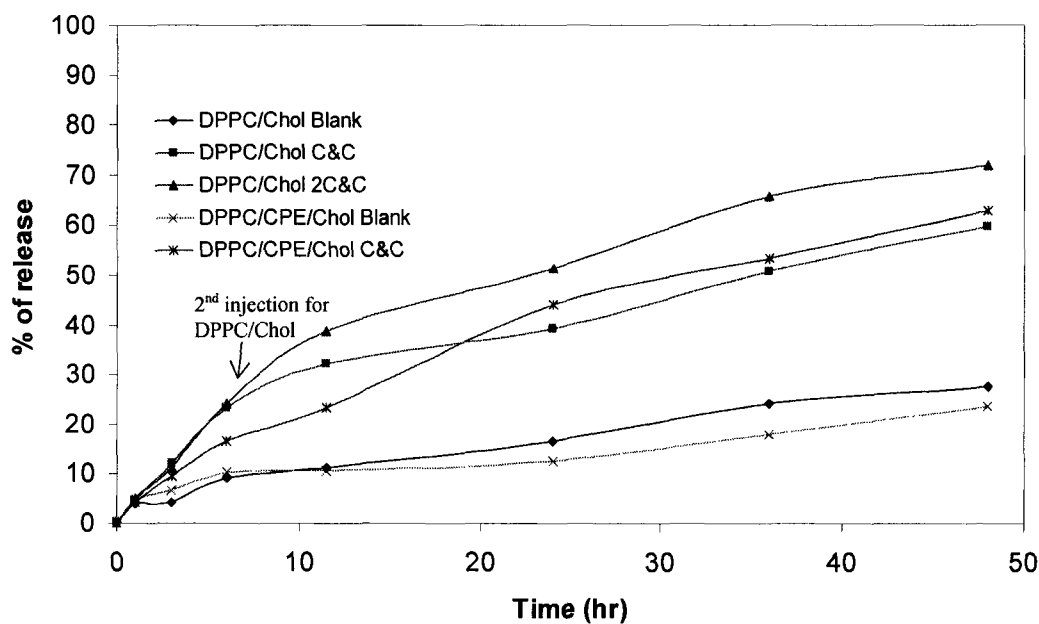


Figure 61 Insulin release at 37°C from different liposomes.

Note that the “DPPPC/Chol 2C&C” and “DPPPC/Chol C&C” samples were having the exact same condition during the first 6 hours, so their release data in the first 6 hours should be the same, and they ARE the same in Figure 61, which shows the reproducibility of our experimental technique and sample handling.

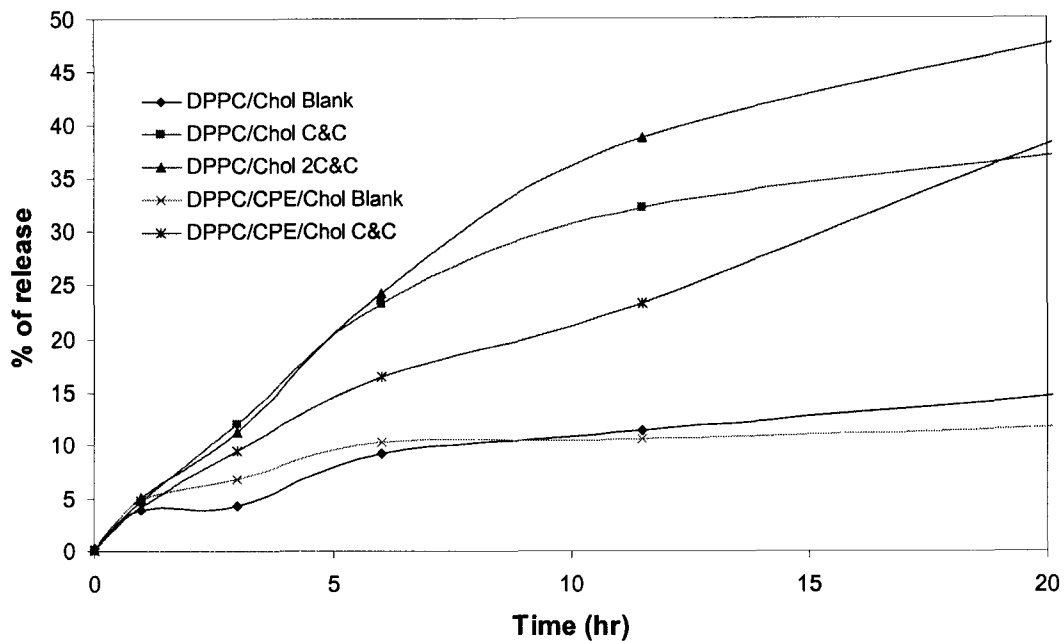


Figure 62 Close-up of Figure 61 at early times.

An important implication of this permeation mechanism is that CPE-215[®] is a SAFE membrane permeation enhancer. There are many kinds of membrane permeation enhancers out in the market. Some of these enhancers cause irritations, but what patients and the FDA are concerned most with is whether they are safe to use, whether they destroy the integrity of the membranes and let everything flow into the human body at the same time as the drug is delivered. Based on our theory, CPE-215[®] can only form transient “pores” in the membrane for a short period of time, and then the barrier function of the membrane is re-established. In our in vitro study, the time from “pore” formation to “pore” resorption was about 6 hours; while in human body, cell metabolism is carried

out at all times, so the in vivo time from “pore” formation to “pore” resorption should be less than 6 hours, which makes CPE-215[®] safer to use than other membrane permeation enhancers.

CHAPTER 5

QUANTITATIVE RELEASE MODEL

We have proposed a theory to describe the process of protein release from liposomes and carried out a set of testing experiments to prove the validity of this theory. In this chapter we developed a mathematical model based on this theory to quantify the release results. A semi-empirical nonlinear equation involving four parameters effectively fits the protein release profiles. Finally we used a neural network approach to correlate the different release condition parameters and the four semi-empirical fitting parameters based on our limited data sets.

5.1. Mathematical Model

Based on our theory, the whole release process is simplified to be the combination of two steps: at the beginning it is the boost release triggered by the permeation enhancers; after the permeation enhancers are evenly distributed inside of the lipid bilayer, it is the self-leakage of liposome.

The part of the triggered boost release can be empirically expressed as a simple linear time dependent event

$$y = a \cdot t + b \quad [5.1]$$

where y is the percentage of protein released from liposome, a is the boost release rate, b represents the systematic error of the experiment (theoretically, b should be zero, but due to the temperature change at time zero and the sample processing time between taking the sample and finishing the separation of protein and liposome, b is always a little bit more than zero).

The self-leakage of liposomes can also be empirically expressed as a simple linear time dependent event

$$y = c \cdot t + d \quad [5.2]$$

where y is the percentage of protein released from liposome, c is the liposome self-leakage rate.

We introduced another parameter, t^* , which is the transition time between the triggered boost release and the self-leakage of liposomes

$$\text{where } a \cdot t^* + b = c \cdot t^* + d \quad [5.3]$$

$$\text{then } d = (a - c) \cdot t^* + b \quad [5.4]$$

and the self-leakage of liposome can be expressed as

$$y = c \cdot t + (a - c) \cdot t^* + b \quad [5.5]$$

Mathematically, we combined both release steps [5.1] and [5.2] through the following equation

$$y = \frac{1}{\frac{1}{a \cdot t + b} + \frac{1}{c \cdot t + (a - c) \cdot t^* + b}} \quad [5.6]$$

or alternatively

$$y = \frac{1}{\left(\frac{1}{(a \cdot t + b)^2} + \frac{1}{(c \cdot t + (a - c) \cdot t^* + b)^2} \right)^{1/2}} \quad [5.7]$$

which could smoothly link the two release steps and represent the whole release process. Practically Equation 5.7 is a better fit than Equation 5.6 to all experimental data. Equation 5.7 was used to express the whole release process.

We used the “Solver” function of Excel[®] to estimate the best a , b , c and t^* values to make the Equation 5.7 fit the experimental data through a least square non-linear curve fit. Figure 63 is an example of the fitting. The complete fitting results for all release curves can be found in Appendix.

The experimental data used in Figure 63 are from the “CPE215” sample in Chapter 3.2.2, shown as square dots. The lines of “ $at+b$ ” and “ $ct+d$ ” are shown in blue and pink colors respectively, and the t^* value can be found in the cross point of these two lines.

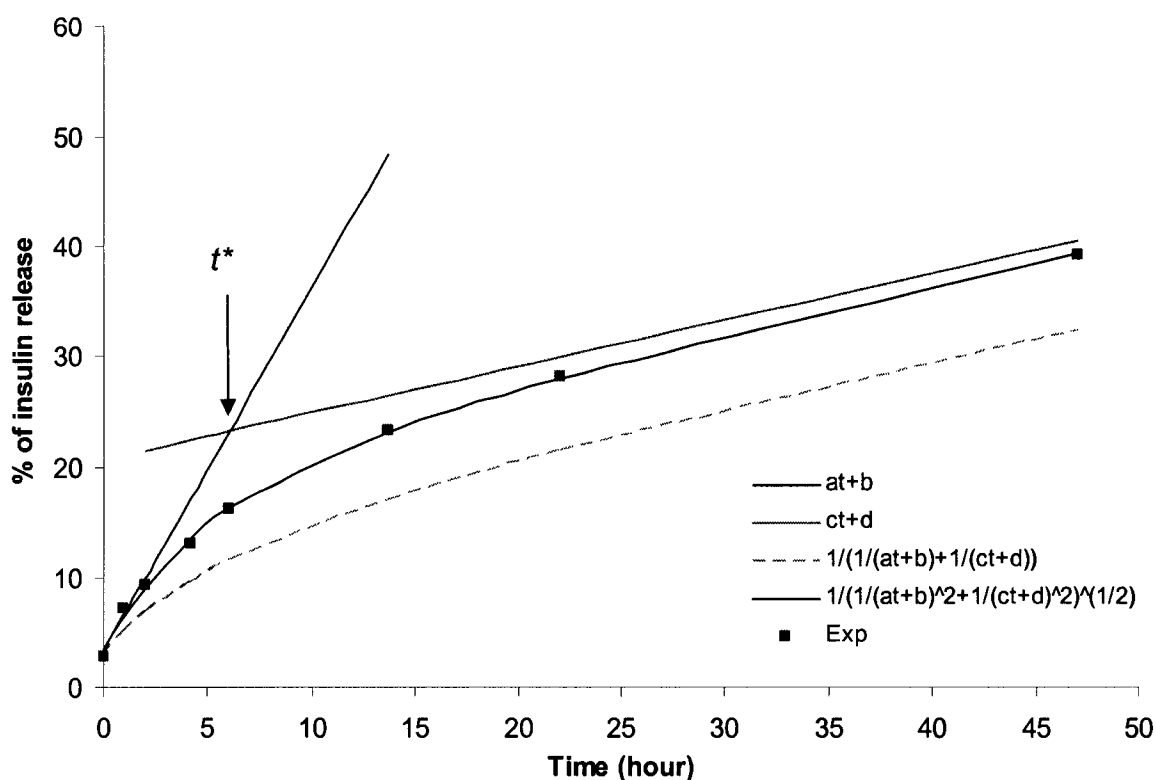


Figure 63 Modeling curves and the experimental release data of the “CPE215” sample in Chapter 3.2.2. The blue line is the “ $at+b$ ”, which represents the boost release; the pink line is “ $ct+d$ ”, which represents the later self-leakage of liposome. The time value of the cross point of the two lines is t^* . The experimental data points are shown as square dots.

Equation 5.7 was used as the modeling equation for all the release experiments, and a , b , c , t^* were obtained from the Excel[®] “Solver” function within reasonable range to generate the best fits. Most modeling curves fit well with the experimental data, which, to some extent, contributes to the validity of our theory. With the values of a , b , c , t^* , we can generate the whole release profile. Table 8 shows the fitting results with Equation 5.7.

Table 8 Modeling parameters for the release experiments.

Chapter #	Sample	a (%·hour ⁻¹)	b (%)	c (%·hour ⁻¹)	t* (hour)
3.2.2	Blank	1.66	10.41	0.48	6.79
3.2.2	CPE215	3.29	3.43	0.42	6.01
3.3.1	B-CD	4.14	12.93	0.15	5.32
3.3.1	CPE&CSO	6.72	8.68	0.19	3.54
3.3.1	B-CD+CPE&CSO	10.65	9.02	0.33	2.20
3.3.1	a-CD+CPE&CSO	15.25	23.07	0.09	3.47
3.3.2	C&C+20x B-CD	14.68	16.79	0.23	2.12
3.3.2	C&C+1x a-CD	9.94	9.86	0.20	2.51
3.3.2	C&C+20x a-CD	14.08	10.43	0.19	1.94
3.3.3	Blank	0.71	49.44	0.20	10.00
3.3.3	CSO+B-CD	11.83	55.55	0.02	1.00
3.3.3	CPE+B-CD	6.57	51.72	0.16	0.65
3.3.3	CPE+CSO+B-CD	11.87	40.41	0.28	0.94
3.4.1	Blank	0.90	2.14	0.70	10.00
3.4.1	CPE-215	2.90	0.41	0.62	2.60
3.4.1	Cottonseed Oil	4.26	0.65	0.30	5.78
3.4.1	CPE+B-CD	4.90	1.34	0.58	6.47
3.4.1	CSO+B-CD	7.11	1.67	0.83	5.14
3.4.2	Blank	0.91	4.02	0.71	54.29
3.4.2	B-CD	4.17	5.59	0.50	5.01
3.4.2	1xCPE&CSO	8.58	3.21	0.45	4.04
3.4.2	3xCPE&CSO	10.20	5.11	0.20	4.22
3.4.2	1xCPE&CSO+B-CD	23.96	9.34	0.39	2.35
3.4.2	3xCPE&CSO+B-CD	29.26	13.66	0.54	1.63
3.5.1	pH7 Blank	0.66	-0.07	0.62	2.45
3.5.1	pH7 C&C+B-CD	20.62	-2.33	0.70	2.53
3.5.2	Blank	0.32	-0.14	0.36	21.75
3.5.2	C&C	1.16	-1.91	0.89	9.04
3.5.2	C&C+B-CD	5.02	-2.33	0.79	14.09
3.5.3	Blank	0.36	-0.73	0.23	16.91
3.5.3	C&C	0.46	-0.37	0.20	23.42
3.5.3	C&C+B-CD	4.16	2.15	1.30	7.87
3.6	Blank	1.32	0.29	0.40	49.04
3.6	CPE	2.10	-0.81	0.50	29.68
3.6	CPE&CSO	4.13	-2.36	0.23	18.83

One can observe that the *a* value, representing the burst release rate, is system dependant and fluctuates widely based on the release conditions from 0.32 %/hour to almost 30 %/hour. The *c* value reflects the leakage rate and should be small and reasonably the same for all systems; in our case, it ranges

from 0.02 %/hour to 1.3 %/hour. Here, $c \leq a$. Although t^* has a physical meaning in the model, which is system dependant and related to the time needed for the liposomes to restore the barrier function, it is hard to find a reasonable explanation to the wild fluctuation of t^* values given by the model in Table 8. The meaning of t^* in the model may need further modification.

5.2. Neural Network

5.2.1. Introduction to Neural Network

A neural network is an information processing paradigm that is inspired by the way biological nervous systems, such as the brain, process information.¹²⁷ The key element of this paradigm is the novel structure of the information processing system. It is composed of a large number of highly interconnected processing elements (neurons) working in parallel to solve specific problems. Neural networks, like people, learn by example. A neural network is configured for a specific application, such as pattern recognition or data classification, through a learning process. Learning in biological systems involves adjustments to the synaptic connections that exist between the neurons, which is true for neural networks as well.

The field of neural network was established before the advent of computers, but many important advances did not appear until the use of fast and inexpensive computers.

Neural networks take a different approach to problem solving than that of conventional computers. Conventional computers use an algorithmic approach,

i.e. the computer follows a set of instructions in order to solve a problem. Unless the specific steps that the computer needs to follow are known, the computer cannot solve the problem. But computers would be so much more useful if they could do things that we don't exactly know how to do. Neural networks process information in a similar way the human brain does. They cannot be programmed to perform a specific task. The examples must be selected carefully otherwise useful time is wasted or even worse the network might be functioning incorrectly. The disadvantage is that because the network finds out how to solve the problem by itself, its operation can be unpredictable.

An artificial neuron (Figure 64) is a device with many inputs and one output. The neuron has two modes of operation; the training mode and the predictive mode. In the training mode, the neuron can be trained to fire (or not), for particular input patterns. In the predictive mode, when a taught input pattern is detected at the input, its associated output becomes the current output.

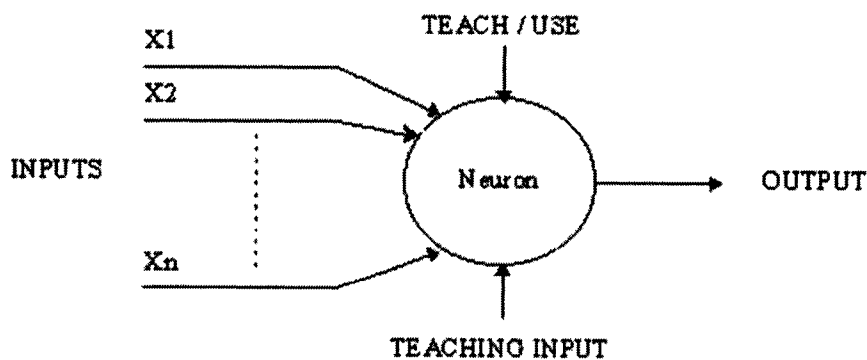


Figure 64 A simple artificial neuron in Neural Network.

The most common type of artificial neural network consists of three layers of neurons: a layer of "input" elements is connected to a layer of "hidden" neurons, which is connected to a layer of "output" neurons (Figure 65). The activity of the input units represents the raw information that is fed into the network. The activity of each hidden unit is determined by the activities of the input units and the weights on the connections between the input and the hidden units. The behavior of the output units depends on the activity of the hidden units and the weights between the hidden and output units.

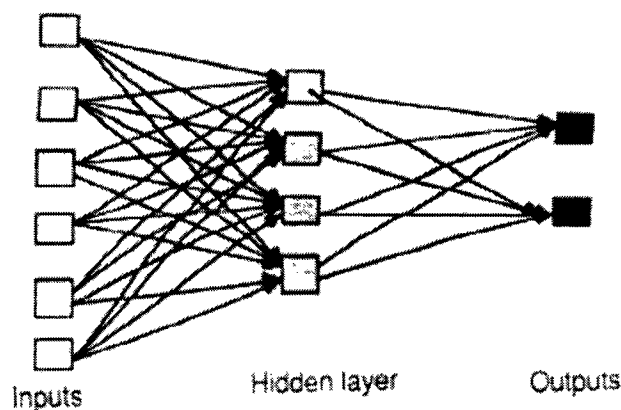


Figure 65 An example of a fully connected feed-forward network.

Every neural network possesses knowledge which is contained in the values of the connections weights (Figure 66). Modifying the knowledge stored in the network as a function of experience implies a learning (training) rule for changing the values of the weights. Information is stored in the weight matrix W of a neural network. Learning (training) is the determination of the weights.

Incoming neural activations (A_i) multiplied by individual connection weights (W_{ij})

Output activation (A_j) multiplied by individual connection weights (W_{jk}) sent to other neurons

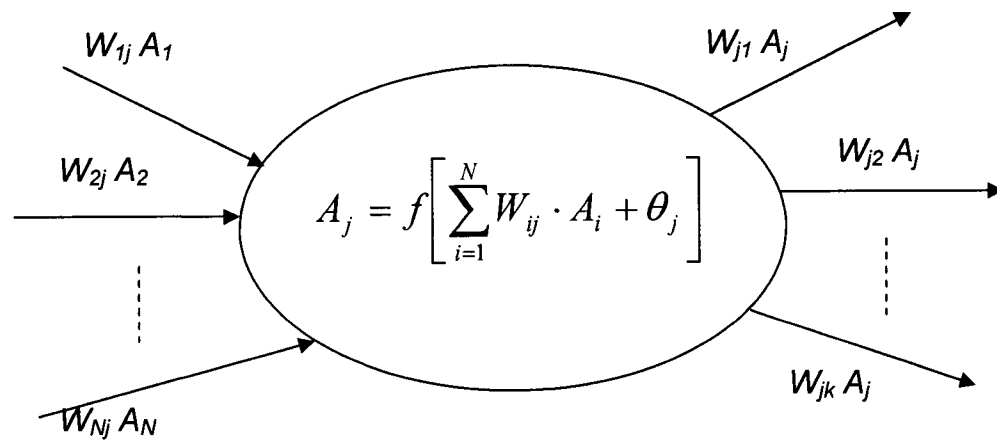


Figure 66 Activation (output) of Neuron j , A_j . W is the individual connection weight; θ_j is the offset or threshold.

Since neural networks are best at identifying patterns or trends in data, they are well suited for prediction or forecasting needs including sales forecasting, industrial process control, customer research, data validation, risk management, target marketing, etc. The ability to learn by example makes neural network very flexible and powerful. Furthermore, there is no need to devise an algorithm in order to perform a specific task; i.e. there is no need to understand the internal mechanisms of that task.

5.2.2. Application of Neural Network Model

One major purpose of modeling is to have the ability to forecast. Although we have proposed a theory and mathematical model for the process of protein release from liposomes with permeation enhancers, we would like to use a neural network to predict the release process, i.e. to predict a , b , c , t^* values, based on given conditions.

There are nine major factors that affect the protein release profile, which means there are nine inputs for our neural network. These inputs are ΔT ($T-T_c$), cholesterol content in lipid bilayer, molecular weight of protein, amount of CPE-215[®], amount of cottonseed oil, ratio of total oil (CPE-215[®] and cottonseed oil) to lipid content (DPPC and cholesterol), percent of β -cyclodextrin in the aqueous phase, percent of α -cyclodextrin in the aqueous phase, and pH.

We listed all nine factors and a , b , c , t^* values for each experimental release curve in Table 9. In order to easily trace back to the experiment, the number of chapter where the experiment was mentioned in this thesis and the sample name were also shown in Table 9. According to our liposome DSC data, the phase transition temperature for 4:1 (w/w) DPPC/Cholesterol liposome is 46 °C, which is the reason why when using DPPC/Cholesterol liposomes at 37 °C, the ΔT is shown as -9. We used insulin dimer for the insulin molecular weight because we know at the release concentration and condition inside of liposomes, insulin mostly existed as dimers, and probably penetrated the liposomes as dimers. Since Table 9 was used for the training of our neural network, two sets of

data (randomly selected), which were used to test the prediction, are not listed here.

Table 9 Neural network matrix

Chap #	Sample	ΔT (C)	Ch (%)	Mw	CPE-215 [®] (g)	oil: lipid (w/w)	CSO (g)	β -CD (%)	α -CD (%)	pH	a (%·hr ⁻¹)	b (%)	c (%·h r ⁻¹)	t* (hour)
3.2.2	Blank	0	0	11600	0	0	0	0	0	7.4	1.66	10.41	0.48	6.79
3.2.2	CPE215	0	0	11600	0.25	40.9	0	0	0	7.4	3.29	3.43	0.42	6.01
3.2.2	β -CD	0	0	11600	0	0	0	0.3	0	7	4.14	12.93	0.15	5.32
3.3.1	CPE&CSO	0	0	11600	0.258	54.5	0.086	0	0	7	6.72	8.68	0.19	3.54
3.3.1	β -CD+CPE&CSO	0	0	11600	0.258	54.5	0.086	0.3	0	7	10.65	9.02	0.33	2.20
3.3.1	α -CD+CPE&CSO	0	0	11600	0.258	54.5	0.086	0	2.1	7	15.25	23.07	0.09	3.47
3.3.2	C&C+20x β -CD	0	0	11600	0.046	8.7	0.015	1	0	7	14.68	16.79	0.23	2.12
3.3.2	C&C+1x α -CD	0	0	11600	0.046	8.7	0.015	0	0.05	7	9.94	9.86	0.20	2.51
3.3.2	C&C+20x α -CD	0	0	11600	0.046	8.7	0.015	0	0.9	7	14.08	10.43	0.19	1.94
3.3.3	Blank	0	0	11600	0	0	0	0	0	7	0.71	49.44	0.20	10.00
3.3.3	CSO+ β -CD	0	0	11600	0	0.6	0.0032	1	0	7	11.83	55.55	0.02	1.00
3.3.3	CPE+ β -CD	0	0	11600	0.0095	1.6	0	1	0	7	6.57	51.72	0.16	0.65
3.3.3	CPE+CSO+ β -CD	0	0	11600	0.0095	2.2	0.0032	1	0	7	11.87	40.41	0.28	0.94
3.4.1	Blank	-9	20	11600	0	0	0	0	0	7	0.90	2.14	0.70	10.00
3.4.1	CPE-215	-9	20	11600	0.0084	1	0	0	0	7	2.90	0.41	0.62	2.60
3.4.1	Cottonseed Oil	-9	20	11600	0	1.1	0.0096	0	0	7	4.26	0.65	0.30	5.78
3.4.1	CPE+ β -CD	-9	20	11600	0.0084	1	0	1.3	0	7	4.90	1.34	0.58	6.47
3.4.2	Blank	-9	20	11600	0	0	0	0	0	7	0.91	4.02	0.71	54.29
3.4.2	β -CD	-9	20	11600	0	0	0	1.7	0	7	4.17	5.59	0.50	5.01
3.4.2	1xCPE&CSO	-9	20	11600	0.009	1.4	0.003	0	0	7	8.58	3.21	0.45	4.04
3.4.2	3xCPE&CSO	-9	20	11600	0.027	4.1	0.009	0	0	7	10.20	5.11	0.20	4.22
3.4.2	1xCPE&CSO+ β -CD	-9	20	11600	0.009	1.4	0.003	1.7	0	7	23.96	9.34	0.39	2.35
3.4.2	3xCPE&CSO+ β -CD	-9	20	11600	0.027	4.1	0.009	1.7	0	7	29.26	13.66	0.54	1.63
3.5.1	pH7 Blank	-9	20	11600	0	0	0	0	0	7	0.66	-0.07	0.62	2.45
3.5.2	Blank	-9	20	11600	0	0	0	0	0	10	0.32	-0.14	0.36	21.75
3.5.2	C&C	-9	20	11600	0.0084	1.3	0.0028	0	0	10	1.16	-1.91	0.89	9.04
3.5.2	C&C+ β -CD	-9	20	11600	0.0084	1.3	0.0028	1.7	0	10	5.02	-2.33	0.79	14.09
3.5.3	Blank	-9	20	11600	0	0	0	0	0	4	0.36	-0.73	0.23	16.91
3.5.3	C&C	-9	20	11600	0.0084	1.3	0.0028	0	0	4	0.46	-0.37	0.20	23.42
3.5.3	C&C+ β -CD	-9	20	11600	0.0084	1.3	0.0028	1.7	0	4	4.16	2.15	1.30	7.87
3.6	Blank	-9	20	66000	0	0	0	0	0	7	1.32	0.29	0.40	49.04
3.6	CPE	-9	20	66000	0.013	1	0	0	0	7	2.10	-0.81	0.50	29.68
3.6	CPE&CSO	-9	20	66000	0.013	1.4	0.0043	0	0	7	4.13	-2.36	0.23	18.83

The neural network software we are using is FORECASTER XL™ from ALYUDA Research, Inc, which is a MS Excel add-in program for forecasting and data analysis using neural network method. We used this program to form the network and forecast *a*, *b*, *c*, *t** values one at a time. In that case, we have nine

inputs and one output each time. We have 33 sets of data to form the network, in which 85% (28) of the data sets would be used for network training and 15% (5) of the data sets would be used for testing purposes by the program; the program requires the data sets should be at least three times more than the number of inputs, and we barely met this minimum requirement.

5.2.3. Neural Network Model Analysis

For neural network modeling, the major task for users is to form the input and output matrix, then the rest is all automatic calculation. We did the calculation for a , b , c and t^* one by one. After each calculation, the program gave a report on the neural network formed.

For the network formed for the purpose of predicting the value of a , the program gave some figures to visualize the deviation of the forecasted value from the actual result. From Figure 67, we can see the forecasted value did not deviate from the actual value significantly, except for a few rows. Given the limited number of experimental data sets, this is a reasonable network model for the prediction the value of a .

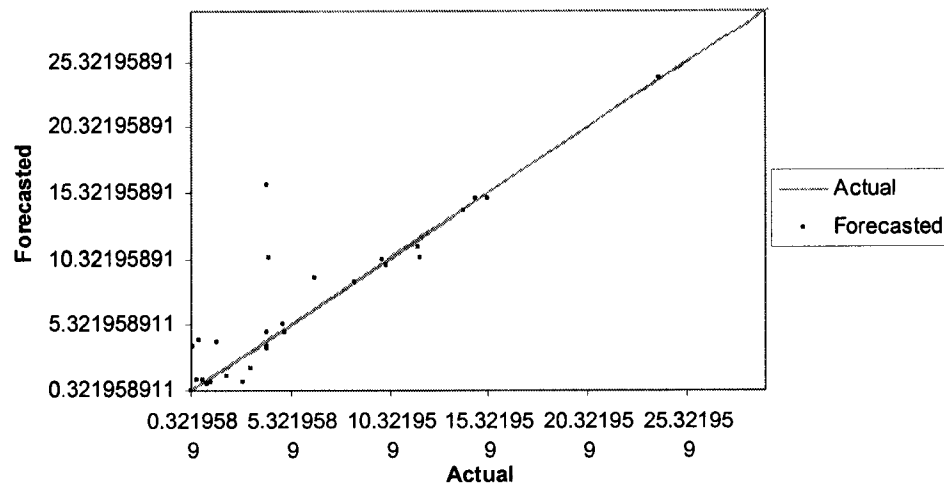


Figure 67 The actual vs. forecast for the neural network for predicting *a*.

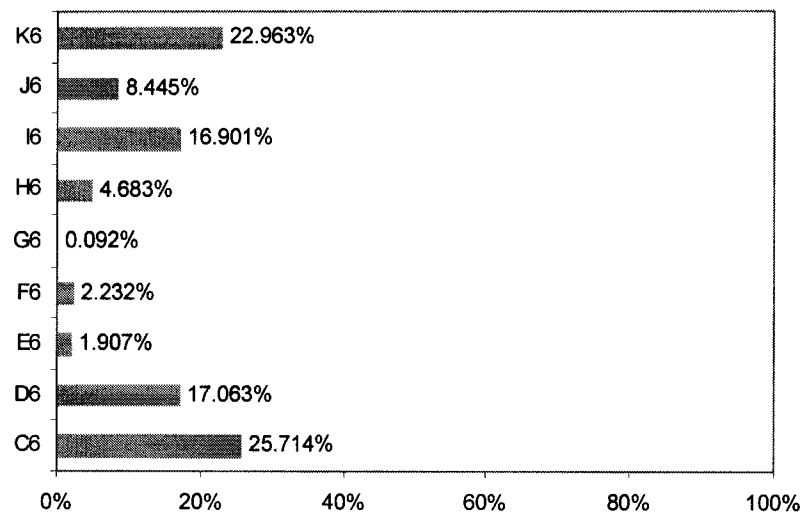


Figure 68 Input importance for each parameter in the network for predicting *a*. C6 is ΔT ($T - T_c$), D6 is the cholesterol content in lipid bilayer, E6 is the molecular weight of protein, F6 is the amount of CPE-215[®], H6 is the amount of cottonseed oil, G6 is the ratio of total oil (CPE-215[®] and cottonseed oil) to lipid content (DPPC and cholesterol), I6 is the percent of β -cyclodextrin in the aqueous phase, J6 is the percent of α -cyclodextrin in the aqueous phase, and K6 is pH.

Figure 68 shows that the parameters of temperature, cholesterol content in lipid bilayer, β -cyclodextrin concentration and pH have significant influence on the a value, which is the rate of triggered boost release at the beginning of the protein release. Based on our knowledge of our protein release system, the major factors that the network picked seem reasonable: the temperature and cholesterol content have significant influence on liposome properties; β -cyclodextrin is an efficient phase transfer agent to transport CPE-215[®] to the membrane; pH would affect the surface charge character of proteins and as a result greatly alter the permeation ability of proteins.

For the neural network formed for the purpose of predicting the value of c , the program also gave some figures to visualize the deviation of the forecasted value from the actual result. From Figure 69, we can see the forecasted value did not deviate from the actual value too much. Again, this is a reasonable network model for the prediction of c value.

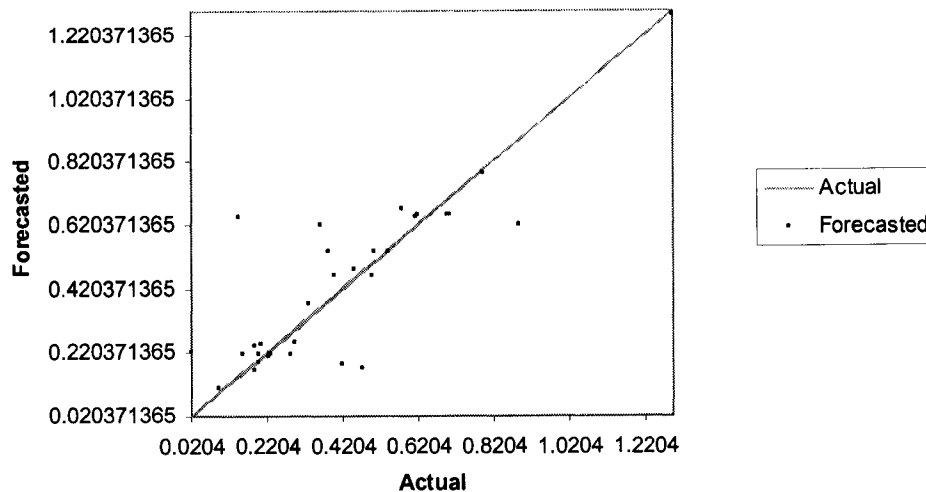


Figure 69 The actual vs. forecast (scatter plot) for the neural network for predicting *c*.

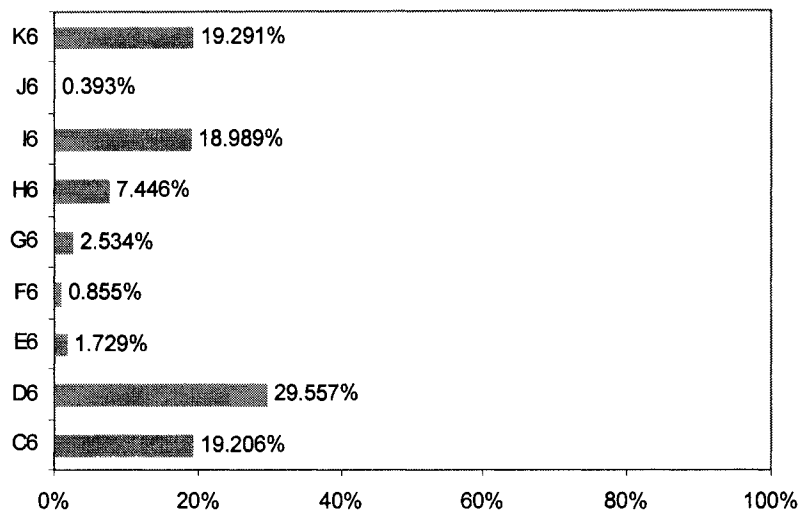


Figure 70 Input importance for each parameter in the network for predicting *c*. C6 is ΔT ($T - T_c$), D6 is the cholesterol content in lipid bilayer, E6 is the molecular weight of protein, F6 is the amount of CPE-215[®], H6 is the amount of cottonseed oil, G6 is the ratio of total oil (CPE-215[®] and cottonseed oil) to lipid content (DPPC and cholesterol), I6 is the percent of β -cyclodextrin in the aqueous phase, J6 is the percent of α -cyclodextrin in the aqueous phase, and K6 is pH.

Figure 70 shows that temperature, cholesterol content in lipid bilayer, β -cyclodextrin concentration and pH have significant influence on the c value, which is similar to what the previous neural network picked for a value. The value of c represents the self-leakage rate of liposomes. Again, this is a reasonable pick of major parameters for the similar reasons.

For the neural network formed for the purpose of predicting the value of t^* , the program also gave some figures to visualize the deviation of the forecasted value from the actual result. The value of t^* represents the time when the permeation enhancers starts to diffuse evenly within the lipid bilayer and the system starts to change from the triggered boost release to liposome self-leakage. From Figure 71, we can see the forecasted value did not deviate from the actual value too much, except for one and actually that one is a "Blank" sample. As to "Blank" samples, t^* does not have meanings for them, because they actually do not have a transition time point. Therefore, this is an effective network model for the prediction of t^* value for non-"Blank" samples.

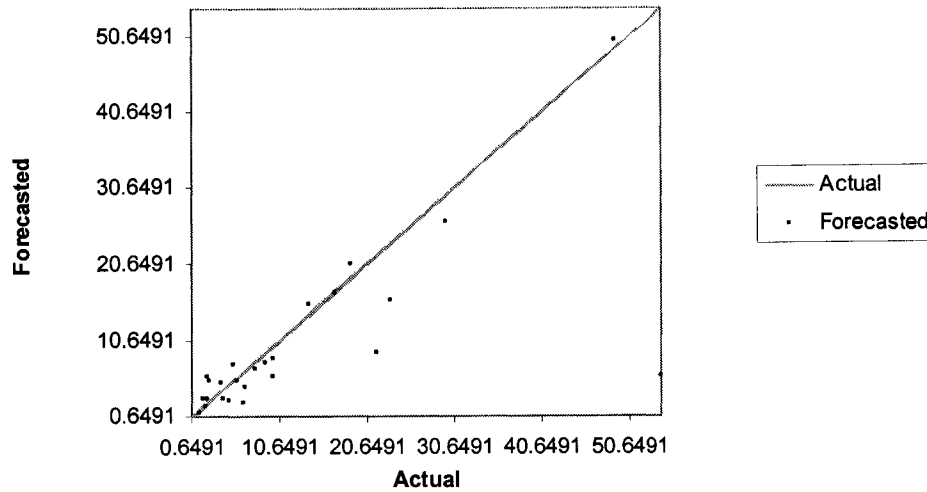


Figure 71 The actual vs. forecast (scatter plot) for the neural network for predicting t^* .

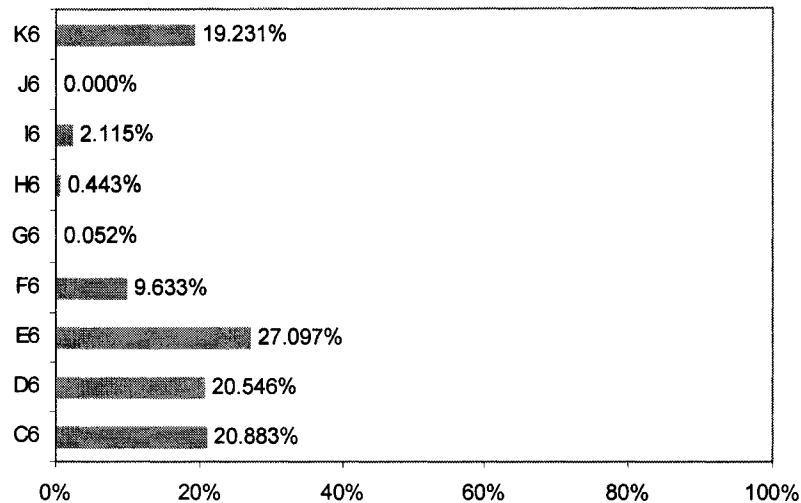


Figure 72 Input importance for each parameter in the network for predicting t^* . C6 is ΔT ($T - T_c$), D6 is the cholesterol content in lipid bilayer, E6 is the molecular weight of protein, F6 is the amount of CPE-215[®], H6 is the amount of cottonseed oil, G6 is the ratio of total oil (CPE-215[®] and cottonseed oil) to lipid content (DPPC and cholesterol), I6 is the percent of β -cyclodextrin in the aqueous phase, J6 is the percent of α -cyclodextrin in the aqueous phase, and K6 is pH.

Figure 72 shows that temperature, cholesterol content in lipid bilayer, protein molecular weight and pH have significant influence on the t^* value. It is easy to understand the influence of temperature and cholesterol content in lipid bilayer on the t^* value, but it is hard to relate t^* to protein molecular weight and pH. Maybe this is due to the limitation in the number of data sets.

Neural network training was performed for b , but the result was not useful as expected. The parameter b has the meaning of systemic error; therefore, there is no real meaning in predicting b value. For the purpose of forecasting, we used $b = 0.01$, since the b value can not be zero.

5.2.4. Neural Network Prediction

After we formed the neural networks for a , c and t^* , we wanted to see if the neural networks can predict reasonable values for a , c and t^* for other release experiments. Table 10 shows the data sets we used to test the neural network prediction. Table 11 gives out the result of neural network prediction values versus the mathematical fit values of a , c and t^* .

Table 10 Experimental data sets for neural network prediction.

Chap #	Sample	ΔT (C)	Chol (%)	Mw	CPE-215 [®] (g)	oil: lipid (w/w)	CSO (g)	β -CD (%)	α -CD (%)	pH
3.4.1	CSO+B-CD	-9	20	11600	0	1.1	0.0096	1.3	0	7
3.5.1	C&C+B-CD	-9	20	11600	0.009	1.4	0.003	1.7	0	7

Table 11 Neural network prediction compared with the math model result.

	CSO+B-CD		C&C+B-CD	
	Math Fit	Neural Network Prediction	Math Fit	Neural Network Prediction
a (%•hour ⁻¹)	7.11	7.88	20.61	24.03
b (%)	1.67	0.01 [†]	-2.33	0.01 [†]
c (%•hour ⁻¹)	0.83	0.68	0.70	0.54
t^* (hour)	5.14	2.39	2.53	2.07

[†] The value of b in Neural Network is not predicted, but arbitrarily put as 0.01.

Figure 73 and Figure 74 show the deviation of the forecasted model curve from the real experimental data. One neural network prediction fits well with the experimental data, while the other only fits the early data. Given the fact that the neural network forecast was based on a , c , and t^* values that were from the empirical mathematical model, which was not exactly the same as the real data, and the limited number of data sets, the prediction are acceptable, though we recognize that they are far from ideal.

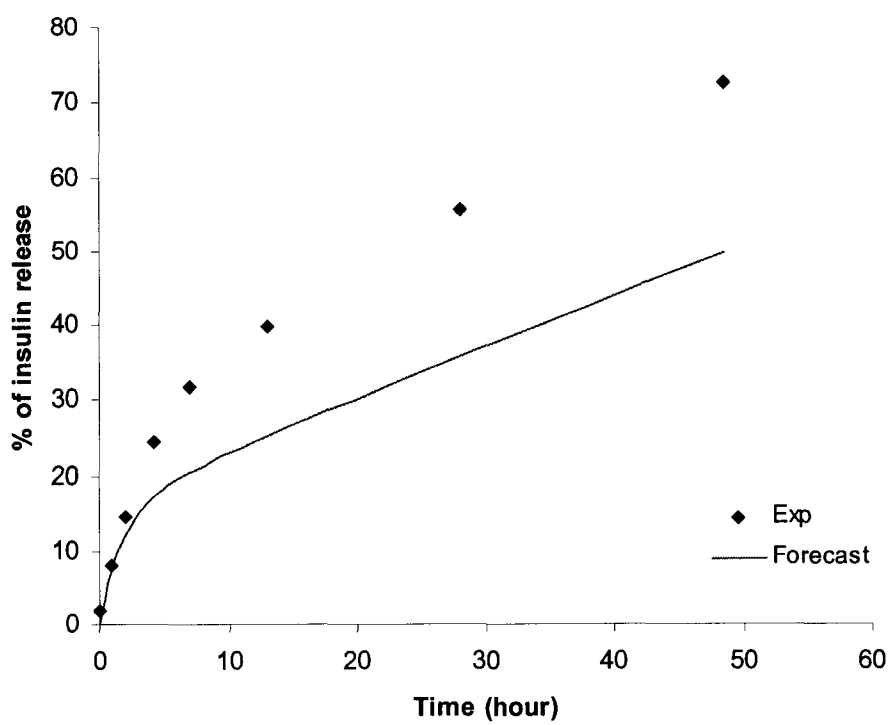


Figure 73 Neural network forecast for “CSO+B-CD” sample in Chapter 3.4.1.

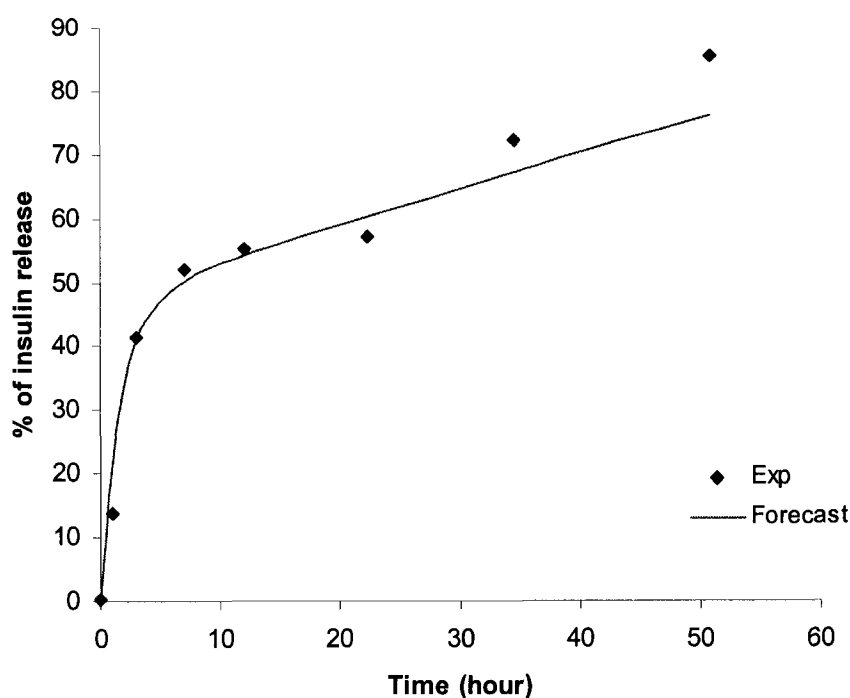


Figure 74 Neural network forecast for “C&C+B-CD” sample in Chapter 3.5.1.

Among the three major parameters a , c , and t^* , a is the one that we are most interested in to do predictions since it is the triggered boost release rate. Based on the neural network we formed, we wanted to know under what conditions the highest a value could be achieved. Figure 68 shows the individual connection weight for each input condition --- temperature, cholesterol content in lipid bilayer, β -cyclodextrin concentration and pH have significant influence on the a value. The neural network predicted the maximum a value could be reached at 37 °C in pH 7 from 4:1 DPPC/Cholesterol liposome with the highest concentrations of phase transfer agents, CPE-215[®] and cottonseed oil. In

practical situations, phase transfer agents have their solubility limit and the amount of CPE-215[®] and cottonseed oil added does have limit. Under the conditions of 37 °C, pH 7, 4:1 DPPC/Cholesterol liposome, insulin dimer, 0.06 g CPE-215[®], 0.02 g cottonseed oil, 1.7% β -cyclodextrin, 2.1% α -cyclodextrin, the neural network predicted the boost release rate, a value, to be 31.9 %•hour⁻¹, which is more than 40 times faster than the liposome leakage rate (0.73 %•hour⁻¹).

CHAPTER 6

CONCLUSION

In our study of the enhancement effect of cyclopentadecanolide (CPE-215[®]) on protein permeation through lipid membranes, we successfully designed and developed a novel in vitro membrane permeability model – liposome. This model system can not only be used to perform in vitro protein release experiments, but also can be used as a tool to select promising intranasal formulations before the expensive animal tests. We effectively labeled the proteins (insulin and BSA) with fluorescein to increase their detection sensitivity at low concentrations. By utilizing the extrusion technique, we can prepare “mono-dispersed” 400 nm large unilamellar vesicles/liposomes; when using 1% (weight) lipid content to make 400 nm unilamellar DPPC liposomes, the encapsulation efficiency is 10%. We prepared different liposomes with DPPC, cholesterol and CPE-215[®], among which DPPC was the major lipid component. We utilized liposomes to encapsulate fluorescein labeled insulin, fluorescein labeled BSA and calcein. We used the centrifugal extraction method to clean the unencapsulated molecules and the molecules adsorbed on the outside surface of liposomes, so that the fluorescence signal outside of liposome was close to the background signal of the buffer solution. We utilized this model to perform a

series of protein release kinetics experiments from liposomes at 37 °C, 42 °C, at pH 7, pH 4, pH 10, in the presence of CPE-215[®], cottonseed oil, cyclodextrins.

The experimental results show that CPE-215[®] is an effective membrane permeation enhancer for proteins; because of the limited solubility of hydrophobic CPE-215[®] in water, a phase transfer agent, for example, cyclodextrins, can further enhance the permeation effect of CPE-215[®]. The pH of the solution has a huge impact on the protein release profile due to the protein surface charge change caused by the pH change. Proteins permeate through lipid bilayers easier at pH levels around its isoelectric point.

Studies on insulin solution properties (self-diffusion and self-association states), the interaction between insulin and liposome, and the interaction between CPE-215[®] and liposomes were carried out to understand the mechanism behind the fact that CPE-215[®] facilitates the protein transport through lipid bilayers. We determined insulin diffusion coefficient at pH 3 at 37 °C to be $1.4 \times 10^{-10} \text{ m}^2/\text{s}$, or $1.4 \times 10^{-6} \text{ cm}^2/\text{s}$ by the pulsed field gradient NMR technique. We determined the binding constant of insulin on a DPPC/Cholesterol liposome surface to be $K = 97 \text{ ml/mg}$, which indicates that insulin only has weak interactions with liposomes. However, we identified that CPE-215[®] almost doubled the insulin adsorption energy on liposome surface by ITC. Based on our calculation, there would be 20 insulin dimers adsorbed on the inner surface of each 400 nm liposome in our release conditions. By modulated DSC, we determined that CPE-215[®] could diffuse across the aqueous phase into the bilayer through limited number of thermal cycles from 10 °C to 90 °C; 20%

(weight) CPE-215[®] can broaden the T_c range, lower the T_c of DPPC liposome by 8 °C and the T_c of DPPC/Cholesterol liposome by 9 °C, and reduce the ΔH of DPPC transition from 37 kJ/mol to 20 kJ/mol.

Based on the mechanism study, our release data and the current liposome leakage theory, we proposed a hypothesis that CPE-215[®] would form a transient “pore” in the lipid bilayer at the beginning of the release experiment; after CPE-215[®] evenly diffused within the bilayer, the barrier function of the lipid bilayer was restored. We performed one set of testing experiments and the result supported our hypothesis theory.

Mathematical modeling approach was used based on our theory. The release kinetics was modeled with Equation 5.7,

$$y = \frac{1}{\left(\frac{1}{(a \cdot t + b)^2} + \frac{1}{(c \cdot t + (a - c) \cdot t^* + b)^2} \right)^{\frac{1}{2}}}$$

where y is the percentage of protein released from liposome, a , c , t^* are adjustable parameters: a is the boost release rate, b represents the systemic error of the experiment, c is the liposome self-leakage rate, t^* is the transition time between the triggered boost release and the self-leakage of liposomes.

Most release data fit well with this model, which further supported our hypothesis theory.

We used the neural network approach to find the internal connections between different release condition parameters based on our limited data sets and tried to predict the protein release profile at new conditions. The values of a , c , t^* were correlated to experimental conditions (temperature difference between

the release temperature and the phase transition temperature of liposome, the cholesterol content in the liposome, the protein molecular weight, the amount of CPE-215[®], the amount of cottonseed oil, the weight ratio of oil (CPE-215[®] and cottonseed oil) to lipid (DPPC and cholesterol), the amount of β -cyclodextrin and α -cyclodextrin, and pH) through neural networks. Neural network predicted the values of a and c within 20% error, and t^* with a 20% to 50% error. The initial burst release rate is the most concerned parameter when the model is used to determine the promising intranasal formulations. The prediction result shows that reasonable neural networks were successfully formed for the major parameters of the mathematical model. The neural network predicted the maximum value of a of 31.9 %·hour⁻¹, for the condition of 37 °C, 4:1 DPPC/Cholesterol liposome at pH 7 with 1.7% of β -cyclodextrin and 2.1% α -cyclodextrin, 0.06 g CPE-215[®] and 0.02 g cottonseed oil, which is more than 40 times faster than the liposome leakage rate.

LIST OF REFERENCES

-
- ¹ Lee, Vincent H. L. Peptide and protein drug delivery: past, present and future. *Drug Targeting and Delivery* (1995), 4, 3-19.
- ² Jain, R. K. The next frontier of molecular medicine: Delivery of therapeutics. *Nature Medicine* (1998), 4, 655-657.
- ³ Akers, Michael J.; Defelippis, Michael R. Peptides and proteins as parenteral solutions. Editor(s): Frokjaer, Sven; Hovgaard, Lars. *Pharmaceutical Formulation Development of Peptides and Proteins* (2000), 145-177. Publisher: Taylor & Francis Ltd., London, UK
- ⁴ Shah, Rakhi B.; Ahsan, Fakhru; Khan, Mansoor A. Oral delivery of proteins: progress and prognostication. *Critical Reviews in Therapeutic Drug Carrier Systems* (2002), 19(2), 135-169.
- ⁵ Lambkin, Imelda; Pinilla, Clemencia. Targeting approaches to oral drug delivery. *Expert Opinion on Biological Therapy* (2002), 2(1), 67-73.
- ⁶ Cleland, Jeffrey L.; Daugherty, Ann; Mrsny, Randall. Emerging protein delivery methods. *Current Opinion in Biotechnology* (2001), 12(2), 212-219.
- ⁷ Gonda, Igor. The ascent of pulmonary drug delivery. *Journal of Pharmaceutical Sciences* (2000), 89(7), 940-945.
- ⁸ Torres-Lugo, Madeline; Peppas, Nikolaos A.. Transmucosal delivery systems for calcitonin: a review. *Biomaterials* (2000), 21(12), 1191-1196.
- ⁹ O'Hagan, D. T.; Illum, L.. Absorption of peptides and proteins from the respiratory tract and the potential for development of locally administered vaccine. *Critical Reviews in Therapeutic Drug Carrier Systems* (1990), 7(1), 35-97.

-
- ¹⁰ Pillai, Omathanu; Nair, Vinod; Jain, Amit Kumar; Thomas, Narisetty Sunil; Panchagnula, Ramesh. Noninvasive transdermal delivery of peptides and proteins. *Drugs of the Future* (2001), 26(8), 779-791.
- ¹¹ Kost, Joseph. Ultrasound-Assisted Insulin Delivery and Noninvasive Glucose Sensing. *Diabetes Technology & Therapeutics* (2002), 4(4), 489-497.
- ¹² Sayani, Aryn P.; Chien, Yie W. Systemic delivery of peptides and proteins across absorptive mucosae. *Critical Reviews in Therapeutic Drug Carrier Systems* (1996), 13(1&2), 85-184.
- ¹³ Senel, Sevda; Kremer, Mary; Nagy, Katalin; Squier, Christopher. Delivery of bioactive peptides and proteins across oral (buccal) mucosa. *Current Pharmaceutical Biotechnology* (2001), 2(2), 175-186.
- ¹⁴ Duvvuri, Sridhar; Majumdar, Soumyajit; Mitra, Ashim K. Drug delivery to the retina: challenges and opportunities. *Expert Opinion on Biological Therapy* (2003), 3(1), 45-56.
- ¹⁵ Dey, Surajit; Mitra, Ashim K.; Krishnamoorthy, Ramesh. Ocular delivery and therapeutics of proteins and peptides. *Drugs and the Pharmaceutical Sciences* (2003), 130(Ophthalmic Drug Delivery Systems (2nd Edition)), 493-514.
- ¹⁶ Yamamoto, Akira; Muranishi, Shozo. Rectal drug delivery systems. Improvement of rectal peptide absorption by absorption enhancers, protease inhibitors and chemical modification. *Advanced Drug Delivery Reviews* (1997), 28(2), 275-299.
- ¹⁷ Okada, Hiroaki; Hillery, Anya M. Vaginal drug delivery. Editor(s): Hillery, Anya M.; Lloyd, Andrew W.; Swarbrick, James. *Drug Delivery and Targeting* (2001), 301-328. Publisher: Taylor & Francis Ltd., London, UK.
- ¹⁸ Langer, R. Drug delivery and targeting. *Nature* (1998), 392, 5-10.
- ¹⁹ Baker, D E. Pegylated interferons. *Rev. Gastroenterol Disord.* (2001), 1, 87-99.

²⁰ Russo, P L., Harrington, G A, Spelman, D W. Needleless intravenous systems: a review. *Am. J. Infect. Control* (1999), 27, 431-434.

²¹ Tobio, M.; Schwendeman, S P; Guo, Y; McIver, J.; Langer, R.; Alonso, M.J. Improved immunogenicity of a core-coated tetanus toxoid delivery system. *Vaccine* (1999), 18, 618-622.

²² Stevenson, C L; Tan, M M. Solution stability of salmon calcitonin at high concentration for delivery of an implantable system. *J. Pept. Res.* (2000), 55, 129-139.

²³ <http://www.mindbranch.com/reports/pdfs/R155-042Sample.pdf>, accessed on January 30, 2004.

²⁴ Drewe, J.; Fricker, G.; Vonderscher, J.; Beglinger, C. Internal absorption of octeotide: absorption enhancement by polyoxyethylene-24-cholesterol ether. *Br. J. Pharmacol.* (1993), 108, 298-303.

²⁵ Gwinup, G.; Elias, A N.; Domurat, E S. Insulin and C-peptide levels following oral administration of insulin in intestinal-enzyme protected capsules. *Gen. Pharmacol.* (1991), 22, 243-246.

²⁶ Wilding, I I.; Hirst, P.; Connor, A. Development of a new engineering-based capsule for human drug absorption studies. *Pharm. Sci. Technol. Today* (2000), 3, 385-392.

²⁷ Sezaki, H. Mucosal penetration enhancement. *J Drug Target* (1995), 3, 175-177.

²⁸ Leone-Bay, A.; Sato, M.; Paton, D.; Hunt, A. H.; Sarubbi, D.; Carozza, M.; Chou, J.; McDonough, J.; Baughman, R. A. Oral delivery of biologically active parathyroid hormone. *Pharm. Res.* (2000), 18, 964-970.

²⁹ Tanaka, K.; Fujita, T.; Yamamoto, Y.; Murakami, M.; Yamamoto, A.; Muranishi, S. Enhancement of intestinal transport of thyrotropin-releasing hormone via a

carrier-mediated transport system by chemical modification with lauric acid. *Biochim. Biophys. Acta* (1996), 1283, 119-126.

³⁰ Gordon Still, J. Development of oral insulin: progress and current status. *Diabetes/metabolism Res. Rev.* (2002), 18 (Suppl 1), S29-S37.

³¹ Nielsen, C U.; Andersen, R.; Brodin, B.; Frokjaer, S.; Taub, M E.; Steffansen, B. Dipeptide model prodrugs for the intestinal oligopeptide transporter. Affinity for and transport via hPepT1 in the human intestinal Caco-2 cell line. *J. Control. Rel.* (2001), 76, 129-138.

³² Kramer, W.; Wess, G.; Enhsen, A.; Falk, E.; Hoffmann, A.; Neckermann, G.; Schubert, G.; Urmann, M. Modified bile acids as carriers for peptides and drugs. *J. Control. Rel.* (1997), 46, 17-30.

³³ Morris, M C; Vidal, P.; Chaloin, L.; Heitz, F.; Divita, G. A new peptide vector for efficient delivery of oligonucleotides into mammalian cells. *Nucleic Acids Res.* (1997), 25, 2730-2736.

³⁴ Hussain, N.; Jaitley, V.; Florence, A. T. Recent advances in the understanding of uptake of microparticulates across the gastrointestinal lymphatics. *Adv. Drug Del. Rev.* (2001), 50, 107-142.

³⁵ Oksendal, A N; Bach-Gansmo, T; Jacobsen, T. F; Eide, H.; Andrew, E. Oral magnetic particles. Results from clinical phase II trials in 216 patients. *Acta Radiol.* (1993), 34, 187-193.

³⁶ Patton, J.S; Platz, R.M. Pulmonary delivery of peptides and proteins for systemic action. *Adv. Drug Deliv. Rev.* (1992), 8, 179-196.

³⁷ Illum, L. The nasal route for delivery of polypeptides. In: *Peptide and Protein Drug Delivery*. Eds. Frokjaer, S., Chrstrup, L., Krogsgaard-Larsen, P., Munksgaard, Copenhagen 1990, p157-170.

³⁸ Behl, C R; Pimplaskar H K; Sileno, A P; Xia W J; deMeireles J C; Romeo, V D. Optimization of systemic nasal drug delivery with pharmaceutical excipients. *Adv. Drug Del. Rev.* (1998), 29, 117-133.

³⁹ Illum, L.; Farraj, N F; Davis, SS. Chitosan as a novel nasal delivery system for peptide drugs. *Pharm. Res.* (1994), 11, 1186-1189.

⁴⁰ Illum, L. Transport of drugs from the nasal cavity to the central nervous system. *Review. Eur. J. Pharm. Sci.* (2000), 11, 1-18.

⁴¹ Frey, W H; Liu, J.; Chen, X.; Thorne, R G.; Fawcett, R G.; Ala, T A.; Rahman, Y-E. Delivery of 125I-NGF to the brain via the olfactory route. *Drug Del.* (1997), 4, 87-92.

⁴² Born, J.; Lange, T.; Kern, W.; McGregor, G P.; Bickel, U.; Fehm, H L. Sniffing neuropeptides: a transnasal approach to the human brain. *Nat. Neurosci.* (2002), 5, 514-516.

⁴³ De Groot, A N.; Vree, T B.; Hekster, Y A.; Pesman, G J.; Sweep, F C.; Van Dongen, P J.; Van Roosmalen, J. Bioavailability and pharmacokinetics of sublingual oxytocin in male volunteers. *J. Pharm. Pharmacol.* (1995), 47, 571-575.

⁴⁴ Modi, P.; Mihic, M.; Lewin, A. The evolving role of oral insulin in the treatment of diabetes using a novel RapidMist(trade mark) System. *Diabetes Metab. Res. Rev.* (2002), 18(suppl 1), S38-S42.

⁴⁵ Owens, D R. New Horizons – alternative routes for insulin therapy. *Nature Reviews* (2002), 1, 529-540.

⁴⁶ Langkjaer, L.; Brange, J.; Grodsky, G M.; Guy, R H. Iontophoresis of monomeric insulin analogues in vitro: effects of insulin charge and skin pre-treatment. *J. Control. Rel.* (1998), 51, 47-56.

⁴⁷ Mitragotri, S.; Blankschtein, D.; Langer, R. Ultrasound-mediated transdermal protein delivery. *Science* (1995), 269, 850-853.

⁴⁸ Cevc, G. Transfersomes, liposomes and other liquid suspensions on the skin: permeation enhancement vesicle penetration and transdermal drug delivery. *Crit. Rev. Ther. Drug Carrier Syst.* (1996), 13, 257-388.

⁴⁹ McAllister, D V.; Allen, M G; Prausnitz, M R. Microfabricated microneedles for gene and drug delivery. *Ann. Rev. Biomed. Eng.* (2000), 2, 289-313.

⁵⁰ Handouts of the Workshop of Formulation Development of Therapeutic Proteins and Drug Delivery Systems for Peptides and Protein Drugs, Chicago, IL, 2003.

⁵¹ <http://ntri.tamuk.edu/cell/membranes.html>, accessed on 02/23/2004.

⁵² Gennis, R. B. *Biomembranes: Molecular Structure and Function*; Springer-Verlag New York Inc: New York, 1989, 24.

⁵³ Gennis, R. B. *Biomembranes: Molecular Structure and Function*; Springer-Verlag New York Inc: New York, 1989, 64.

⁵⁴ Hilgers, Allen R.; Conradi, Robert A.; Burton, Philip S. Caco-2 cell monolayers as a model for drug transport across the intestinal mucosa. *Pharmaceutical Research* (1990), 7(9), 902-910.

⁵⁵ Karlsson, Johan; Artursson, Per. A method for the determination of cellular permeability coefficients and aqueous boundary layer thickness in monolayers of intestinal epithelial (Caco-2) cells grown in permeable filter chambers. *International Journal of Pharmaceutics* (1991), 71(1-2), 55-64.

⁵⁶ Kansy, Manfred; Senner, Frank; Gubernator, Klaus. Physicochemical High Throughput Screening: Parallel Artificial Membrane Permeation Assay in the Description of Passive Absorption Processes. *Journal of Medicinal Chemistry* (1998), 41(7), 1007-1010.

⁵⁷ Avdeef, Alex; Strafford, Melissa; Block, Eric; Balogh, Michael P.; Chambliss, Walter; Khan, Ikhlas. Drug absorption in vitro model: filter-immobilized artificial membranes 2. Studies of the permeability properties of lactones in Piper methysticum Forst. *European Journal of Pharmaceutical Sciences* (2001), 14(4), 271-280.

⁵⁸ Sugano, Kiyohiko; Hamada, Hirokazu; Machida, Minoru; Ushio, Hidetoshi. High throughput prediction of oral absorption: Improvement of the composition of the lipid solution used in parallel artificial membrane permeation assay. *Journal of Biomolecular Screening* (2001), 6(3), 189-196.

⁵⁹ Wohnsland, Frank; Faller, Bernard. High-Throughput Permeability pH Profile and High-Throughput Alkane/Water log P with Artificial Membranes. *Journal of Medicinal Chemistry* (2001), 44(6), 923-930.

⁶⁰ Drummond, Daryl C.; Kirpotin, Dmitri; Benz, Christopher C.; Park, John W.; Hong, Keelung. Liposomal drug delivery systems for cancer therapy. Editor(s): Brown, Dennis M. *Drug Delivery Systems in Cancer Therapy* (2004), 191-213. Publisher: Humana Press Inc., Totowa, N. J

⁶¹ Martin, Francis J.; Huang, Tony. STEALTH liposomal technology: current therapies & future directions. *Drug Delivery Technology* (2003), 3(5), 66-73.

⁶² Antonietti, Markus; Foerster, Stephan. Vesicles and liposomes: A self-assembly principle beyond lipids. *Advanced Materials* (Weinheim, Germany) (2003), 15(16), 1323-1333.

⁶³ Jorgensen, Kent; Hoyrup, Pernille; Pedersen, Tina B.; Mouritsen, Ole G. Dynamical and structural properties of lipid membranes in relation to liposomal drug delivery systems. *Cellular & Molecular Biology Letters* (2001), 6(2A), 255-263.

⁶⁴ de Gier, J. Osmotic behavior and permeability properties of liposomes. *Chemistry and Physics of Lipids* (1993), 64(1-3), 187-96.

⁶⁵ <http://www.avantilipids.com/PreparationOfLiposomes.html>, accessed on 04/23/2004.

⁶⁶ Bangham, A. D.; Standish, M. M.; Watkins, J. C. Diffusion of univalent ions across the lamellae of swollen phospholipids. *Journal of Molecular Biology* (1965), 13(1), 238-52.

⁶⁷ Deamer, D.; Bangham, A. D. Large volume liposomes by an ether vaporization method. *Biochimica et Biophysica Acta* (1976), 443(3), 629-34.

⁶⁸ Schieren, H.; Rudolph, S.; Finkelstein, M.; Coleman, P.; Weissmann, G. Comparison of large unilamellar vesicles prepared by a petroleum ether vaporization method with multilamellar vesicles: ESR, diffusion and entrapment analyses. *BIOCHIMICA ET BIOPHYSICA ACTA* (1978 Aug 3), 542(1), 137-53.

⁶⁹ Deamer, David W.. Preparation and properties of ether-injection liposomes. *Annals of the New York Academy of Sciences* (1978), 308 250-8.

⁷⁰ Papahadjopoulos, D.; Vail, W. J.; Jacobson, K.; Poste, G. Cochleate lipid cylinders. Formation by fusion of unilamellar lipid vesicles. *Biochimica et Biophysica Acta* (1975), 394(3), 483-91.

⁷¹ Szoka, Francis; Papahadjopoulos, Demetrios. Liposomes: preparation and characterization. *Research Monographs in Cell and Tissue Physiology* (1981), 7(Liposomes: Phys. Struct. Ther. Appl.), 51-82.

⁷² Szoka, Francis, Jr.; Papahadjopoulos, Demetrios. Procedure for preparation of liposomes with large internal aqueous space and high capture by reverse-phase evaporation. *Proceedings of the National Academy of Sciences of the United States of America* (1978), 75(9), 4194-4198.

⁷³ Szoka F; Olson F; Heath T; Vail W; Mayhew E; Papahadjopoulos D Preparation of unilamellar liposomes of intermediate size (0.1-0.2 μm) by a combination of reverse phase evaporation and extrusion through polycarbonate membranes. *BIOCHIMICA ET BIOPHYSICA ACTA* (1980 Oct 2), 601(3), 559-571.

⁷⁴ Olson, F.; Hunt, C. A.; Szoka, F. C.; Vail, W. J.; Papahadjopoulos, D. Preparation of liposomes of defined size distribution by extrusion through polycarbonate membranes. *Biochimica et Biophysica Acta* (1979), 557(1), 9-23.

⁷⁵ Gregoriadis, G.; Kirby, C.; Meehan, A.; Senior, J. Targeting of liposomes: some prerequisites for success. *Liposomes, Drugs Immunocompetent Cell Funct.*, [Proc. Conf.] (1981), 29-51.

⁷⁶ Papahadjopoulos, Demetrios; Miller, Nigel. Phospholipid model membranes. I. Structural characteristics of hydrated liquid crystals. *Biochimica et Biophysica Acta* (1967), 135(4), 624-638.

⁷⁷ Huang C Studies on phosphatidylcholine vesicles. Formation and physical characteristics. *BIOCHEMISTRY* (1969), 8(1), 344-352.

⁷⁸ Batzri, Shmuel; Korn, Edward D. Single bilayer liposomes prepared without sonication. *Biochimica et Biophysica Acta* (1973), 298(4), 1015-1019.

⁷⁹ Milsmann, Manfred H. W.; Schwendener, Reto A.; Weder, Hans Georg. The preparation of large single bilayer liposomes by a fast and controlled dialysis. *Biochimica et Biophysica Acta* (1978), 512(1), 147-155.

⁸⁰ Battelle Memorial Institute, British Patent Application 2001929A, 1979.

⁸¹ Bonina, F.; Montenegro, L.; Rosa, C. La; Gasparri, F.; Leonardi, R. Comparison of different separative techniques in the quantitative determination of active compound enclosed in liposomal systems. *International Journal of Cosmetic Science* (1994), 16(5), 183-197.

⁸² Tortorella, Domenico; Ulbrandt, Nancy D.; London, Erwin. Simple centrifugation method for efficient pelleting of both small and large unilamellar vesicles that allows convenient measurement of protein binding. *Biochemistry* (1993), 32(35), 9181-9188.

⁸³ Vemuri, Sriram; Rhodes, C. T. Separation of liposomes by a gel filtration chromatographic technique: a preliminary evaluation. *Pharmaceutica Acta Helvetiae* (1994), 69(2), 107-113.

⁸⁴ Ohki, Shinpei. Properties of lipid bilayer membranes. Determination of membrane thickness. *Journal of Theoretical Biology* (1969), 23(1), 158-168.

⁸⁵ Ostrowsky, N.; Hesse-Bezot, C. Dynamic light scattering study of the conformational change and fusion phenomenon of phospholipid vesicles. *Chemical Physics Letters* (1977), 52(1), 141-144.

⁸⁶ Ohno, Hiroyuki; Maeda, Yukio; Tsuchida, Eishun. Proton NMR study of the effect of synthetic polymers on the fluidity, transition temperature and fusion of dipalmitoyl phosphatidylcholine small vesicles. *Biochimica et Biophysica Acta* (1981), 642(1), 27-36.

⁸⁷ *Stability and Characterization of Protein and Peptide Drugs: Case Histories*, edited by Y. John Wang and Rodney Pearlman. Plenum Press, New York 1993.

⁸⁸ Helfrich, John P.. Flow-mode dynamic laser light scattering technology for 21st century biomolecular characterization. *American Biotechnology Laboratory* (1998), 16(11), 64-66.

⁸⁹ Deamer, D.W. ; Uster, P.S. *Liposome Preparation: Methods and Mechanism*. *Liposomes* (M.J. Ostro, Ed.) (1983), 27-51. Marcel Dekker, New York.

⁹⁰ <http://class.fst.ohio-state.edu/fst601/Lectures/LIPID.htm>, accessed on 04/23/2004.

⁹¹ Parrish, M. A. Cyclodextrins - a review. *Speciality Chemicals Magazine* (1987), 7(6), 366, 370, 372, 374, 378-380.

⁹² Vlachou, Marilena; Papaioannou, George. Preparation and characterization of the inclusion complex of furosemide with hydroxypropyl- β -cyclodextrin. *Journal of Biomaterials Applications* (2003), 17(3), 197-206.

⁹³ Sankaram, Mantripragada B.; Thompson, Thomas E.. Cholesterol-induced fluid-phase immiscibility in membranes. *Proceedings of the National Academy of Sciences of the United States of America* (1991), 88(19), 8686-8690.

⁹⁴ Larsson, Marcus; Larsson, Kare; Nylander, Tommy; Wollmer, Per. The bilayer melting transition in lung surfactant bilayers: the role of cholesterol. *European Biophysics Journal* (2003), 31(8), 633-636.

⁹⁵ Wintersteiner, Oskar; Abramson, Harold A. The isoelectric point of insulin. Electrical properties of adsorbed and crystalline insulin. *Journal of Biological Chemistry* (1933), 99, 741-753.

⁹⁶ Gennis, R. B. *Biomembranes: Molecular Structure and Function*; Springer-Verlag New York Inc: New York, 1989, 265.

⁹⁷ Gutknecht, J. Proton/hydroxide conductance through lipid bilayer membranes. *Journal of Membrane Biology* (1984), 82(1), 105-112.

⁹⁸ Johnson, C. S., Jr. Diffusion ordered nuclear magnetic resonance spectroscopy: principles and applications. *Progress in Nuclear Magnetic Resonance Spectroscopy* (1999), 34(3,4), 203-256.

⁹⁹ Le Bihan, D. *Diffusion and Perfusion Magnetic Resonance Imaging. Application to Functional MRI*. Raven Press, New York, 1995.

¹⁰⁰ Lin, Mengfen; Larive, Cynthia K. Detection of insulin aggregates with pulsed-field gradient nuclear magnetic resonance spectroscopy. *Analytical Biochemistry* (1995), 229(2), 214-220.

¹⁰¹ Jeffrey, P. D.; Coates, J. H. An equilibrium ultracentrifuge study of the self-association of bovine insulin. *Biochemistry* (1966), 5(2), 489-498.

¹⁰² Pekar, Allen H.; Frank, Bruce H. Conformation of proinsulin. Comparison of insulin and proinsulin self-association at neutral pH. *Biochemistry* (1972), 11(22), 4013-4016.

¹⁰³ Goldman, Jose; Carpenter, Frederick H. Zinc binding, circular dichroism, and equilibrium sedimentation studies on insulin (bovine) and several of its derivatives. *Biochemistry* (1974), 13(22), 4566-4574.

¹⁰⁴ Blundell, Tom; Dodson, Guy; Hodgkin, Dorothy; Mercola, Dan. Insulin: The structure in the crystal and its reflection in chemistry and biology. *Advances in Protein Chemistry* (1972), 26, 279-402.

¹⁰⁵ Uversky, Vladimir N.; Garriques, Liza Nielsen; Millett, Ian S.; Frokjaer, Sven; Brange, Jens; Doniach, Sebastian; Fink, Anthony L. Prediction of the association state of insulin using spectral parameters. *Journal of Pharmaceutical Sciences* (2003), 92(4), 847-858.

¹⁰⁶ Svedberg, The; Nichols, J. B. Application of the oil turbine type of ultracentrifuge to the study of the stability region of carbon monoxide-hemoglobin. *Journal of the American Chemical Society* (1927), 49, 2920-2934.

¹⁰⁷ Shipley, G. G. Recent X-ray diffraction studies of biological membranes and membrane components. *Biol. Membranes* (1973), 2, 1-89.

¹⁰⁸ Blume, A. Apparent molar heat capacities of phospholipids in aqueous dispersion. Effects of chain length and head group structure. *Biochemistry* (1983), 22, 5436-5442.

¹⁰⁹ Bernard, E.; Faucon, F. J.; Dufourcq, J. Phase separations induced by melittin in negatively-charged phospholipid bilayers as detected by fluorescence polarization and differential scanning calorimetry. *Biochimica et Biophysica Acta* (1982), 688, 152-162.

¹¹⁰ Ortiz, A.; Villalain, J.; Gomez-Fernandez, J. C. Interaction of diacylglycerols with phosphatidylcholine vesicles as studied by differential scanning calorimetry and fluorescence probe depolarization. *Biochemistry* (1988), 27, 9030-9036.

¹¹¹ Rolland, A.; Brzokewicz, A.; Shroot, B.; Jamouille, C.J. Effect of penetration enhancers on the phase transition of multilamellar liposomes of dipalmitoylphosphatidylcholine. A study by differential scanning calorimetry. *International Journal of Pharmaceutics* (1991), 76, 217-224.

-
- ¹¹² Brumm, T.; Joergensen, K.; Mouritsen, O. G.; Bayer, T. M. The effect of increasing membrane curvature on the phase transition and mixing behavior of a dimyristoyl-sn-glycero-3-phosphatidylcholine/distearoyl-sn-glycero-3-phosphatidylcholine lipid mixture as studied by Fourier transform infrared spectroscopy and differential scanning calorimetry. *Biophysical Journal* (1996), 70, 1373-1379.
- ¹¹³ Menczel, J. D.; Judovits, L. Literature status on temperature-modulated differential scanning calorimetry. *Journal of Thermal Analysis and Calorimetry* (1998), 54, 419-436.
- ¹¹⁴ Hutchinson, J. M. Studying the glass transition by DSC and TMDSC. *Journal of Thermal Analysis and Calorimetry* (2003), 72, 619-629.
- ¹¹⁵ Zhang, Xuan; Qi, Xianrong; Zhang, Qiang. Interaction between insulin with liposome. *Yaoxue Xuebao* (2002), 37(5), 370-373.
- ¹¹⁶ Langmuir, Irving. Evaporation, condensation and reflection of molecules, and the mechanism of adsorption. *Physical Review* (1916), 8, 149-176.
- ¹¹⁷ Hauser, H.; Pascher, I.; Pearson, R. H.; Sundell, S. Preferred conformation and molecular packing of phosphatidylethanolamine and phosphatidylcholine. *Biochimica et Biophysica Acta* (1981), 650(1), 21-51.
- ¹¹⁸ Freire, Ernesto; Mayorga, Obdulio L.; Straume, Martin. Isothermal titration calorimetry. *Analytical Chemistry* (1990), 62(18), 950A-959A.
- ¹¹⁹ Chellani, Mohan. Isothermal titration calorimetry: biological applications. *American Biotechnology Laboratory* (1999), 17(11), 14, 16, 18.
- ¹²⁰ Walter, Anne; Gutknecht, John. Permeability of small nonelectrolytes through lipid bilayer membranes. *Journal of Membrane Biology* (1986), 90(3), 207-217.

¹²¹ Lieb, William R.; Stein, Wilfred D. Non-Stokesian nature of transverse diffusion within human red cell membranes. *Journal of Membrane Biology* (1986), 92(2), 111-119.

¹²² Pink, David A.; Lookman, Turab; MacDonald, A. Leo; Zuckermann, Martin J.; Jan, Naeem. Lateral diffusion of gramicidin S, M-13 coat protein and glycophorin in bilayers of saturated phospholipids. Mean field and Monte Carlo studies. *Biochimica et Biophysica Acta* (1982), 687(1), 42-56.

¹²³ Tamm, Lukas K.; McConnell, Harden M. Supported phospholipid bilayers. *Biophysical Journal* (1985), 47(1), 105-113.

¹²⁴ Georgallas, A.; MacArthur, J. D.; Ma, X. P.; Nguyen, C. V.; Palmer, G. R.; Singer, M. A.; Tse, M. Y. The diffusion of small ions through phospholipid bilayers. *Journal of Chemical Physics* (1987), 86(12), 7218-7226.

¹²⁵ Ohno, Hiroyuki; Ukaji, Kazuo; Tsuchida, Eishun. Temperature dependence of the leakage of carboxy fluorescein from an inner aqueous phase of liposomes or mixed liposomes. *Journal of Colloid and Interface Science* (1986), 120(2), 486-494.

¹²⁶ Hays, L. M.; Crowe, J. H.; Wolkers, W.; Rudenko, S. Factors affecting leakage of trapped solutes from phospholipid vesicles during thermotropic phase transitions. *Cryobiology* (2001), 42(2), 88-102.

¹²⁷ Mukesh, D. Applications of neural computing for process chemists: I. Introduction to neural network. *Journal of Chemical Education* (1996), 73(5), 431-433.

APPENDIX

In Chapter 5.1, we developed a mathematical model, based on our theory of protein release from liposomes, to quantify the release results. Equation 5.7 was used as the modeling equation to express the whole protein release process.

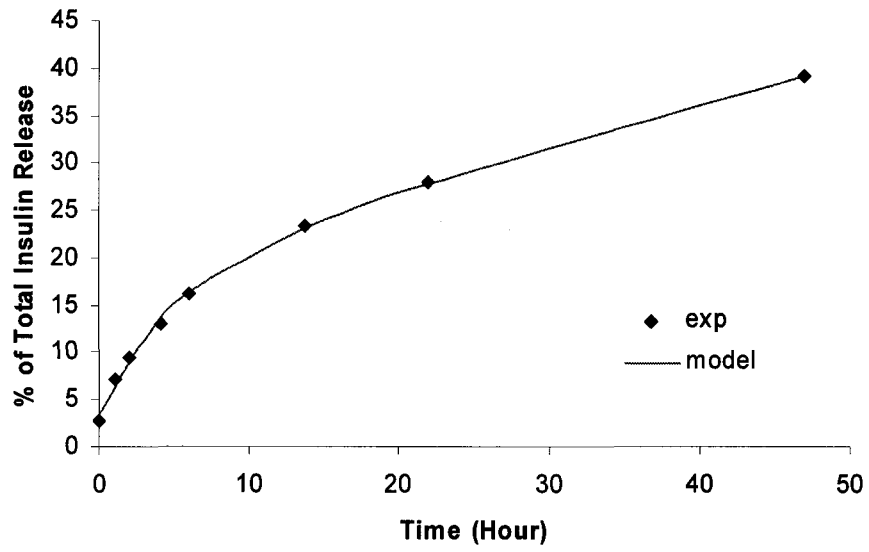
$$y = \frac{1}{\left(\frac{1}{(a \cdot t + b)^2} + \frac{1}{(c \cdot t + (a - c) \cdot t^* + b)^2} \right)^{1/2}} \quad [5.7]$$

We used the “Solver” function of Excel® to estimate the best a , b , c and t^* values to make the Equation 5.7 fit the experimental data through a least square non-linear curve fit. Table 6 listed the result of the curving fitting. The figures in the Appendix show the detail curve fitting for each release curve: the diamond dots are the experimental data points and the line is the fitting curve. The R^2 value was also given by

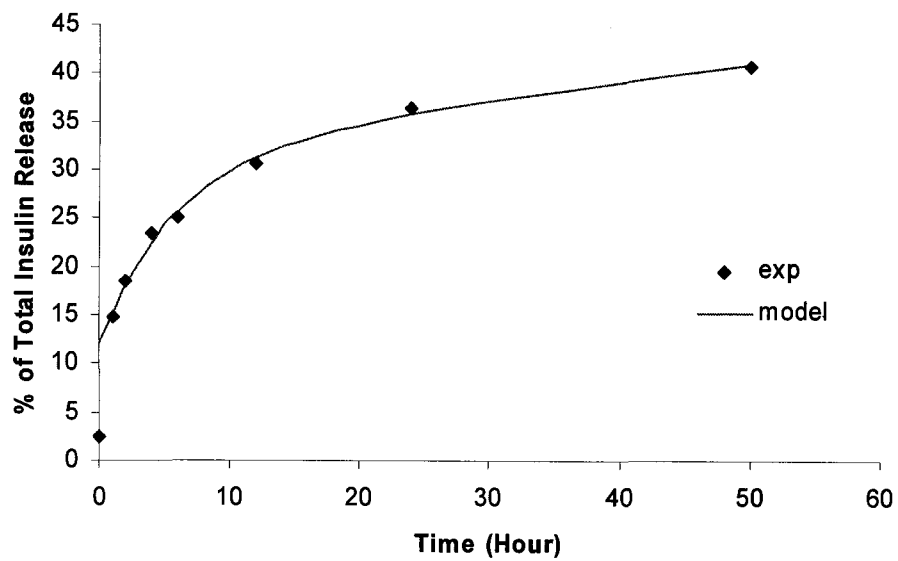
$$R^2 = 1 - \frac{\sum_{i=1}^n (y_i - \hat{y}_i)^2}{\sum_{i=1}^n (y_i - \bar{y})^2}$$

where y_i is the experimental protein percent release value, \hat{y}_i is the predicted percent release value, \bar{y} is the mean.

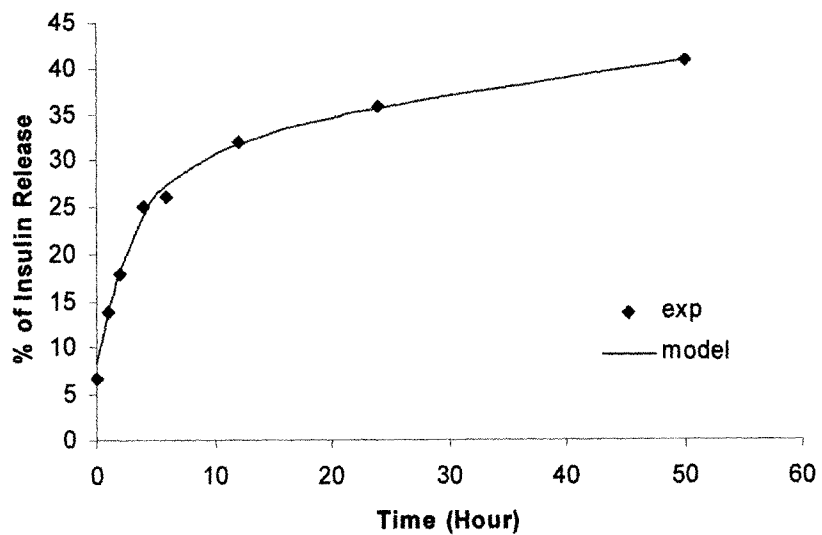
Sample "CPE215" in Chapter 3.2.2 ($R^2=0.999$)



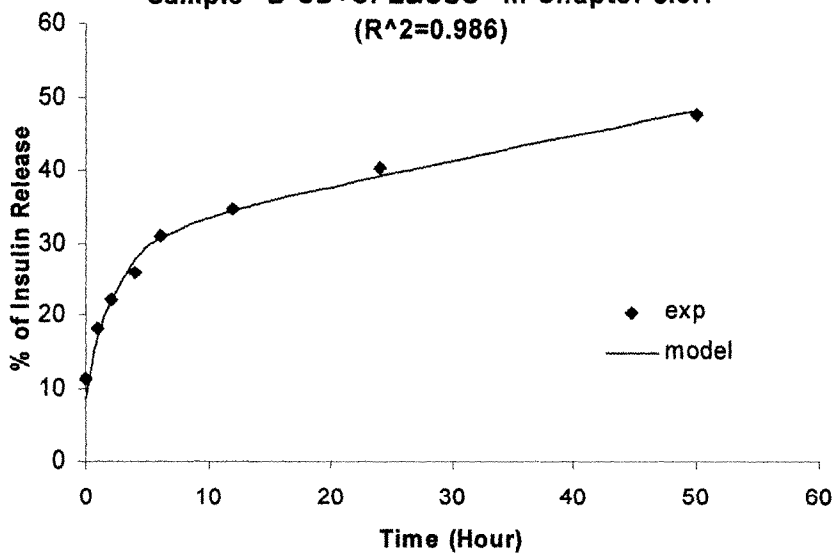
Sample "B-CD" in Chapter 3.3.1 ($R^2=0.917$)

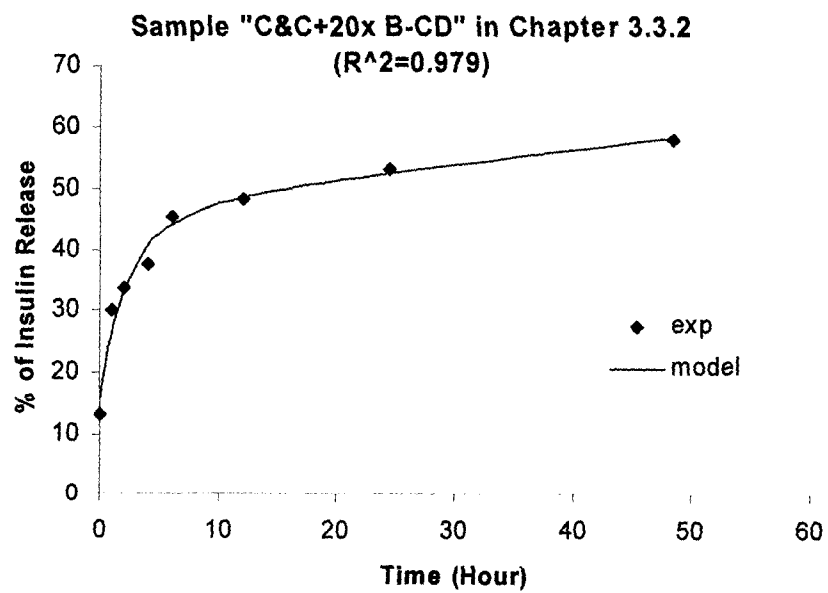
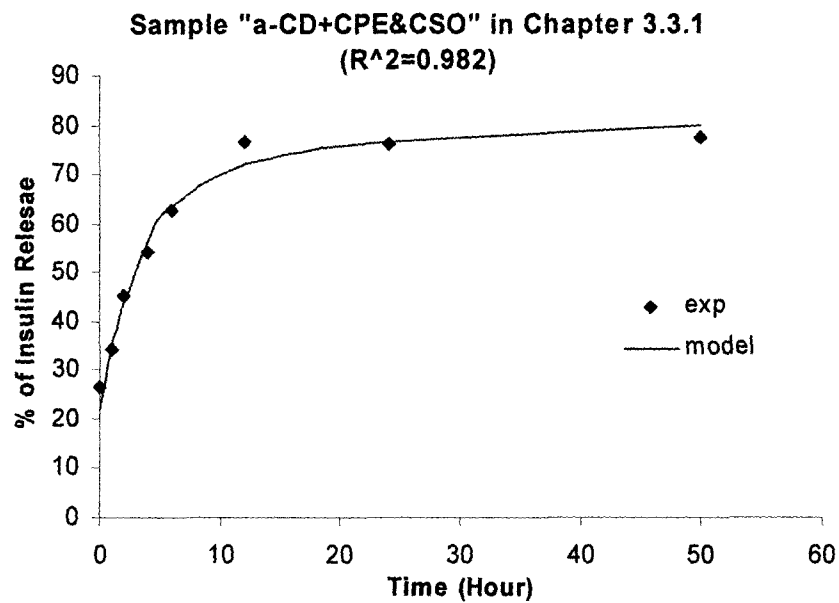


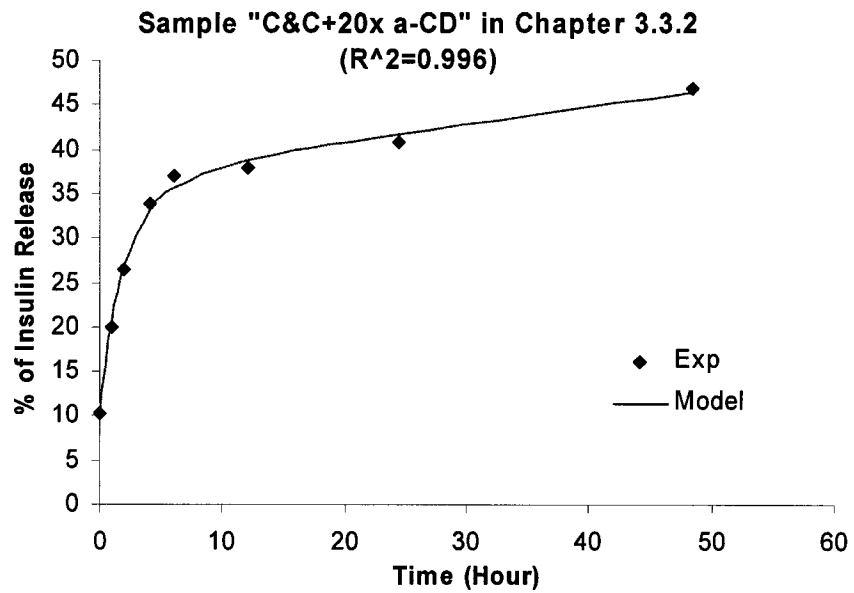
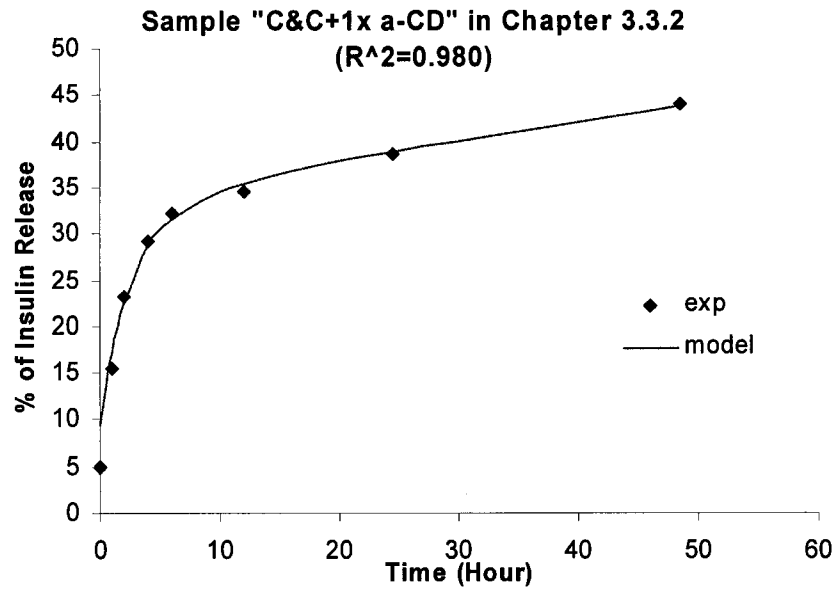
Sample "CPE&CSO" in Chapter 3.3.1 ($R^2=0.994$)

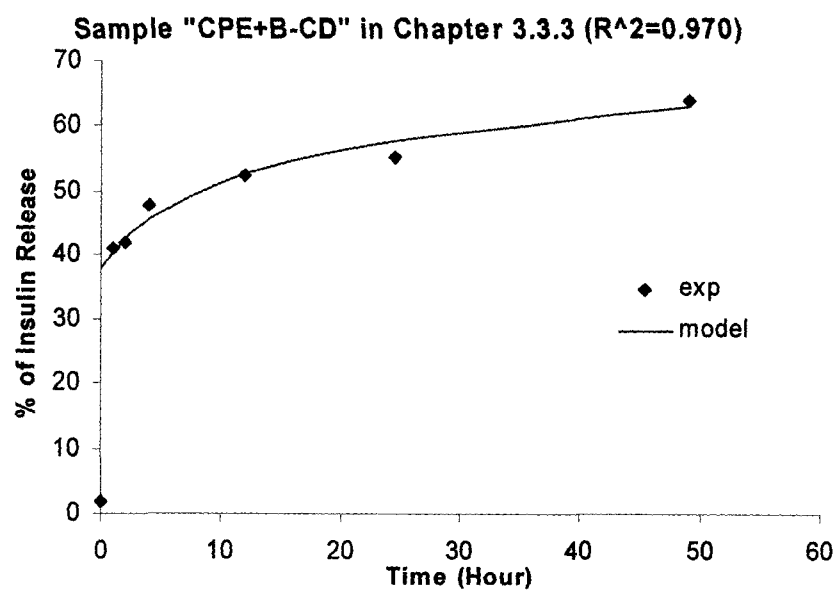
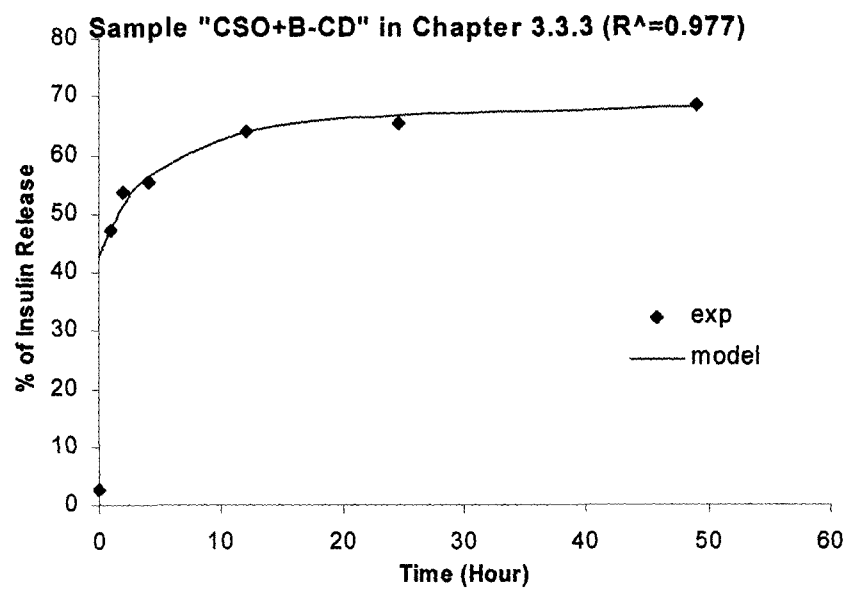


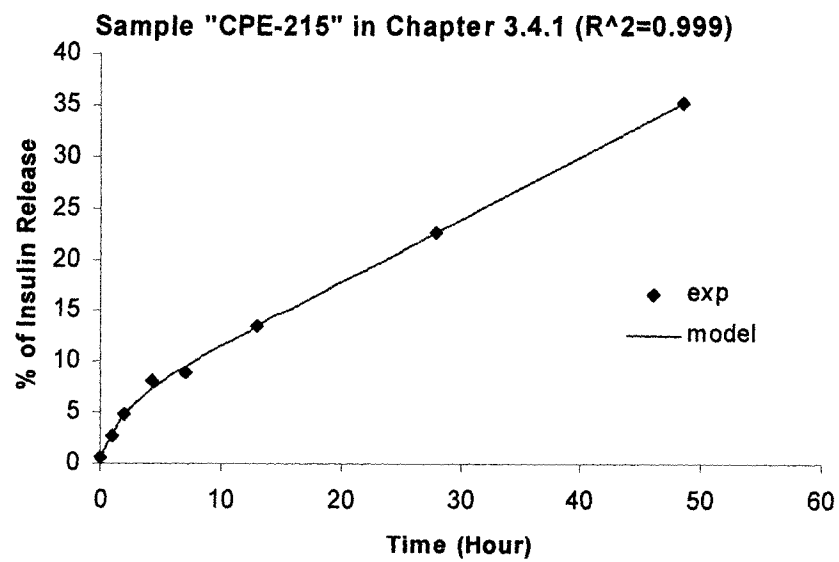
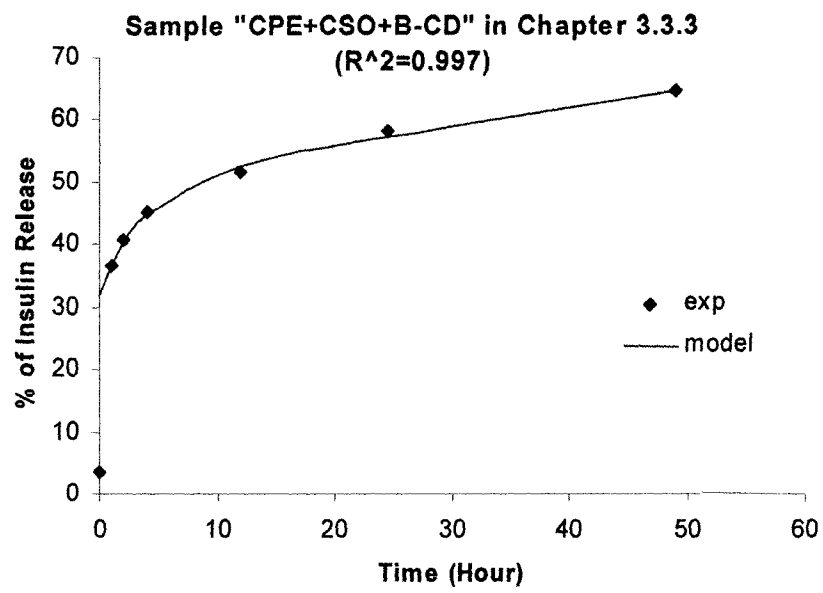
Sample "B-CD+CPE&CSO" in Chapter 3.3.1
($R^2=0.986$)

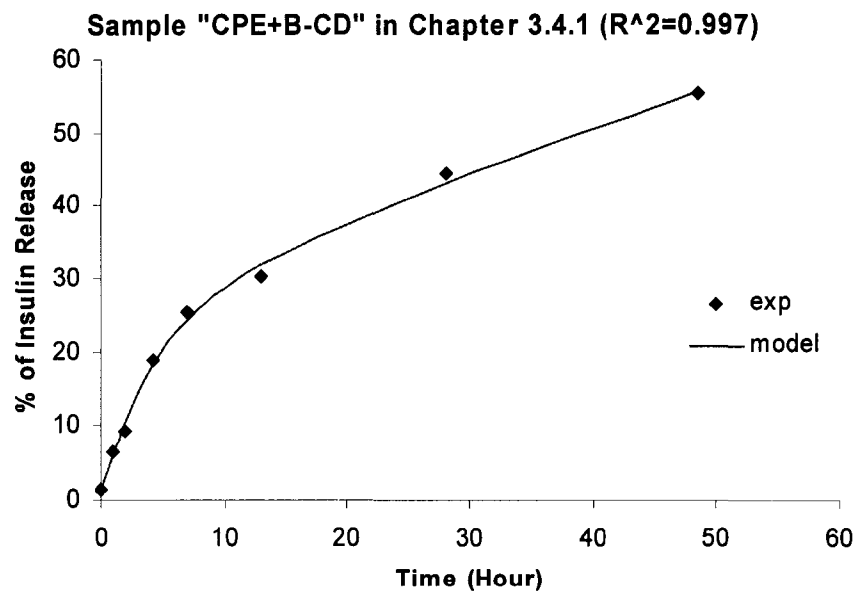
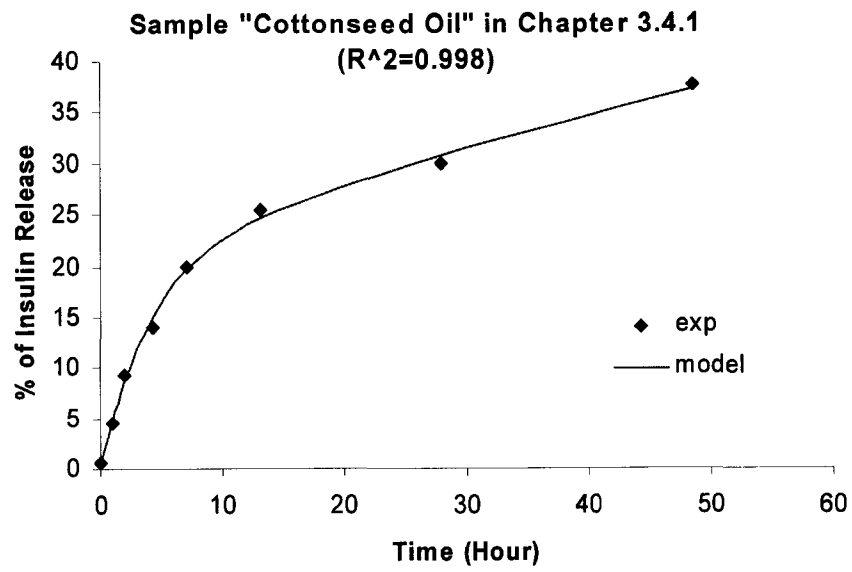


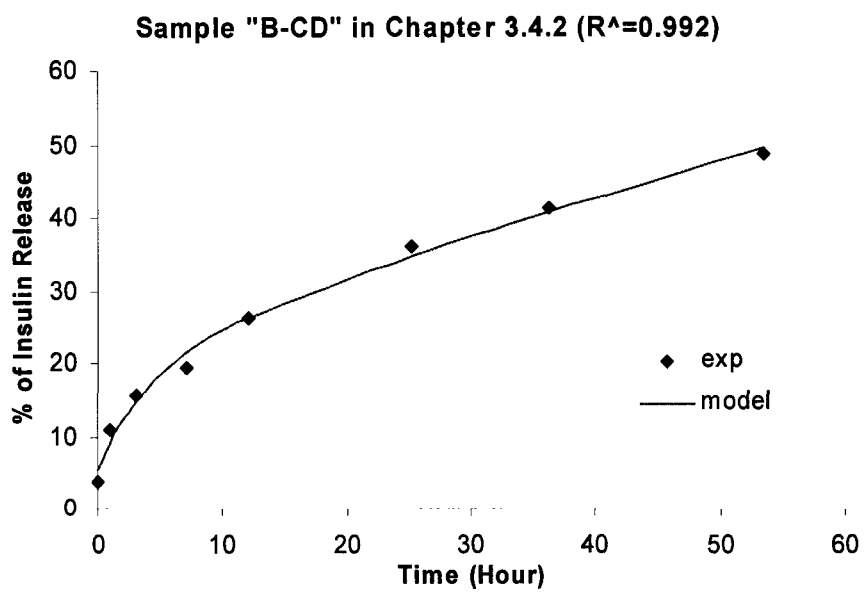
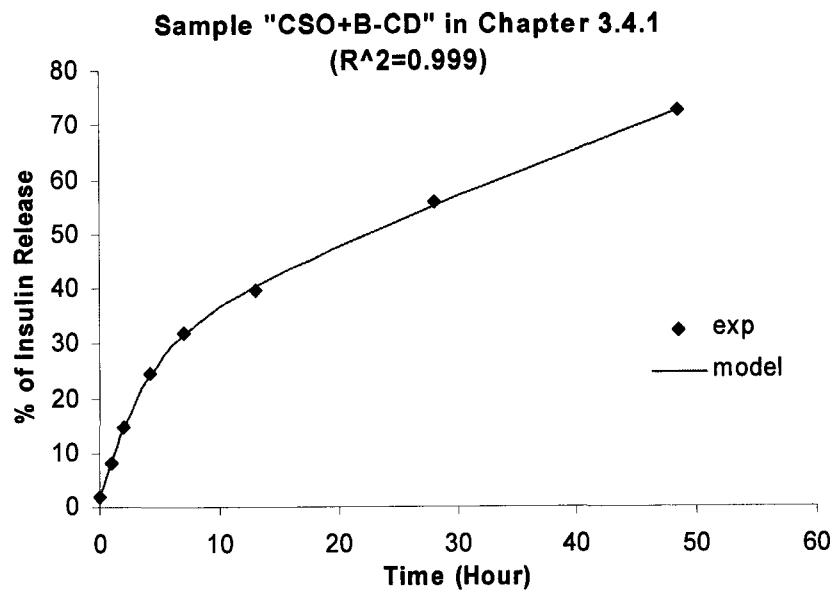


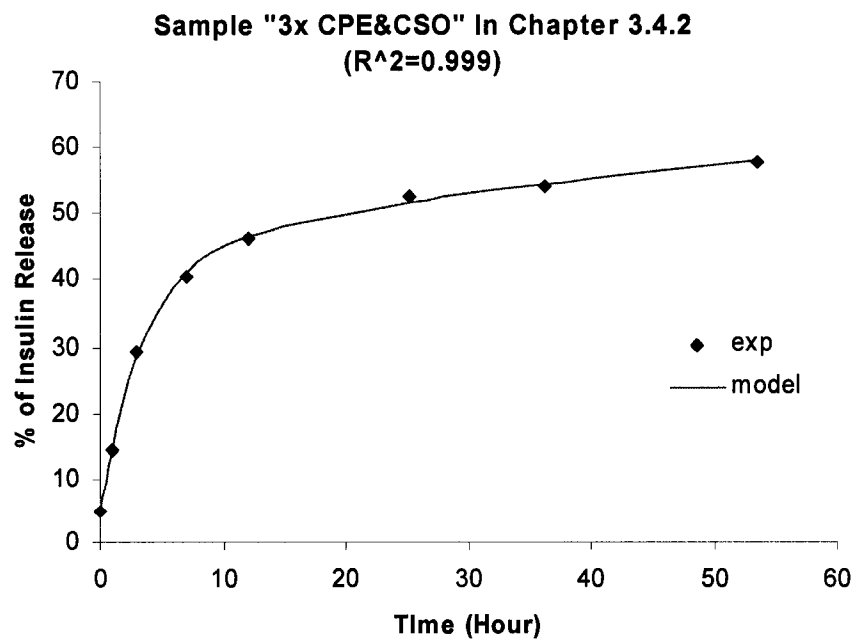
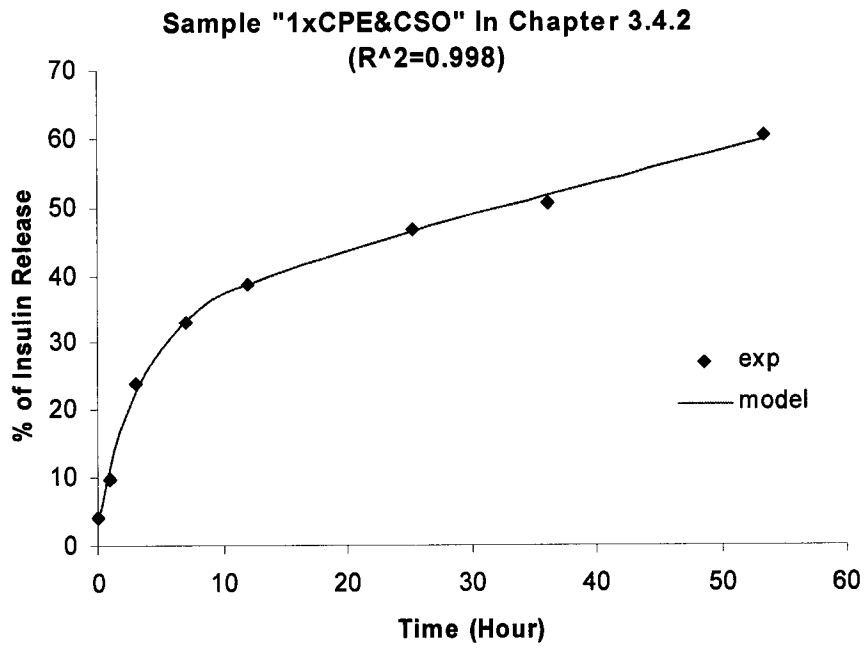


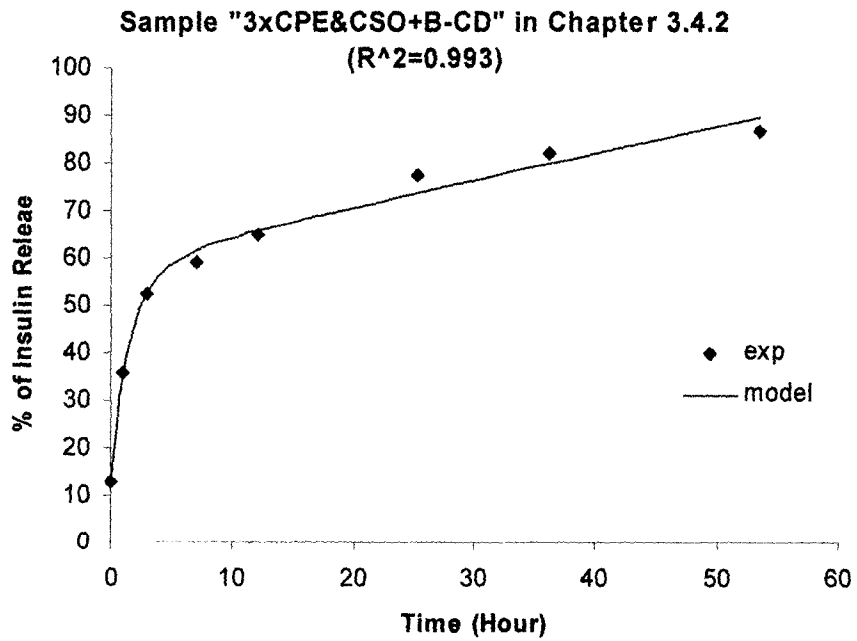
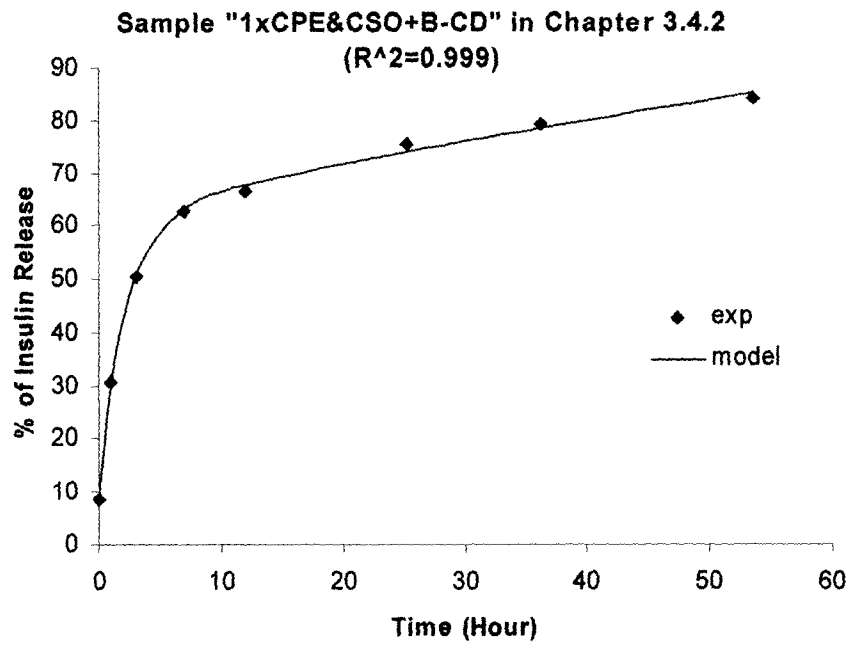


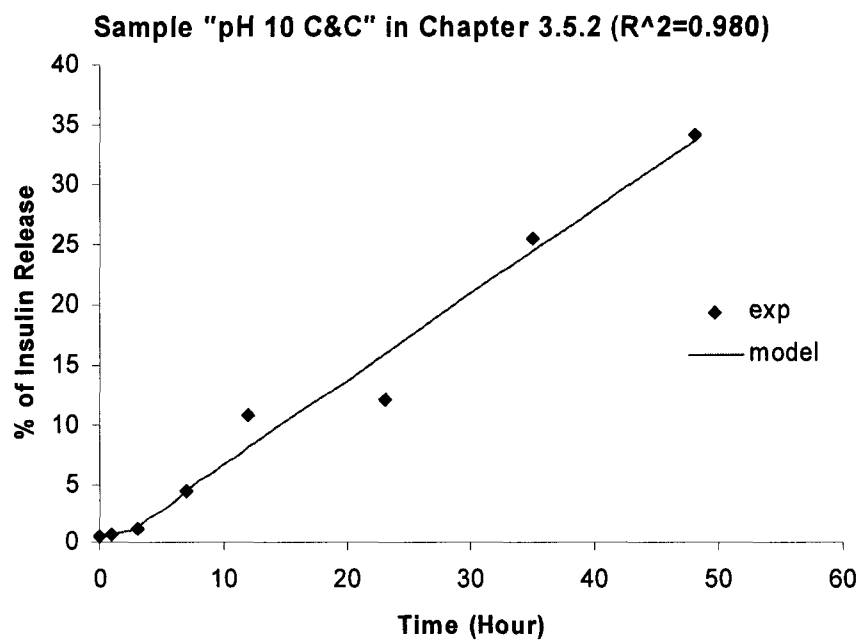
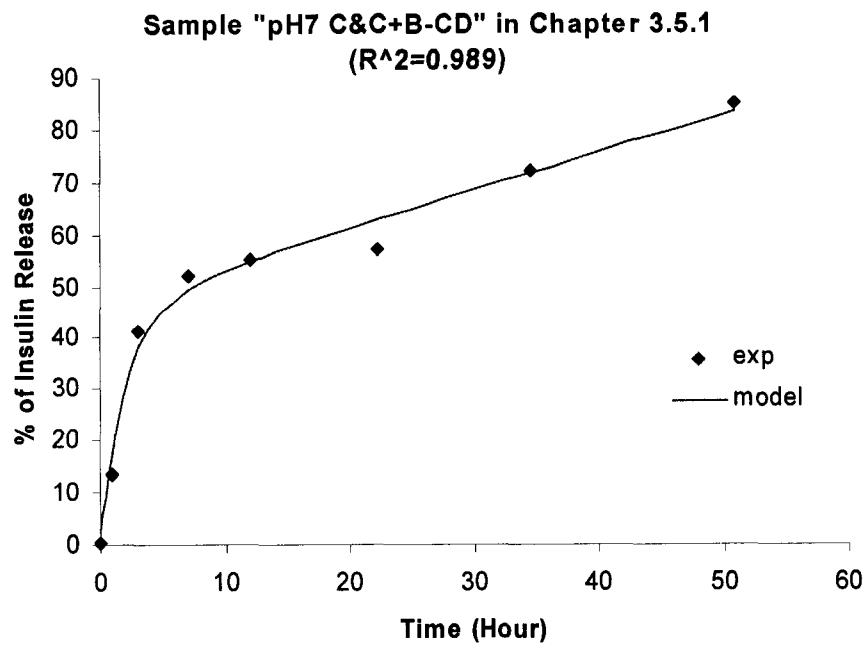


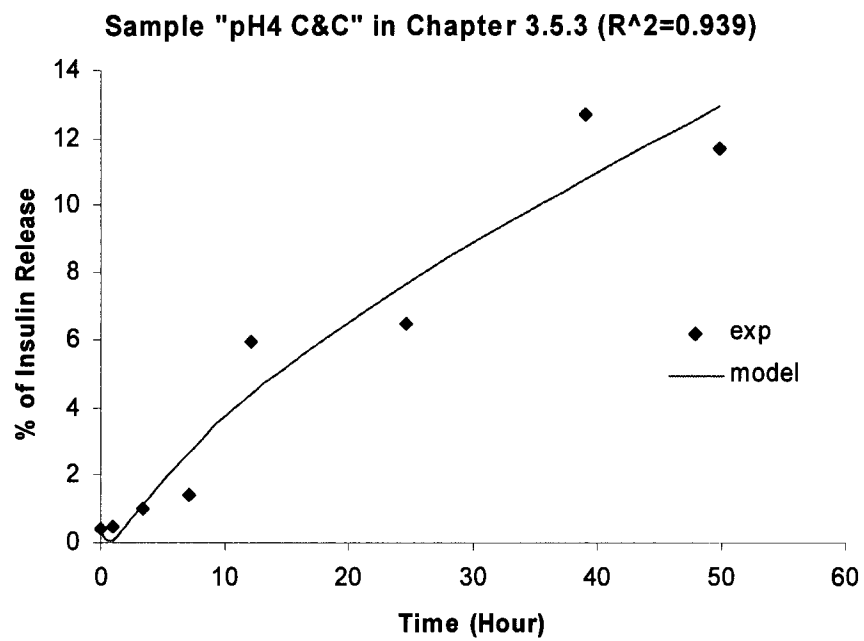
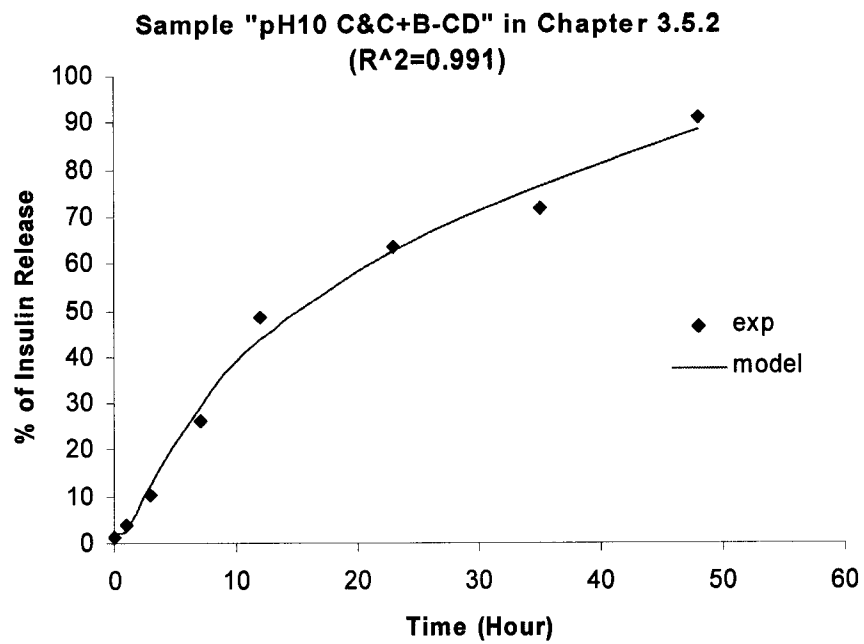




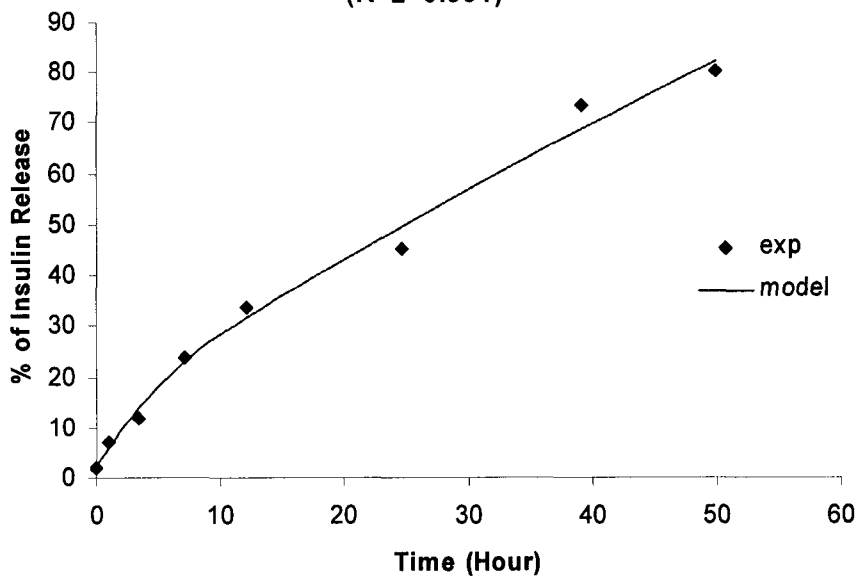








Sample "pH4 C&C+B-CD" in Chapter 3.5.3
($R^2=0.991$)



Sample "CPE" in Chapter 3.6 ($R^2=0.996$)

